Modeling of the price microstructure and applications of stochastic control to algorithmic trading.

Pietro Fodra

HAL Id: tel-01161734

https://theses.hal.science/tel-01161734

Submitted on 9 Jun 2015

UNIVERSITÉ PARIS DIDEROT (PARIS 7)
SORBONNE PARIS CITÉ
U.F.R. DE MATHÉMATIQUES
ÉCOLE DOCTORALE DE SCIENCES MATHÉMATIQUES
DE PARIS CENTRE
Laboratoire LPMA

THÈSE DE DOCTORAT

Discipline : Mathématiques Appliquées

Présentée par
PIETRO FODRA

MODELING OF THE PRICE MICROSTRUCTURE AND APPLICATIONS OF STOCHASTIC CONTROL TO ALGORITHMIC TRADING

Modélisation de la microstructure du prix et applications du contrôle stochastique au trading algorithmique

---

Thèse dirigée par **Huyên PHAM**
Soutenue le **17 Février 2015**

Jury

Frédéric ABERGEL	Rapporteur
Michael LUDKOVSKI	Rapporteur
Álvaro CARTEA	Membre du jury
Olivier GUEANT	Membre du jury
Charles-Albert LEHALLE	Membre du jury
Huyên PHAM	Membre du jury
Mathieu ROSENBAUM	Membre du jury

Special thanks

I would like to thank all the people that have been close to me during these years of research and work, since their help has been a wonderful gift.

First of all, I would like to thank my Ph.D. advisor, *Huyên Pham*, whose patience and experience have guided me through this long work. His advice has been fundamental, and his encouragement has been my most precious ally.

A special thank to the *LPMA*, that allowed me to participate to the research activity in a culturally rich environment, with seminars, workshops and conferences all around the Europe. I had the pleasure to exchange ideas with a vast community of students and professors with different mathematical backgrounds. I thank all my Ph.D. colleagues, who fully understand all the efforts, the doubts, the hard work which comes with a thesis, especially in a period of economic crisis, but also the joy of discovering and sharing new results. An extra thank to *Marc-Antoine*, *Maud*, *Anna* and *Tommaso*, with whom I shared the office for a long time, and with whom it has always been a pleasure to talk.

I want to thank my referees *Frédéric Abergel* and *Michael Ludkovski* for their detailed reports, and the other jury members *Álvaro Cartea*, *Olivier Guéant*, *Charles-Albert Lehalle* and *Mathieu Rosenbaum*, for having accepted to examine my work and partecipate to the defence.

I thank *Jacques Lucas*, *Philippe de Gouville*, *J.G.Grebet*, and all my colleagues, who have believed in me, and allowed me to develop many professional skills in an outstanding working environment, made of daily intellectual challenges and collaborations between colleagues driven by enthusiasm and passion. A special thank goes to *Aurélien*, for all the time he devoted me to improve my coding style, and for its contagious passion for Computer Science, *Mauricio*, who contributed to one of the four papers, and *Gwen*, for all the interesting discussions had together and his great curiosity.

I want to thank *Mamma*, *Babbo*, *Azzurra*, *Fabio* and the kids, *Ettore* and *Giulio*, who gave me a unconditional support. A special thank goes to my dad, for all the love he gave me, and for having scarifying everything, especially his time, so that I could have the best chances to succeed. This thesis is dedicated to him and his memory.

I want to thank my girlfriend, *Federica*, who has lived this journey of more than three years in symbiosis with me, who has listened, understood, loved, supported and got me calm, either by the other side of the phone, more than 1000 km away, or by the other side of the table, after a long day spent in front of my computer.

Spending these years in Paris has been a human and professional privilege, an unforgettable experience that will be a part of me for the rest of my life. I want to thank the city, and France in general, who has welcomed me and given me many presents: a high-level education, a work, the possibility of projecting me in the future, a lot of fun, and the chance to enjoy her beauty. Here I have found a place that I can call home: I hope to repay my debt in the forthcoming years.

A final thank is dedicated to me, for having held on.

Contents

Chapter 1

Introduction

1.1   A introduction to the limit order book

During the last decades, electronic markets have gained an enormous popularity among investors, and cover now the majority of the transaction volume, especially in U.S. market. Their success is due to fast, public and traceable transactions, in exchange for small fees to pay to the stock exchange for the service provided.

Humans are replaced by automatons (luckily still programmed by humans!) sending orders to the electronic market, a veritable revolution in the finance world. The intrinsic limits of human speed have been widely overcome by computers, that are able to send several orders in a fraction of second following complicated and systematic algorithms. A new kind of trader is born: the high frequency one. Despite the success, their participation to the market has been widely debated both in terms of moral and regulatory issues: the emblematic flash crash of 6th May 2010 on the U.S. market has highlighted the necessity of better understanding how high frequency traders affect, impact and drive the market, in particular since an algorithm, and the chain reaction of others in the next milliseconds, can deeply modify the value of a stock in few seconds. At present time, a large academic literature (e.g. [55], [48]) has focused on the flash crash, trying to attack or defend these traders from being responsible of one of the most spectacular event in the modern finance, but empirical evidences do not suggest a unique interpretation of these "wild" minutes of trading. Furthermore, it would be restrictive to consider only extreme scenarios in the analysis of such a complex phenomenon as electronic (and in particular high-frequency) trading. Its original mission, which has been successfully accomplished, was, and still is, to bring liquidity at a small price: public concurrence of several investors in the electronic market has contributed to improve significantly the market liquidity, lowering the cost of market participation, and this seems to guarantee a future to this activity.

The FIFO matching engine: be what you want!

The key behind this success is a simple queueing system handling the inter-play between sellers and buyers, liquidity providers and takers.

In the simplest and most popular case, the price-time FIFO (first-in-first-out) electronic book, several liquidity providers, also called **market makers**, make public the price they are willing to sell or buy a lot, as well as the liquidity (the number of lots) they make available at that price. These passive orders are called **limit orders**. Sellers (buyers) are ranked in terms of priority according to the lower (higher) price offered, with the convention that:

  i) for sellers or buyers offering liquidity at the same price, the priority is determined by the timestamp of the limit order (**price-time priority**),

 ii) the best selling (buying) price is called **best-ask** (**best-bid**),

iii) the difference between the best-ask price and the best-bid price is called the **bid-ask spread**, while their average the **mid-price**.

Notice that the bid-ask spread is always positive: the best-ask price is always bigger than the best-bid one, since otherwise there would be an agreement between a buyer and a seller, and thus an immediate transaction.

Now, liquidity takers can accept to buy or sell at the price offered by liquidity providers, sending active orders, also called **market orders**. Of course, if their demand of liquidity is small, a buyer (seller) accepts to treat at the best-ask (best-bid) only. However, if their demand excesses the liquidity supplied at the best level, they first consume it, and then go for deeper levels in the book, widening the market spread and altering the current mid-price.

This snapshot of the limit order book should be though dynamically: liquidity providers and liquidity takers continuously send market and limit orders, improve the current best price to gain priority, clear levels when a big amount of liquidity is needed, etc... The same investor can be, during one day, buyer and seller, liquidity provider and liquidity taker. This is one of the key of the success of electronic trading compared to monopolistic market where one external liquidity provider establishes the best quotes for all the liquidity takers, and no role exchange is possible.

Even if the latter is the most popular type of electronic market, this is not the only one: several markets exist, with different priority rules (e.g. pro-rata, where the displayed liquidity is more rewarded than timestamp in terms of priority), different fees (e.g. markets where market makers pay a fixed initial fee not to be charged on each transaction), different visibility (e.g. dark pools, where limit orders are hidden to liquidity takers), and so on. Since all the models in this work are inspired to the FIFO matching engine, we will not add further details on other types of market.

The tick size

So far, we have mentioned that market makers are allowed to send limit orders displaying the price and the liquidity they are willing to offer. In a price-time priority market, it would be enough to improve the current best price of any $\epsilon > 0$ to be the first in the queue. In an electronic market, this would create an extremely unstable environment where each market maker, as soon as she is not the best offerer, sends a new limit order to improve the current best price of a small quantity. This problem is solved by the introduction of apparently harmless but powerful tool: **the tick**.

Fixed by the stock exchange, the tick size represents the minimum distance between two levels in the limit order book, which implies that all the limit orders have prices living on the tick grid and that **a bid-ask spread of 1 tick cannot be improved**, forcing any new market maker to wait to be first served in the line. The timestamp priority becomes a crucial factor, which justifies the enormous amount of money spent by big financial investors to reduce the latency between the time when the order is sent and when it is actually received by the exchanxge.

The choice of the tick size is a delicate subject, and the recent work of [31] has focused on how to determine the optimal size for the exchange in order to guarantee the functional behavior of the market. Assets can be roughly divided in **large tick** or **small tick** assets, comparing the size of the tick with the asset price.

In large tick assets, the distance between two consecutive levels represents an important amount of money (recall that high frequency traders make several transactions a day), and lots of market makers are fine to offer liquidity at levels close to the mid-price. As a consequence, if the bid-ask spread is more than one tick, there is likely to be one market maker willing to improve it and fill the gap: for large tick assets the liquidity is concentrated on the first levels and the bid-ask spread is almost constantly one tick. The liquidity structure of the limit order book is dense around the mid-price, which is trapped into two walls of market makers offering resistance to the price movement, making the mid-price jumps mostly of one tick at the time.

In assets with small tick, the situation is quite the opposite: the displayed liquidity is spread all over the book, and holes can appear (levels where no liquidity is displayed) also in levels close to the mid-price. As a result, the spread is not constantly one tick, and the mid-price enjoys a large freedom of movement, which makes it jump several times and often of multiple ticks. The difference between the two market is illustrated by Figure 1.1.
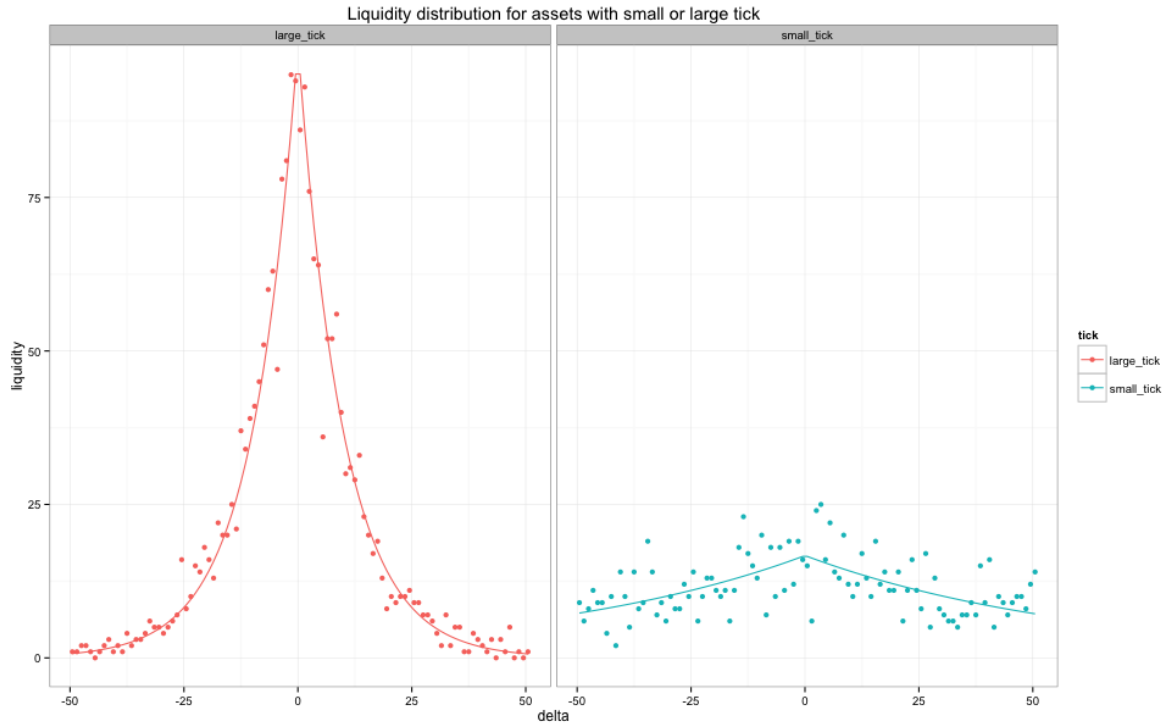
Figure 1.1: liquidity distribution for assets with different ticks (simulated data), with the convention that $\delta = 0$ is the mid-price, and $\delta > 0$ (< 0) corresponds to the ask (bid) side. Asset with large tick displays liquidity close to the mid price $\delta = 0$, while in the small tick case the liquidity is distributed more uniformly.

Summing up, the (mid) price of large tick assets changes less often than in the small tick case, since the minimal jump possible represents an important amount of money, and usually of one tick at the time. Nevertheless, assets with different tick size and different frequency of jump can be highly correlated (see the Eurostoxx and the Dax), since the effect of multiple jumps of a small tick assets are replicated by few jumps of the large tick asset.

Stylized facts and models for the stock price

The pricing literature has developed over the last 40 years a lot of models for the stock price based on daily observations, for which continuous processes, as the geometric Brownian motion and its sophisticated extensions, are well adapted, both in terms of accuracy and tractability for pricing formulae.

At the micro-structure scale, the choice of a continuous process is arguable. The effect of the tick size naturally discretizes the stock price, which is a piece-wise constant process jumping on the tick grid.

This dynamic has direct consequences on the stock price, which exhibits, at the micro-structure scale, several stylized facts.

We illustrate the most common ones.

i) *micro-structure noise*: the stock price exhibits a mean reverting behavior, i.e. a strong anti-correlation between two consecutive jumps. This phenomenon is due to the particular structure of the limit order book, where the price is the result of the interplay between

liquidity providers and takers. When market orders consume all the liquidity offered by market makers at one of the best prices, the mid price jumps in the corresponding direction, up (down) if theses orders match the best-ask (best-bid) price. The spread suddenly enlarges, and new market makers are likely to fill the gap: if the price jumps upwards (downwards), the new best-ask (best-bid) displays a pre-existing liquidity offered by market makers that were waiting on the second level on the ask (bid) side, while the new best-bid (best-ask) offers a brand new liquidity due to market makers filling the gap in the spread. Since the new level offers less liquidity than the older one, the price is likely to jump downwards (upwards) the next time, and so on... This creates a mechanical mean reversion (see Figure 5.2), which is stronger for assets where the liquidity is concentrated around the mid price, i.e. large tick assets. The phenomenon can be quantified by measuring the frequency of two consecutive jumps in the opposite direction, i.e.

$$\mathbb{P}[\uparrow\downarrow \ \ or \ \ \downarrow\uparrow].$$

for large tick assets, it widely overcomes 50% (the random walk): the stock price is not, at the micro-structure level, a martingale, since the directional information coming from the last jump (actually jumps!) influences its future evolution.

ii) *Volatility clusters:* while micro-structure noise is a stylized fact typical of micro-structure, volatility clusters can be found both at the micro and macro-structure scales. Empirical evidences suggest that phases of high activity (read volatility) are persistent in time: the pricing literature has tackled this problem introducing stochastic volatility (GARCH, Heston , SABR, etc...), and we will see that the micro-structure one has chosen a very similar approach, employing point processes with stochastic intensity.

iii) *Mean signature plot:* volatility estimation is crucial in option pricing (and almost everywhere in quantitative finance), since volatility represents a risk an agent is likely to hedge against. High frequency databases guarantees an impressive number of observations, which should improve the standard volatility estimator by shrinking its confidence interval. Unfortunately, the microscopic mean reversion leads to a standard estimator that explodes when the observation frequency increases. In particular the mean signature plot

$$\bar{\mathcal{V}}(\tau) := \frac{1}{\tau} \mathbb{E}\left[(P_{t+\tau} - P_t)^2\right] \neq \sigma^2,$$

as it should be if (P_t) were driven by $dP_t = \sigma dW_t$. Empirical evidences suggest that $\bar{\mathcal{V}}(\tau)$ is a decreasing function of τ, and this phenomenon cannot be explained by diffusive models.

iv) *Diffusive behaviour on the long run:* most of the stylized facts appearing in the micro-structure world tend to disappear as soon as observations become less frequent, especially for the micro-structural mean-reversion and the decreasing shape of the signature plot. Pricing literature has been focusing on continuous price models for years, and the arrival of the electronic market has not altered the diffusive nature of the stock price at the macroscopic scale.

v) *Epps effect:* even if not treated in this work, it is worth mentioning the Epps effect. Empirical evidences suggest that increasing the observation frequency, the correlation between two assets tends to disappear, even if at the macroscopic scale they are highly correlated. This can be interpreted as the cross correlation counter-party of the mean signature plot, and its cause has to be looked for in the discrete nature of the price.

We will detail how different models in the micro-structure literature replicate these stylized facts, but first it is important to make a remark concerning applications. Trading applications based on optimal control techniques are often a sophisticated and powerful tools to design an algorithmic strategy. However, optimality, like magic, comes with a price: sophisticated systems are usually high-dimensional, complex and difficult to handle both analytically and numerically.

An electronic trading application should address at least the price model and the execution mechanism: a faithful description of the entire environment would lead to intractable models. Often, something must be sacrificed. In the available literature, the most popular choices are to consider the price as a Brownian motion, or the arrival of market orders in the book as a Poisson process. Both hypothesis are somehow inconsistent, but in some case tolerable. In particular, when the agent horizon is big, the micro-structure stylized facts tends to compensate, leaving space for easier models. For a daily horizon for example, assets with small tick can still be thought as diffusive, since their jump activity is so high that the stock price can be considered continuous. For large tick assets instead, the piece-wise constant feature cannot be ignored, and point processes should be preferred to continuous ones.

A literature background on price modelling at high frequency

The modelling of tick-by-tick asset prices has attracted a growing interest in the statistical and quantitative finance literature with the availability of high frequency data. The properties of the stock price, and more generally of whole the limit order book, have been widely investigated by several econometric and econophysic papers, which focused on the empirical property of the book starting from minimal assumptions. Some examples are provided by the seminal papers [13, 58], studying the distribution of incoming limit order around the mid-price, enlightening its power shape nature, [32], where the the authors observe the role of liquidity providers in the magnitude of price variation, or [52, 12], studying long memory persistence of the order flow and the price increments.

We introduce some of the existing models to provide an overview of how different authors has tackled this problem and to explain the philosophy guiding them. The literature is basically split into two categories.

i) *The macro-to-microscopic (or econometric) approach:* (see e.g. [39], [3], [60]) it interprets the observed price as a noisy representation of an unobserved one, typically assumed to be a continuous Itô semi-martingale: in this framework several results exist on the robust estimation of the realized volatility, but these models seem not to be adapted to high frequency trading problems and stochastic control techniques, mainly because the state variables are latent rather than observed.

ii) *The micro-to-macroscopic approach:* (see e.g. [9], [7], [25], [1], [35], [17], [29] and [30]) it exploits point processes, in particular Hawkes and renewal processes (as in our case), to drive the asset price, either moving on the tick grid or on the real line. In contrast with the macro-to-microscopic approach, these models do not rely on the arguable assumption of the existence of a fair or fundamental price, focusing only on observable quantities, which makes the statistical estimation usually simpler.

Two of the most beautiful examples in the macro-to-microscopic approach are represented by the rounding model and the uncertainty zone model. In the **rounding model**, the price process is given by

$$P_t := \lfloor \widehat{P}_t \rfloor,$$

(assuming that the tick size is unitary), where $(\widehat{P}_t)$ is a continuous semi-martingale (e.g. a Brownian motion). The tick rounding guarantees the reproduction of the micro-structural noise, while by construction the process has a diffusive behaviour for large scale observations. For this model [39] and [46] illustrate several statistical properties and provide a volatility estimator for the hidden price process, overcoming the problem of the explosion of the mean signature plot. The **uncertainty zone model** of [60] instead, assumes that a continuous semi-martingale drives a hidden price, with the observed price that changes only when the hidden price hits some hidden barriers, strategically placed to reproduce the micro-structure noise. An efficient estimation procedure allows to detect the hidden price dynamic (e.g. its volatility in the Brownian motion

case) and the position of the barriers, and once again the process tends to a diffusive behavior for large scale observations by construction. As previously said, these efficient models are rather difficult to translate into trading applications using optimal control techniques, since the knowledge of the current value of the hidden process is a necessary ingredient to use dynamic programming.

The micro-to-macroscopic literature instead bases her description on observed quantities only. No hidden process exists, and the stock price is assumed to be driven by piece-wise constant point processes. The most popular are Hawkes processes. In the seminal paper of [7] the stock price is given by

$$P_t = N_t^+ - N_t^- \,,$$

where $(N_t = (N_t^+, N_t^-))$ is a **Hawkes process** with stochastic intensity

$$\begin{pmatrix} h_t^+ \\ h_t^+ \end{pmatrix} = \begin{pmatrix} \mu^+ \\ \mu^- \end{pmatrix} + \int_{-\infty}^t \begin{pmatrix} \nu^{++}(t-u) & \nu^{+-}(t-u) \\ \nu^{-+}(t-u) & \nu^{--}(t-u) \end{pmatrix} \begin{pmatrix} dN_t^+ \\ dN_t^- \end{pmatrix} \,.$$

The base intensity $\mu = (\mu^+, \mu^-)$ represents the minimal intensity of two components, while the kernel ν handles their covariance structure. This model is able to reproduce the microstructure noise choosing an antidiagonal kernel: as a result, when the price jump upwards (downwards), i.e. N_t^+ (N_t^-) jumps, the downwards (upwards) intensity λ_t^- (λ_t^+) jumps as well, increasing the probability of a downward (upwards) jump of the stock price. This kind of Hawkes process are called cross exciting, since the activity of the two components are reciprocally activated. This model is able to reproduce efficiently volatility clusters, i.e. the persistence in time of period of high jump intensity. This key ingredient is provided by the convolution term $\int_{-\infty}^t \nu(t-u)dN_t$, that determines both the feedback effect of a price jump on the jump intensity, and how the stochastic intensity decays towards the base intensity μ. According to the choice of the kernel (usually exponential or power type), the influence of the past activity fades away slowly or quickly, determining big or small clusters of activity. One of the most elegant results are provided by the closed form for the signature plot and the long-run behavior, i.e. the functional convergence

$$\lim_{T \to \infty} \frac{P_{tT}}{\sqrt{T}} \overset{\mathcal{L}}{=} \sigma W_t \,, \quad t \in [0,1] \,,$$

where W_t is a Brownian motion whose volatility is known analytically. A non-parametric estimation procedure for the kernel shape is provided by [8], and some important generalization made this model extremely popular. The model can be extended in fact to the multivariate case, where multiple assets are mutually influenced by the kernel structure, which replaces the covariance structure of the diffusive Itô case. Once again, results for the large scale observations are available in closed form that gives the corresponding diffusive covariance starting from the point process kernel. Another generalization consists in linking the price process to the arrival or market orders to create a complex system of Hawkes process given by

$$\widehat{N}_t := \left(N_t^a, N_t^+, N_t^-, N_t^b \right) \,,$$

where (N_t^+, N_t^-) counts stock price upwards/downwards jumps, while (N_t^a, N_t^b) counts market orders arriving at the best ask/bid price: their intensity is given by

$$\begin{pmatrix} \widehat{\lambda}_t^+ \\ \widehat{h}_t^+ \\ \widehat{h}_t^- \\ \widehat{\lambda}_t^- \end{pmatrix} = \widehat{\mu} + \int_{-\infty}^t \widehat{\nu}(t-u)d\widehat{N}_t \,, \quad \widehat{\nu}(t) \in \mathbb{R}^{4 \times 4} \,.$$

This elegant approach has a major inconvenient in applications, because of its dimension. The only case where this system can be embedded in a Markov system is when the kernel is exponential, and in that case the dimension is (at least) 5 (the time dimension plus an extra one for each intensity).

The **marked point process** approach, given by [17], subordinates the price dynamic to the market order ones. In particular the stock price is given by

$$P_t = P_0 \exp \left(\sum_{i=1}^{M_t} \xi_i \right),$$

where $\xi_i > 0$ ($\xi_i < 0$) is the price shock corresponding to a single buy (sell) limit order, counted by (M_t): the latter can be a renewal process (as in [17]) and (ξ_i) an i.i.d sequence, but one can generalise this approach choosing a different model for (M_t), e.g. a self-existing point process, and give a more complex probabilistic structure to (ξ_i), e.g. a Markov chain. The exponential transformation guarantees the positiveness of the stock price, which cannot be achieved by arithmetic point processes, as the Hawkes one, but does not guarantee that the stock price moves on the tick grid.

To conclude this non-exhaustive list of examples, [25] proposes an entire **endogenous reconstruction of the price formation**, providing the dynamic of the first two levels of the limit order book (i.e. the best-ask and the best-bid). A couple of random variables models the liquidity offered on both levels, which is gradually consumed by market driven by general point processes. Every time the stock price jumps, the liquidity offered at the two best prices is reformed according to a new couple of random variables taking into account the natural imbalance of the two levels immediately after the jump: this reproduces the micro-structural mean reversion. Furthermore, several results are available for the asymptotic behaviour of the book, in particular for the long-run law of the stock price.

The market making problem

Market making is a non-directional trading strategy based on taking a profit from providing liquidity to the market. Sending two limit orders, one on the ask side and one on the bid one (not necessarily at the best quote), the market maker offers a liquidity that can be consumed on both sides. Assume that both limit orders have size N, and that the ask order is sent at A_t, while the bid one at B_t (notice that $A_t > B_t$). If both limit orders are fulfilled, the agent sells at A_t and buys at B_t a package of N lots, creating a profit of $N(A_t - B_t) > 0$, while her inventory is unchanged ($-N + N = 0$). **The market maker is rewarded for providing liquidity collecting several bid-ask spreads** during the trading day. We say that this strategy is non-directional, since the market maker is not interested following the market, but wants to be paid for the service she provides: on the contrary, she wants to be as market independent as possible, and in order to achieve this result, she has to control her inventory, avoiding large positions (both short and long) that would expose her to market risk (called **inventory risk**).

Market making is a continuous activity all along the day and electronic trading guarantees (almost) real time reaction to the market: orders are sent, cancelled, replaced or modified in a short amount of time by all the market makers. Since potential transactions are much more than in the classic (human) market, liquidity providers can tighten their spread and improve the market liquidity.

Trivial at first sight, market making is a complex trading activity, since, beyond the inventory one, there are hidden risks that the market maker takes on her shoulder. Since the liquidity risk decreases for liquidity takers in an electronic platform, this risk must be carried by someone else. Market makers are exposed in a subtle way: their orders are always likely to be executed in the least profitable way. When liquidity takers hit several times the ask (bid) side, market makers sell (buy) inventory, but since the market pressure pushes the price upwards (downwards), they sell (buy) an asset whose value is increasing (decreasing). This is an intrinsic property of the book, called **adverse selection**, and allows liquidity takers to transfer their risk to market makers by paying the spread: a general investor wanting to buy (sell) the asset, can either send a market order at the best ask (bid) price, or send a limit order at a lower (higher) price, decreasing her chances to be executed. Liquidity takers chose to send market orders, and pay to

get free of the risk of not being executed, while market makers chose to wait and risk a random execution in exchange of a small, but frequent reward.

Furthermore, the effect of inventory risk and adverse section combines. The market maker can accumulate, because of adverse selection, a huge long (short) position due to the downwards (upwards) market pressure. Suddenly, she has a large position she is averse to: in order not be exposed to inventory risk, she may decide to sell her liquidity cheaper to revert her inventory to 0. In this case, she suffers a double loss, the directional one due to adverse selection, and the one due the urgency of getting free of her new inventory, that would expose her to market risk. The intrinsic execution reward due to liquidity providing can be strongly mitigated, or in the worst case widely overcome, by adverse selection and inventory risk. That is why optimal control is necessary to reach a trade-off between liquidity providing and risk controlling. A standard (see [44]) approach consists in finding a market making strategy maximizing

$$ V_T - \eta \int_t^T Y_u^2 d\langle P \rangle_u \,, \quad \text{or } V_T - \eta Y_T^2 \,, \quad \text{or } \exp\left(-\eta\left(V_T\right)\right) \,, $$

where T is the trading horizon, while $\eta > 0$ is the subjective risk aversion controlling the portfolio variance. In both cases the portfolio mean performance is penalized by its variance: in the linear case the penalization is given either all along the trading day (the integral term) or at the horizon, but in both cases the variance control is equivalent to avoid large positions, which is exactly the source of the inventory risk. In the exponential case, the exponential utility function allows to reach a compromise between mean and variance: the variance and the inventory control are, in the end, the same thing. In the seminal paper of [6], the market maker is allowed to send (unitary) limit orders on both sides, and their probability of execution decreases with the distance from the mid-price. Other papers, as in [44], the agent sends limit orders only at the best levels. The choice depends essentially from the market. For assets with small ticks, the stock price can be assumed continuous, and because of the sparsity of the liquidity in the limit order book and the rounding error is relatively small, we assume that limit orders can be placed at any (real) distance from the mid-price. For large tick assets instead, the stock price is usually better described by point processes, and since liquidity is concentrated on the levels being closest to the mid price (often the first one), one can allow the market maker to send order at the existing best price only. In our work we will adopt both approaches, according to the type of asset we are dealing with (we will develop further details later).

The main difficulties in electronic trading application is, by far, providing analytic formulae for the optimal strategy. This is due to the intrinsic problem complexity, where several random processes come into play, making the problem dimension explode. Thanks to several variable changes, and asymptotic developments, some closed formulae are available, illustrating the interaction between the agent and the market components, and improving the financial interpretability of those results. The usual approach is to

◇ give the market model,

◇ define the agent admissible strategies,

◇ formulate the control problem in terms of maximization of an utility function,

◇ write the HJB equation associated to the control problem,

◇ simplify the HJB equation dimension thanks to multiple variable changes,

◇ solve numerically the remaining part.

Two out of three times, we will exploit the perturbation theory (see [11]) to provide an asymptotic expansion of the value function and the optimal controls in the risk aversion parameter. The risk aversion parameters allows the agent to control her inventory: we will prove that the value function of a risk neutral agent (no risk aversion) is independent of her current inventory.

This allows to reduce the problem dimension and access to analytic formula. When small risk aversion is introduced, the agent profile slightly changes, and deforms her value function and her optimal policy. This approach leads to much more explicit formulae, that are easier to understand and test in real algorithmic strategy.

Using $\exp\left(-\eta\left(V_T\right)\right)$ as terminal payoff (see e.g. [44], where the utility function is the exponential one), we would be able to capture the total risk associated to the agent position. Unfortunately, this kind of problem formulation represents an obstacle for tractability: using $V_T - \eta \int_t^T Y_u^2 d\langle P\rangle_u$ or $V_T - \eta Y_T^2$ (or combining the two approaches), since the payoff has a polynomial shape in the inventory, we can look for solutions, or approximations, of the same form, which would not be possible for a general utility function. For the exponential utility function, the case with no risk aversion ($\eta = 0$) has no sense, and perturbation methods becomes a hard path to follow. Furthermore, the choice of the integral or the terminal penalisation allows the agent to privilege one of the two different form of the inventory risk: the one associated to holding inventory during all the trading day and the one associated to the terminal inventory only. According to the agent profile, one penalisation can suit better than another, and in both cases its interpretation is straightforward, while the exponential utility function handles all the risks in a unique, elegant but somehow opaque form. Nevertheless, all of the three methods remain an excellent way to control both inventory and risk, which are intrinsically connected with each other, and the choice remains a matter of taste or (computational) convenience.

A panoramic of the different models and optimal policy results

Before detailing the content of our work, we would like to explain the reason of approaching the market making problem under different angles and with different models, reconstructing the *iter* that chains one paper to the following and comparing our results with the literature ones.

In Chapter 2, we follow the work of [6, 42] and generalise it to a class of assets from which we only know their expected incrementation and quadratic variation. In this framework, market maker limit orders are posted at both sides and at a certain (real, not discrete) distance from the mid price and executed at a rate decreasing with the limit order distance. For this kind of models, quotes are adjusted in real time to follow the mid-price dynamic, and the optimal bid-ask (agent) spread consists in a symmetric position with the respect to the stock price,

⋄ whose centre is translated by the market direction or by the necessity of reverting the inventory to zero,

⋄ while its width is increased by the level of risk (both objective, the market risk, and subjective, the agent risk aversion).

The problem of this model is that the rounding error on optimal quotes (that in real life must be on the tick grid) due to the discrete nature of the book has an important impact on strategies performance, especially on assets with large tick (i.e. where the tick size is large with respect to the standard volatility of the price arithmetic increments). Furthermore, the model has no market impact, since the probability of a limit order fulfilment does not depend on the recent price trend. Market impact and adverse selection can be added (see e.g. [23]) to this framework: however, we have preferred a different approach, focusing our work to a model where both the stock price and the agent bid-ask policy live on the tick grid.

Chapters 3 and 4, as in [44, 43], answer this need and deal with discrete value agent quotes. We define a semi-Markov model for the stock price, whose increments are driven by a Markov chain on $\{-1, +1\}$ with random inter-arrival times depending both on the departure and the arrival state. With a discrete mid-price living on the half-tick, orders can be systematically placed (or not, determining the agent policy) at the real best ask or best bid price. In this model, we show that adverse selection can be included (actually we describe two kinds of adverse selection), by correlating the execution with the price movements. The main result of these chapter is that, because of the micro-structural mean reversion, i.e. the mid-price repeated oscillation around a

theoretical fair price, the agent should not place order at the fair price level (we call it the weak side of the book) to protect herself against the inflation of transaction costs, and place limit orders mostly at one tick far from it (we call it the strong side),

⋄ unless her risk aversion forces to modify this strategy to revert her inventory to zero,

⋄ or the stock price has not moved for a rather long time (in the high-frequency trading scale), indicating a temporary stabilisation of the market.

Market making focuses on providing liquidity, and exploiting the bid-ask bouncing previously mentioned, these actors are rewarded for the service offered to the market. Liquidity strategies can be enriched and mixed with directional strategies, as shown in the Chapter 2, in order to have a complete strategy able to adapt itself to the market condition. Chapter 5 answers this need. This time the theoretical fair price previously described is the center of our framework, and a long-memory model describes its increments (either +1 or -1). This paper is a natural consequence of the long-memory of the market ([52]), which is reflected in the stock price (and in many other components). Thanks to huge database of market data, complex model can be estimated with care, and VLMC proposed in this paper offers an elegant solution to improve the semi-Markov setting previously mentioned. This analysis shows that the theoretical fair-price filters the high-frequency mean reversion and shows trend that can be captured by aggressive limit orders. So, once again, the market maker can exploit the mean-reversion of the stock price (which translated to a stability of the fair-price) with passive limit orders and be rewarded for her liquidity provision, plus she can follow the market with aggressive limit orders as soon as she has information on its trend.

We have provided a quick glance to the problems treated in this work, and underlined the importance of optimal control. The next sections are devoted to an overview of the four papers collected in this thesis, with a list of models and results.

1.2 Directional bets and the power of information in market making

We address the problem of optimal market making for assets with small tick. Even though market making is not a directional strategy per se, an agent detaining information on the future evolution of the stock price should be able to take advantage from it, and adapt her non-directional strategy. Most of the existing literature on market making assumes that the stock price is an undrifted Brownian motion, which simplifies the HJB equation and substantially implies that the optimal strategy is independent from the current mid-price. But what happens in the general case? And in particular, if the martingale dynamic is slightly deformed, how does it deform the market making optimal policy? And what about stochastic volatility? We will see that the agent information translate the agent spread centre in the market direction, creating a mix directional/market making strategy, while volatility widens the spread.

The market is made by an uncontrolled process, i.e. the stock price, which is assumed exogenous and independent from the agent strategy which does not impact them (small agent assumption), and the controlled ones, describing the agent portfolio and how her limit orders are matched.

The uncontrolled processes: the mid-price

We assume that $(t, P_t, \tilde{P}_t) =: (t, Z_t)$ is a Markov process, not necessarily continuous, where (P_t) is the stock price, while the vectorial process $(\tilde{P}_t)$ makes the triplet Markovian and independent from the arrival of market orders in the limit order book. We set to $\mathcal{L}$ the infinitesimal generator of (Z_t) and assume that $(P_t) \in \mathbb{R}$[1] admits finite moment generating function conditionally to

---

[1]The mid-price is not assumed to be positive, since in intraday high-frequency trading application, the initial price is nothing but a reference price.

its initial value. Its finiteness guarantees that the agent has a finite value function. The only assumption we made is that

$$\mathbb{E}_{t,z}\left[P_T\right] - p := \varepsilon(t, z)\,, \tag{1.2.1}$$

$$d\langle P\rangle_t := \sigma^2(t, Z_t)dt = \sigma_t^2 dt\,. \tag{1.2.2}$$

The controlled processes: the agent wealth and her inventory

We borrow the market framework from [6], where the agent places, continuously and on both sides, limit orders of unitary size at a certain distance $((\delta_\pm)_t) \in \mathbb{R}$ from the opposite best quotes, with the convention that $+/-$ refers to the ask/bid side. As in [6], we assume that orders placed at distance $\delta_\pm$ from the opposite market best policies are matched by two independent Cox processes having stochastic intensity $(\lambda_\pm)_t := Ae^{-k(\delta_\pm)t}$, for some $A, k \geq 0$. We assume that every transaction is subjected to a fixed cost φ. The goal of the agent is to find an optimal policy $((\delta_\pm)_t)$ maximizing the gain function (called $\mathbf{j}^{(\eta,\varepsilon)}$), i.e

$$\mathbf{u}^{(\eta,\varepsilon)}(t, x, y, z) := \max_{(\delta_\pm)_t}\mathbf{j}^{(\eta,\varepsilon)}(t, x, y, z; \delta_\pm)\,,$$

$$\mathbf{j}^{(\eta,\varepsilon)}(t, x, y, z; \delta_\pm) := \mathbb{E}_{t,x,y,z}\left[X_T\left[\delta_\pm\right] + Y_T\left[\delta_\pm\right]P_T - \eta\left(\beta Y_T^2\left[\delta_\pm\right] + \int_t^T Y_u^2\left[\delta_\pm\right]d\langle P\rangle_u\right)\right]\,,$$

where $[\delta_\pm]$ denotes the controlled process induced by the strategy between braces. **We emphasize the dependence on η (chosen by the agent) and ε (observed on the market), since we will explicitly show how, for small values, they deform the agent value function and her optimal policy**.

The explicit solution in the no risk aversion case

For $\eta = 0$, we are able to derive explicitly the value function and optimal controls:

$$\mathbf{u}^{(0,\varepsilon)} = \underbrace{x + y\mathbf{h}^{(\varepsilon)}}_{\textit{buy-and-hold}} + \underbrace{\mathbf{m}^{(\varepsilon)}}_{\textit{market-making}}\,,$$

$$\mathbf{h}^{(\varepsilon)}(t, z) := p + \varepsilon(t, z) = \mathbb{E}_{t,z}\left[P_T\right]\,,$$

$$\mathbf{m}^{(\varepsilon)}(t, z) := 2c\int_t^T \mathbb{E}_{t,z}\left[\cosh(k\varepsilon(u, P_u))\right]du\,, \quad c := \frac{A}{k}e^{-k(1/k+\varphi)}\,.$$

Furthermore, optimal controls are given by

$$\delta_\pm^{(0,\varepsilon)} := 1/k + \varphi \pm \varepsilon\,,$$

and can be alternatively expressed in terms of

$$\begin{aligned}\text{semi-width}^{(0,\varepsilon)} &:= 1/k + \varphi &= \text{semi-width}^{(0,0)}\,, \\ \text{center}^{(0,\varepsilon)} &:= p + \varepsilon &= \text{center}^{(0,0)} + \varepsilon.\end{aligned}$$

where semi-width$^{(\eta,\varepsilon)}$ and center$^{(\eta,\varepsilon)}$ are the semi-width and the centre of the agent spread. The controls $\delta_\pm^{(0,0)}$ are associated to an agent with no risk aversion and a stock price having $\varepsilon \equiv 0$, i.e. a martingale: in the general case, for $\eta = 0$, **the centre of the optimal spread is linearly impacted by the directional information provided by ε.** If $\varepsilon > 0$ (< 0), the agent estimates that a holding a long (short) position until T is profitable. In order to increase her chances to buy (sell) and decreases those to sell (buy), she entirely translates her spread of ε, becoming more aggressive on the bid (ask) and more passive on the opposite one. Thanks to this "spread shift", the agent reaches an optimal trade-off between anticipating the market and providing liquidity, creating a mixed directional/liquidity policy.

The perturbation approach for positive risk aversion

We extend the previous result to the case of (positive) small risk aversion. We prove that the value function is $O(\eta^2)$-approximated by

$$\mathbf{u}^{(\eta,\varepsilon)} \approx \widehat{\mathbf{u}}^{(\eta,\varepsilon)} := \mathbf{u}^{(0,\varepsilon)} - \eta \widehat{\mathbf{v}}^{(\varepsilon)},$$

where $\mathbf{u}^{(0,\varepsilon)}$ is the risk-neutral value function, $\mathbf{u}^{(\eta,\varepsilon)} - \widehat{\mathbf{u}}^{(\eta,\varepsilon)} \geq 0$, and the risk aversion deformation is approximated by $\widehat{\mathbf{v}}^{(\varepsilon)} = \widehat{\rho}_0 + 2y\widehat{\rho}_1 + y^2\widehat{\rho}_2 \geq 0$, where

$$\widehat{\rho}_2(t,z) = \beta + \mathbb{E}_{t,z}\left[\int_t^T d\langle P \rangle_u\right] \geq 0,$$

$\widehat{\rho}_1$ has probabilistic representation

$$\widehat{\rho}_1(t,z) = \mathbb{E}_{t,y=0,z}\left[\int_t^T Y_u\left[\delta_\pm^{(0,\varepsilon)}\right] d\langle P \rangle_u + \beta Y_T\left[\delta_\pm^{(0,\varepsilon)}\right]\right],$$

while $\widehat{\rho}_0$ is solution of

$$-\left(\partial_t + \mathcal{L}\right)\widehat{\rho}_0 - 2kc\left(\widehat{\rho}_2 \cosh(k\varepsilon) + \widehat{\rho}_1 \sinh(k\varepsilon)\right) = 0, \quad \rho_0(T,) = 0.$$

Furthermore, optimal controls are $O(\eta^2)$-approximated by

$$\delta_\pm^{(\eta,\varepsilon)} \approx \widehat{\delta}_\pm^{(\eta,\varepsilon)} := \delta_\pm^{(0,\varepsilon)} + \underbrace{\eta\left(\mp 2\widehat{\rho}_1 + (1 \mp 2y)\widehat{\rho}_2\right)}_{risk\ aversion}.$$

The introduction of the risk aversion has the effect of widening the agent spread of a multiple of η, so that a risk averse agent would adopt a more cautious policy. Widening the spread, the probability of being executed decreases, while the wealth deriving from a round trip execution increases. On the other side, the optimal agent spread centre is affect by $-2y\rho_2$, which adjusts the agent spread according to her position.

The special case of small information

The computation or the interpretation of $\widehat{\rho}_1$ may represent an obstacle for the determination of the optimal policies. The results obtained for small risk aversion can be improved, in terms of interpretability, assuming that $\varepsilon(t,z) \to 0$, i.e that the stock price is close to a martingale. This hypothesis is consistent with the non-arbitrage theory where the stock price, assuming that interest rates are zero, is a martingale, so that $\varepsilon \equiv 0$. We prove that for small risk aversions ($\eta \to 0^+$) and small martingale deviations ($\varepsilon \to 0$ point-wisely), the value function is approximated at the first order by

$$\widetilde{\mathbf{u}}^{(\eta,\varepsilon)} = \underbrace{x + yp + y\varepsilon}_{forward\ value} + \underbrace{\mathbf{m}^{(0)}\left(1 - \eta D\right)}_{market\ making} - \underbrace{\eta\widetilde{\rho}_2 y^2}_{inventory\ risk},$$

$$D(t,z) := k\left(\beta + \frac{1}{T-t}\mathbb{E}_{t,z}\left[\int_t^T \int_u^T d\langle P \rangle_\xi\right]\right) \geq 0.$$

Notice that the value function is discounted by the factor ηD, that penalizes the risk-neutral value function under the martingale regime. Another penalisation is provided by $\eta\widetilde{\rho}_2 y^2$, which has a bigger impact on exposed portfolios. Furthermore, optimal controls are approximated by

$$\delta_\pm^{(\eta,\varepsilon)} \approx \widetilde{\delta}_\pm^{(\eta,\varepsilon)} := \delta^{(0,0)} + \varepsilon + \eta\left(1 \mp 2y\right)\widetilde{\rho}_2,$$

or equivalently

$$
\begin{aligned}
\widetilde{\text{semi-width}}^{(\eta,\varepsilon)} &:= 1/k + \varphi + \eta\widetilde{\rho}_2 &= \widetilde{\text{semi-width}}^{(0,0)} + \eta\widetilde{\rho}_2 &= \widetilde{\text{semi-width}}^{(\eta,0)}, \\
\widetilde{\text{center}}^{(\eta,\varepsilon)} &:= p - 2\eta y\widetilde{\rho}_2 + \varepsilon &= \widetilde{\text{center}}^{(0,0)} + \varepsilon - 2\eta y\widetilde{\rho}_2 &= \widetilde{\text{center}}^{(\eta,0)} + \varepsilon.
\end{aligned}
$$

Notice that these controls are a linear deformation of $\delta^{(0,0)}$ both in ε and η. In particular the spread semi-width is impacted only by the risk-aversion, which, as in the previous case, widens the agent spread. The spread centre is translated by ε to follow the market direction and by $-2\eta y \widetilde{\rho}_2$ to avoid the inventory risk.

Conclusion and further developments

We have extended the work of [6] and understand how conditional information on the stock price affects the optimal market making. Thanks to perturbation techniques, closed-form formulae are available, that explains how information linearly translates the spread, while risk aversion widens it. This model is not suitable for large tick assets, where most of the liquidity is concentrated on the first level, which implies that the impact of rounding the $\mathbb{R}$-optimal quotes to the tick grid alters the agent performance. In what follows, will study the large tick asset case, introducing a simple model for the stock price using point processes, and giving a market making application complementing these results.

1.3 Semi Markov model for market microstructure

For large tick assets, the stock price cannot be assumed continuous anymore, and point processes replaces Itô diffusion. This approach is general, and suitable for small tick assets as well. We use a Markov renewal process (MRP) to describe the random sequence (T_n, J_n). Markov renewal theory [53] is largely studied in reliability for describing failure of systems and machines, and one purpose is to show how it can be applied to market micro-structure. By considering a suitable Markov chain modeling for (J_n), we are able to reproduce the mean-reversion of price returns, while allowing arbitrary jump size, i.e. the price can jump of more than one tick. On the other hand, the counting process (N_t), which may depend on the Markov chain, models the jump activity, and in particular the alternation of high and low activity phases. Finally, MRPs ensure a Brownian motion behavior of the price process at macroscopic scales, which is consistent with the classic diffusive approach in the case of daily observations. Our MRP model is a rather simple but robust model, easy to understand, simulate and estimate, both parametrically and non-parametrically. An important feature of the MRP approach is the semi-Markov property: the price process can be embedded into a Markov system with few additional and observable state variables, ensuring the tractability of the model for applications to market making and statistical arbitrage. We underline that one of our main prerogative is to provide a model involving only observable variables, so that non-parametric estimation is easy and no optimization routine is necessary (as in [19] e.g.), which is a common issue when hidden components are present. MRPs are powerful tools to model the dependence between jump timestamps and marks, dependence which is empirically shown (and theoretically supported by [25]), and for which an explanation relying on the nature of the LOB is provided.

Data sample

The used database is the EURIBOR 3M future (front contract) quoted on the LIFFE electronic platform (London), from 2010-01-04 to 2010-12-31, observed every day from 10:00 to 14:00 London time. Since the bid-ask spread is 99% of the time equal to one tick, this corresponds to most of the observations.

We describe the tick-by-tick fluctuation of a univariate stock price by means of a marked point process $(T_n, J_n)_{n\in\mathbb{N}}$. The increasing sequence (T_n) represents the jump (tick) times of the asset price, while the marks sequence (J_n) valued in the finite set $E = \{+1, -1, \ldots, +m, -m\} \subset \mathbb{Z} \setminus \{0\}$, represents the price increments, where positive (negative) marks stands for upwards (downwards) jumps.

Here, we have normalized the tick size to 1. We write the price arithmetic returns as $J_n =$

$\widehat{J}_n \xi_n$, where $\widehat{J}_n := \text{sign}(J_n)$ valued in $\{+1, -1\}$ is an irreducible Markov chain with probability transition matrix

$$\widehat{Q} = \left(\begin{array}{cc} \frac{1+\alpha}{2} & \frac{1-\alpha}{2} \\ \frac{1-\alpha}{2} & \frac{1+\alpha}{2} \end{array} \right), \quad \alpha = \text{corr}_\pi \left(\widehat{J}_n, \widehat{J}_{n-1} \right),$$

(we impose $\alpha \neq 1$ to guarantee the Markov chain irreducibility) while (ξ_n) is an i.i.d. sequence valued in $\{1, \ldots, m\}$, independent of $(\widehat{J}_n)$, with distribution law: $p_i = \mathbb{P}\left[\xi_n = i\right] \in (0, 1)$, $i = 1, \ldots, m$. On the given database, $\alpha \approx -85\%$, which is equivalent to a high level of mean reversion due to a very large tick.

We assume that conditionally on the jump marks (J_n), (S_n) is an independent sequence of positive random times, with distribution depending on the current and next jump mark:

$$F_{ij}(t) = P[S_{n+1} \leq t | J_n = i, J_{n+1} = j], \quad (i, j) \in E.$$

Here, we allow in general dependency between jump marks and renewal times, and we refer to the symmetric case when F_{ij} depends only on the sign of ij, by setting

$$F_+(t) = F_{ij}(t), ij > 0, \quad F_-(t) = F_{ij}(t), ij < 0.$$

In other words, F_+ (F_-) is the distribution function of inter-arrival times given two consecutive jumps in the same (opposite) direction, called trend (mean-reverting) case. The hazard function associated to the MRP is given by

$$h_{ij}(t) := p_j \left(\frac{1 + \text{sign}(ij)\alpha}{2} \right) \frac{f_{\text{sign}(ij)}(t)}{1 - F(t)}, \quad F(t) := \frac{1+\alpha}{2} F_+(t) + \frac{1-\alpha}{2} F_-(t),$$

that describes the instantaneous jump activity. We analyse the parametric and the non-parametric estimation procedures for $F_\pm$ and $h_\pm$: empirical evidences suggest that the hazard function is a decreasing function of the elapsed time since the last jump of the stock price, which can be translated in high activity immediately after a jump, decaying while the stock price is unchanged.

Scaling limit

We now characterize the large scale limit of the price process constructed from our Markov renewal model. We assume that the mean sojourn time μ is finite. By classical regenerative arguments, it is known (see [40]) that the Markov renewal process obeys a strong law of large numbers, which means the long run stability of price process:

$$\lim_{t \to \infty} \frac{P_t}{t} = 0, \quad \text{a.s.}.$$

We next define the normalized price process:

$$P_t^{(T)} = \frac{P_{tT}}{\sqrt{T}}, \quad t \in [0, 1],$$

and address the macroscopic limit of $P^{(T)}$ at large scale limit $T \to \infty$. From the functional central limit theorem for Markov renewal process, we obtain

$$\lim_{T \to \infty} P^{(T)} \stackrel{(d)}{=} \sigma_\infty W, \quad \sigma_\infty^2 := \frac{1}{\bar{\mu}} \left[\text{Var}(\xi_n) + \mathbb{E}[\xi_n]^2 \frac{1+\alpha}{1-\alpha} \right],$$

where $W = (W_t)_{t \in [0,1]}$ is a standard Brownian motion, and σ_∞ its macroscopic variance.

Mean Signature plot

We are able to provide by our Markov renewal model a quantitative justification of the signature plot effect, described in the introduction. We consider the symmetric and stationary case, i.e.:
(H) (N_t) is a delayed renewal process: for $n \geq 1$, S_n has distribution function F (independent of i, j), with finite mean $\bar{\mu} < \infty$, and finite second moment, and S_1 has a distribution with density $(1 - F(t))/\bar{\mu}$.

It is known that the process N is stationary under **(H)** (see [28]), and so the price process is also stationary under the stationary probability P_π, i.e. the distribution of $P_{t+\tau} - P_t$ does not depend on t but only on increment time τ. In this case, the empirical mean signature plot is written as $(P_0 = 0)$:

$$\bar{\mathcal{V}}(\tau) := \frac{1}{T} \sum_{i\tau \leq T} \mathbb{E}_\pi \left[\left(P_{i\tau} - P_{(i-1)\tau} \right)^2 \right] = \frac{1}{\tau} \mathbb{E}_\pi \left[P_\tau^2 \right] .$$

Notice that if $P_t = \sigma W_t$, where W_t is a Brownian motion, then $\bar{\mathcal{V}}$ is a flat function: $\bar{\mathcal{V}}(\tau) = \sigma^2$, while it is well known that on real data $\bar{\mathcal{V}}$ is a decreasing function on τ with finite limit when $\tau \to \infty$. This is mainly due to the anti-correlation of returns: on a short time-step the signature plot captures fluctuations due to returns that, on a longer time-steps, mutually cancel. We obtain the closed-form expression for the mean signature plot, and give some qualitative properties about the impact of price returns autocorrelation. Under **(H)**, we prove that

$$\bar{\mathcal{V}}(\tau) = \sigma_\infty^2 + \left(\frac{-2\alpha(\mathbb{E}[\xi_n])^2}{1 - \alpha} \right) \frac{1 - G_\alpha(\tau)}{(1 - \alpha)\tau} ,$$

where σ_∞^2 is the macroscopic variance and $G_\alpha(t) := \mathbb{E}[\alpha^{N_t}]$ is given via its Laplace-Stieltjes transform:

$$\widehat{G}_\alpha(s) = 1 - \frac{1}{\bar{\mu}}(1 - \alpha) \frac{1 - \widehat{F}(s)}{s(1 - \alpha\widehat{F}(s))} , \quad \alpha \neq 0 , \quad \widehat{F}(s) := \int_{0^-}^\infty e^{-st} dF(t) .$$

The term σ_∞^2 equal to the limit of the mean signature plot when time step observation τ goes to infinity, corresponds to the macroscopic variance, and $\bar{\mathcal{V}}(0^+) = \frac{1}{\bar{\mu}} \mathbb{E}[\xi_n^2]$ is the micro-structural variance. Notice that while σ_∞^2 increases with the price returns autocorrelation α, the limiting term $\bar{\mathcal{V}}(0^+)$ does not depend on α, and the mean signature plot is flat if and only if price returns are independent, i.e. $\alpha = 0$. In the case of mean-reversion $(\alpha < 0)$, $\bar{\mathcal{V}}(0^+) > \sigma_\infty^2$, while in the trend case $(\alpha > 0)$, we have: $\bar{\mathcal{V}}(0^+) < \sigma_\infty^2$.

Conclusion and further developments

Having in mind a direct application purpose, we decided to sacrifice the autocorrelation of inter-arrival times in order to have a fast and simple non-parametric estimation, perfect simulation and the suitable setup for a market making application, presented afterwards in this work.

Aware of the model limits, and with an eye to statistical arbitrage, the next step is to extend the structure of the counting process (N_t), for example to Hawkes process, to have a better fit, and the structure of the Markov chain (J_n) to a longer memory binary processes, able to recognize patterns, which will be treated later as well.

1.4 HFT and asymptotics for small risk aversion in a Markov renewal model

We study an optimal high frequency trading problem for large tick assets, using a market micro-structure model reaching a good compromise between accuracy and tractability. The stock price is driven by a Markov Renewal Process (MRP), as previously described, while market orders arrive in the limit order book via a point process correlated with the stock price itself.

Data sample

Market data are taken from tick-by-tick observation of the 3-month future EUROSTOXX50, on February 2011, from 09:00:000 to 17:00:00.000 (CET).

The stock price

We shall rely on the previous section (see also [36]), where we show how Markov Renewal processes are an extremely flexible and pertinent tool to model the stock price at high frequency, as well as easy to estimate, simulate and understand. **We assume that the bid-ask spread is constantly one tick and the stock price jumps of one tick**, which is consistent with liquid large tick assets.

By modeling the stock price by a pure jump process, we are able to introduce probabilistic and mechanical dependences between the price evolution and the trades arrival. We can easily introduce correlation between the next price jump and proportion of ask/bid trades before the next jump, as well as the jump risk. In the context of option pricing, jumps represent a source of market incompleteness, leading to unhedgeable claims: similarly, jumps of the stock price in the electronic market are a real source of risk for the market maker. More precisely, the agent faces two kind of risk due to the stock price jump.

  i) *Market risk:* when the price suddenly jumps, the whole agent inventory is re-evaluated, changing the portfolio value in no time (i.e. a finite amount of risk in no time, whereas the Brownian motion has quadratic variation proportional to the interval length).

 ii) *Adverse selection risk:* in our model, we assume that an upwards (downwards) jump at time t corresponds to a big market order clearing the liquidity on the best ask (bid) price level. If the agent posts a **small** limit order, say on the bid side, the latter has to be executed, since (we guess that) the goal of the big market order was to clear all the available liquidity rather than consuming a fixed amount of it. In this sense, the agent does not affect the market dynamics. In this scenario, the agent is systematically penalized, since she sells liquidity at t_- for less than its value at t. This risk, known as **adverse selection**, can and will be incorporated, measured and hedged, thanks to our market model.

Market order flow modeling and adverse selection

We introduce a suitable modeling of the market order flow, taking into account the real dependence with the stock price dynamics. **Our model is price rather than trade centered**, since we assume that trades (no matter their side) are counted by a Cox process subordinated to the stock price. Trades arrive more frequently after a price jump, while their arrival rate decreases as the price stabilizes. In this sense, events have a much richer dynamic than a Poisson process, and they are not independent from the stock price, as often assumed. We focus on small market orders that we model by a marked point process (θ_n, Z_n).

  i) *Timestamps:* the increasing sequence (θ_n) represents the arrival timestamps of (small) market orders.

 ii) *Marks:* the marks $(Z_n) \in \{-1, +1\}$, represent the side of the exchange, with the convention that when $Z_n = -1(+1)$, the trade is exchanged at the best bid (ask) price, i.e. market sell (buy) order has arrived.

We do not take into account the size of trades. On one hand, we assume that the counting process (M_t) associated to (θ_n) is a Cox process with conditional intensity $\lambda(S_t)$, where S_t is the time spent since the last price jump. On the other hand, we assume that market order trade and stock price in the LOB are correlated via the relation:

$$Z_n := \Gamma_n I_{\theta_n-},$$

where $\Gamma \equiv (\Gamma_n)$ is an i.i.d. sequence, independent of all other processes, and distributed according to a Bernoulli law on $\{-1, +1\}$ with parameter $(1 + \rho)/2$, with $\rho \in (-1, 1)$, where $\rho = \mathrm{Corr}(Z_n, I_{\theta_n^-})$. We define the concordant $(+)$ and discordant $(-)$ trade intensity as

$$\lambda_\pm(s) := \left(\frac{1 \pm \rho}{2}\right) \lambda(s), \quad s \geq 0.$$

This definition is consistent with the one of $h_\pm(s)$, where $\pm$ indexes the concordance $(+)$ or discordance $(-)$ of two consecutive jumps. Estimation on real data leads to a value of ρ around -50%. This means that about 3 over 4 trades arrive on the weak side of the limit order book. Adding marks (determining the trade exchange side) to the Cox process counting the trade events, we are able to reproduce the *adverse selection* risk appearing in a weak and strong form, the first limiting the agent profit, the second penalizing it, forcing the agent to play a less aggressive policy.

i) *Weak adverse selection:* it comes from the small trades flow, made of those trades that are unable to move the market stock price. For this flow, a limit order is more likely to be matched on the less profitable side: if the price is likely to jump downwards (upwards), few trades would arrive at the best ask (bid) price, limiting the chances of building a short (long) position (that would be profitable w.r.t. to the market direction). Thanks to this feature, the extra gain (w.r.t. to a market order) due to a limit order execution is compensated by an unfavorable execution probability.

ii) *Strong adverse selection:* differently from the weak adverse selection risk, the strong one comes from big trades affecting immediately the stock price. We assume that a limit order is automatically executed as soon as the stock price jumps over the corresponding level, i.e., for an order at the best ask (bid), when the price jumps upwards (downwards). In this scenario, the agent systematically loses, beyond the transaction cost, half-a-tick w.r.t. to the new mid-price. Making the stock price change its value, big trades put the market maker in a bad position, since the sudden execution forces her to sell liquidity at less than its current value.

The market making problem

The agent strategy consists in placing continuously limit orders of constant small size $L \in \mathbb{N} \backslash (0)$, (where small is meant w.r.t. to the total liquidity provided by all the market makers) on both sides, and at the best price available. The market making strategy is then described by a pair of predictable processes $(\ell_+, \ell_-)_t$ valued in $\{0, 1\}$. When $\ell_+ = 1$ $(\ell_- = 1)$, a limit order of size L is posted at time t on the strong (weak) side, while in the opposite case no limit order is submitted or the limit order is cancelled. We denote by $\mathcal{A}$ the set of market making controls $\boldsymbol{\ell} = (\ell_+, \ell_-)$.

Every time a small market order arrives in the limit order book, if the agent has placed an order on the corresponding side, the latter is executed according to a random variable. We consider the distributions

$$\vartheta_\pm(dk, L) \text{ on } \{0, \ldots, L\}, \quad \Phi_\pm^m(L) := \int k^m \vartheta_\pm(dk, L), \quad m = 1, 2,$$

where $\vartheta_-(dk, L)$ $(\vartheta_+(dk, L))$ is the distribution of the executed quantity of limit order of size L in the concordant (discordant), i.e. strong (weak) side, of the limit order book.

Finally, the value function associated to the market making problem is

$$\mathbf{u}^{(\eta)}(t, p, i, s, x, y) := \max_{\boldsymbol{\ell} \in \mathcal{A}} \mathbb{E}_{t,p,i,s,x,y}\left[V_T - \eta Y_T^2\right].$$

The no risk aversion case

In the special case where $\eta = 0$, we prove that

$$\mathbf{u}^{(0)} = \mathbf{u}_{hold} + \mathbf{u}_{mm} \,,$$
$$\mathbf{u}_{hold}(t, p, i, s, x, y) = x + yp + iy\theta(t, s) \,, \quad \mathbf{u}_{mm}(t, s) = \omega(t, s) \geq 0 \,,$$

with $\omega(t, s)$ is the unique bounded viscosity solution to

$$-\frac{\partial \omega}{\partial t} - \frac{\partial \omega}{\partial s} - \sigma^2(s) \Delta \omega(t, 0) - \sum_{\nu \in \pm} \max\left(G_\nu(t, s), 0\right) = 0 \,, \quad \omega(T,) = 0 \,,$$

$$G_\pm(t, s) := \lambda_\pm(s)\left(\delta - \varphi \mp \theta(t, s)\right) \Phi_\pm^1(L) - h_\pm(s)\left(\delta + \varphi + \theta(t, 0)\right) L \,,$$
$$\sigma^2(s) := h_+(s) + h_-(s) \,,$$

and probabilistic representation

$$\omega(t, s) = \sum_{\nu \in \pm} \mathbb{E}_{t,s}\left[\int_t^T \max\left(G_\nu(u, S_u), 0\right) du\right] \,.$$

Moreover, the optimal controls are given in feedback form by:

$$\hat{\ell}_\pm^{(0)}(t, s) = \mathbb{1}\{G_\pm(t, s) > 0\} \,.$$

Optimal controls are naturally decomposed into

$$G_\pm(t, s) = G_\pm^{\mathrm{trd}}(t, s) - G_\pm^{\mathrm{jmp}}(t, s)$$
$$:= \lambda_\pm(s)\left(\delta - \varphi \mp \theta(t, s)\right) \Phi_\pm^1(L) - h_\pm(s)\left(\delta + \varphi + \theta(t, 0)\right) L \,.$$

i) The **trade part** $G_\pm^{\mathrm{trd}}$: the agent orders are matched by small market orders (not impact-ing the stock price) of random size, distributed according to $\vartheta_\pm(dk, L)$, arriving at rate $\lambda_\pm(s)(S_t)$. For each executed lot she gains the half-spread thanks to passive execution (market making gain), she loses the transaction costs, and since her inventory changes, she loses the martingale distance $\theta(t, s)$ that she would gain (in average) keeping her position until the horizon (attention: this quantity might be negative). This scenario is favourable for the agent, since she has the time to close her spread before the stock price jumps again and she has gained half a tick w.r.t. to the mid-price evaluation of the stock: this profit comes from small uninformed traders, that are unable to make the stock price jump and need the liquidity provided by the market maker.

ii) The **jump part** $G_\pm^{\mathrm{jmp}}$: the agent orders are cleared (fulfilled) at rate $h_\pm(S_t)$ by big market orders impacting the stock price. As before, for each executed lot, she gains the half-spread thanks to passive execution (market making gain), but loses a spread because of the stock price jumps, ending with a passive of half a spread, she loses the transaction costs, and since her inventory changes, she loses the martingale distance $\theta(t, 0)$ (the price has just jumped). We prove that

$$h_\pm(s)\left(\delta + \varphi + \theta(t, 0)\right) \geq 0 \,,$$

which implies that the limit order execution due to big orders is a source of risk for the agent, called **strong adverse selection**. This is due to the fact that large market orders makes the price jump, and thus do not allow the agent to close her spread. On the contrary, the agent finds herself buying/selling L lots (the maximum admissible size) when the stock price is suddenly decreasing/increasing value.

We have that $\hat{\ell}_\pm^{(0)}(t,s)$ converges for large horizon to the stationary value:

$$\lim_{T\to\infty} \hat{\ell}_\pm^{(0)}(t,s) = \mathbb{1}\{\bar{G}_\pm(s) > 0\}\,,$$

$$\bar{G}_\pm(s) := \lambda_\pm(s)\left(\delta - \varphi \mp \bar{\theta}(s)\right)\Phi_\pm^1(L) - h_\pm(s)\left(\delta + \varphi + \bar{\theta}(0)\right)L\,,$$

$$\bar{\theta}(s) := \lim_{T\to\infty} \theta(t,s) = \frac{\bar{\alpha}(s)}{1-\alpha}\,, \quad \bar{\alpha}(s) := \sum_{\nu\in\pm} \nu\left(\frac{1+\nu\alpha}{2}\right)\left(\frac{1-F_\nu(s)}{1-F(s)}\right)\,.$$

The small risk aversion case

We first give the exact solution of the problem in terms of a non-explicit deformation of the $(\eta = 0)$-value function, that one can evaluate numerically if not wanting to involve approximation arguments. This result will help us to illustrate, in terms of probabilistic representation, how a particular strategy affects the value function. We prove that the value function is

$$\mathbf{u}^{(\eta)} := \mathbf{u}^{(0)} - \mathbf{v}^{(\eta)}\,,$$

where $\mathbf{u}^{(0)}(t,p,i,s,x,y)$ is the solution of the control problem in the no risk aversion case, while $\mathbf{v}^{(\eta)}(t,s,q := iy)$ is nonnegative and the unique viscosity solution with quadratic growth in q of a certain PDE, while optimal controls are given in feedback form by in terms of the value function.

The deformation function $\mathbf{v}^{(\eta)}$ due to risk aversion is solution to a certain semi-linear PDE, which can be solved numerically. We use instead a perturbation approach for deriving a first-order expansion of $\mathbf{v}^{(\eta)}$ for small risk aversion η, that proves that the function $\mathbf{v}^{(\eta)}(t,s,q)$ can be linearly approximated in $\eta > 0$ by

$$\mathbf{v}^{(\eta)}(t,s,q) = \eta\left(q^2 + 2q\zeta_1(t,s) + \zeta_0(t,s)\right) - \mathbf{R}^{(\eta)}(t,s,q)\,, \tag{1.4.1}$$

where

i) $\zeta_1(t,s)$ is expressed as

$$\zeta_1(t,s) := \mathbb{E}\left[\hat{Y}_T\big|S_{t-} = s, I_{t-} = +, Y_{t-} = 0\right]\,,$$

where $(\hat{Y}_t)$ is the inventory process controlled by the optimal strategy for $\eta = 0$;

ii) $\zeta_0(t,s)$ is the viscosity solution of

$$-\frac{\partial \zeta_0}{\partial t} - \frac{\partial \zeta_0}{\partial s} - \sigma^2(s)\Delta\zeta_0(t,0)$$

$$-\sum_{\nu\in\pm}\left(h_\nu(s)\left(L^2 - 2L\zeta_1(t,0)\right) + \lambda_\nu(s)\left(\Phi_\nu^2(L) - 2\nu\Phi_\nu^1(L)\zeta_1(t,s)\right)\right)\hat{\ell}_\nu^{(0)}(t,s) = 0\,,$$

$$\zeta_0(T,) = 0\,;$$

iii) the remainder $\mathbf{R}^{(\eta)}(t,s,q)$ is a non-negative $o(\eta)$.

Furthermore, we get an approximate optimal limit order control given by

$$\widetilde{\ell}_\pm^{(\eta)}(t,s) := \mathbb{1}\{G_\pm(t,s) > \langle \mathcal{C}_\pm, \widetilde{\mathbf{v}}^{(\eta)}\rangle\}\,,$$

$$\langle \mathcal{C}_\pm, \mathfrak{g}\rangle := h_\pm(s)\left(\mathfrak{g}(t,0,\pm q - L) - \mathfrak{g}(t,0,\pm q)\right) + \lambda_\pm(s)\int \Delta\mathfrak{g}(t,s,q\mp k)\vartheta_\pm(dk,L)\,,$$

and the approximate optimal feedback control can be rewritten as

$$\widetilde{\ell}_\pm^{(\eta)}(t,s) := \mathbb{1}\{G_\pm(t,s) > \eta\left(\mathbf{C}_\pm^0(t,s) \mp 2q\mathbf{C}_\pm^1(t,s)\right)\}\,,$$

$$\mathbf{C}_\pm^0(t,s) := h_\pm(s)\left(L^2 - 2L\zeta_1(t,0)\right) + \lambda_\pm(s)\left(\Phi_\pm^2(L) \mp 2\Phi_\pm^1(L)\zeta_1(t,s)\right)\,,$$

$$\mathbf{C}_\pm^1(t,s) := h_\pm(s)L + \lambda_\pm(s)\Phi_\pm^1(L) \geq 0\,.$$

The control adjustment due to risk aversion can be understood as follows.

i) The **inventory independent part** in affects the agent strategy even when her inventory is $q = y = 0$: in the no risk aversion case, the agent places a limit order if $G_\nu(t, s) > 0$, but when $\eta > 0$, this trading barrier - depending on the couple (t, s) - is raised by a multiple of the risk aversion itself. The agent becomes cautious and decides to enter the market only in the most profitable cases, but renounces to trade if expected gain is small, even if positive. This result is shown by Figure 4.8, where the non trading region for $q = 0$ grows w.r.t. the case $\eta = 0$, reflecting the increased trading aversion of the agent.

ii) The **linear part in the inventory** is in charge of controlling the absolute value of the inventory, in order to reduce the exposure of the agent to inventory and market risk. For $q = iy > 0$, the adjustment of the strong side (weak side) turns the trading barrier down (up) by a multiple of η: the agent decides to trade on the strong (weak) side under less (more) restrictive conditions in order to reduce (not to increase) her absolute inventory. This result is summarized by the summarised by the stationary control, where for large values of the inventory the agent plays, independently on s, on one side only, in order to revert the absolute position to a smaller value.

Conclusion and further developments

We have exploited the MRP framework previously described in order to provide an application to a market making problem. Thanks to a Cox model, we are able to include the matching engine and complete the order book model of the best levels: only small trades are described directly, while big market orders affecting the stock price are included in the stock price dynamics itself. The perturbation technique adopted to derive optimal controls as a deformation of the no risk aversion case has helped us to improve financial interpretability and reduce the dimension problem as well as the computational cost of its numerical solution. For further developments, more complicated stock price model can introduce statistical arbitrage opportunity, that we may capture by means of optimal control techniques.

1.5 Long memory patterns in high-frequency trading

We present a long memory model, based on marked point processes, which describes the stock price in the limit order book: its marks are driven by a VLMC (an efficient modeling of high-order Markov chains), while the inter-arrival times (between two consecutive jumps of the price) are represented by a self-exciting and independent univariate Hawkes process. Instead of modeling directly the mid-price, we introduce the fair price process, with the intent to reduce the micro-structure noise and represent the fundamental value of the asset: empirical evidences show that micro-structural trends, a source of statistical arbitrage, emerge after noise reduction. The agent participates to the market both via impulsive (pseudo) market orders and limit orders, whose execution is modeled by Cox processes. Once the system is embedded into a Markovian one, we illustrate a trading algorithm based on optimal control techniques: we reduce the complex HJB equation associated to the problem to a simple system of variational ODE's, for which an explicit Euler scheme gives a computationally non-expensive solution. Finally, Monte Carlo simulations show that the VLMC strategy over-performs the benchmark of a uninformed agent modeling the fair price as a simple Markov chain.

We address a **high-frequency trader wanting to detect short-term patterns of the stock price, controlling the market risk associated to her portfolio**. We work with liquid large tick assets (see [31] for a rigorous quantitative definition), where the price jumps and the bid-ask spread are unitary.

The fair price

It is well-known that the mid-price is subjected to micro-structural mean-reversion: as pointed out by the empirical literature (e.g. [36], [25] and [60]), at least on a big class of assets having large tick ([31]), two consecutive jumps of the mid-price are often in opposite directions. Consequently, **multiple jumps in the opposite direction clear themselves and do not affect the fundamental value of the asset**. We define, for a mid-price jumping at (T_n^M) of (J_n^M) such that $M_{T_n} = M_n$,

$$P_n := M_n - \frac{1}{2}\text{sgn}\left(J_n^M\right), \quad k \in \mathbb{N}^*.$$

and extract from (T_n^M) the subsequence of (T_n) such that $P_n \neq P_{n-1}$. Notice that (P_t) jumps if and only if (M_t) does it twice consecutively in the same direction, while it is stable under noise reversion (see Figure 5.3). We choose (P_t) as the new reference price instead of the mid-oine. We assume that (N_t) and (J_n) are independent. Getting free of the mutual dependence allows to use more complex models and describe **long memory patterns for both** (N_t) **and** (J_n). Since (see Figure 5.5) **inter-arrival times exhibit strong positive autocorrelation**: a natural candidate to model (N_t) is thus a univariate Hawkes self-exciting process with intensity

$$h_t := \mu_t + \alpha \sum_{T_i < t} \exp(-\beta(t - T_i)),$$

where μ_t reproduces the typical U-shaped intraday seasonality.

Marks exhibit positive auto-correlation: most of the literature focuses on the short-term mean-reversion, but the latter seems to vanish once we pass from the mid-price price to the fair one, while trends emerge: these trends are caused by the strong positive autocorrelation of trade sides, mostly due to splitting of meta-orders. **Our goal is to perform an arbitrage of these trends**, hedging against fees and market risk.

Since more than 99% of the price jumps are of the same size of the tick, we can assume that $|J_n| = 1$ a.s., and $J_n = J_{n-1}U_n$, for $k \in \mathbb{N}^*$ and $(U_n) \in \{-1, +1\}$. We assume that (U_n) is a stationary Variable Length Markov Chain (VLMC) of finite memory whose dynamic of (U_n) is given by

i) a satured tree with alphabet $E \in \{-1, +1\}$, whose leaves (terminal nodes) are called "contexts" and form a set denoted by $\mathbb{C}$;

ii) a family of probability $\{\wp_\pm(c)\}_{c \in \mathbb{C}}$, such that for every u right infinite word on E

$$\mathbb{P}\left[U_0 = \pm \middle| U_{-1}U_{-2}\cdots = u\right] = \frac{1 \pm \alpha(\pi(u))}{2}, \quad \pi : \prod_{k=1}^{\infty} E^{(k)} = E^{\mathbb{N}^*} \to \mathbb{C},$$

where π is the context function associated to the tree, mapping the right infinite sequence u to the only context $c := \pi(u)$ being prefix of u.

Unfortunately, a VLMC cannot be directly embedded in a Markov chain on its context set $\mathbb{C}$. We prove that the VLMC tree can be properly grown without altering the induced probabilistic structure in such a way that the Markov embedding and dynamic programming are possible. From now, on, we assume that (U_n) is embedded in a Markov chain on its context set $\mathbb{C}$, so that, for all $u \in \mathbb{C}$, $\pi(+u)$ and $\pi(-u)$ is well defined, where $\pm u$ indicates the word starting with $\pm$ and continuing with u.

The agent strategy

We divide limit orders into level-0 and level-1 limit orders.

A level-0 limit order is sent at the fair price level: its price either coincides with the best price, or improves the existing best quotes, in which case, since the spread is unitary, it is immediately converted to a market order and executed. Notice that, if the price reverts, the order is necessarily filled before the reversion and, since reversions are frequent for large tick assets (see [36]), a first approximation is to consider level-0 limit orders as (pseudo) market orders, filled with probability $\delta \in [0, 1]$. In order to prevent the agent to affect the exogenous dynamic of the price, i.e. to limit her market impact, and to make impulsive control easier, an admissible policy will allow only $n \in \mathbb{N}$ pseudo market orders per fair price jump. We denote by

⋄ (θ_j, m_j) the sequence of timestamps θ_j at which the agent sends a level-0 limit order of size $|m_j| \in \mathbb{N}$, where if $I_{\theta_{j_-}} m_j > 0 \ (< 0)$, the order of buy (sell) type.

⋄ (K_t) the process counting the number of level-0 limit orders since the last fair price jump: notice that (K_t) increments of 1 when the agent sends an order, while jumps to 0 at each fair price jump.

A level-1 limit order is sent at the fair price level ± 1 **tick**, $+1 \ (-1)$ for sell (buy) limit orders: they are used to gain an extra tick thanks to the execution, as in the market making case, when no statistical pattern is known, or simply to improve the performance. We assume that the agent sends orders of small size, that are entirely filled at a random time given by the first jump of a Cox process having conditional intensity w.r.t. to the current context c

$$h_t \lambda \frac{1 \pm I_t \alpha(c)}{2}, \quad \text{on the ASK/BID side},$$

where $\lambda \geq 0$ is non-negative constant. Notice that the total intensity on both sides is $h_t \lambda$, which does not depend on the current context, while the coefficient $\frac{1 \pm I_t \alpha(c)}{2}$ tells that if the price is likely to jump in a certain direction, the same imbalance are reflected in the agent execution, adding **adverse selection** to the model, since an order is more likely to be executed if the price is going in the same direction.

The optimal trading problem

We assume that the agent admissible controls are given by $((\ell_t), (I_j)) \in \mathbb{A}$, where

⋄ $\ell_t := (\ell_+, \ell_-)_t$ is a continuously controlled process in $\mathbb{L} := \{0, \dots, L\}$, predictable w.r.t. $\mathbb{F}_t$ (the market filtration), where $\ell_{\pm I_{t_-}}$ represents the agent level-1 position at time t on the ask $(+)$ and bid $(-)$ side;

⋄ $I_j := (\theta_j, m_j)$ is an impulsive sequence of level-0 limit orders such that $K_t \leq k_{\max}$, and $m_j \in \{-m_{\max}, \dots, -m_{\max}\} := \mathbb{M} \subset \mathbb{Z}$;

⋄ the inventory (Y_t) satisfies $\mathbb{Y} := \{-y_{\max}, \dots, +y_{\max}\} = -\mathbb{Y} \subseteq \mathbb{Z}$.

In order to ease computation, we consider the optimal control problem with a very specific random horizon, i.e.:

$$\mathbf{u}_k(t, \tau, h, x, y, p, c, i) := \max_{\ell \in \mathbb{A}} \mathbb{E}_{t, \tau, h, x, y, p, c, i} \left[V_T - \eta \int_t^T Y_u^2 d\langle P \rangle_u \right],$$

where $T := \inf \left\{ u : \tau_u := \int_0^u \lambda_s ds = \tau_{\max} \right\}$, for some constant $\tau_{\max}$. We prove that the optimal control problem is solved by $\mathbf{u}_k = x + yp + \mathbf{v}_k$, where $\mathbf{v}_k(\tau, q, c)$ is the viscosity solution of

$$\min \left\{ -\frac{\partial \mathbf{v}_k}{\partial \tau} - \mathcal{C}(\mathbf{v}_k), \mathcal{I}\mathbf{v}_k \right\} = 0, \quad \mathbf{v}_k(\tau_{\max},) = 0,$$

where $\mathcal{C}$ and $\mathcal{I}$ are differential operators defined at Theorem 5.1 (in the body of this work).

Notice that neither the value function, nor the optimal controls depend on this state variable h, while estimating the parameters of the Hawkes process can be even more expensive that computing the value function itself! Such an effort is unfortunately still necessary, since the role of the stochastic intensity is hidden behind the random horizon T: $\langle P \rangle_t$ is indeed predictable w.r.t. to the agent filtration, but only once the parameters determining its dynamic are known. Long story short, the estimation of the Hawkes process N_t is necessary if and only if we want to know what the current τ is. Luckily, we observe numerically that the optimal policy stabilizes after few backward steps. So, rather than a time dependent optimal policy, we can use its long-horizon version all over the trading day, losing more and more the optimal behaviour as we get closer to horizon. Using this recipe, the estimation of the Hawkes process parameters is less relevant under the performance point of view, though it is a good advice to perform it to validate the model assumptions.

Numerical results

We illustrate numerical result concerning the optimal trading problem previously described. Figure 5.11 shows both the continuous (level-1) and impulsive (level-0) policy, on the buy and on the sell side for the slice $k = \tau = 0$ (i.e. immediately after a fair price jump, and at the beginning of the trading day). We find the inventory on the x-axis and the current context on y-axis: a coloured circle means that for the system occupying the state (q, c), the agent sends an order. The side convention is for $i = +$: in the opposite case the sell and the buy side are exchanged. Limit orders are of unitary size, i.e. $L = 1$, while $k_{\max} = 1$. Comparing the upper side with the lower one, we immediately notice that the agent is more active on the level-1 limit order, since it is almost always optimal to send a passive limit order one tick away from the fair price. Level-1 limit orders lead to a big potential gain with few risk. On the contrary, impulsive order are widely used for large values of $|q|$, in order to bring the agent inventory back to zero with few uncertainty on the execution. Furthermore, notice that the level-0 strategy is much more sensitive to the context variable c: this is due to the fact that impulsive order are able to change position quickly and allow the agent to follow the market, rather than being rewarded for providing liquidity, which is rather market independent instead. Comparing the left side with the right one, we notice an asymmetry: the agent tends to be more active on the buy side. In particular, for specify contexts, buying (for i=+, sell otherwise) is optimal both on level-0 and the level-1 even when q is already positive. This is due to the micro-structural trends emerging after the VLMC estimation (see Figure 5.7), that leads the agent to exploit her anticipation on the market to align her position to the market direction. We do not show the result, for $k = 1$, since on the level-1 limit order no big changes exist, while no level-0 limit orders are allowed. Figure 5.13 illustrate the behaviour of the value function for various levels of risk aversion (η). We plot $q \mapsto \frac{1}{\tau_{\max}} \sum_{c \in \mathbb{C}} \mathbf{v}_0(0, q, c) \, \mathbb{Q}^*(c)$, where $\mathbb{Q}^*$ is the stationary probability of the VLMC process seen as a Markov chain on its context set $\mathbb{C}$.

Chapter 2

Directional bets and the power of information in market making

Abstract

In this paper we study a control problem related to a market maker having directional information on the mid-price. She places unitary limit orders on the bid and ask sides simultaneously, at a certain distance from the mid-price, hoping for a double execution that would yield the spread between her quotes, leaving her inventory unchanged. Our goal is to understand how stochastic drift and volatility are reflected into her strategy: we prove that drift translates into limit orders placed asymmetrically w.r.t. to the mid price, even when she has no inventory, while volatility widens the agent spread and encourage the inventory reversion to 0. This creates a mixed policy that enables to exploit a double source of gain, the one due to liquidity providing and the one due to market anticipation, while controlling the inventory to prevent market risk.

In a the first part of the paper we solve explicitly the problem in the no risk aversion case, and compare the results with an uninformed trader, who sees the stock price as a martingale: our conclusion is that the directional information leads to an extra gain explained by the even moments of the mid-price. In the second part, we allow for a small risk aversion and small martingale deviation, i.e. we assume that the stock price dynamic is close to the martingale one. In this case we provide a first deformation of the solution in terms of the previous case: the associated strategy sacrifices part of the expected gain to control the agent inventory and the associated risk. This is obtained by widening the spread and shifting its center conveniently in the opposite side of the current inventory. To conclude, we generalize these results to the multi-dimensional framework.

keywords: Quantitative Finance, High-Frequency Trading, Market-Making, Inventory Risk, Markov Processes, Hamilton-Jacobi-Bellman, Stochastic Control, Optimal Control

Introduction

The market microstructure literature has developed several tools, mostly based on stochastic optimal control techniques, in order to deal with two fundamental problems of algorithmic trading:

  i) the minimization of the execution cost of a large position,

  ii) the maximization of the expected reward of a liquidity provider.

In the first case, from the seminal paper of [5] (using market orders and a mixed permanent/volatile impact approach) a lot of work has been done in the first direction, performing liquidation, just to provide some examples, *a*) using limit orders, as in e.g. [10] and [41], in order to avoid market impact *b*) using static limit order strategies derived from stochastic algorithm techniques as in [51], *c*) using mixed limit/market strategies as in [44], *d*) tracking the VWAP, as in [57] and [21].

Our paper falls in the second category: a market maker is defined as a participant of the electronic book who posts limit orders on both the sell (+) and the buy (-) side, with the intent of gaining the spread deriving by a double-side (or round-trip) execution, in which case she would obtain a profit without any position change, avoiding the associated market risk. Our main references on optimal market-making are [6], [42], [44] and [18]: we share the same execution model of these papers, assuming that limit orders at distance $((\delta_\pm)_t)$ from the mid-price are filled by two independent Cox processes, whose rate decays exponentially with $((\delta_\pm)_t)$.

In [23], the authors have made a different choice, and treat the same problem in a sophisticated execution environment based on Hawkes processes, including news and adverse selection, where the local drift includes a mean-reverting component. In our paper instead, we **focus on the directional bets made by the market maker**, i.e. how the agent forecasts the evolution of the stock price **without specifying any dynamic for the stock price**, as in [23]. Furhermore, we include transaction costs in order to create a realistic application. Differently from [23], we do not systematically make any restriction on the optimal policy, that is free to take negative values that are translated to market orders in real trading. In the general case, we follow the classical model of [6], where the book has an exponential shape, but in the case of small perturbation of the martingale deviation and for small risk aversion, we release as in [23] the exponential hypothesis for the order book shape and deal with the general case: we will see that, in this particular case and provided that the market maker has a backtest engine, no estimation of the order arrival is needed to obtain the optimal policy, that can be obtained by a mixed historical/optimal control approach.

We choose to add an extra inventory penalisation depending on the portfolio terminal position, which allows to provide a double control on the inventory (along the path and at expiration) and detail how risk aversion deforms the optimal strategy of a risk neutral agent, to whom we dedicate a section to enlighten the role of agent information on the stock price, and take into account what happens if such an information is ignored. On intraday horizons, the agent may dispose of several signals (based on news, machine learning techniques, technical indicators, etc. . .) detecting trends or mean reversions: this information can be incorporated in a **policy that takes advantage from**

  ⋄ **the reward due to pure liquidity providing,**

  ⋄ **the understanding of the market direction and the market risk.**

We prove that all the ingredient we need to derive (asymptotic results for) the optimal policies are given by the expectation of the terminal value of the stock price and its integrated variance. In order to simplify calculations, market-making models are usually assuming that the stock price is a martingale (an undrifted Brownian motion in most cases), so that optimal strategies exclude

gains coming from directional forecasting. We aim converting potential risks, as unexpected trends of the stock price, in potential gains.

However, **liquidity providing and directional trading are in a natural conflict**. A pure liquidity provider (having no inventory) keeps her two best policies at the same distance from the mid-price. On the contrary, a pure directional bet leads to open a profitable position as soon as possible, sending a market order or placing a limit order relatively close to the mid-price (on one side only). The equilibrium between these two forces is not trivial, and optimal control is a fundamental tool in this sense.

The stock price

At the current stage, many models for the stock price exist. The papers of [26] and [25] describes the price formation is terms of the interplay between incoming trades and the existing liquidity, while [62] provides a complete picture of the book, looking at the price as a singular component of the whole system. In [24] the price formation follows the trades arriving in the market, where the latter are driven by a renewal process. The papers [7] and [8] instead, develop a complex theory using Hawkes processes, incorporating feedback and mean reversion in the stochastic intensities driving the process components. A different approach consists in assuming the existence of a latent, unobserved stock price, as in the seminal work of [46], or the recent uncertainty zone model of [60], that reconstructs the observed price as a representation of an observed diffusion hitting barriers.

We have been looking for a trade-off between the two literature streams, the first assuming a very simple price model guaranteeing tractability, the other providing a very realistic but complex environment, leading to non-closed formula and high-dimensional problems. The goal of this paper is to **understand how the directional information on the mid-price, as the anticipation of a trend or a mean reversion, can improve the market-making policy**. For this purpose we obtain some results on the Brownian motion with local drift, and provide some numerical examples for the Ornstein-Uhlenbeck process.

Following [44] and [23], we maximize the expectation of a linear utility function (and not the exponential one, to ease computations), adding a penalty to keep the agent inventory within a small range. This choice leads to an explicit solution for no risk aversion, while for small risk aversions, thanks to a perturbation technique, we derive optimal controls as a deformation of the previous case. The semi-explicit results, mostly expressed in terms of conditional moments, are fairly easy to understand and enlighten the role of directional bets in the policy: **the agent adjusts her optimal spread by an entire translation in the convenient direction, in order to anticipate the price movement**.

Plan of the paper

Section 2.1 introduces the setting: we detail the stochastic processes involved in the model, distinguishing between the uncontrolled processes (the mid-price) and the controlled ones (the matching engine determining how limit orders are executed, the agent wealth and her inventory). Section 2.2 deals with the explicit problem solution in the special case of no risk aversion. Thanks to a variable change, the problem dimension reduces drastically: we deduce that **directional information shifts the optimal spread of an uninformed agent in the market direction**. In Section 2.3 we solve the problem in the general case thanks to a regular perturbation technique and provide optimal controls as a deformation of the no risk aversion case. We prove that **the introduction of the risk aversion unconditionally widens the spread, and adds an extra shift to its center in the opposite direction of the agent inventory, if any.** Assuming that the stock price is close to a martingale, we improve the results finding explicit formulae for the linear approximation (in the risk aversion parameter) both of the value function and the optimal controls. Section 2.4 contains two practical examples, where the underlying assets follows either an Ornstein-Uhlenbeck dynamic or an arithmetic Heston one: these

two models provides examples of diffusion with stochastic local drift (Ornstein-Uhlenbeck) and stochastic volatility (Heston). In both cases the asymptotic expansions of the value function and the optimal control are completely explicit. Section 2.5 is devoted to the numerical illustration of the small martingale deviation policy, an explicit policy for small risk aversion and mid-price dynamic close to the martingale one. Finally Section 2.6 generalizes the previous results to the multi-dimensional framework.

2.1　　The market framework and the control problem

Let us recall the setting of the market-making problem, taken from [6], where

⋄ the agent places, continuously and on both sides, limit orders of unitary size at a certain distance $((\delta_\pm)_t)$ from the opposite best policies;

⋄ orders are matched by two independent Cox processes having intensities decaying with $((\delta_\pm)_t)$.

For the rest of the paper we assume that the time variable t ranges in $[0, T]$, $T < \infty$.

The uncontrolled processes: the mid-price

We assume that $(t, P_t, \tilde{P}_t) =: (t, Z_t)$ is a Markov process, not necessarily continuous, where (P_t) represents the stock price, while the vectorial process $(\tilde{P}_t)$ makes the triplet Markovian and independent from the arrival of market orders in the limit order book. We set to $\mathcal{L}$ the infinitesimal generator of (Z_t) and assume that $(P_t) \in \mathbb{R}^1$ admits finite moment generating function conditionally to its initial value. Its finiteness guarantees that the agent has a finite value function. This includes for example stochastic volatility models, as the arithmetic Heston one, choosing $\tilde{P}_t = \sigma_t$, where

$$dP_t = \alpha_t dt + \sigma_t dW_t \,,$$
$$d\sigma_t = a(b - \sigma_t)dt + \nu dW_t' \,, \quad \langle dW_t, dB_t \rangle = \rho dt \,,$$

or a jump model as the Hawkes one of [7]. The only assumption we made is that

$$\mathbb{E}_{t,z}[P_T] - p := \varepsilon(t, z) \,, \tag{2.1.1}$$
$$d\langle P \rangle_t := \sigma^2(t, Z_t)dt \,, \tag{2.1.2}$$

with the convention that $\mathbb{E}_{t,z}[\bullet] = \mathbb{E}[\bullet | Z_{t-} = z]$. Since jumps are taken into account, all the expectation are taken at $t-$ in order to guarantee that the controls are predictable.

The main idea of our paper is to **understand how conditional information on the mid-price (drift and volatility) affect the market-making optimal policy**. We will show how, in the martingale case, the current value of the mid-price does not lead to any contribution to the optimal policy, while otherwise the agents adjusts her spread center to exploit information on the asset.

The controlled processes: the agent wealth and her inventory

A market-making policy is defined by a couple of $\mathbb{R}$-valued predictable processes $((\delta_\pm)_t)$, where $(\delta_\pm)_t$ represents the distance of the agent limit order price from the mid-price at time t, with the convention that $+/-$ refers to the ask/bid side. Unfortunately, in order to guarantee the tractability of this system, we cannot exclude negative strategies, that can be translated, in real-trading application, to market orders.

---

[1]The mid-price is not assumed to be positive, since in intraday high-frequency trading application, the initial price is nothing but a reference price.

DEFINITION 2.1. *(Matching engine) We assume that orders placed at distance $\delta_\pm$ from the opposite market best policies are matched by two independent Cox processes $(N_t^\pm)$ having stochastic intensity*

$$(\lambda_\pm)_t = Ae^{-k(\delta_\pm)_t}, \quad A, k \geq 0. \tag{2.1.3}$$

The decreasing shape of the intensity in δ reflects the fact the farther is a limit order from market order price, the lower is its probability of execution. Orders are matched at rate $Ae^{-k\delta_\pm}$ (decreasing in $\delta_\pm$), leading to a gain of $\delta_\pm$ (increasing in $\delta_\pm$) w.r.t. to the mid-price: a good policy has to reach a trade-off between two quantities, but not only. The agent must take into account the inventory change: her portfolio should change according to the market anticipation, always keeping in mind that a large inventory would expose her to market risk.
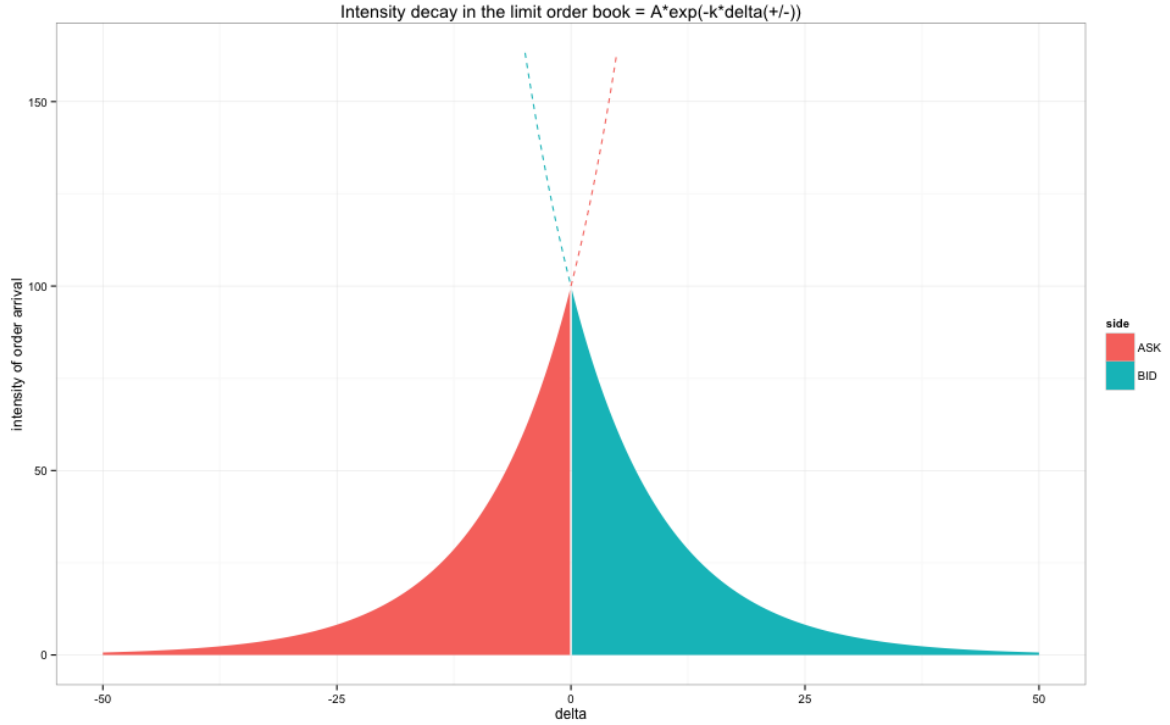
Figure 2.1: market order intensities $\lambda_\pm$.

DEFINITION 2.2. *(The wealth and the inventory process) We assume that every transaction is subjected to a fixed cost φ (usually positive, but not always, as in the case of rebates). The wealth process (X_t), representing the agent cash flow, and her inventory (Y_t), are given by*

$$dX_t = dX_t[\delta_\nu] = \sum_{\nu \in \pm} (\nu P_t + (\delta_\nu)_t - \varphi)dN_t^\nu, \tag{2.1.4}$$

$$dX_t = dY_t[\delta_\nu] = dN_t^- - dN_t^+, \tag{2.1.5}$$

where the notation $[\delta_\nu]$ means that the two controlled processes are induced by a certain strategy. We will adopt this notation only when necessary and drop it when the underlying strategy is clear from the context.

As one can see from (2.1.4)-(2.1.5), a round trip execution for $\varphi = 0$ leads to

$$X_t - X_{t-} \big| N_t^+ - N_{t-}^+ = N_t^- - N_{t-}^- = 1 = \sum_{\nu \in \pm} (\delta_\nu)_t dN_t^\nu \geq 0,$$

$$Y_t - Y_{t-} \big| N_t^+ - N_{t-}^+ = N_t^- - N_{t-}^- = 1 = 0.$$

i.e. a gain without any inventory change, i.e. a statistical arbitrage. Mathematically speaking, $(N_t^{\pm})$ almost surely never jump simultaneously: the purpose of the previous equations is just to enlighten the interest of the market maker to have both limit orders matched in a "short" period.

The stochastic optimal control problem

The goal of the agent is to find an optimal policy $((\delta_{\pm})_t)$ maximizing the gain function (called $\mathbf{j}^{(\eta,\varepsilon)}$), i.e

$$\mathbf{u}^{(\eta,\varepsilon)}(t,x,y,z) := \max_{(\delta_{\pm})_t} \mathbf{j}^{(\eta,\varepsilon)}(t,x,y,z;\delta_{\pm}), \tag{2.1.6}$$

$$\mathbf{j}^{(\eta,\varepsilon)}(t,x,y,z;\delta_{\pm}) := \mathbb{E}_{t,x,y,z}\left[X_T\left[\delta_{\pm}\right] + Y_T\left[\delta_{\pm}\right]P_T - \eta\left(\beta Y_T^2\left[\delta_{\pm}\right] + \int_t^T Y_u^2\left[\delta_{\pm}\right]\,d\langle P\rangle_u\right)\right],$$

where:

⋄ $z = (p, \tilde{p})$, $\tilde{p} \in \mathbb{R}^n$;

⋄ $\eta \geq 0$ describes the agent risk aversion to the inventory risk;

⋄ $\varepsilon(t,z)$ has been defined in (2.1.1);

⋄ $\mathbb{E}_{t,x,y,z}[]$ is the conditional expectation given the values of all variables at time $t-$, i.e.

$$\mathbb{E}_{t,x,y,z}[\cdot] = \mathbb{E}_{t,x,y,z}[\cdot|X_{t-} = x, Y_{t-} = y, Z_{t-} = z];$$

⋄ the gain function $\mathbf{j}^{(\eta,\varepsilon)}$ represents the gain function under a particular policy: we use the convention that, for any pair of (resp. single) constants $c^{\pm}$, $\mathbf{j}^{(\eta,\varepsilon)}(\ldots;c^{\pm})$ is the gain function under $((\delta_{\pm})_t) \equiv c^{\pm}$ (resp. $((\delta_{\pm})_t) \equiv c$).

We emphasise the dependence on η (chosen by the agent) and ε (observed on the market), since we will explicitly show how, for small values, they deform the agent value function and her optimal policy.

The penalty terms

In this paper we adopt a double approach to control the agent inventory, **discouraging large portfolios both during the trading day and at maturity**.

i) *Liquidity risk:* βY_T^2, $\beta \in \mathbb{R}_+$, represents the liquidity component of the inventory risk. An intraday trader does not want to be exposed to over-night risk, and consequently liquidates her position at T with a market order. Choosing a quadratic form, we are able penalize both short and long positions, and reproduce the non-linearity of the market impact[2] due to the final market order. Notice that this quantity does not depend on the asset volatility, since liquidation is instantaneous. Furthermore, since this penalty is applied at maturity, it propagates backwards from T to t, so that an inventory control takes place all along the day.

ii) *Market risk:* the integral term reflects the agent aversion to risky portfolios. The path-integration allows to control the variance of the portfolio all over the trading day. This penalty is applied all over the trading day, depends on the asset volatility, and decreases as t approaches T, since the agent is exposed for a shorter time.

---

[2]The polynomial form of $\mathbf{m}^{(0)}$ will be crucial to allow computations of the value function approximation.

The HJB equation associated to the optimal control problem

Throughout the rest of our paper, we use the following compact notation for every function $\mathfrak{g}(x)$, for a fixed x lying in some domain,

$$\Delta_x \mathfrak{g}(x') = \mathfrak{g}(x') - \mathfrak{g}(x),$$

and simply denote $\Delta = \Delta_x$ where no ambiguity is present. We can finally provide the HJB equation associated to (2.1.6) for a generic function $\mathfrak{g}$:

$$-(\partial_t + \mathcal{L})\,\mathfrak{g} - A \sum_{\nu \in \pm} \max_\delta e^{-k\delta} \Delta \mathfrak{g}(t, x \pm \nu p + \delta - \varphi, y \mp \nu, z) = -\eta\sigma^2 y^2\,, \qquad (2.1.7)$$

$$\mathfrak{g}(T,) = -\eta\beta y^2\,.$$

2.2 The explicit solution in the no risk aversion case

In this section we derive explicitly the value function and optimal controls for $\eta = 0$. Being not risk averse leads the agent to an optimal policy which is independent of the state variable y, simplifying the HJB equation (2.1.7). The main result of this section is the following.

PROPOSITION 2.1 (Informed agent with no risk aversion). *The risk-neutral value function is given by*

$$\mathbf{u}^{(0,\varepsilon)} = x + y\mathbf{h}^{(\varepsilon)} + \mathbf{m}^{(\varepsilon)}\,,$$

where

$$\mathbf{h}^{(\varepsilon)} = \mathbf{h}^{(\varepsilon)}(t,z) := p + \varepsilon(t,z) = \mathbb{E}_{t,z}\left[P_T\right]\,, \qquad (2.2.1)$$

$$\mathbf{m}^{(\varepsilon)} = \mathbf{m}^{(\varepsilon)}(t,z) := 2c \int_t^T \mathbb{E}_{t,z}\left[\cosh(k\varepsilon(u, Z_u))\right] du \geq 0\,, \qquad (2.2.2)$$

$$c = c(A, k, \varphi) := \frac{A}{k} e^{-k(1/k + \varphi)}\,. \qquad (2.2.3)$$

Furthermore, $\mathbf{m}^{(\varepsilon)}$ can be expressed in terms of solution of (2.2.6), while optimal controls are given by

$$\delta_\pm^{(0,\varepsilon)} := 1/k + \varphi \pm \varepsilon\,. \qquad (2.2.4)$$

Proof. Assuming the ansatz

$$\mathfrak{g}(t,z) = x + y\mathfrak{h}(t,z) + \mathfrak{m}(t,z)\,,$$

(2.1.7) takes the form

$$-(\partial_t + \mathcal{L})(y\mathfrak{h} + \mathfrak{m}) - \sum_{\nu \in \pm} \max_\delta f^\nu(\delta, t, z) = 0\,, \quad \mathfrak{m}(T,) = 0\,, \quad \mathfrak{h}(T,) = p\,, \qquad (2.2.5)$$

with $f^\pm(\delta, t, z) = A e^{-k\delta}(\pm p + \delta - \varphi \mp \mathfrak{h})$. Using elementary Calculus we find that its maximum is attained at

$$\delta_\pm^{(0,\varepsilon)} := 1/k + \varphi \pm (\mathfrak{h} - p)) \Rightarrow f^\pm\left(\delta_\pm^{(0,\varepsilon)}, t, z\right) = \frac{A}{k} e^{-k\delta_\pm^{(0,\varepsilon)}}\,,$$

so that (2.2.5) reduces to

$$-(\partial_t + \mathcal{L})(y\mathfrak{h} + \mathfrak{m}) - 2c\cosh(k\varepsilon) = 0\,, \quad \mathfrak{m}(T,) = 0\,, \quad \mathfrak{h}(T,) = p\,.$$

We split the previous equation into two parts, one for each one of our unknowns, according to the degree of y. We obtain in the first degree

$$-(\partial_t + \mathcal{L})\mathfrak{h} = 0\,, \quad \mathfrak{h}(T,) = p\,,$$

whose solution, provided by the Feymann-Kac theorem, is $h(t,z) = p + \varepsilon(t,z)$. Now, m is solution of

$$-(\partial_t + \mathcal{L})\mathfrak{m} - 2c\cosh(k\varepsilon) = 0\,, \quad \mathfrak{m}(T,) = 0\,, \tag{2.2.6}$$

and has probabilistic representation (2.2.2).

$\square$

2.2.1   A financial interpretation of the value function

In this section we decompose the value function at Proposition 2.1 in the buy-and-hold and market-making components.

DEFINITION 2.3. *We denote by*

$$\varepsilon_t := \varepsilon(t, Z_t)\,, \tag{2.2.7}$$

$$\Theta_{t,z}^{(j)}(u) := \mathbb{E}_{t,z}\left[\varepsilon_u^j\right]\,, \quad k \in \mathbb{N}, u \in [t,T]\,. \tag{2.2.8}$$

Notice that $\varepsilon(t,z)$ represents a measure of the deviation of the mid-price from the martingale dynamic, while $\Theta_{t,z}^{(j)}(u)$ is conditional moment of $\varepsilon(u, Z_u)\big|Z_t = p$. We see how these quantities play a crucial role in the analysis of the market-making value function.

The buy-and-hold component

COROLLARY 2.1 (The buy-and-hold, or forward, portfolio).

$$x + y\mathbf{h}^{(\varepsilon)}(t,z) = \mathbf{j}^{(0,\varepsilon)}(t,x,y,z;+\infty)\,.$$

Proof. If $((\delta_\pm)_t) \equiv +\infty$, the agent does not participate to the market, which implies that (X_t) and (Y_t) are constant process, i.e.:

$$\begin{aligned}
\mathbf{j}^{(0,\varepsilon)}(t,x,y,z;+\infty) &= \mathbb{E}_{t,x,y,z}\left[X_T\left[\infty\right] + Y_T\left[\infty\right]P_T\right] \\
&= x + y\,\mathbb{E}_{t,z}\left[P_T\right] = x + y\mathbf{h}^{(\varepsilon)}(t,z)\,.
\end{aligned}$$

$\square$

The previous corollary shows that $x + y\mathbf{h}^{(\varepsilon)}(t,z)$ is a component of the value function corresponding to hold the portfolio until T without participating to the market, i.e. the forward value of the portfolio. There is no option on this term: independently on its value being positive or negative, the over-all performance depends on this quantity. This is due to the fact that the optimal policy does not depend on the current inventory: consequently the current portfolio is held for all the trading day, while a new one, starting from $y = 0$, is used for market-making.

The market-making component

Using a Taylor expansion:

COROLLARY 2.2 (The market-making portfolio).

$$\mathbf{m}^{(\varepsilon)}(t,z) = 2c\sum_{j=0}^{\infty}\frac{k^{2j}}{(2j)!}\int_t^T \Theta_{t,z}^{(2j)}(u)\,du\,. \tag{2.2.9}$$

This components of the value function is the profit due to playing a dynamic (i.e. high-frequency) market-making policy, as the integral from t to T suggests. Notice that it does not depend on the current inventory, and that, since $\cosh \geq 1$:

COROLLARY 2.3.

$$\mathbf{m}^{(\varepsilon)}(t, z) \geq 2c(T - t) := \mathbf{m}^{(0)}(t) \, . \tag{2.2.10}$$

The introduction of the market-making policy improves the performances (recall that $\mathbf{m}^{(\varepsilon)} \geq 0$). An important observation is that **the worst mid-price dynamic is the martingale one**: the function $\xi \mapsto \cosh(\xi) \geq 1$ has a strict minimum for $\xi = 0$, and in the martingale case $\varepsilon \equiv 0$. This is due to the fact the current value of the mid-price does not provide any directional information on its future evolution.

Notice that $\mathbf{m}^{(\varepsilon)}$ is a complex object, with a much richer structure that ε: in particular, in the Gaussian case, it depends on both the mean and volatility of the process. Even though in the general case no explicit formula is available, a Monte Carlo simulation or a numerical PDE scheme allows to compute $\mathbf{m}^{(\varepsilon)}$: luckily, optimal controls do not depend on this quantity, so that its evaluation is not necessary to determine the agent policy. Nevertheless we can use (2.2.9) to develop $\mathbf{m}^{(\varepsilon)}$ in terms of conditional moments $\Theta^{(j)}$ (see (2.2.8)). Notice that:

⋄ only even moments $\Theta^{(2j)} \geq 0$ are included in the power series;

⋄ at the 0th order we have $\mathbf{m}^{(0)}$, i.e. the value of $\mathbf{m}^{(\varepsilon)}$ when the stock price is martingale: we interpret the remaining positive part as the mean advantage brought by information w.r.t. an unformed trader.

The market parameters

For the market parameters A, k and φ, their contribution appears in the constant $c(A, k, \varphi)$. **The market-making policy is proportional to the ratio A/k**, i.e. directly proportional to the arrival rates of market orders and inversely to the intensity decay, while transaction costs represent an exponential discount, as shown in:

COROLLARY 2.4 (Asymptotics for big transaction costs).

$$\lim_{\varphi \to \infty} \mathbf{m}^{(\varepsilon)}(t, z) \equiv 0 \, .$$

Proof. The claim can be derived from the value function (see (2.2.2)), or looking at optimal controls (2.2.4), that explode for big transaction costs, implying that the agent does not participate at all to the market.

□

2.2.2 A financial interpretation of the optimal controls

Summing up, directional bets are not reflected by the hold policy, but by the market-making one. The agent, aware of the average value of the forward portfolio, adjusts her optimal spread in order reach an optimal trade-off between the gain due to liquidity providing and the directional information. In particular, the semi-width and the center of the agent spread are given by:

POLICY 2.1. *The policy associated to the control $\delta_{\pm}^{(0,\varepsilon)}$ (see (2.2.4)) is equivalent to*

$$\begin{aligned}
semi\text{-}width^{(0,\varepsilon)} &:= 1/k + \varphi &= semi\text{-}width^{(0,0)} \, , \\
center^{(0,\varepsilon)} &:= p + \varepsilon &= center^{(0,0)} + \varepsilon.
\end{aligned}$$

Notice that semi-width$^{(0,\varepsilon)}$ does not depend on ε, i.e. on the directional bet, while center$^{(0,\varepsilon)}$ is obtained as a linear deformation of center$^{(0,0)}$ in $\varepsilon(t, z)$. In the next section we will also show how the introduction of risk aversion deforms the agent policy, widening and shifting her spread.

The spread width and the round-trip execution

The width of the optimal spread is constant over time, and does not depend on any state variable. It depends on the shape parameter k of the limit order book, saying that faster is the intensity decay, the smaller is the agent spread. As expected, **fixed costs widen the optimal spread**, since the agent has to compensate the market participation cost: for $\varphi \to \infty$, the agent eventually avoids the market.

On the contrary, **the profit of a round-trip execution does not depend on the transaction costs**: the market maker always expects the same reward from a single round-trip execution, no matter the value of φ, even thought the probability of the event decreases with φ, as shown by the term $c(A, k, \varphi)$ given in (2.2.3), which is an exponential discount (in φ) of the value function.

The spread center

The center of the optimal spread is impacted by the directional bet through the martingale deviation $\varepsilon(t, z)$. If $\varepsilon(t, z) > 0$ (resp. < 0), the agent estimates that a holding a long (resp. short) position until T is profitable. In order to increase her chances to buy (resp. sell) and decreases those to sell (resp. buy), she entirely translates her spread of $\varepsilon(t, z)$, becoming more aggressive on the bid (resp. ask) and more passive on the opposite one. Thanks to this "spread shift", the agent reaches an optimal trade-off between anticipating the market and providing liquidity, creating a mixed directional/liquidity strategy.

The martingale policies and the information advantage

By definition, strategies for no risk aversion are extremely exposed to market and inventory risk, since the directional component is extremely strong. Inventory is not necessarily bounded (notice that the optimal policy does not depend on the current inventory level) and the directional bets incorporated in the optimal policy lead to high-risk-high-reward profiles. Directional bets comes from the agent awareness of the non-martingality of the stock price: under no information, the agent guesses (committing an error) that the mid-price is a martingale, i.e. that $\varepsilon \equiv 0$, and her trading policy is given by

$$\delta^{(0,0)} = 1/k + \varphi \,. \tag{2.2.11}$$

Adopting this martingale policy:

LEMMA 2.1 (Uninformed agent).

$$\mathbf{j}^{(0,\varepsilon)}(t, x, y, z; \delta^{(0,0)}) = x + y\mathbf{h}^{(\varepsilon)} + \mathbf{m}^{(0)} \,. \tag{2.2.12}$$

Proof. We use the ansatz

$$x + y\mathfrak{h}(t, z) + \mathfrak{m}(t, z) \,.$$

Injecting the constant martingale controls at (2.2.11) in the HJB equation (2.1.7) (where the max is replaced by injecting the given policies), we are left to solve

$$-(\partial_t + \mathcal{L})\mathfrak{h} = 0 \,, \quad \mathfrak{h}(T,) = p \,,$$

and

$$-(\partial_t + \mathcal{L})\mathfrak{m} - 2c = 0 \,, \quad \mathfrak{m}(T,) = p \,,$$

whose solution are $\mathbf{h}^{(\varepsilon)}$ and $\mathbf{m}^{(0)}$ (see (2.2.1) and (2.2.10)).

$\square$

Notice the $x + y\mathbf{h}^{(\varepsilon)}(t, z)$ is the forward value of the current portfolio, where the mid-price dynamic is not the martingale one, while $\mathbf{m}^{(0)}$ rewards the agent as if the mid-price were a martingale.

The extra gain due to information is the difference between the value function of two agents in the <u>same</u> market, playing respectively $\delta_{\pm}^{(0,\varepsilon)}$ and $\delta^{(0,0)}$:

$$\mathbf{j}^{(0,\varepsilon)}(t, x, y, z; \delta_{\pm}^{(0,\varepsilon)}) - \mathbf{j}^{(0,\varepsilon)}(t, x, y, z; \delta^{(0,0)})$$

$$= \mathbf{u}^{(0,\varepsilon)}(t, x, y, z) - \mathbf{j}^{(0,\varepsilon)}(t, x, y, z; \delta^{(0,0)})$$

$$= \mathbf{m}^{(\varepsilon)}(t, z) = 2c \frac{k^{2j}}{(2j)!} \int_t^T \Theta_{t,z}^{(2j)}(u)\, du \geq 0. \tag{2.2.13}$$

The martingale policies as the best symmetric policies

Since the martingale policies are constant and symmetric, it is interesting to see if they can be outperformed by policies of the same type.

COROLLARY 2.5. *For $\eta = 0$, $\delta^{(0,0)}$ are the optimal policies among all the constant symmetric policies, i.e.*

$$\mathbf{j}^{(0,\varepsilon)}(t, x, y, z; \delta^{(0,0)}) = \max_{\delta \in \mathbb{R}} \mathbf{j}^{(0,\varepsilon)}(t, x, y, z; \delta).$$

Proof. Once again, injecting the generic constant symmetric policies $\delta_{\pm} = \delta$ in the HJB equation, and using the ansatz

$$\mathbf{j}^{(0,\varepsilon)}(t, x, y, z; \delta) = x + y\mathbf{h}^{(\varepsilon)}(t, z) + \mathfrak{m}^{\delta}(t, z),$$

we obtain

$$-(\partial_t + \mathcal{L})(x + y\mathbf{h}^{(\varepsilon)} + \mathfrak{m}^{\delta}) - \sum_{\nu \in \pm} A e^{-k\delta}(\nu p + \delta - \varphi - \nu \mathfrak{m}^{\delta}(t, z))$$

$$= -(\partial_t + \mathcal{L})\mathfrak{m}^{\delta} - 2A e^{-k\delta}(\delta - \varphi) = 0.$$

By the comparison principle,

$$\mathbf{j}^{(0,\varepsilon)}(t, x, y, z; \delta) \leq \mathbf{j}^{(0,\varepsilon)}(t, x, y, z; \delta_*), \quad \text{for } \delta_* := \arg\max e^{-k\delta}(\delta - \varphi) = \delta^{(0,0)},$$

which implies that

$$\max_{\delta} \mathbf{j}^{(0,\varepsilon)}(t, x, y, z; \delta) = \mathbf{j}^{(0,\varepsilon)}(t, x, y, z; \delta_*) = \mathbf{j}^{(0,\varepsilon)}(t, x, y, z; \delta^{(0,0)}).$$

$\square$

Getting free of the exponential shape of the limit order book

Assume that the agent has no knowledge of the limit order book, but can backtest her strategy and knows that the stock price is a martingale. In this case we can prove the following result:

PROPOSITION 2.2 (Free book shape). *Assume that the shape of the book has symmetric arbitrary (not necessarily continuos) shape $\lambda(\delta) > 0$ such that $\lambda(\delta)(\delta - \varphi)$ has a unique positive maximum $\delta^{(0,0)}$. Then if $\varepsilon \equiv 0$ (martingale stock price) and $\eta = 0$, the optimal policy is constant, given by $\delta^{(0,0)}$, while the value function is given by*

$$\mathbf{u}^{(0,0)}(t, x, y, z) = x + yp + \mathbf{m}^{(0)}(t)$$

$$= x + yp + 2c(T - t), \quad c := \lambda(\delta^{(0,0)}).$$

Before giving the trivial proof of the proposition, it is important to understand the previous result. Reaching optimal strategy by backtesting is hard: a search grid approach is impossible since a strategy is described by too many parameters. However, since in this case we know that the optimal strategy is constant, we can optimize backtesting a family of strategies depending on a unique parameter, and choose the best outcome. This implies no parameter estimation whatsoever and, since we have made no assumption on regularity of λ, we can think it is piecewise constant between two tick levels, so that the optimal policies lies on the (market) tick grid. Furthermore, since $\delta^{(0,0)} \geq 0$, guarantees that optimal quotes are non-negative.

Proof. The proof is a straightforward, and mimics the one of Proposition 2.1.

$\square$

2.3   The perturbation approach for positive risk aversion

In this section we extend the result of Proposition 2.1 to the case of (positive) small risk aversion. We prove that the value function can be approximated in the general case by a first order deformation of the value function for no risk aversion. In a similar fashion, optimal controls are derived in terms of the no risk aversion ones. Recall that we have an explicit formula for the solution $\mathbf{u}^{(0,\varepsilon)}$. Therefore, we use perturbation methods on η to reconstruct the value function and the optimal controls as a first order deformation in the risk aversion parameter. More precisely, we propose the following ansatz:

$$\mathbf{u}^{(\eta,\varepsilon)}(t,x,y,z) = \mathbf{u}^{(0,\varepsilon)}(t,x,y,z) - \eta \mathbf{v}^{(\eta,\varepsilon)}(t,y,z)\,.$$

Injecting the previous ansatz in the HJB equation (2.1.7), we obtain that $\mathbf{v}^{(\eta,\varepsilon)}$ solves the following PDE in the unknown $\mathfrak{g}$

$$-(\partial_t + \mathcal{L})(\mathbf{u}^{(0,\varepsilon)} - \eta\mathfrak{g}) - \sum_{\nu \in \pm} \max_\delta f^\nu(\delta,t,y,z) = -\eta\sigma^2 y^2\,, \tag{2.3.1}$$

$$\mathfrak{g}(T,) = \beta y^2\,,$$

where

$$f^\pm(\delta,t,y,z) = Ae^{-k\delta}\left(\delta - \varphi \mp \varepsilon(t,z) - \eta\Delta\mathfrak{g}(t,y\mp 1,z)\right)\,. \tag{2.3.2}$$

Once again, using elementary Calculus, we obtain the optimal controls in the feedback form

$$\delta_\pm^{(\eta,\varepsilon)}(t,y,z) = 1/k + \varphi \pm \varepsilon(t,z) + \eta\Delta\mathfrak{g}(t,y\mp 1,z)\,,$$
$$= \delta_\pm^{(0,\varepsilon)}(t,z) + \eta\Delta\mathfrak{g}(t,y\mp 1,z)\,, \tag{2.3.3}$$

where $\delta_\pm^{(0,\varepsilon)}$ are given by (2.2.4), while plugging (2.3.3) in (2.3.2) we obtain

$$f^\pm(\delta_\pm^{(\eta,\varepsilon)}) = ce^{\mp k\varepsilon(t,z) - \eta k\Delta\mathfrak{g}(t,y\mp 1,z)}\,. \tag{2.3.4}$$

We can now prove the following result:

THEOREM 2.1 (Informed agent with small risk aversion). *The value function is $O(\eta^2)$-approximated by*

$$\mathbf{u}^{(\eta,\varepsilon)} \approx \widehat{\mathbf{u}}^{(\eta,\varepsilon)} := \mathbf{u}^{(0,\varepsilon)} - \eta\widehat{\mathbf{v}}^{(\varepsilon)}\,,$$

where

i) $\mathbf{u}^{(0,\varepsilon)}$ is the risk-neutral value function provided in Proposition 2.1;

ii) $\mathbf{u}^{(\eta,\varepsilon)} - \widehat{\mathbf{u}}^{(\eta,\varepsilon)} \geq 0$;

iii) the risk aversion deformation is approximated by

$$\widehat{\mathbf{v}}^{(\varepsilon)} = \widehat{\rho}_0 + 2y\widehat{\rho}_1 + y^2\widehat{\rho}_2 \geq 0, \tag{2.3.5}$$

where

$$\widehat{\rho}_2(t,z) = \beta + \mathbb{E}_{t,z}\left[\int_t^T d\langle P\rangle_u\right] \geq 0, \tag{2.3.6}$$

$\widehat{\rho}_1(t,z)$ *has probabilistic representation*

$$\widehat{\rho}_1(t,z) = \mathbb{E}_{t,y=0,z}\left[\int_t^T Y_u\left[\delta_\pm^{(0,\varepsilon)}\right] d\langle P\rangle_u + \beta Y_T\left[\delta_\pm^{(0,\varepsilon)}\right]\right], \tag{2.3.7}$$

and is solution of

$$-\left(\partial_t + \mathcal{L}\right)\widehat{\rho}_1 - 2kc\sinh(k\varepsilon)\widehat{\rho}_2 = 0, \tag{2.3.8}$$
$$\rho_1(T,) = 0,$$

while $\widehat{\rho}_0$ *is solution of*

$$-\left(\partial_t + \mathcal{L}\right)\widehat{\rho}_0 - 2kc\left(\widehat{\rho}_2\cosh(k\varepsilon) + \widehat{\rho}_1\sinh(k\varepsilon)\right) = 0, \tag{2.3.9}$$
$$\rho_0(T,) = 0.$$

Furthermore, optimal controls are $O(\eta^2)$-approximated by

$$\delta_\pm^{(\eta,\varepsilon)} \approx \widehat{\delta}_\pm^{(\eta,\varepsilon)} := \delta_\pm^{(0,\varepsilon)} + \underbrace{\eta\left(\mp 2\widehat{\rho}_1 + (1\mp 2y)\,\widehat{\rho}_2\right)}_{\text{risk aversion}}, \tag{2.3.10}$$

where $\delta_\pm^{(0,\varepsilon)}$ *are given by* (*2.2.4*).

Proof. Using (2.2.6) we have

$$(\partial_t + \mathcal{L})\mathbf{u}^{(0,\varepsilon)} = -c\sum_{\nu\in\pm} e^{-\nu k\varepsilon},$$

and (2.3.1) reduces to

$$-(\partial_t + \mathcal{L})\mathfrak{g} - c\sum_{\nu\in\pm} e^{-k\nu\varepsilon} N_\eta^\nu(\mathfrak{g}) = \sigma^2 y^2, \quad \mathfrak{g}(T,) = \beta y^2, \tag{2.3.11}$$

for

$$N_\eta^\pm(\mathfrak{g}) := \frac{1 - e^{-\eta k\Delta\mathfrak{g}(t,y\mp 1,z)}}{\eta} = \underbrace{k\Delta\mathfrak{g}(t, y\mp 1, z)}_{:= L^\pm(\mathfrak{g})} - \frac{1}{\eta}R(\eta\Delta\mathfrak{g}(t, y\mp 1, z)),$$

where $N_\eta^\pm(\mathfrak{g}) \leq L^\pm(\mathfrak{g})$, $R \geq 0$, $x \in \mathbb{R}$ and $R(x)$ is an $O(x^2)$ for $x^2 \downarrow 0$.

Since the remaining PDE is non-linear, our only hope to find something explicit is to replace the non-linear operators $N_\eta^\pm$ for its linearisation $L^\pm$ and ignore the remaining non-linear part. Injecting the ansatz

$$\mathfrak{g}(t,y,z) = \widehat{\rho}_0(t,z) + 2y\widehat{\rho}_1(t,z) + y^2\widehat{\rho}_2(t,z), \tag{2.3.12}$$

in (2.3.11), where $N_\eta^\pm$ is replaced by $L^\pm$, we obtain

$$-(\partial_t + \mathcal{L})\left(\widehat{\rho}_0 + 2y\widehat{\rho}_1 + y^2\widehat{\rho}_2\right) - kc\sum_{\nu\in\pm}e^{-k\nu\varepsilon}\left(-2\nu\widehat{\rho}_1 + (1-\nu 2y)\widehat{\rho}_2\right) = \sigma^2 y^2\,, \qquad (2.3.13)$$

$$\widehat{\rho}_0(T,) = \widehat{\rho}_1(T,) = 0\,,$$
$$\widehat{\rho}_2(T,) = \beta y^2\,.$$

Assume we can find a solution to (2.3.13). In order to prove ii), we claim that

$$\widehat{\mathbf{v}}^{(\varepsilon)} \geq \mathbf{v}^{(\eta,\varepsilon)} \geq 0\,.$$

Injecting $\underline{v} \equiv 0$ in (2.3.11) we obtain

$$-\sigma^2 y^2 \leq 0\,, \quad \underline{v}(T,) = 0 \leq \beta y^2\,,$$

which immediately implies, by the comparison principle, that $\underline{v} \equiv 0$ is a sub-solution of (2.3.11), i.e. that $\mathbf{v}^{(\eta,\varepsilon)} \geq 0$. Now, since $N_\eta^\pm \leq L^\pm$, applying once again the comparison principle we immediately have that $\widehat{\mathbf{v}}^{(\varepsilon)} \geq \mathbf{v}^{(\eta,\varepsilon)} \geq 0$, which proves the claimed result.

In order to prove iii), we need to find a solution to (2.3.13), that can decompose it, as for the proof of Proposition 2.1, and solve them recursively using the Feynman-Kac formula. The first equation, which regroups the terms in y^2, is given by

$$-(\partial_t + \mathcal{L})\widehat{\rho}_2 = \sigma^2\,, \quad \widehat{\rho}_2(T,) = \beta\,, \qquad (2.3.14)$$

and its solution is provided by (2.3.6), while the first and second degrees term in y leads to $\widehat{\rho}_1$ and $\widehat{\rho}_0$, given in the body of theorem as the solutions of (2.3.9) and (2.3.8).

We are left to prove the probabilistic representation of $\widehat{\rho}_1$ given in (2.3.7), for which we (re)define

$$\mathfrak{g}(t,x,y,z) := \mathbb{E}_{t,z}\left[\int_t^T Y_u\left[\delta_\pm^{(0,\varepsilon)}\right]d\langle P\rangle_u + \beta Y_T\left[\delta_\pm^{(0,\varepsilon)}\right]\right]\,.$$

We guess that

$$\mathfrak{g}(t,x,y,z) = y\mathfrak{a}(t,z) + \mathfrak{b}(t,z)\,,$$

and, use the PDE representation of $\mathfrak{g}$, given by

$$-(\partial_t + \mathcal{L})\mathfrak{g} - \sum_{\nu\in\pm}Ae^{-k\delta_\nu^{(0,\varepsilon)}}\Delta\mathfrak{g}(t,y-\nu,z) - \sigma^2 y =$$

$$-(\partial_t + \mathcal{L})\mathfrak{g} - \sum_{\nu\in\pm}Ae^{-k(1/k+\varphi+\nu\varepsilon)}\Delta\mathfrak{g}(t,y-\nu,z) - \sigma^2 y =$$

$$-(\partial_t + \mathcal{L})(y\mathfrak{a}+\mathfrak{b}) - 2c\sum_{\nu\in\pm}e^{-k\nu\varepsilon}\Delta\mathfrak{g}(t,y-\nu,z) - \sigma^2 y =$$

$$-(\partial_t + \mathcal{L})(y\mathfrak{a}+\mathfrak{b}) - 2c\sum_{\nu\in\pm}e^{-k\nu\varepsilon}\nu\mathfrak{a} - \sigma^2 y =$$

$$y\left(-(\partial_t + \mathcal{L})\mathfrak{a} - \sigma^2\right) + \left(-(\partial_t + \mathcal{L})\mathfrak{b} - 2c\sinh(\varepsilon)\mathfrak{a}\right) = 0$$
$$\mathfrak{g}(T,) = y\mathfrak{a}(T,) + \mathfrak{b}(T,) = \beta y\,.$$

We have

$$-(\partial_t + \mathcal{L})\mathfrak{a} - \sigma^2 = 0\,, \quad \mathfrak{a}(T,) = \beta \Rightarrow \mathfrak{a} = \widehat{\rho}_2\,,$$

and

$$-(\partial_t + \mathcal{L})\mathfrak{b} - 2c\sinh(\varepsilon)\widehat{\rho}_2 = 0\,, \quad \mathfrak{b}(T,) = 0 \Rightarrow k\mathfrak{b} = \widehat{\rho}_1\,,$$

Finally, setting $y = 0$, we have

$$k\mathfrak{g}(t,x,y=0,z) = \widehat{\rho}_1(t,z)\,,$$

which conclude the proof.

$$\square$$

2.3.1 A financial interpretation of the value function

LEMMA 2.2 (Monotonicity in the risk aversion).

$$\mathbf{u}^{(\eta_2,\varepsilon)} \leq \mathbf{u}^{(\eta_1,\varepsilon)}, \quad \forall \eta_2 \geq \eta_1.$$

Proof. Since $\beta Y_T^2 + \int_t^T Y_u^2 d\langle P \rangle_u \geq 0$, the lemma is a straightforward consequence of the

$$X_T + Y_T P_T - \eta \left(\beta Y_T^2 + \int_t^T Y_u^2 d\langle P \rangle_u \right)$$

is an a.s. decreasing random variable in the parameter η.

$\square$

However, even if the introduction of the risk aversion parameter η penalizes the agent performance, the risk aversion is able to control the variance of the portfolio by controlling the inventory, leading to more cautious strategies.

The reason why small risk aversions are taken into account is not only for computational reasons: for large risk aversion, following the market direction induces a risk that the agent is not willing to pay, and the profits deriving from the optimal policies (Policy 2.1) and martingale ones (see (2.2.11)) do not differ significantly. The directional bets leads to a consistent advantage only if the market maker has the courage to risk, following the trend or the mean reversion, while a high level of risk aversion makes information valueless.

The term $\widehat{\rho}_2$

Looking at the function $\widehat{\rho}_2(t,z)$ at (2.3.6), we understand how liquidity risk and market risk impacts the agent performance. In particular, the value function is penalized by the current square inventory times the sum of the unitary market impact (β) and the future realized volatility. The first term penalizes the agent in a time-independent way, while the second one is monotone, increasing function of $T - t$ and penalizes large position at the beginning of the trading day, since they risk to exposed for a longer time, while for $T \to t^+$, this term becomes small.

2.3.2 A financial interpretation of the optimal controls

The spread width and the round trip execution

The introduction of the risk aversion has the effect of widening the optimal spread of η, so that a risk averse agent would adopt a more cautious policy. Widening the spread, the probability of being executed decreases, while the wealth deriving from a round trip execution increases. As a result, the agent plays less often, partially compensating by larger spread, even though widening the spread does not fully compensate the missing gain due to less market participation.

The spread center

The introduction of the risk aversion has a double effect.

i) *Inventory reversion:* the linear part $-2y\widehat{\rho}_2$ adjusts the agent spread according to her position. In order to avoid inventory risk, she keeps her position close to 0: when $y > 0$ (resp. $y < 0$), her spread is translated downwards (resp. upwards), so that the limit order placed on the ask (resp. bid) side increases (reap. decreases) its execution probability. Notice that for large $|y|$, this correction can lead to negative strategies, that should be interpreted in real life as market orders.

ii) *Reduction of the market participation:* the term ρ_1 is a first order compensation of $\mathbf{m}^{(\varepsilon)}$ (see Policy 2.1): this term shifts the agent spread center in the opposite direction of the market. The agent becomes more cautious and tends to avoid extremely directional strategies, i.e. she comes back to the "classic" market-making approach, where the mid-price is thought as a martingale.

Looking at Theorem 2.1, the risk aversion infinitesimally deforms the optimal policies for $\eta = 0$ (see Policy 2.1), as shown in:

POLICY 2.2. *The policy associated to the control $\widehat{\delta}_{\pm}^{(\eta,\varepsilon)}$ (see (2.3.10)) is equivalent to*

$$\widehat{semi\text{-}width}^{(\eta,\varepsilon)} := semi\text{-}width^{(0,\varepsilon)} + \eta\widehat{\rho}_2 \,,$$

$$\widehat{center}^{(\eta,\varepsilon)} := center^{(0,\varepsilon)} - 2\eta\left(\widehat{\rho}_1 + y\widehat{\rho}_2\right) \,.$$

2.3.3 The special case of small martingale deviation

Because of its complexity, $\widehat{\rho}_1$ may represent an obstacle for the determination of the optimal policies. The results obtained for small risk aversion in Theorem 2.1 can be improved, in terms of interpretability, assuming that

$$\varepsilon(t,z) = \mathbb{E}_{t,z}\left[P_T\right] - p \to 0 \,, \quad \forall(t,z) \,.$$

This hypothesis is consistent with the non-arbitrage theory where the stock price, assuming that interest rates are zero, is a martingale, so that $\varepsilon(t,z) \equiv 0$. High-frequency traders, being the fastest market participant, are supposed to be the first to take profit from existing arbitrages, which disappear after their intervention. However, these statistical arbitrages are (in average) only fractions of the tick, on which the high-frequency traders bets several times during the day.

THEOREM 2.2 (Agent with small risk aversion and mid-price close to a martingale). *For small risk aversions ($\eta \to 0^+$) and small martingale deviations ($\varepsilon(t,z) \to 0$ point-wisely), the value function (2.1.6) is approximated at the first order (in the risk aversion and the martingale deviation) by:*

$$\mathbf{u}^{(\eta,\varepsilon)} \approx \widetilde{\mathbf{u}}^{(\eta,\varepsilon)} = \mathbf{u}^{(0,0)} + y\varepsilon - \eta\left(\widetilde{\rho}_0 + \widetilde{\rho}_2 y^2\right) \,, \tag{2.3.15}$$

with $\mathbf{u}^{(0,0)}$ given by Proposition 2.1

$$\widetilde{\rho}_0(t,z) := 2kc\left(\beta(T-t) + \mathbb{E}_{t,z}\left[\int_t^T \int_u^T d\langle P\rangle_\xi \, du\right]\right) \geq 0 \,, \tag{2.3.16}$$

$$\widetilde{\rho}_2(t,z) := \widehat{\rho}_2(t,z) \geq 0 \,. \tag{2.3.17}$$

Furthermore, optimal controls are approximated by

$$\delta_{\pm}^{(\eta,\varepsilon)} \approx \widetilde{\delta}_{\pm}^{(\eta,\varepsilon)} := \delta^{(0,0)} + \varepsilon + \eta\widetilde{\rho}_2\left(1 \mp 2y\right) \,, \tag{2.3.18}$$

where $\delta^{(0,0)}$ is defined at (2.2.11).

Proof. For $\eta = \varepsilon \equiv 0$, the value function (2.1.6) is given by $\mathbf{u}^{(0,0)} = x + yp + \mathbf{m}^{(0)}$, satisfying $-(\partial_t + \mathcal{L})\mathbf{u}^{(0,0)} = 2c$, For small η and ε, the HJB equation (2.3.1) for a generic function $\mathfrak{g}$ linearizes as

$$- (\partial_t + \mathcal{L})(\mathbf{u}^{(0,0)} - \eta\mathfrak{g}) - \sum_{\nu\in\pm} f^\nu(\delta_\nu^{(\eta,\varepsilon)}(t,z)) - \eta\sigma^2 y^2$$

$$\approx -(\partial_t + \mathcal{L})(-\eta\mathfrak{g}) - c\sum_{\nu\in\pm}\left((1 - k\left(\nu\varepsilon(t,z) - \eta\Delta\mathfrak{g}(t, y-\nu, z)\right)) - 1\right) - \eta\sigma^2 y^2$$

$$= -\eta\Big(- (\partial_t + \mathcal{L})\mathfrak{g} - kc\sum_{\nu\in\pm}\Delta\mathfrak{g}(t, y-\nu, z) - \sigma^2 y^2\Big) \,.$$

Dividing by $-\eta$ and using the ansatz

$$\mathfrak{g}(t, y, z) = \widetilde{\rho}_0(t, z) + y^2 \widetilde{\rho}_2(t, z),$$

we obtain

$$\Delta\mathfrak{g}(t, y - 1, z) + \Delta\mathfrak{g}(t, y + 1, z) = 2\widetilde{\rho}_2(t, z),$$

which simplifies the HJB equation to

$$-(\partial_t + \mathcal{L})\left(\widetilde{\rho}_0 + y^2 \widetilde{\rho}_2\right) - 2kc\widetilde{\rho}_2 = \sigma^2 y^2, \tag{2.3.19}$$
$$\widetilde{\rho}_0(T,) + y^2 \widetilde{\rho}_2(T,) = \beta y^2.$$

Splitting by the y degrees we look for the solution of

$$-(\partial_t + \mathcal{L})\widetilde{\rho}_2 = \sigma^2, \quad \widetilde{\rho}_2(T,) = \beta,$$

and

$$-(\partial_t + \mathcal{L})\widetilde{\rho}_0 - 2kc\widetilde{\rho}_2 = 0, \quad \widetilde{\rho}_0(T,) = 0,$$

which are given by $\widetilde{\rho}_2$, defined at (2.3.6), and

$$\widetilde{\rho}_0(t, z) = 2kc\, \mathbb{E}_{t,z}\left[\int_t^T (\beta + \rho_2(u, Z_u))\, du\right],$$

equivalently expressed by (2.3.16). Finally, approximated controls are obtained injecting $\mathfrak{g}$ in (2.3.3).

$\square$

The value function

We can write the value function as

$$\widetilde{\mathbf{u}}^{(\eta,\varepsilon)} = \underbrace{x + yp + y\varepsilon}_{forward\ value} + \underbrace{\mathbf{m}^{(0)}\left(1 - \eta D\right)}_{market\ making} - \underbrace{\eta\widetilde{\rho}_2 y^2}_{inventory\ risk}, \tag{2.3.20}$$
$$D(t, z) := k\left(\beta + \frac{1}{T - t}\,\mathbb{E}_{t,z}\left[\int_t^T \int_u^T d\langle P\rangle_\xi\, du\right]\right) \geq 0,$$

that decomposes the value function in its forward value, the market making component and the penalisation due to the inventory risk. The introduction of the risk aversion linearly deforms the market making performance $\mathbf{m}^{(0)}$ by a relative discount of $D(t, z)$, which is inventory independent, but depends (monotonically) on k (the fastest is the intensity decay, the least is the gain opportunity), β (bigger impact of the final market order), and $\frac{1}{T-t}\,\mathbb{E}_{t,z}\left[\int_t^T d\langle P\rangle_u\right]$ (bigger exposure of the current inventory). On the contrary, the inventory risk part impacts quadratically the value function, proportionally to $\widetilde{\rho}_2$.

The small martingale deviation policy

POLICY 2.3. *The policy associated to the control $\widetilde{\delta}_\pm^{(\eta,\varepsilon)}$ (see (2.3.18)) is equivalent to*

$$\widetilde{semi\text{-}width}^{(\eta,\varepsilon)} := 1/k + \varphi + \eta\widetilde{\rho}_2 = semi\text{-}width^{(0,0)} + \eta\widetilde{\rho}_2 = \widetilde{semi\text{-}width}^{(\eta,0)},$$
$$\widetilde{center}^{(\eta,\varepsilon)} := p - 2\eta y\widetilde{\rho}_2 + \varepsilon = center^{(0,0)} + \varepsilon - 2\eta y\widetilde{\rho}_2 = \widetilde{center}^{(\eta,0)} + \varepsilon.$$

Notice that the small martingale deviation policy is a linear deformation of the martingale one (see Policy 2.1) both in ε and η. In particular the spread semi-width is impacted only by the risk-aversion, which, as in the previous case, widens the agent spread. The spread centre is translated by ε to follow the market direction and by $-2\eta y \widetilde{\rho_2}$ to avoid the inventory risk.

Figure 2.2 displays how optimal policy varies in different market conditions: reading from the left to right, one can see how agent spread changes when only one feature varies. The mid-price is assumed to be $p = 0$ and $\rho_2 \equiv 1$ for simplicity:

⋄ when $y = \varepsilon = \eta = 0$, the agent is placed symmetrically around the mid-price;

⋄ changing (only) $\varepsilon(t, z)$ to 0.2, the whole spread is translated upwards by $\varepsilon(t, z) = 0.2$;

⋄ increasing (only) η to 0.2, the spread widens of η, keeping its center invariant;

⋄ finally, changing (only) y to 1, the spread is translated downwards, in order to increase (resp. decrease) the probability of being executed on the ask (resp. bid) side: the upward shift of the spread center due to the directional is completely compensated by the necessity of reverting the current inventory to 0.
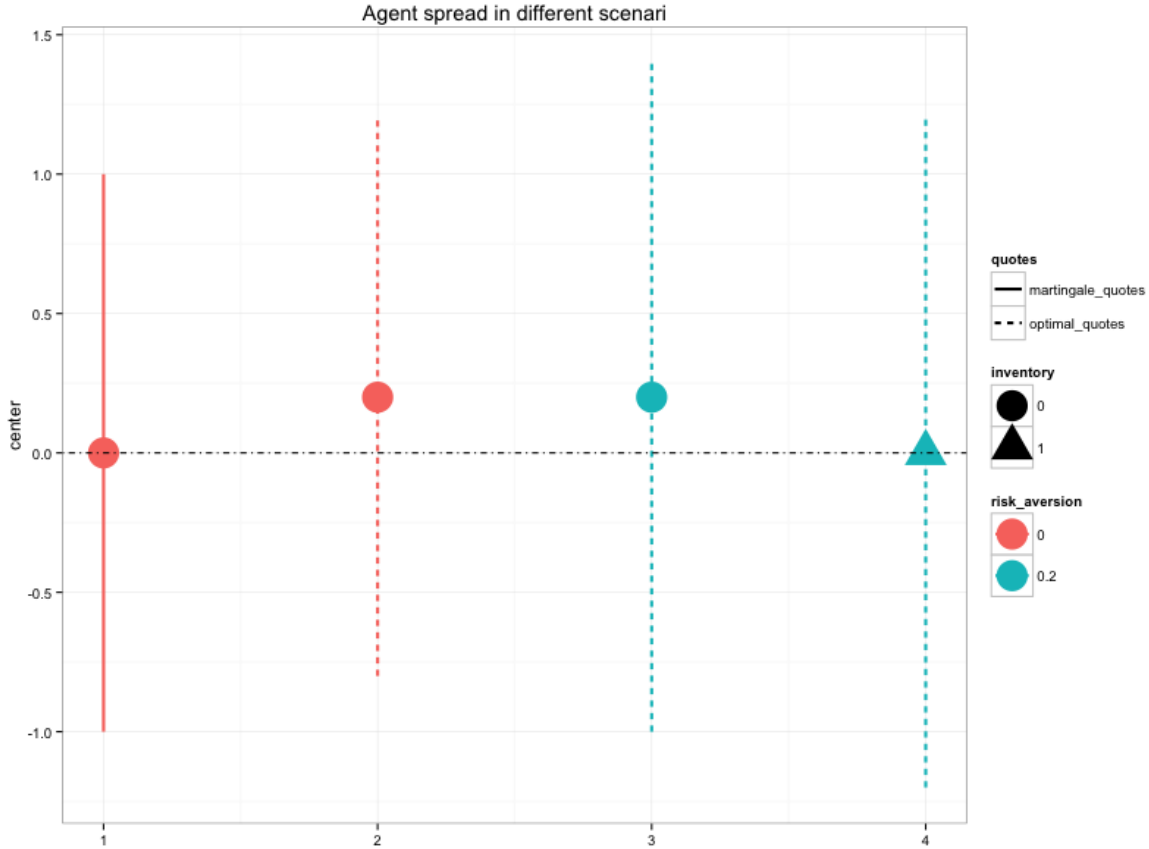

Figure 2.2: agent spread in different scenarios.

2.4   Examples

In this two examples we focus on the small martingale deviation policies into two different cases:

i) the first example considers a mean reverting process with stochastic (local) drift and constant quadratic variation (Ornstein Uhlenbeck);

ii) the second example is an arithmetic process with constant drift and mean reverting positive volatility (e.g. the arithmetic Heston model).

The two examples considers two classical generalisations of the drifted Brownian motion, one enriching the drift structure, the other on the volatility one. Of course, the two examples can be combined to obtain an Ornstein Uhlenbeck process with CIR stochastic volatility. We have preferred to keep them separate in order to focus on one component at the time.

2.4.1 The Ornstein-Uhlenbeck process

Assume that the stock price follows[3]

$$dP_t = -aP_t dt + \sigma dW_t, \quad a, \sigma > 0.$$ (2.4.1)

In this case we have

$$\varepsilon(t, z) = p\left(e^{-a(T-t)} - 1\right),$$ (ε Ornstein-Uhlenbeck)

that goes to 0 when the parameter a does. Using (2.3.18) and (2.3.20), we are left to compute $\approx \rho_2$ and D to have an approximation of the value function and the optimal policy. We easily obtain:

$$\widetilde{\rho}_2(t, z) = \beta + \sigma^2(T - t),$$ ($\widetilde{\rho}_2$ Ornstein-Uhlenbeck)

$$D(t, z) := k\left(\beta + \frac{1}{2}\sigma^2(T - t)\right).$$ (D Ornstein-Uhlenbeck)

Thanks to the simple structure of the process, we are also able to provide an asymptotic expansion of $\mathbf{m}^{(\varepsilon)}$ for $(T - t) \to 0$, i.e. the market making gain for a risk neutral agent. Truncating (2.2.9) at the second order leads to[4]:

$$\mathbf{m}^{(\varepsilon)}(t, z) = 2c\left((T - t) + \psi(T - t, z)\right),$$ (2.4.2)

$$\psi(\tau, z) := k^2\left(\frac{\sigma^2\tau}{2a} + \frac{e^{-2a\tau} - 1}{2a}\left(\frac{\sigma^2}{2a} - p^2\right)\right) + \dots.$$ (2.4.3)

By (2.4.2), we notice a that the spread acts as a discount factor, while (2.4.3) is an increasing function of σ^2. More volatility means more risk, but also wider movements to anticipate, and the agent can exploit this information to improve her performance. The model independent part (τ) corresponds to the uninformed trader, who sees the process as a Brownian motion (notice that the Brownian motion volatility does not come into play). Notice that

$$\frac{\psi(t, z)}{\tau} \approx k^2\frac{\sigma^2}{2a} + \dots, \quad \text{as } \tau \to \infty,$$

where $1 + k^2\frac{\sigma^2}{2a}$ can be used as an approximation of the market-making mean gain per time unit.

2.4.2 The arithmetic Heston model

The Ornstein Uhlenbeck process provides an excellent example of a how a local drift deforms the martingale market making policy. Now instead, we focus on a stochastic volatility model, i.e. an arithmetic model with mean reverting volatility. We assume that

$$dP_t = \alpha_t dt + \sigma_t dW_t,$$
$$d\sigma_t^2 = a(\sigma_\infty^2 - \sigma_t^2)dt + \nu\sigma_t dB_t, \quad a, \sigma_\infty^2, \nu > 0,$$
$$d\langle W, B\rangle_t = \rho dt.$$

---

[3]Without loss of generality, we assume the stock price mean reverts to 0, since for any other value p_∞, replacing P_t by $P_t - p_\infty$ we would fall in the previous case.

[4]Computations are provided by `sympy`, an open source symbolic calculation written in `Python`, that we suggest if one wants to calculate further orders of the Taylor series.

In this case the Markov system is given by $(t, Z_t) = (t, P_t, \sigma_t^2)$, and, choosing $\alpha_t = \mu$ as a constant drift, we have

$$\varepsilon(t, z) = \mathbb{E}_{t,z}\left[\int_t^T \alpha_s ds\right] = \mu(T - t). \qquad (\varepsilon \text{ Heston})$$

We now are interested in determining $\widetilde{\rho}_2$ and D, that, injected in (2.3.20) and (2.3.18), provide an approximation for the value function and the optimal policy. Notice that, by the Itô formula, defining

$$\bar{\sigma}_t^2 := e^{at}(\sigma_t^2 - \sigma_\infty^2),$$

we have

$$d\bar{\sigma}_t^2 = ae^{at}(\sigma_t^2 - \sigma_\infty^2) + e^{at}(a(\sigma_\infty^2 - \sigma_t^2)dt + \nu\sigma_t dB_t) = e^{at}\nu\sigma_t dB_t,$$

which implies that $(\bar{\sigma}_t^2)$ is a local-martingale. From [27], we know that for $2a\sigma_\infty^2 > \nu^2$ this local martingale is actually a positive martingale. Using the martingale property, We obtain

$$\begin{aligned}
\mathbb{E}_{u,Z_u}\left[\int_u^T \sigma_s^2 ds\right] &= \mathbb{E}_{u,Z_u}\left[\int_u^T e^{-as}\bar{\sigma}_s^2 ds\right] + \sigma_\infty^2(T - u) \\
&= \bar{\sigma}_u^2\int_u^T e^{-as}ds + \sigma_\infty^2(T - u) \\
&= (\sigma_u^2 - \sigma_\infty^2)\frac{1 - e^{-a(T-u)}}{a} + \sigma_\infty^2(T - u),
\end{aligned}$$

which implies

$$\widetilde{\rho}_2(t, z) = \beta + (\sigma^2 - \sigma_\infty^2)\frac{1 - e^{-a(T-t)}}{a} + \sigma_\infty^2(T - t). \qquad (\widetilde{\rho}_2 \text{ Heston})$$

Integrating both terms, using once again the martingale property,

$$\mathbb{E}_{t,z}\left[\int_t^T (\sigma_u^2 - \sigma_\infty^2)\frac{1 - e^{-a(T-u)}}{a}du\right] = (\sigma_t^2 - \sigma_\infty^2)\frac{e^{-a(T-t)} - 1 + a(T - t)}{a^2}$$

$$\mathbb{E}_{t,z}\left[\int_t^T \sigma_\infty^2(T - u)du\right] = \frac{1}{2}\sigma_\infty^2(T - t),$$

and finally

$$\widetilde{\rho}_0(t, z) = \beta(T - t) + \frac{1}{2}(\sigma^2 - \sigma_\infty^2)\frac{e^{-a(T-t)} - 1 + a(T - t)}{2a^2} + \frac{1}{2}\sigma_\infty^2(T - t)$$

$$D(t, z) = k\left(\beta + \frac{1}{2}(\sigma^2 - \sigma_\infty^2)\frac{e^{-a(T-t)} - 1 + a(T - t)}{2a^2(T - t)} + \frac{1}{2}\sigma_\infty^2\right). \qquad (D \text{ Heston})$$

2.5 Numerical experiments

We test the small martingale deviation policy for the Ornstein-Uhlenbeck dynamic (2.4.1) via numerical simulations, in order to prove that these explicit policies still give good results, both in terms of performances and inventory risk. These simulation are intended to show how the small martingale deviation policy associated to $\widetilde{\delta}_\pm^{(\eta,0)}$ (Policy 2.3) behaves with respect to the one associated to $\widetilde{\delta}_\pm^{(\eta,0)} = \widehat{\delta}_\pm^{(\eta,0)}$, where the stock price is considered as a martingale. The spread is assumed constant, while stock price is driven by (2.4.1). For all the Monte Carlo simulations, 10^4 trajectories are considered, while $T = 30$ minutes. The price, on short scales, has an arithmetic dynamic, so that translating the system in order to start at 0 is always possible: $p = 0$ is only a reference, and the price can take negative values.

The martingale policy against the small martingale deviation ones

As shown by Figure 2.4, the martingale policies loses in terms of performance against the small martingale deviation ones (which coincides with the optimal policies since $\eta = 0$) as expected, even though the performance profile has a lower variance. Including directional bets in market-making policy improves the average performance, but the directional nature leads to new variance and fatter distribution tails.

i) *Cautious agent:* an agent averse to portfolio variance should limit herself to a pure market-making policy, where no information of the evolution of the price is taken into account.

ii) *Risky agent:* an agent having market anticipation and who is ready to trade variance for profit, should play the small martingale deviation policy, mixing directional views and pure market-making.

The role of the transaction cost

As expected, a higher level of fixed costs reduces the policy performances, as shown by Figure 2.5.

The role of the risk aversion

As shown by Figure 2.6 and Figure 2.7, introducing risk aversion allows the agent to control her inventory, who reverts to zero as soon as it becomes too big. As a side effect, the agent performance is penalized in terms of profit, but not in terms of variance, which is considerably reduced. A higher risk aversion leads to more conservative strategies, where profit is not exchanged for variance: reducing distribution tail and variance have the highest priority, so that directional bets becomes not relevant for $\eta >> 0$.

2.6 Appendix: the multi-asset model

In this section we wish to extend the previous framework to the multidimensional case.

Notation

In this section we will use the following notations:

$\diamond$ $\forall v \in \mathbb{R}^n$, we will denote by v^i its ith component;

$\diamond$ $\mathbb{1}_n$ is the vector $(1, \ldots, 1) \in \mathbb{R}^n$;

$\diamond$ $\forall v_1, v_2 \in \mathbb{R}^n$, $v_1' v_2$ stands for the inner product in $\mathbb{R}^n$;

$\diamond$ $\forall v \in \mathbb{R}^n$, $\text{diag}(v)$ is the corresponding diagonal matrix filled by v;

$\diamond$ $\forall M \in \mathbb{R}^{n \times n}$, $\text{diag}(M)$ is the matrix diagonal.

The uncontrolled process: the mid-price and the spread

Assume that we have n different assets in n different markets. As in the scalar case, we assume that $(t, Z_t) = (t, P, \tilde{P}_t)$ is a Markov process, such that

$$\varepsilon_i(t, z) := \mathbb{E}_{t,z}[(P_i)_T] - p_i = \mathbb{E}_{t,z}\left[\int_t^T \alpha_i(u, Z_u)\, du\right], \quad i = 1, \ldots, n$$

$$\langle P_i, P_j \rangle_t := \Sigma_{ij}^2(t, Z_t) dt, \quad i, j = 1, \ldots, n.$$

The controlled processes: the agent wealth and the inventory process

As in the scalar case, we define an n-dimensional couple

$$\left(N_t^+, N_t^-\right) = \begin{pmatrix} (N_1^+)_t & (N_1^-)_t\,, \\ \vdots & \vdots\,, \\ (N_n^+)_t & (N_n^-)_t \end{pmatrix} \in \mathbb{R}^{n\times 2},$$

determining the limit order matching of all ask/bid limit orders posted on the n market: we assume that the ith component is a Cox process has **controlled** intensity decaying exponentially with $(\delta_\pm)_i$, depending on A_i and k_i, $i = 1, \ldots, n$, where all the components of the limit order matcher (N_t) are assumed independent between each other, in order to ease computation. With these notations, the wealth and the inventory have the same dynamic of the uni-dimensional case, i.e. the agent wealth and inventory follow

$$dX_t\left[\delta_\pm\right] = \sum_{\nu \in \pm} \left(\nu P_t + (\delta_\nu)_t - \varphi\right)' dN_t^\nu\left[\delta_\pm\right]\,, \quad X_t \in \mathbb{R}\,, \tag{2.6.1}$$

$$dY_t\left[\delta_\pm\right] = dN_t^-\left[\delta_\pm\right] - dN_t^+\left[\delta_\pm\right]\,, \quad Y_t \in \mathbb{Z}^n\,. \tag{2.6.2}$$

Notice that in the multi-dimensional case, **the wealth process** (X_t) **is a scalar process**, while the inventory (Y_t) lives in $\mathbb{Z}^n$.

The stochastic optimal control problem

As in (see (2.1.6)), the target of the agent is to find an optimal policy $((\delta_\pm)_t)$ maximizing her utility function, i.e.

$$\mathbf{u}^{(\eta,\varepsilon)}(t, x, y, z) := \max_{(\delta_\pm)_t} \mathbf{j}^{(\eta,\varepsilon)}(t, x, y, z; \delta_\pm)\,, \tag{2.6.3}$$

$$\mathbf{j}^{(\eta,\varepsilon)}(t, x, y, z; \delta_\pm) := \mathbb{E}_{t,x,y,z}\left[X_T\left[\delta_\pm\right] + Y_T'\left[\delta_\pm\right] P_T - \eta\left(\Omega_T^{(1)}\left[\delta_\pm\right] + \int_t^T \Omega_u^{(2)}\left[\delta_\pm\right] du\right)\right]\,,$$

where

$$\Omega_T^{(1)}\left[\delta_\pm\right] := \sum_{i=1}^n \beta_i \left(Y_i^2\right)_T\left[\delta_\pm\right] \geq 0\,, \beta_i \geq 0$$

$$\Omega_t^{(2)}\left[\delta_\pm\right] := Y_t'\left[\delta_\pm\right] \Sigma^2(t, Z_t) Y_t\left[\delta_\pm\right] \geq 0\,.$$

An important consequence of the choice of $\Omega^{(2)}$ is that the agent limit orders would not drive her portfolio towards a smaller portfolio in the canonical L2-norm sense, but towards a smaller portfolio in the L2-norm induces by Σ. One can imagine this risk reduction as an attempt of the agent to drag the portfolio towards the position $(0, \ldots, 0) \in \mathbb{Z}^n \subseteq \mathbb{R}^n$: in order to do so the agent choses the smallest path from Y_t to 0, whose length is given in the metric induced by inner product associated to the volatility matrix and not identity one!

The stochastic optimal control problem and the associated HJB equation

The HJB equation associated to (2.6.3) is given by

$$-\left(\partial_t + \mathcal{L}\right)\mathfrak{g} - \sum_{i=1}^n \sum_{\nu \in \pm} \max_\delta A_i e^{-k_i \delta} \Delta\mathfrak{g}(t, x \pm \nu p_i + \delta - \varphi_i, y \mp \nu e_i, z) = \eta \sum_{i,j=1}^n \Sigma_{ij}^2 y_i y_j\,,$$

$$\mathfrak{g}(T,) = -\eta \sum_{i=1}^n \beta_i y_i^2\,,$$

where $\mathcal{L}$ is the infinitesimal generator of (P_t).

2.6.1 The no risk aversion case

We again use perturbation methods on η: for this we first need the solution in the special case $\eta = 0$. Using the same technique of Proposition 2.1, we obtain, after tedious but straightforward calculations, the following result.

PROPOSITION 2.3. *In the no risk aversion case, the value function associated to the control problem (2.6.3) is*

$$\mathbf{u}^{(0,\varepsilon)} = \underbrace{x + y'\mathbf{h}^{(\varepsilon)}}_{\text{buy-and-hold}} + \underbrace{\mathbb{1}_n' \, \mathbf{m}^{(\varepsilon)}}_{\text{market-making}} \quad , \quad \mathbf{m}^{(\varepsilon)}, \mathbf{h}^{(\varepsilon)} \in \mathbb{R}^n \, ,$$

with

$$\mathbf{h}_i^{(\varepsilon)}(t, z) := p_i + \varepsilon_i(t, z) \, ,$$

$$\mathbf{m}_i^{(\varepsilon)}(t, z) := 2c_i \, \mathbb{E}_{t,z}\left[\int_t^T \cosh\left(k_i \varepsilon_i(u, Z_u)\right) du\right] \, , \quad c_i := \frac{A_i}{k_i} e^{-k_i(1/k_i + \varphi_i)} \, . \tag{2.6.4}$$

Finally, optimal controls are given by

$$\delta_{\pm}^{(0,\varepsilon)} = 1/k + \varphi \pm \varepsilon \in \mathbb{R}^n \, . \tag{2.6.5}$$

2.6.2 The case of small risk aversion under small martingale deviation

We now switch to general case of $\eta \to 0^+$. We generalize Theorem 2.2, and leave the vectorial case of Theorem 2.1 to the reader.

THEOREM 2.3 (Risk averse agent detaining small martingale deviation). *For $\eta \downarrow 0$ and $\epsilon \downarrow 0$, the solution of the optimal control problem (2.1.6) is given by*

$$\mathbf{u}^{(\eta,\varepsilon)} \approx \widetilde{\mathbf{u}}^{(\eta,\varepsilon)} = \mathbf{u}^{(0,0)} + \underbrace{y'\varepsilon}_{\text{directional}} - \underbrace{\eta\left(\widetilde{\rho}_0 + y'\widetilde{\rho}_2 y\right)}_{\text{risk aversion}}, \tag{2.6.6}$$

where $\mathbf{u}^{(0,0)}$ is the solution for $\eta = 0$ (Proposition 2.3), and

$$\widetilde{\rho}_2(t, z) := \operatorname{diag}(\beta_1, \dots, \beta_n) + \mathbb{E}_{t,z}\left[\int_t^T \Sigma^2(u, Z_u) du\right] \in \mathbb{R}^{n \times n} \, , \tag{2.6.7}$$

$$\widetilde{\rho}_0(t, z) := \sum_{i=1}^n 2k_i c_i \left(\beta_i(T - t) + \mathbb{E}_{t,z}\left[\int_t^T \int_u^T \Sigma_{ii}^2(\xi, Z_\xi) d\xi \, du\right]\right) \in \mathbb{R} \, . \tag{2.6.8}$$

Furthermore, optimal controls (in vectorial form) are approximated by

$$\delta_{\pm}^{(\eta,\varepsilon)} \approx \widetilde{\delta}_{\pm}^{(\eta,\varepsilon)} := \delta_{\pm}^{(0,0)} \underbrace{\pm\varepsilon(t, z)}_{\text{directional}} + \underbrace{\eta\left(\operatorname{diag}\left(\widetilde{\rho}_2\right) \pm 2\widetilde{\rho}_2 y\right)}_{\text{risk-aversion}},$$

where $\delta_{\pm}^{(0,\varepsilon)}$ are given by (2.6.5).

Proof. We briefly recall the main steps of the proof, which mimics the one of Theorem 2.2. Using the ansatz

$$\mathbf{u}^{(0,0)}(t, x, y, z) - \eta\mathfrak{g}(t, y, z) \, ,$$

the ith components of the optimal controls is given by

$$1/k_i + \varphi_i \pm \varepsilon_i(t, z) + \eta\Delta\mathfrak{g}(t, y \mp e_i, z) = \delta_{\pm}^{(0,\varepsilon)}(t, z)_i + \eta\Delta\mathfrak{g}(t, y \mp e_i, z) \, , \tag{2.6.9}$$

and following the proof of Theorem 2.2, taking into account the necessary vectorial adjustment, we find a linear approximation in ε and η taking $\mathfrak{g}$ as solution of

$$-(\partial_t + \mathcal{L})\mathfrak{g} - \sum_{i=1}^{n} k_i c_i \sum_{\nu \in \pm} \Delta\mathfrak{g}(t, y - \nu e_i, z) = \sum_{i,j=1}^{n} \Sigma_{ij}^2 y_i y_j \,,$$

$$\mathfrak{g}(T,) = \sum_{i=1}^{n} \beta_i y_i^2 \,.$$

Using the ansatz $\mathfrak{g}(t, y, z) := \widetilde{\rho}_0(t, z) + y'\widetilde{\rho}_2(t, z)y$, we obtain

$$\Delta\mathfrak{g}(t, y - e_i, z) + \Delta\mathfrak{g}(t, y + e_i, z) = 2e_i'\widetilde{\rho}_2(t, z)e_i \,, \quad i = 1, \ldots, n \,,$$

which leads to

$$-(\partial_t + \mathcal{L})\left(\widetilde{\rho}_0 + y'\widetilde{\rho}_2 y\right) - 2\sum_{i=1}^{n} k_i c_i e_i'\widetilde{\rho}_2 e_i = \sum_{i,j=1}^{n} \Sigma_{ij}^2 y_i y_j \,,$$

$$\widetilde{\rho}_0(T,) + y'\widetilde{\rho}_2(T,)y = \sum_{i=1}^{n} \beta_i y_i^2 \,.$$

Once again, splitting by the inventory degree we obtain

$$-(\partial_t + \mathcal{L})\widetilde{\rho}_2 = \Sigma \,, \quad \widetilde{\rho}_2(T,) = \mathrm{diag}\left(\beta_1, \ldots, \beta_n\right) \,,$$

(where the previous system is meant for all component-wise), whose solution is (2.6.7), while

$$-(\partial_t + \mathcal{L})\widetilde{\rho}_0 - 2\sum_{i=1}^{n} k_i c_i e_i'\widetilde{\rho}_2 e_i = 0 \,, \quad \widetilde{\rho}_0(T,) = 0 \,,$$

whose solution is given by (2.6.8). Finally, approximated controls are determined injecting $\mathfrak{g}$ in (2.6.9).

$\square$

Approximation error = max |v−v_approx|
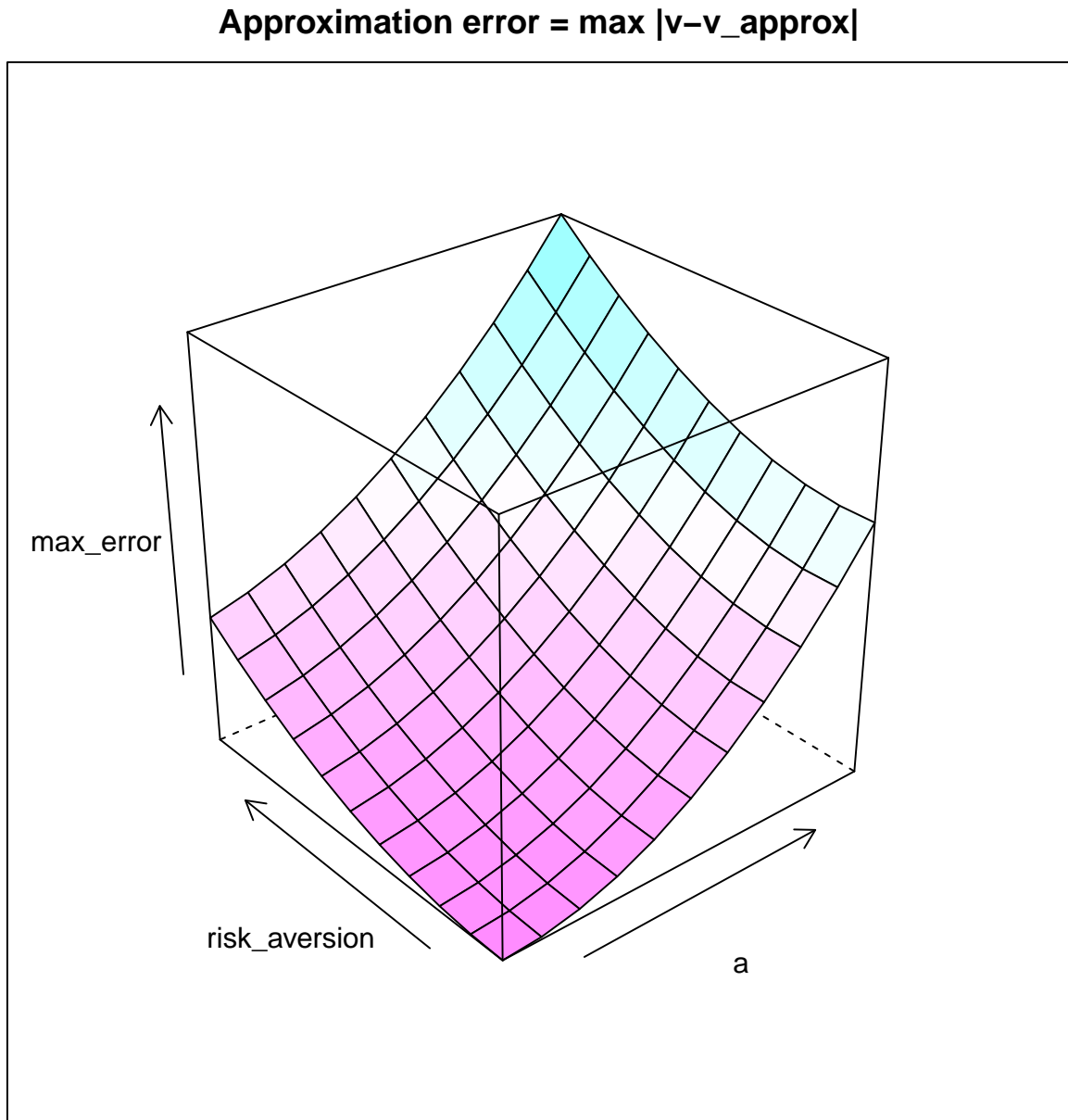
Figure 2.3: (numerically computed) approximation error, i.e. $||\mathbf{u}^{(\theta,\eta)} - \mathbf{u}^{(\theta,\eta)}||_\infty$ letting go η and the a parameter of the Ornstein Uhlenbeck (see (2.4.1)) towards 0.
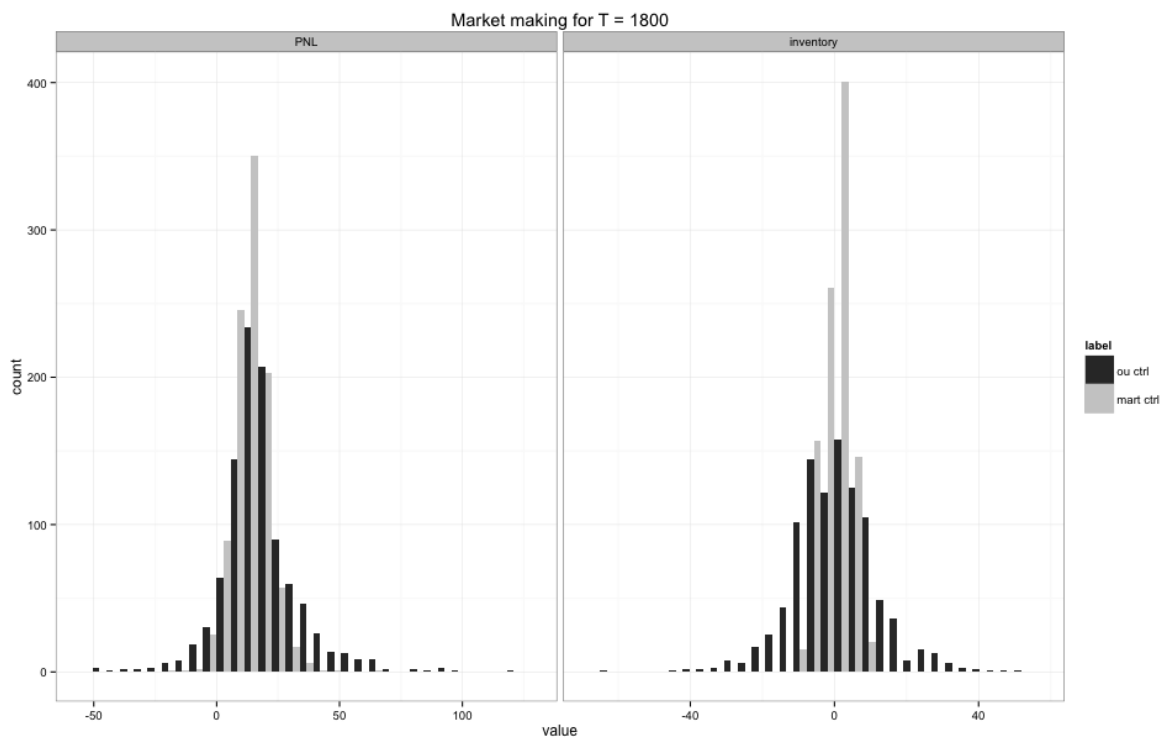
Figure 2.4: Monte Carlo simulation comparing the small martingale deviation policies agains the martingale ones for $\eta = 0$.
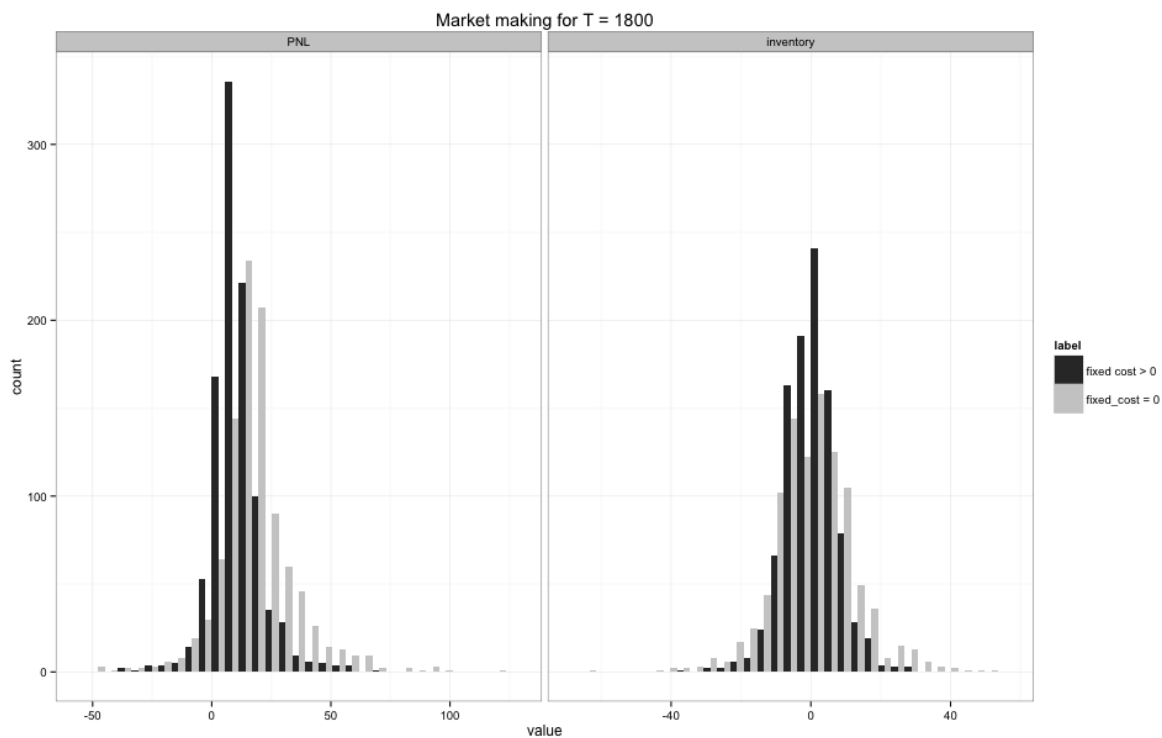
Figure 2.5: Monte Carlo simulation of the small martingale deviation policy for different value of the transaction cost parameter φ.
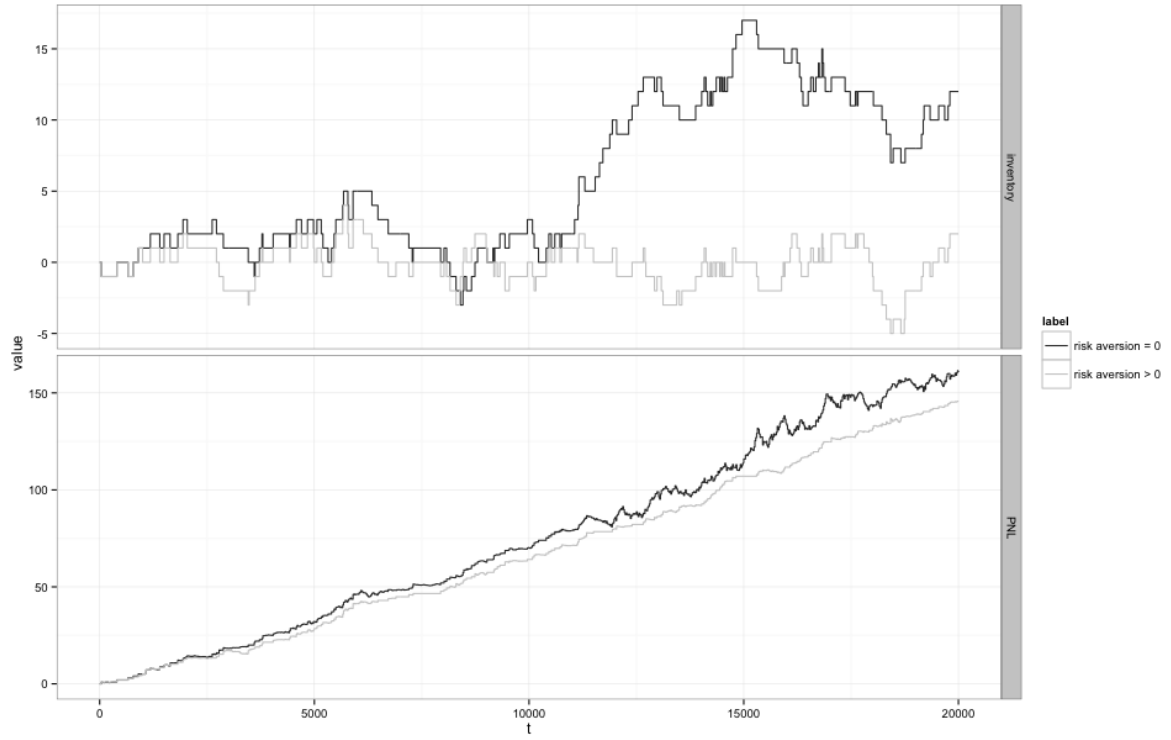
Figure 2.6: one trading trajectory (on a large horizon) for the small martingale deviation policies for different value of the risk aversion parameter η.
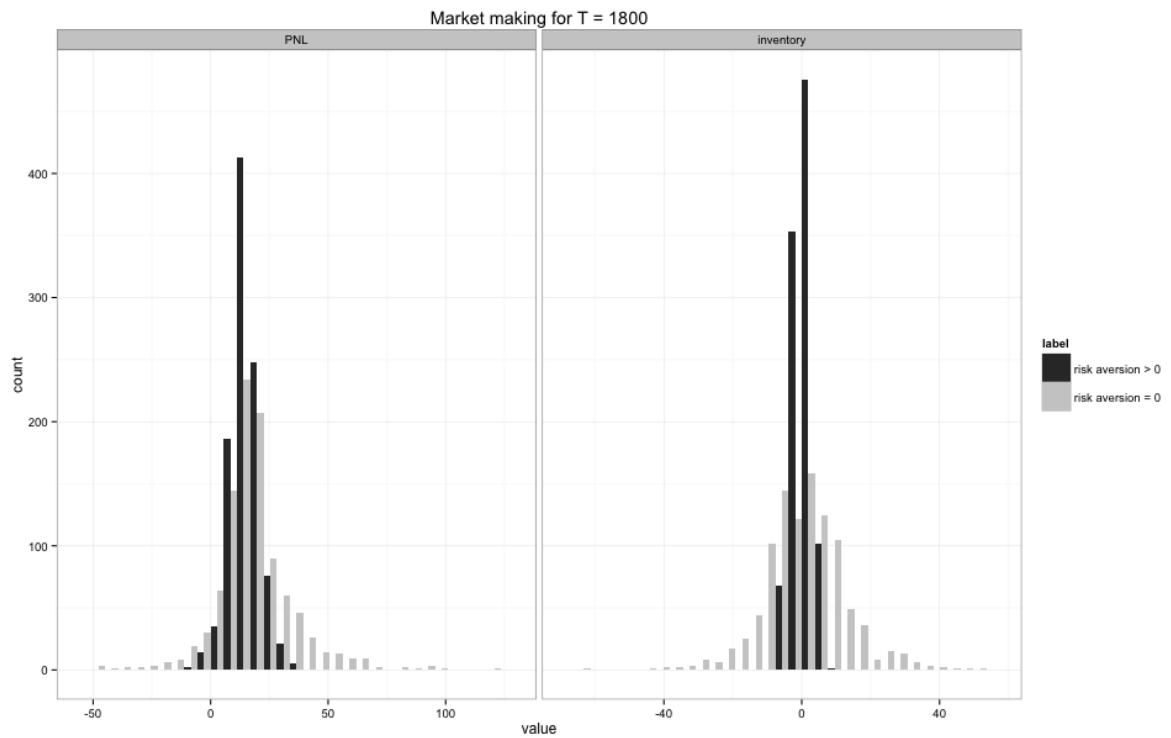
Figure 2.7: Monte Carlo simulation of the small martingale deviation policy for different value of the risk aversion parameter η.

Chapter 3

Semi Markov model for market microstructure

Abstract

We introduce a new model based on Markov renewal processes describing the fluctuations of a tick-by-tick single asset price. We consider a point process associated to the timestamps of the price jumps, with marks associated to price increments. By modeling the marks with a suitable Markov chain, we can reproduce the strong mean-reversion of price returns, a phenomenon known as microstructure noise. Moreover, using Markov renewal processes, we can model the alternating of time intervals with high and low market activity, and consider dependence between price increments and jump times. We also provide simple parametric and non-parametric statistical procedures for the estimation of our model. We obtain closed-form formula for the mean signature plot, and show the diffusive behavior of our model at large scale limit. We illustrate our results by numerical simulations, and find that our model is consistent with available empirical data.

Keywords: Microstructure noise, Markov renewal process, Signature plot, Scaling limit.

Introduction

The modelling of tick-by-tick asset prices has attracted a growing interest in the statistical and quantitative finance literature with the availability of high frequency data. It is basically split into two categories, according to the philosophy guiding the modeling.

- i) *The macro-to-micro (or econometric) approach:* (see e.g. [39], [3], [60]) it interprets the observed price as a noisy representation of an unobserved one, typically assumed to be a continuous Itô semi-martingale: in this framework several results exist on robust estimation of the realized volatility, but these models seem not to be adapted to high frequency trading problems and stochastic control techniques, mainly because the state variables are latent rather than observed. In this paper, we shall discuss in particular the uncertainty zones model introduced in [60], for which we detail the connections with our work.

- ii) The micro-to-macroscopic approach: (see e.g. [9], [7], [25], [1], [35], [17], [29] and [30]) it exploits point processes, in particular Hawkes and renewal processes (as in our case), to drive the asset price, either moving on the tick grid or on the real line. In contrast with the macro-to-microscopic approach, these models do not rely on the arguable assumption of the existence of a fair or fundamental price, focusing only on observable quantities, which makes the statistical estimation usually simpler. These models differ according to the magnifying glass used to look at the limit order book (LOB).

A first category, to which our paper belongs, describes the stock price directly: the choice of the point process determines entirely the model, since the stock price is considered as the primitive random component and no price formation is involved. In general, these models address problems as the reproduction of fine stylized facts concerning the stock price (in the multi-asset framework as well), but does not deal with other aspects of the electronic book. An example is provided by [7], where a bivariate Hawkes process describes the upwards and downwards jump of the stock price: a kernel rules the memory of the process while the branching matrix reproduces the microstructure noise. In this setting, result on the explosion of the signature plot and volatility clustering, as well as non-parametric estimation and diffusive limits are also available in the multi-asset case. Another example is provided by [29] and [30], where indexed and weighted semi-Markov chains describe the geometric returns of the asset price, focusing on the first passage time and the autocorrelation of returns, integrating theoretical results with numerical simulations.

A second category in this literature looks at the price dynamics as a result of an endogenous component plus the impact of the market order flow, and addresses a wide range of problems. A bridge between the previous category and this one is provided by the work [8], where a four-dimensional Hawkes process drives a single asset market, each component describing a different event in the book (trades at the best ask/bid, jump upwards/downwards of the stock price), and the price is driven by an endogenous component plus a market impact one. A completely different approach is presented in [19], where each trade determines a random, and possibly zero, revision of the log-price, which is assumed to be a continuous time process on $\mathbb{R}$, and a hidden Markov chain drives the market, inducing different arrival rates for trades and different reactions of the price for each regime. In [24] the authors address a different target (option pricing starting from a microstructure model) and exploit renewal processes to describe the trade inter-arrival times (which are seen as an i.i.d. sequence of positive random times), while the stock price moves, at the arrival of each trade, according to a continuous random variable independent of tick time process. In [23] instead, the stock price is the result of a diffusive exogenous component and a random drift which is determined by influential market orders arriving in the book and a mean-reverting component. The market order flow is modeled by a complex system of branched Hawkes processes, where investors are classified according to their influential status (e.g. institutional investors affecting the price drift) or not (e.g. small investors or market maker adjusting their position), and each group action determines a different jump

in the global market intensity. As an application, explicit optimal market making strategies are provided for asymptotically small risk aversions.

The autoregressive model of [34] models the timestamps between events with an autoregressive sequence representing the inter-arrival counterpart of the GARCH model commonly used for financial returns. Therefore, depending whether this model is used for trade inter-arrivals (as in the original paper) or for price jump, it may be classified into the first or the second category.

Finally, an extreme approach consists in modeling the entire limit order book (quotes, cancellation, trades, posting of limit order, etc...) and deducing the price consequently. The paper [26] describes an electronic market where every level is modified by the Poissonian arrival of new events (market orders, limit order postings or cancellations, etc...). In a similar fashion, the paper [25] focuses on the first levels of the book (best ask, best bid) and models the asymmetry in the liquidity provided by the two sides after every price jump. The trade flow is modeled by general point processes and the main results concern large-scale asymptotic diffusive behavior of the stock price. Other important contributions in the study of the limit order book shape and dynamics, with particular focus on the resilience and price formation, are given by [62] and [50].

A brief introduction to our work and connections to the existing literature

In this paper, we aim to provide a tractable tick-by-tick model for the price of liquid assets with large tick, in view of an application to an optimal high frequency trading problem (studied in the companion paper [37]). This feature guarantees that the bid-ask spread in the limit order book is almost always constant and equal to one tick, as shown in [31], and leads to a much easier modeling of the book itself. Our goal is to reproduce some of the well-known stylized facts on high frequency data, see e.g. [38], [14], such as:

i) *Microstructure noise:* high-frequency returns are extremely anticorrelated, leading to a short-term mean reversion effect, which is mechanically explicable by the structure of the limit order book. This effect manifests through an increase of the realized volatility estimator (*signature plot*) when the observation frequency decreases from large to fine scales.

ii) *Intermittence of durations:* markets alternates, independently of the intraday seasonality, between phases of high and low activity.

iii) *Diffusive behaviour:* at large scale, the price process displays a *diffusive* behaviour.

Our starting point is a model-free description of the mid-price, the arithmetic mean of the best bid and best ask quotes. The latter is a piecewise constant process defined by a random sequence (T_n, J_n), a marked point process where the timestamps (T_n) represent the jump times of the asset price associated to a counting process (N_t), and the marks (J_n) are the price increments. For the modeling of this bivariate sequence, we use a Markov renewal process (MRP). Markov renewal theory [53] is largely studied in reliability for describing failure of systems and machines, and one purpose of this paper is to show how it can be applied to market microstructure.

By considering a suitable Markov chain modeling for (J_n), we are able to reproduce the mean-reversion of price returns, while allowing arbitrary jump size, i.e. the price can jump of more than one tick. On the other hand, the counting process (N_t), which may depend on the Markov chain, models the jump activity, and in particular the alternation of high and low activity phases. Finally, MRPs ensure a Brownian motion behavior of the price process at macroscopic scales, which is consistent with the classic diffusive approach in the case of daily observations.

Our MRP model is a rather simple but robust model, easy to understand, simulate and estimate, both parametrically and non-parametrically. An important feature of the MRP approach is its semi-Markov property: the price process can be embedded into a Markov system with few additional and observable state variables, ensuring the tractability of the model for applications to market making and statistical arbitrage.

In the classification mentioned above, our paper is placed in the micro-to-macro-structure models describing directly the stock price. We underline that one of our main prerogative is to provide a model involving only observable variables, so that non-parametric estimation is easy and no optimization routine is necessary (as in [19] e.g.), which is a common issue when hidden components are present. This choice naturally leads us to deal with a piecewise constant price moving on the grid tick, where no diffusive components are present and where jumps are integer-valued (and not real-valued) processes. MRPs are powerful tools to model the dependence between jump timestamps and marks, dependence which is empirically shown (and theoretically supported by [25]), and for which an explanation relying on the nature of the LOB is provided. Since our goal is to give closed formula on stylized facts of the stock price, by modeling directly the latter and not its formation (trade = price movement), we obtain a simpler framework to deal with.

Plan of the paper

The outline of the paper is the following. In Section 3.1, we describe the MRP model for the asset mid-price, and provides statistical inference. We show how to simulate the model, and the semi-Markov property of the price process. We also discuss the comparison of our model with the uncertainty zones model, and Hawkes processes used for modeling asset prices and microstructure noise. Section 3.2 studies the diffusive limit of the asset price at macroscopic scale. In Section 3.3, we derive analytical formula for the mean signature plot, and compare with real data. We conclude by a paper summary and some possible extensions for future research.

Data sample

The used database is the EURIBOR 3M future (front contract) quoted on the LIFFE electronic platform (London), from 2010-01-04 to 2010-12-31, observed every day from 10:00 to 14:00 London time. In the Appendix we will perform an analysis of the EUROSTOXX 3M future quoted on the EUREX platform, from 2010-03-22 to 2010-06-18, observed from 10:00 to 11:00 Frankfurt time. For both assets, the analyzed price is the mid one, only those falling at the half of the tick. Since the bid-ask spread is 99% of the time equal to one tick, this corresponds to most of the observations.

3.1   Semi-Markov model

We describe the tick-by-tick fluctuation of a univariate stock price by means of a marked point process $(T_n, J_n)_{n \in \mathbb{N}}$. The increasing sequence (T_n) represents the jump (tick) times of the asset price, while the marks sequence (J_n) valued in the finite set

$$E = \{+1, -1, \ldots, +m, -m\} \subset \mathbb{Z} \setminus \{0\},$$

represents the price increments, where positive (resp. negative) marks stands for upwards (resp. downwards) jumps. The continuous-time price process is a piecewise constant, pure jump process, given by

$$P_t = P_0 + \sum_{n=1}^{N_t} J_n, \quad t \geq 0, \tag{3.1.1}$$

where (N_t) is the counting process associated to the tick times (T_n), i.e.

$$N_t = \inf \left\{ n : \sum_{k=1}^{n} T_k \leq t \right\}.$$

Here, we have normalized the tick size (the minimum variation of the price) to 1, and the asset price (P_t) is considered e.g. as the last quotation for the mid-price, i.e. the mean between the best-bid and best-ask price. Let us mention that the continuous time dynamics (3.1.1) is a model-free description of the piecewise constant price in the electronic market. We decouple the modeling of the jump activity via the point process (N_t), while the microstructure noise is described via the random marks (J_n).

3.1.1   Price return modelling

We write the price return as

$$J_n = \hat{J}_n \, \xi_n \,, \quad n \geq 1 \,, \tag{3.1.2}$$

where $\hat{J}_n := \text{sign}(J_n)$ valued in $\{-1, +1\}$ indicates whether the price jumps upwards or downwards, and $\xi_n := |J_n|$ is the absolute size of the price increment. In order to simplify the model and guarantee some explicit computations, we consider that the dependence of the price returns occurs through their direction, and assume that only the current price direction will impact the next jump one.

REMARK 3.1. *This assumption is not satisfied empirically as shown by the autocorrelation function of $(\hat{J}_n)$ (Figure 3.1), which displays the existence of long-lasting memory in the sequence. In particular the left side of Figure 3.1 exhibits an alternate-sign memory for $(\hat{J}_n)$, which translates into a positive autocorrelation function $(B_n := \hat{J}_{n-1}\hat{J}_n)$, as shown on the right side. However, the goal of this paper is to explain some basic stylized facts: since the microstructure noise and the explosion of the mean signature plot are essentially a consequence of the high-frequency mean reversion, a first order approximation as the Markov chain (3.1.2) fits our needs. Nevertheless, a more sophisticated model encoding the richer structure of the return sequence, and addressing in particular statistical arbitrage applications, is in our agenda.*
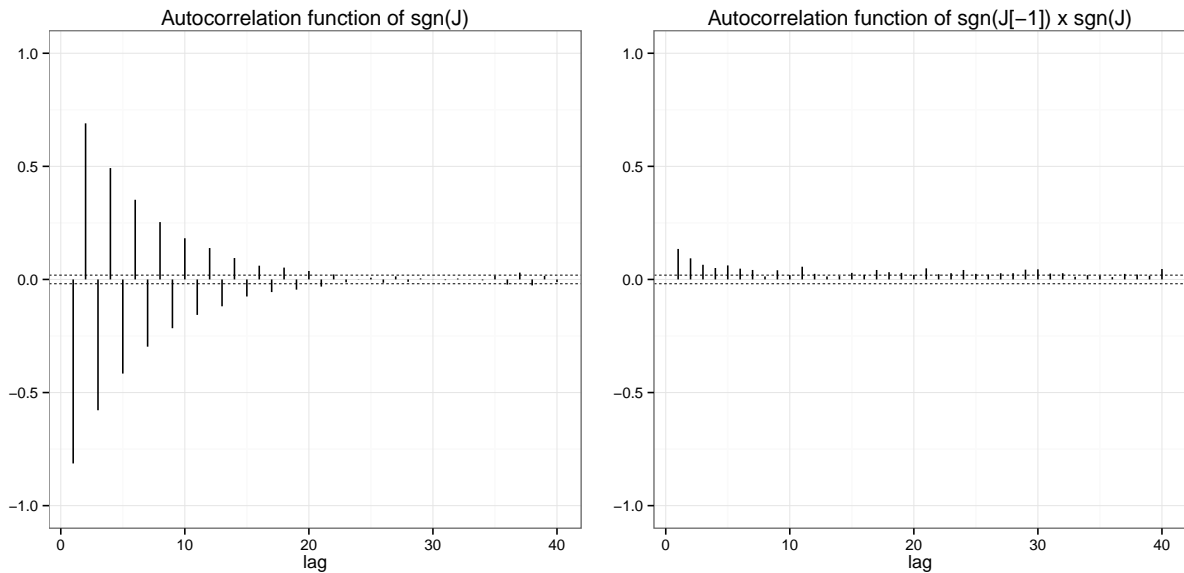
Figure 3.1: Autocorrelation function of the sequences $(\hat{J}_n)$ and $(\hat{J}_{n-1}\hat{J}_n)$.

Moreover, we assume that the absolute size of the price returns are independent and also independent of the direction of the jumps. Formally, this means that

⋄ $(\hat{J}_n)$ is an irreducible Markov chain with probability transition matrix

$$\hat{Q} = \begin{pmatrix} \frac{1+\alpha_+}{2} & \frac{1-\alpha_+}{2}, \\ \frac{1-\alpha_-}{2} & \frac{1+\alpha_-}{2} \end{pmatrix} \,, \tag{3.1.3}$$

with $\alpha_+, \alpha_- \in [-1, 1)$.

◇ (ξ_n) is an i.i.d. sequence valued in $\{1, \ldots, m\}$, independent of $(\hat{J}_n)$, with distribution law:
$p_i = \mathbb{P}[\xi_n = i] \in (0, 1)$, $i = 1, \ldots, m$.

In this case, (J_n) is an irreducible Markov chain with probability transition matrix given by

$$Q = \begin{pmatrix} p_1 \hat{Q} & \cdots & p_m \hat{Q} \\ \vdots & \ddots & \vdots \\ p_1 \hat{Q} & \cdots & p_m \hat{Q} \end{pmatrix}. \tag{3.1.4}$$

We could model in general (J_n) as a Markov chain with transition matrix $Q = (q_{ij})$ involving $2m(2m-1)$ parameters, while under the above assumption, the matrix Q in (3.1.4) involves only $m + 1$ parameters to be estimated. Actually, on real data, we often observe that the number of consecutive downward and consecutive upward jumps are roughly equal. One can easily see that

$$\alpha_\pm = \pm \mathbb{E}[\hat{J}_n \,|\, \hat{J}_{n-1} = \pm].$$

We have estimated the two empirical means: both a t-test and the intersection of their confidence interval, as shown in Figure 3.2, suggest that we can specialize to the *symmetric case* where

$$\alpha_+ = \alpha_- =: \alpha. \tag{3.1.5}$$
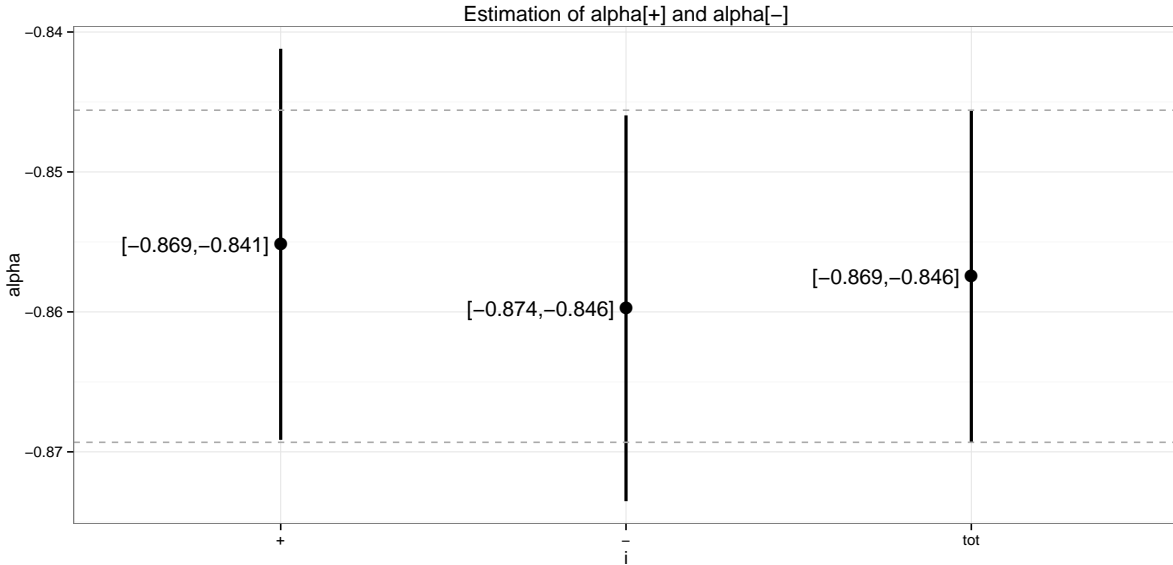
Figure 3.2: Estimation and confidence interval for $\alpha, \alpha_\pm$.

In this case, as shown by the following lemma, we have an intuitive interpretation of the parameter $\alpha \in [-1, 1)$ as the correlation between two consecutive price return directions: in the case $\alpha = 0$ price returns are independent, while when $\alpha < 0$ (resp. $\alpha > 0$) they are subjected to mean-reversion (resp. trends).

LEMMA 3.1. *In the symmetric case, the invariant distribution of the Markov chain $(\hat{J}_n)$ is $\hat{\pi} = (\frac{1}{2}, \frac{1}{2})$, and the invariant distribution of (J_n) is $\pi = (p_1 \hat{\pi}, \ldots, p_m \hat{\pi})$. Moreoever, we have:*

$$\alpha = \mathrm{corr}_\pi \left(\hat{J}_n, \hat{J}_{n-1} \right), \quad \forall n \geq 1, \tag{3.1.6}$$

where corr_π denotes the correlation under the stationary probability P_π starting from the initial distribution π.

Proof. We easily check that under the symmetric case, $\hat{\pi}\hat{Q} = \hat{\pi}$ for $\hat{\pi} = (1/2, 1/2)$, which means that $\hat{\pi}$ is the invariant distribution of the Markov chain $(\hat{J}_n)$. Consequently, $\pi = (p_1\hat{\pi}, \dots, p_m\hat{\pi})$ satisfies $\pi Q = \pi$, i.e. π is the invariant distribution of (J_n), and so under P_π, $(\hat{J}_n)$ (resp. (J_n)) is distributed according to $\hat{\pi}$ (resp. π). Therefore, $\mathbb{E}_\pi[\hat{J}_n] = 0$ and $\mathrm{Var}_\pi[\hat{J}_n] = 1$. We also have for all $n \geq 1$, by definition of $\hat{Q}$:

$$\mathbb{E}_\pi\left[\hat{J}_n\hat{J}_{n-1}\right] = \mathbb{E}_\pi\left[\frac{1+\alpha}{2}\left(\hat{J}_{n-1}\right)^2 - \frac{1-\alpha}{2}\left(\hat{J}_{n-1}\right)^2\right] = \alpha\,,$$

which proves the relation (3.1.6) for α.

$\square$

We also have another equivalent formulation of the Markov chain, whose proof is trivial and left to the reader.

LEMMA 3.2. *In the symmetric case, the Markov chain $(\hat{J}_n)$ can be written as:*

$$\hat{J}_n = \hat{J}_{n-1}B_n\,, \quad n \geq 1\,, \tag{3.1.7}$$

where (B_n) is a sequence of i.i.d. random variables with Bernoulli distribution on $\{-1, +1\}$, and parameter $(1+\alpha)/2$, i.e. of mean $\mathbb{E}[B_n] = \alpha$. The price increment Markov chain (J_n) can also be written in an explicit induction form as:

$$J_n = \hat{J}_{n-1}\zeta_n\,, \tag{3.1.8}$$

where (ζ_n) is a sequence of i.i.d. random variables valued in $E = \{+1, -1, \dots, +m, -m\}$, and with distribution

$$P[\zeta_n = k] = p_k(1 + sign(k)\alpha)/2\,.$$

The above lemma is useful for an efficient estimation of α. By the strong law of large numbers, we have a consistent estimator given by α:

$$\hat{\alpha}^{(n)} = \frac{1}{n}\sum_{k=1}^n \frac{\hat{J}_k}{\hat{J}_{k-1}} = \frac{1}{n}\sum_{k=1}^n \hat{J}_k\hat{J}_{k-1}\,.$$

The variance of this estimator is known, equal to $1/n$, so that the latter is efficient, with a confidence interval given by the central limit theorem:

$$\sqrt{n}(\hat{\alpha}^{(n)} - \alpha) \xrightarrow{(d)} \mathcal{N}(0, 1)\,, \quad \text{as } n \to \infty\,.$$

The estimated parameter for the chosen dataset is $\hat{\alpha} \approx -86\%$, which shows as expected a strong anticorrelation of price returns. Figure 3.3 shows the result of the estimation procedure: splitting the sample in three consecutive and disjoint subsamples, the corresponding confidence intervals intersect both with each other and with the one obtained by estimation on the whole dataset. This proves the stability of the estimator over time.

In the case of several tick jumps $m > 1$, the probability $p_i = P[\xi_n = i]$ may be estimated from the classical empirical frequency

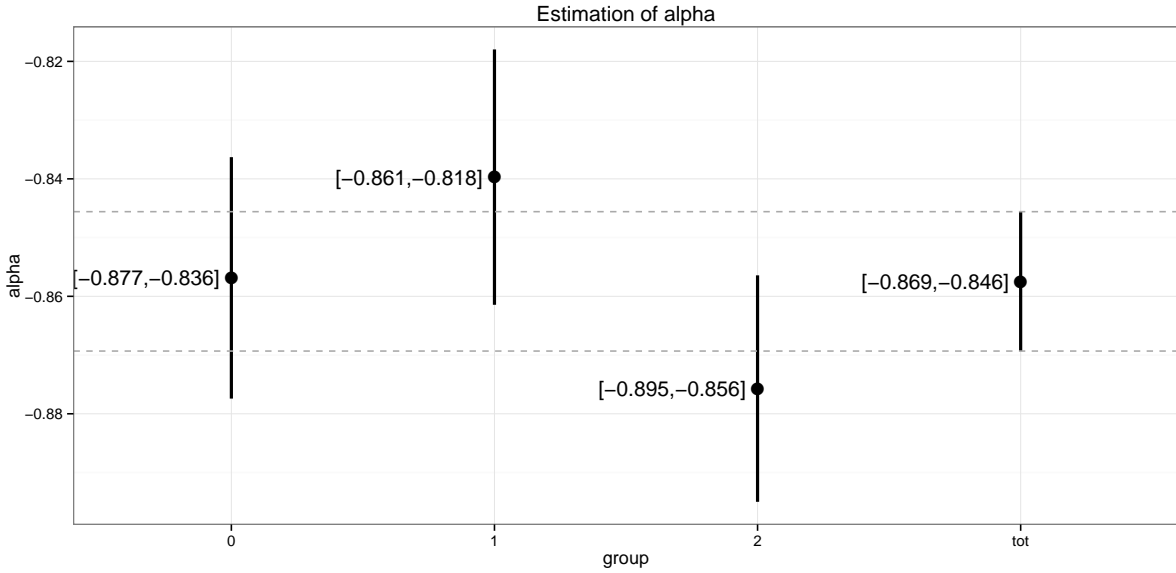$$\hat{p}_i^{(n)} = \frac{1}{n}\sum_{k=1}^n \mathbb{1}\{\xi_k = i\}\,, \quad i = 1, \dots, m\,.$$

Figure 3.3: confidence intervals for the estimators $\hat{\alpha}$ and $\hat{\alpha}_i, i = 1, 2, 3$, where $\hat{\alpha}_i$ are obtained by partitioning the sample in three disjoint and consecutive subsamples and performing estimation on each one.

3.1.2 Tick times modeling

In order to describe the jump activity, we consider a counting process (N_t) with stochastic intensity decaying while the stock price is constant and bumping up when the latter jumps. In this paper we investigate a model based on Markov renewal processes. In what follows, we briefly recall the standard setting, mainly to fix notations.

Let us denote by $S_n = T_n - T_{n-1}$, $n \geq 1$, the inter-arrival times associated to (N_t). We assume that conditionally on the jump marks (J_n), (S_n) is an independent sequence of positive random times, with distribution depending on the current and next jump mark:

$$F_{ij}(t) = P[S_{n+1} \leq t | J_n = i, J_{n+1} = j], \quad (i, j) \in E.$$

We then say that (T_n, J_n) is a Markov Renewal Process (MRP) with transition kernel:

$$P[J_{n+1} = j, S_{n+1} \leq t | J_n = i] = q_{ij} F_{ij}(t), \quad (i, j) \in E,$$

In the particular case where F_{ij} does not depend on i, j, the point process (N_t) is independent of (J_n), and called a renewal process. Moreover, if F is the exponential distribution, N is a Poisson process. Here, we allow in general dependency between jump marks and renewal times, and we refer to the symmetric case when F_{ij} depends only on the sign of ij, by setting

$$\begin{aligned}
F_+(t) &= F_{ij}(t), \quad ij > 0, \\
F_-(t) &= F_{ij}(t), \quad ij < 0.
\end{aligned} \tag{3.1.9}$$

In other words, F_+ (resp. F_-) is the distribution function of inter-arrival times given two consecutive jumps in the same (resp. opposite) direction, called trend (resp. mean-reverting) case.

REMARK 3.2 (Connection to the uncertainty zones model). *A classical approach for modeling microstructure noise in the financial econometrics literature is to consider an additive noise independent of a latent efficient price process. Recently, in the works [60] and [61], the authors propose to make endogenous the microstructure noise through a model with uncertainty zones. Their model (in short UZM) is basically constructed as follows. Starting from a continuous time Itô process X representing the efficient price, they define the times (T_n) of change in transaction price as the exit times of the efficient price from uncertainty zones of size , a around the mid-tick*

grid value. The associated transaction price P_{T_n} is then defined as the value of X_{T_n} rounded to the nearest multiple of the tick size, and $(P_t)_{t\geq 0}$ is the càd-làg piecewise constant process built from (T_n, P_{T_n}). Denoting by $J_n = P_{T_n} - P_{T_{n-1}}$ the price increments, and in the case where X is a Brownian motion, it appears that (T_n, J_n) is a Markov renewal process with symmetric kernel.

   i) *Conditional distribution: F_+ and F_- are given by the first hitting time distribution of the Brownian motion against $\mathcal{B}_+$ and $\mathcal{B}_-$, where the two barriers are given by*

$$\mathcal{B}_+ = 1,$$
$$\mathcal{B}_- = \frac{1}{2a}.$$

   This is due to the fact that when the latent price hits a barrier, we know its value, which coincides with the barrier itself. Now the latent price can either hit the closest barrier, at distance $\mathcal{B}_-$, causing a reversion ($B_n = -1$), or the farther one, at distance $\mathcal{B}_+$, causing a trend ($B_n = +1$). So, conditionally to $B_n = \pm$, the next jump time is distributed as the first hitting time of the latent price against $\mathcal{B}_\pm$.

   ii) *Marks: (J_n) is a $\{\pm\}$-valued Markov chain with symmetric transition matrix, where the relation between the bandwidth size , a and α is explicitly given by*

$$\alpha = \frac{2a - 1}{2a + 1}.$$

   Indeed, since Brownian motion is a martingale with constant volatility, we have: $B_n = +1$ (resp. $B_n = -1$) if the latent price hits $\mathcal{B}_+$ (resp. $\mathcal{B}_-$) first, which happens with probability $\frac{2a}{1+2a}$ (resp. $\frac{1}{1+2a}$), and leads to the above formula.

Let us now introduce the marked hazard function:

$$h_{ij}(t) = \lim_{\delta \downarrow 0} \frac{1}{\delta} P[t \leq S_{n+1} \leq t + \delta, \, J_{n+1} = j | S_n \geq t, \, J_n = i], \quad t \geq 0, \qquad (3.1.10)$$

for $i, j \in E$, which represents the instantaneous probability of a jump with mark j, given that there have not been any jump during the elapsed time t, and the current mark is i. By assuming that the distributions F_{ij} of the renewal times S_n admit a density f_{ij}, we may write h_{ij} as:

$$h_{ij}(t) = q_{ij} \frac{f_{ij}(t)}{1 - \sum_{j \in E} q_{ij} F_{ij}(t)} =: q_{ij} \lambda_{ij},$$

where

$$\sum_{j \in E} q_{ij} F_{ij}(t) = P[S_{n+1} \leq t | J_n = i],$$

is the conditional distribution of the renewal time in state i. In the symmetric case (3.1.5), (3.1.9), we have

$$h_{ij}(t) = p_j \left(\frac{1 + \text{sign}(ij)\alpha}{2} \right) \lambda_{\text{sign}(ij)}(t),$$

with jump intensity

$$\lambda_\pm(t) = \frac{f_\pm(t)}{1 - F(t)}, \qquad (3.1.11)$$

where $f_\pm$ is the density of $F_\pm$, and

$$F(t) = \frac{1 + \alpha}{2} F_+(t) + \frac{1 - \alpha}{2} F_-(t).$$

Markov renewal processes are used in many applications, especially in reliability. Classical examples of renewal distribution functions are the ones corresponding to the Gamma and Weibull distribution, with density given by:

$$f_{Gam}(t) = \frac{t^{\beta-1}e^{-t/\theta}}{\Gamma(\beta)\theta^{\beta}},$$

$$f_{Wei}(t) = \frac{\beta}{\theta}\left(\frac{t}{\theta}\right)^{\beta-1}e^{-\beta t/\theta},$$

where $\beta > 0$, and $\theta > 0$ are the shape and scale parameters, and Γ (resp. Γ_t) is the Gamma (resp. lower incomplete Gamma) function:

$$\Gamma(\beta) = \int_0^{\infty} s^{\beta-1}e^{-s}ds,$$

$$\Gamma_t(\beta) = \int_0^{t} s^{\beta-1}e^{-s}ds. \tag{3.1.12}$$

3.1.3   Statistical inference

We design simple statistical procedures for the estimation of the distribution and jump intensities of the renewal times. Over an observation period, pick a subsample of i.i.d. data

$$\{S_k = T_k - T_{k-1} : k : J_{k-1} = i, J_k = j\},$$

and set

$$I_{ij} := \{k : J_{k-1} = i, J_k = j\},$$
$$I_i := \{k : J_{k-1} = i\},$$

with cardinality respectively n_{ij} and n_i. In the symmetric case, we also denote by

$$I_{\pm} := \{k : sgn(J_{k-1}J_k) = \pm\},$$

with cardinality $n_{\pm}$. We describe both parametric and non-parametric estimation.

Parametric estimation.

We discuss the parametric estimation of the distribution F_{ij} of the renewal times when considering Gamma or Weibull distributions with shape and scale parameters β_{ij}, θ_{ij}. We can indeed consider the Maximum Likelihood Estimator (MLE) $(\hat{\beta}_{ij}, \hat{\theta}_{ij})$, which are solution to the equations:

$$\ln\hat{\beta}_{ij} - \frac{\Gamma'(\hat{\beta}_{ij})}{\Gamma(\hat{\beta}_{ij})} = \ln\left(\frac{1}{n_{ij}}\sum_{k=1}^{n_{ij}}S_k\right) - \frac{1}{N}\sum_{k=1}^{n_{ij}}\ln S_k,$$

$$\hat{\theta}_{ij} = \frac{1}{\hat{\beta}_{ij}}\bar{S}_{n_{ij}}, \quad \bar{S}_{n_{ij}} := \frac{1}{n_{ij}}\sum_{k=1}^{n_{ij}}S_k.$$

There is no closed-form solution for $\hat{\beta}_{ij}$, which can be obtained numerically e.g. by Newton method. Alternatively, since the first two moments of the Gamma distribution $S \rightsquigarrow \Gamma(\beta, \theta)$ are explicitly given in terms of the shape and scale parameters, namely:

$$\beta = \frac{\mathbb{E}[S]^2}{\text{Var}[S]},$$

$$\frac{1}{\theta} = \frac{\mathbb{E}[S]}{\text{Var}[S]}, \tag{3.1.13}$$

i	j	shape	scale
+1	+1	0.27651097	2187
-1	-1	0.2806104	2565.371
+1	-1	0.07442401	1606.308
-1	+1	0.06840708	1508.155

Table 3.1: Parameter estimates for the renewal times of a Gamma distribution

we can estimate β_{ij} and θ_{ij} by moment matching method, i.e. by replacing in (3.1.13) the mean and variance by their empirical estimators, which leads to:

$$\tilde{\beta}_{ij} = \frac{n_{ij}\bar{S}_{n_{ij}}^2}{\sum_{k=1}^{n_{ij}}(S_k - \bar{S}_{n_{ij}})^2}\,,$$

$$\frac{1}{\tilde{\theta}_{ij}} = \frac{n_{ij}\bar{S}_{n_{ij}}}{\sum_{k=1}^{n_{ij}}(S_k - \bar{S}_{n_{ij}})^2}\,.$$

We performed moment matching estimation on our dataset, and obtain the following estimates in Table 3.1. We observed that the shape and scale parameters depend rather on the product ij rather than on i and j separately. In other words, the distribution of the renewal times are symmetric in the sense of (3.1.9). Hence, we have performed again in Table 3.2 the parametric estimation $(\tilde{\beta}_+, \tilde{\theta}_+)$ and $(\tilde{\beta}_-, \tilde{\theta}_-)$ for the shape and scale parameters by distinguishing only samples for $ij = 1$ (the trend case) and $ij = -1$ (the mean-reverting case). We also provide in Figure 3.4 graphical tests of the goodness-of-fit for our estimation results, where the empirical distributions of F_+ and F_- are compared to theoretical densities of the gamma distribution with the estimated parameters both via an histogram versus density plot and a qqplot.

The estimated value $\tilde{\beta}_+$, and $\tilde{\beta}_- < 1$ for the shape parameters, can be interpreted when considering the hazard rate function of S_{n+1} given current and next marks:

$$\hat{\lambda}_\pm(t) := \lim_{\delta \downarrow 0} \frac{1}{\delta} P[t \le S_{n+1} \le t + \delta | S_n \ge t, \text{sign}(J_n J_{n+1}) = \pm]$$

$$= \frac{f_\pm(t)}{1 - F_\pm(t)}\,, \quad t \ge 0\,,$$

when $F_\pm$ admits a density $f_\pm$ (Notice that $\hat{\lambda}_\pm$ differs from $\lambda_\pm$). $\hat{\lambda}_+(t)$ (resp. $\hat{\lambda}_-(t)$) is the instantaneous probability of price jump given that there were no jump during an elapsed time t, and the current and next jump are in the same (resp. opposite) direction. For the Gamma distribution with shape and scale parameters (β, θ), the hazard rate function given by (3.1.11) is decreasing in time if and only if the shape parameter $\beta < 1$, which means that the more the time passes, the less is the probability that an event occurs. Therefore, the estimated values $\hat{\beta}_+$, and $\tilde{\beta}_- < 1$ are consistent with the following phenomenon: when a jump occurs, the probability of another jump in a short period is high, but if the event does not take place soon, then the price is likely to stabilize. Using this modelling, a long period of constant price corresponds to a renewal time in distribution tail. On the contrary, since renewal times are likely to be small when $\beta < 1$, most of the jumps will be extremely close. We also notice that the parameters in the trend and mean-reverting case differ significantly. This can be explained as follows: trends (two consecutive jumps in the same direction) are extremely rare (recall that $\alpha \approx -90\%$), since, in order to take place, market orders either have to clear two walls of liquidity or there must be a big number of cancellations. Since these events are caused by specific market dynamic, it is not surprising that their renewal law differ from the mean-reverting case.

Non-parametric estimation.

Since the renewal times form an i.i.d. sequence, we are able to perform a non-parametric estimation by kernel method of the density f_{ij} and the jump intensity. We recall the smooth

i j	shape	scale
+1 (trend)	0.276225	2397.219
-1 (mean-reverting)	0.07132677	1561.593

Table 3.2: Parameter estimates in the trend and mean-reverting case
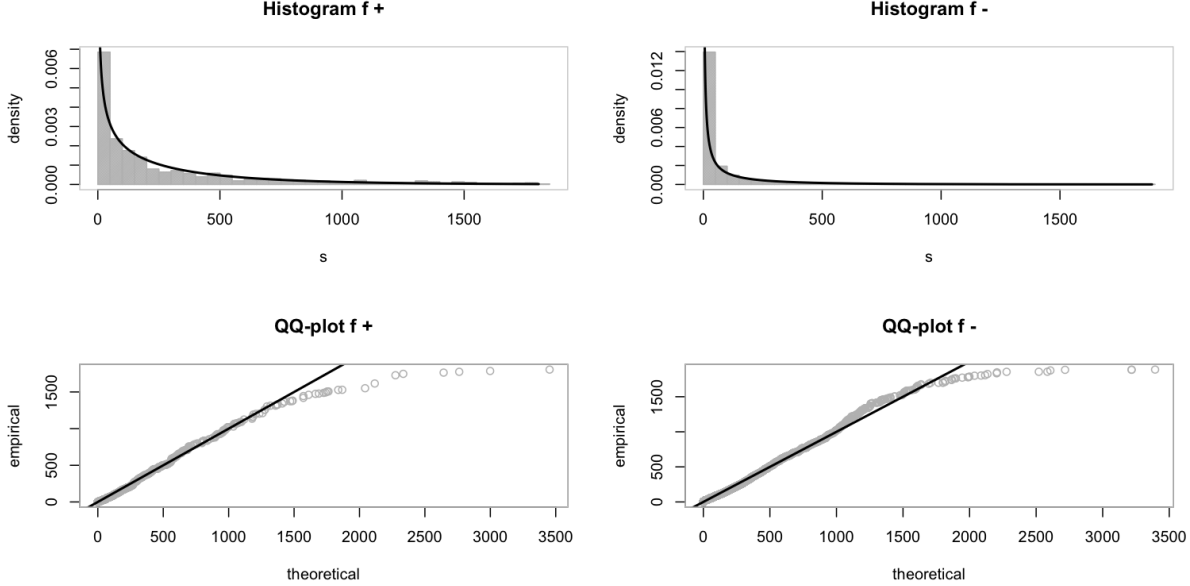
Figure 3.4: qq-plot and histogram of the distributions F_-(left) and F_+(right).

kernel method for the density estimation, and, in a similar way, we will give the one for h_{ij} and λ_{ij}. Let us start with the empirical histogram of the density, which is constructed as follows. For every collection of breaks

$$\{0 < t_1 < ... < t_M \leq \infty\}, \quad \delta_r := t_{r+1} - t_r,$$

we bin the sample $(S_k = T_k - T_{k-1})_{k=1,...,n}$ and define the empirical histogram of f_{ij} as

$$f_{ij}^{hst}(t_r) = \frac{1}{\delta_r} \frac{\#\{k \in I_{ij} | t_r \leq S_k < t_{r+1}\}}{n_{ij}}.$$

By the strong law of large numbers, when $n_{ij} \to \infty$, this estimator converges to

$$\frac{1}{\delta_r} \mathbb{P}\left[t_r \leq S_k < t_{r+1}\right],$$

which is a first order approximation of $f_{ij}(t_r)$. This estimator depends on the choice of the binning, which has not necessarily small (nor equal) δ_r's. The corresponding non-parametric (smooth kernel) estimator of the density is given by a convolution method:

$$f_{ij}^{np}(t) = \frac{1}{n_{ij}} \sum_{k \in I_{ij}} K_b(t - S_k) = (K_b * F_{ij}^{np})(t),$$

where $K_b(x)$ is a smoothing scaled kernel with bandwidth b and $F_{ij}^{np}(t)$ is non-parametric estimator of the cumulative distribution function given by

$$F_{ij}^{np}(t) = \frac{\#\{k \in I_{ij} : S_k \leq t\}}{n_{ij}}. \tag{3.1.14}$$

In our example we have chosen the Gaussian one, given by the density of the normal law of mean 0 and variance b^2. In practice, many softwares provide already optimized version of non-parametric estimation of the density, with automatic choice of the bandwidth and of the kernel (here Gaussian). For example in R, this reduces to the function `density`, applied to the sample $\{S_k | k \in I_{ij}\}$.
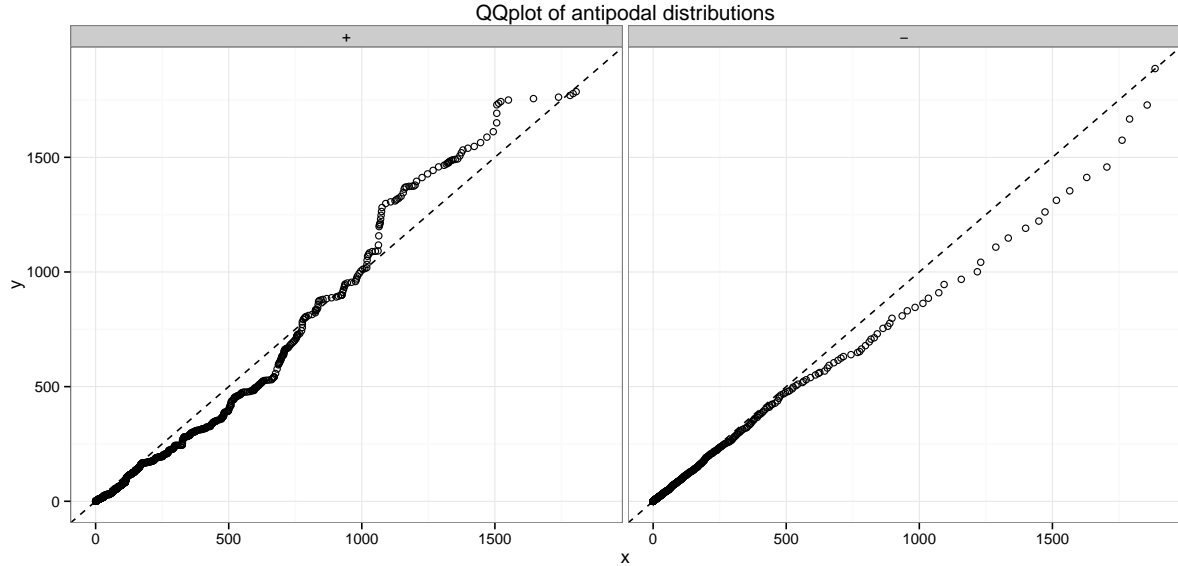

Figure 3.5: empirical qqplot comparing f_{--} against f_{++} (left) and f_{-+} against f_{-+} (right) on the whole sample.

In the symmetric case, which is the case as shown in Figure 3.5, the histogram reduces to:

$$f_{\pm}^{hst}(t_r) = \frac{1}{\delta_r} \frac{\#\{k \in I_{\pm} | t_r \le S_k < t_{r+1}\}}{n_{\pm}},$$

while the kernel estimator is given by:

$$f_{\pm}^{np}(t) = \frac{1}{n_{\pm}} \sum_{k \in I_{\pm}} K_b(t - S_k).$$

Figure 3.7 shows the result obtained for the kernel estimation of $f_{\pm}(t)$ in a logarithmic scale. The non-parametric estimation confirms the decreasing form of both densities, whose interpretation is that most of the jump of the stock price takes place in a short period of time (less than second), even though some renewal times can go to hours. Figure 3.6 shows a goodness-of-fit test for the null hypothesis that the probability transform sequence $(F_{B_n}(S_n))$ is an i.i.d. sequence of uniform random variables. The empirical cumulative distribution functions are obtained by interpolating linearly the piecewise constant estimator given in (3.1.14). As expected, MRP allows us to fit perfectly the stationary distribution of the inter-arrival time, but cannot reproduce the dependence reflected by the autocorrelation function (ACF) on the right. As in the case of the autocorrelation function of the sequence (J_n), MRPs prevent us to catch the long memory behaviour of the process, but allow us to provide explicit formula reproducing stylized facts and a reasonable framework for market making application, explored in [37].

Furthermore, Figure 3.8 is a qqplot of the sequence $(S_n | B_n = \pm)$ against $(S_n^{(i)} | B_n = \pm)$, where the $S_n^{(i)}$ correspond to a partition of the whole sample. This picture shows that the estimation of f_+ and f_- are rather stable over time.

We use a similar technique to estimate the marked hazard function h_{ij} defined in (3.1.10) and the cumulative hazard function $H_{ij}(t) = \int_0^t h_{ij}(u)du$. The Nelson-Aalen estimator for H_{ij} is
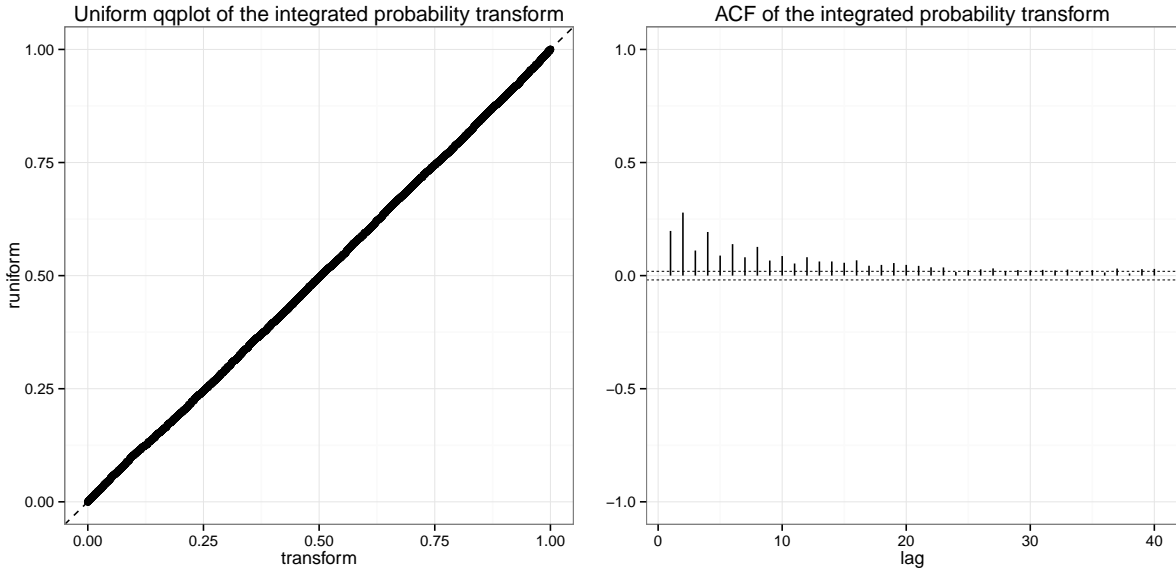
Figure 3.6:   uniform QQplot and ACF of the sequence $(F_{B_n}(S_n))$
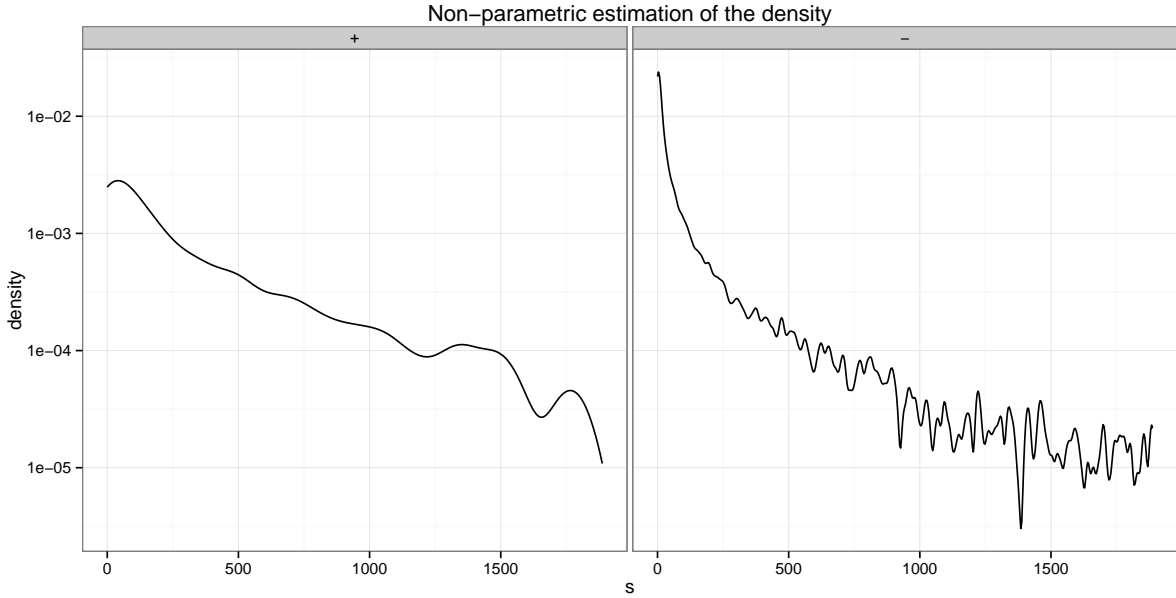
Figure 3.7: Non-parametric estimation of the densities f_+ (bandwith $= 24.17$) and f_- (y-axis in log10 scale, bandwith $= 1.44$)

given by the piecewise constant function given by

$$H_{ij}^{np}(t) := \sum_{k \in I_{ij}} \frac{1}{\#\{k \in I_i | S_k \geq t\}} \,,$$

and, in the symmetric case, by

$$H_{\pm}^{np}(t) := \sum_{k \in I_{\pm}} \frac{1}{\#\{k | S_k \geq t\}} \,. \tag{3.1.15}$$

The result of the estimation is shown in Figure 3.9. By writing

$$h_{ij}(t) = \lim_{\delta \to 0} \frac{1}{\delta} \frac{\mathbb{P}\left[t \leq S_k < t + \delta, J_k = j \middle| J_{k-1} = i\right]}{\mathbb{P}\left[S_k \geq s \middle| J_{k-1} = i\right]} \,,$$
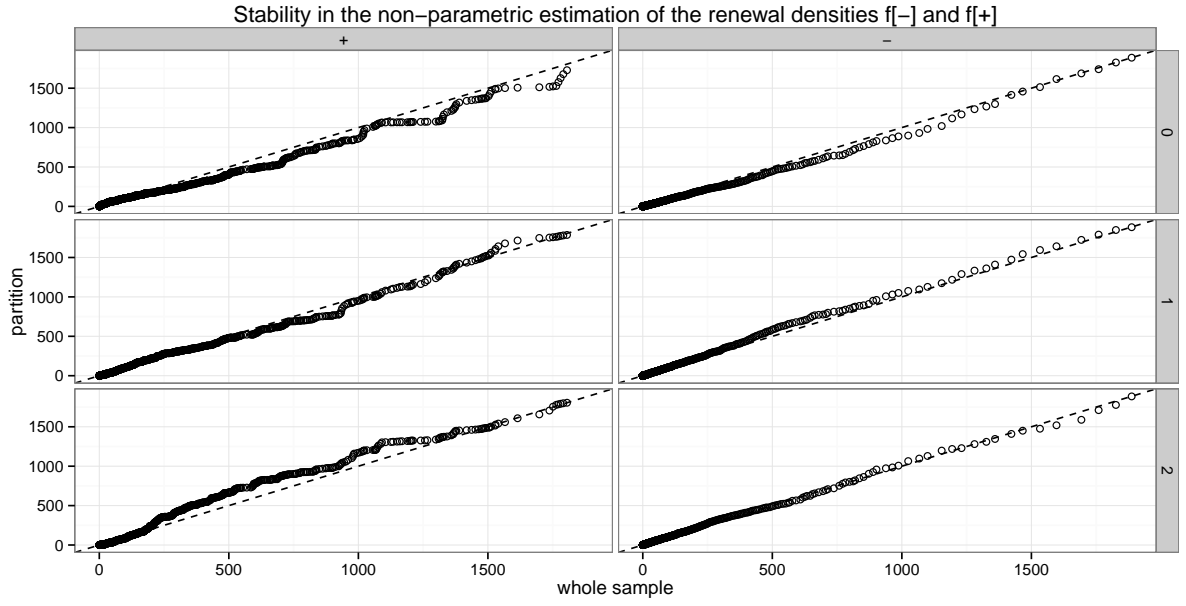
Figure 3.8: empirical qqplot of the $(S_n|B_n = \pm)$ (x-axis) against $(S_n^{(i)}|B_n = \pm)$, where the $S_n^{(i)}$ correspond to a partition of the whole sample.
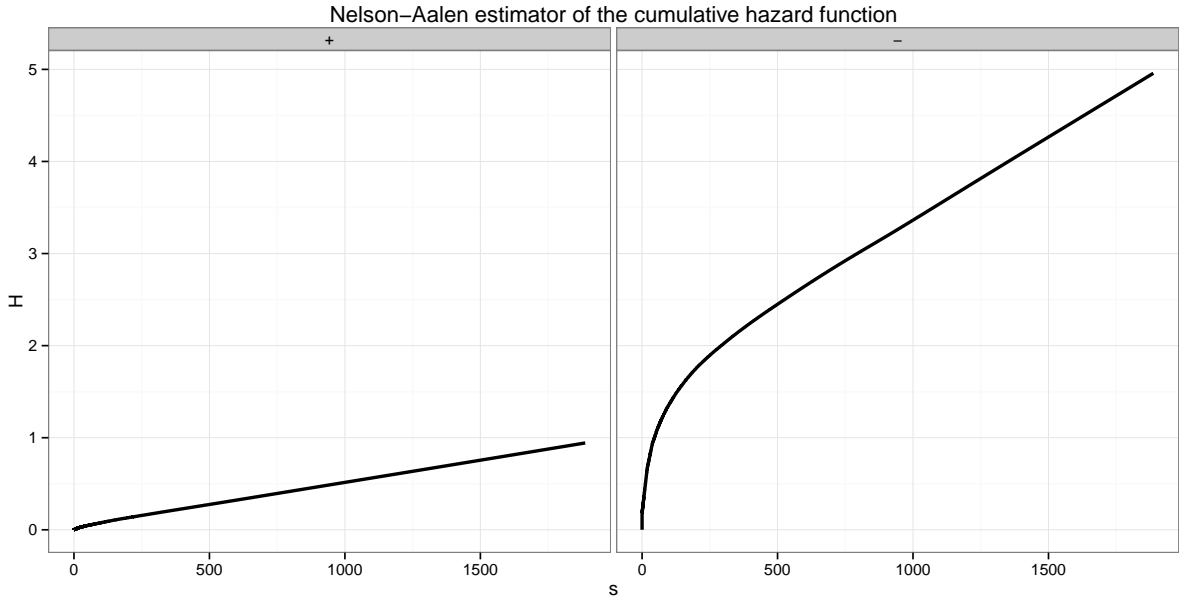
Figure 3.9: Nelson-Aalen non-parametric estimator of the cumulative hazard functions $H_\pm$.

we can define the empirical histogram of h_{ij} as

$$h_{ij}^{hst}(t_r) = \frac{1}{\delta_r} \frac{\#\{k \in I_{ij} | t_r \le S_k < t_r + \delta\}}{\#\{k \in I_i | S_k \ge t_r\}} ,$$

and the associated smooth kernel estimator by

$$h_{ij}^{np}(t) = \sum_{k \in I_{ij}} K_b(t - S_k) \frac{1}{\#\{k \in I_i | S_k \ge t\}} = K_b * H_{ij}^{np} .$$

Notice that this non-parametric estimator is factored as

$$h_{ij}^{np}(t) = \left(\frac{n_{ij}}{n_i}\right) \left(\frac{n_i}{n_{ij}} h_{ij}^{np}(t)\right) ,$$

where $\frac{n_{ij}}{n_i}$ is the estimator of q_{ij} and $\frac{n_i}{n_{ij}}h_{ij}^{np}(t)$ is the kernel estimator of the jump intensity $\lambda_{ij}(t) = \frac{f_{ij}(t)}{1-\sum_j F_{ij}F_{ij}(t)}$. Thus, we can either estimate λ_{ij} and multiply by the estimator of q_{ij} to obtain h_{ij} or vice versa, obtaining the same estimators. In the symmetric case, we have:

$$h_\pm^{hst}(t_r) = \frac{1}{\delta_r}\frac{\#\{k \in I_\pm | t_r \le S_k < t_r + \delta\}}{\#\{k|S_k \ge t_r\}},$$

while

$$h_\pm^{np}(t) = \sum_{k \in I_\pm} K_b(t - S_k)\frac{1}{\#\{k|S_k \ge t\}}.$$

Figure 3.10 shows the result obtained for $h_\pm$. The interpretation is the following: immediately after a jump the price is in an unstable condition, which will probably leads it to jump again soon. If it does not happen, the price gains in stability with time, and the probability of a jump becomes smaller and smaller. Moreover, due to mean-reversion of price returns, the intensity of consecutive jumps in the opposite direction is larger than in the same direction, which explains the higher value of h_- compared to h_+.
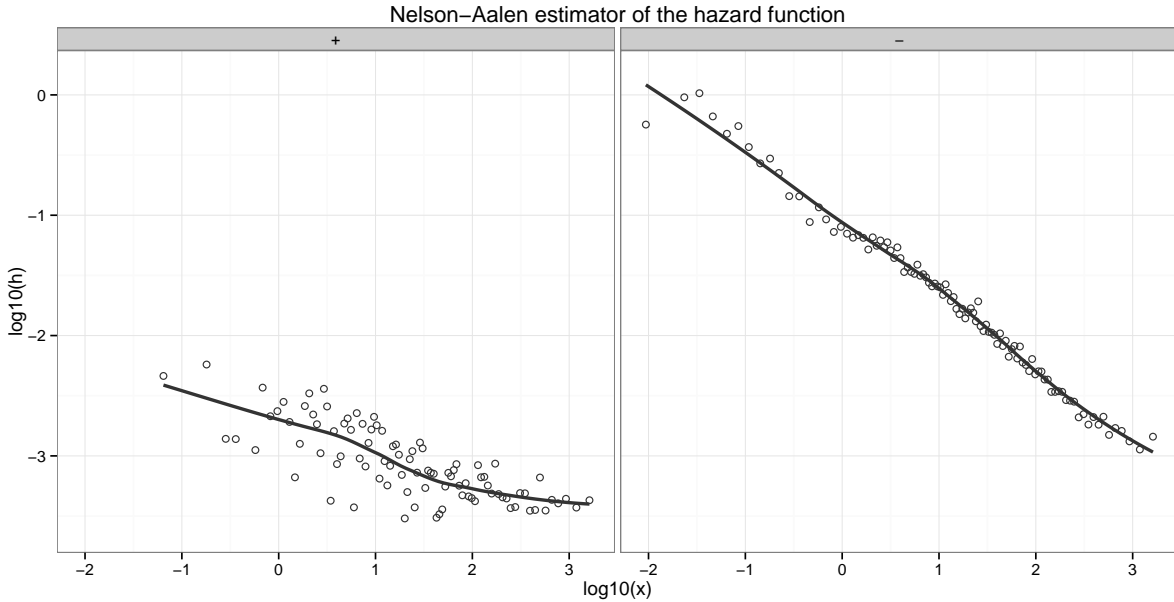
Figure 3.10: Non-parametric estimation of the hazard function $h_\pm$: points represent the histogram, while the black solid line the non-parametric estimator.

3.1.4   Price simulation

The simulation of the price process (3.1.1) with a Markov renewal model is quite simple, much easier than any other point process modelling microstructure noise. This would allow the user, even when (N_t) is better fit by a more complex point process, to have a quick proxy for its price simulation. Choose a starting price P_0 at initial time T_0.

i) *Initialization step:* k = 0 (starting points).

   ◇ Set $\hat{P}_0 = P_0$.
   ◇ Draw J_0 from initial (e.g. stationary) law π.

ii) *Inductive step:* $k - 1 \to k$ (next price and next timestamp).

   ◇ Draw J_k according to the probability transition, and set $\hat{P}_k = \hat{P}_{k-1} + J_k$;

◇ draw $S_k \to F_{J_{k-1} J_k}$, and set $T_k = T_{k-1} + S_k$.

Once $(T_k, \hat{P}_k)_{k \in \mathbb{N}}$ is known, the price process is given by the piecewise constant process

$$P_t = \hat{P}_k \,, \quad T_k \le t < T_{k+1} \,.$$

We show in Figure 3.11 one trajectory of the price process based on the estimated parameters.
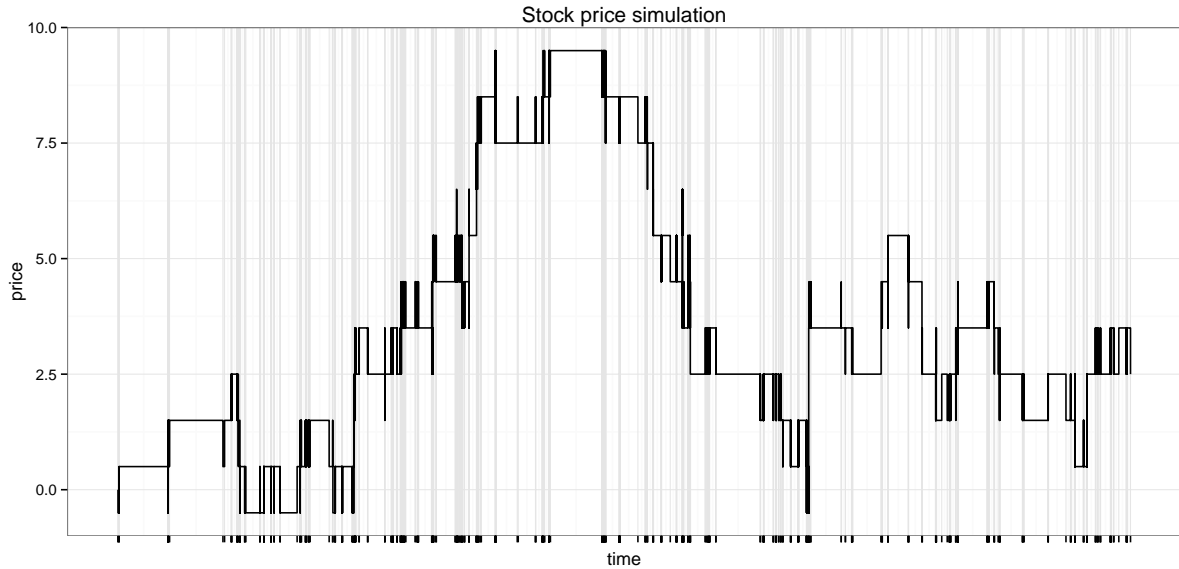
Figure 3.11: Simulation of one trajectory of a MRP with estimated parameters on empirical data.

3.1.5 Semi-Markov property

The main purpose of this paper is to provide a Markov framework for an application of stochastic control theory to high-frequency trading. In what follows, we recall the existence of Markov embedding for the stock price. Let us define the pure jump process

$$I_t = J_{N_t} \tag{3.1.16}$$

which represents the last price increment. Then, I is a *semi-Markov* process in the sense that the pair (I_t, S_t) is a Markov process, where

$$S_t = t - T_n \,, \quad T_n \le t < T_{n+1} \,,$$

is the time spent from the last jump price. Moreover, the price process (P_t) is embedded in a Markov process with three observable state variables: (P_t, I_t, S_t) is a Markov process with infinitesimal generator

$$\mathcal{L}\varphi(p, i, s) = \frac{\partial \varphi}{\partial s} + \sum_{j \in E} h_{ij}(s) \Delta \varphi(p + j, j, 0) \,,$$

which is written in the symmetric case (3.1.5) and (3.1.9) as

$$\mathcal{L}\varphi(p, i, s) = \frac{\partial \varphi}{\partial s} + \lambda_+(s) \left(\frac{1 + \alpha}{2} \right) \sum_{j=1}^m p_j \Delta \varphi(p + \text{sign}(i)j, \text{sign}(i)j, 0) \,,$$

$$+ \lambda_-(s) \left(\frac{1 - \alpha}{2} \right) \sum_{j=1}^m p_j \Delta \varphi(p - \text{sign}(i)j, -\text{sign}(i)j, 0) \,,$$

where $\lambda_{\pm}$ is the jump intensity defined in (3.1.11).

3.1.6   Comparison with respect to Hawkes processes

In a recent work [7] (see also [35]), the authors consider a tick-by-tick model for asset price by means of cross-exciting Hawkes processes. More precisely, the stock price jumps by one tick according to the dynamics:

$$P_t = N_t^+ - N_t^-, \tag{3.1.17}$$

where $(N_t^\pm)$ is a point process corresponding to the number of upward and downward jumps, with coupling stochastic intensities:

$$\lambda_t^\pm = \lambda_\infty + \int_{-\infty}^t \varphi(t-u)dN_u^\mp, \tag{3.1.18}$$

where $\lambda_\infty > 0$ is an exogenous constant intensity, and φ is a positive decay kernel. This model, which takes into account in the intensity the whole past of the price process, provides a better good-fit of intraday data than the MRP approach, and can be easily extended to the multivariate asset price case. However, it is limited to unitary jump size, and presents some drawbacks especially in view of applications to trading optimization problem. The price process in (3.1.17)-(3.1.18) is embedded into a Markovian framework only for the case of exponential decay kernel, i.e. for

$$\varphi(t) = \gamma e^{-\beta t}\mathbb{1}\{\mathbb{R}_+\}(t),$$

with $0 < \gamma < \beta$. In this case, the Markov price system consists of P together with the stochastic intensities (λ^+, λ^-). But in contrast with the MRP approach, the additional state variables (λ^+, λ^-) are not directly observable, and have to be computed from their dynamics (3.1.18), which requires a "precise" estimation of the three parameters λ_∞, γ, and β. In that sense, the MRP approach is less sensitive to the propagation of estimation errors than the Hawkes one. Notice also that in the MRP approach, we can deal not only with parametric forms of the renewal distributions (which involves only two parameters for the usual Gamma and Weibull laws), but also with non-parametric form of the renewal distributions, and so of the jump intensities. Simulation and estimation in MRP model are simple since they are essentially based on (conditional) i.i.d. sequence of random variables, with the counterpart that MRP model can not reproduce the correlation between inter-arrival jump times as in Hawkes model.

We finally mention that one can use a combination of Hawkes process and semi-Markov model by considering a counting process (N_t) associated to the jump times (T_n), independent of the price return (J_n), and with stochastic intensity

$$\lambda_t = \lambda_\infty + \gamma \int_0^t e^{-\beta(t-u)}dN_u, \tag{3.1.19}$$

with $\lambda_\infty > 0$, and $0 < \gamma < \beta$. In this case, the pair (I_t, λ_t) is a Markov process, and (P_t, I_t, λ_t) is a Markov process with infinitesimal generator:

$$\mathcal{L}\varphi(p,i,\ell) = \beta(\mu - \ell)\frac{\partial \varphi}{\partial \ell} + \ell \sum_{j \in E} q_{ij}\Delta\varphi(p+j,j,\ell+\gamma),$$

which is written in the symmetric case (3.1.5) as:

$$\mathcal{L}\varphi(p,i,\ell) = \beta(\mu - \ell)\frac{\partial \varphi}{\partial \ell},$$
$$+ \ell\left(\frac{1+\alpha}{2}\right)\sum_{j=1}^m p_j\Delta\varphi(p+\text{sign}(i)j, \text{sign}(i)j, \ell+\gamma),$$
$$+ \ell\left(\frac{1-\alpha}{2}\right)\sum_{j=1}^m p_j\Delta\varphi(p-\text{sign}(i)j, -\text{sign}(i)j, \ell+\gamma).$$

3.2 Scaling limit

We now study the large scale limit of the price process constructed from our Markov renewal model. We consider the symmetric case (3.1.5) and (3.1.9), and denote by

$$F(t) = \frac{1+\alpha}{2} F_+(t) + \frac{1-\alpha}{2} F_-(t),$$

the distribution function of the sojourn time S_n. We assume that the mean sojourn time is finite:

$$\bar{\mu} = \int_0^\infty t dF(t) < \infty, \quad \text{and we set } \bar{\lambda} = \frac{1}{\bar{\mu}},$$

By classical regenerative arguments, it is known (see [40]) that the Markov renewal process obeys a strong law of large numbers, which means the long run stability of price process:

$$\frac{P_t}{t} \longrightarrow c, \quad \text{a.s.},$$

when t goes to infinity, with a limiting constant c given by:

$$c := \frac{1}{\bar{\mu}} \sum_{i,j \in E} \pi_i q_{ij} j,$$

where $E = \{1, -1, \ldots, m, -m\}$, $\bar{\mu}_{ij} = \int_0^\infty t dF_{ij}(t)$, $Q = (q_{ij})$ is the transition matrix (3.1.4) of the embedded Markov chain (J_n), and $\pi = (\pi_i)$ is the invariant distribution of (J_n). In the symmetric case (3.1.5) and (3.1.9), we have $q_{ij} = p_{|i|}(1 + \text{sign}(j)\alpha)/2$, $\pi_i = p_{|i|}/2$, and so $c = 0$. We next define the normalized price process:

$$P_t^{(T)} = \frac{P_{tT}}{\sqrt{T}}, \quad t \in [0,1],$$

and address the macroscopic limit of $P^{(T)}$ at large scale limit $T \to \infty$. From the functional central limit theorem for Markov renewal process, we obtain the large scale diffusive behavior of price process.

PROPOSITION 3.1.

$$\lim_{T \to \infty} P^{(T)} \overset{(d)}{=} \sigma_\infty W,$$

where $W = (W_t)_{t \in [0,1]}$ is a standard Brownian motion, and σ_∞, the macroscopic variance, is explicitly given by

$$\sigma_\infty^2 = \bar{\lambda} \left[\text{Var}(\xi_n) + (\mathbb{E}[\xi_n])^2 \frac{1+\alpha}{1-\alpha} \right]. \tag{3.2.1}$$

Proof. From [40], we know that a functional central limit theorem holds for Markov renewal process so that

$$P^{(T)} \overset{(d)}{\to} \sigma_\infty W,$$

when T goes to infinity (here $\overset{(d)}{\to}$ means convergence in distribution), where σ_∞ is given by $\sigma_\infty^2 = \bar{\lambda} \tilde{\sigma}_\infty^2$ with $\bar{\lambda} = 1/\bar{\mu}$, and

$$\tilde{\sigma}_\infty^2 = \sum_{i,j \in E} \pi_i q_{ij} H_{ij}^2,$$

with

$$H_{ij} = j + g_j - g_i \,,$$
$$g = (g_i)_i = (I_{2m} - Q + \Pi)^{-1} b \,,$$
$$b = (b_i), b_i = \sum_{j \in E} Q_{ij} j \,,$$

and Π is the matrix defined by $\Pi_{ij} = \pi_j$. In the symmetric case (3.1.5), a straightforward calculation shows that

$$b_i = \text{sign}(i)\alpha \sum_{j=1}^{m} j p_j = \text{sign}(i)\alpha \mathbb{E}[\xi_n] \,,$$

and then

$$g_i = \text{sign}(i)\frac{\alpha}{1-\alpha}\mathbb{E}[\xi_n] \,, \quad i \in E = \{1, -1, \dots, m, -m\} \,.$$

Thus,

$$H_{ij} = \left\{ \begin{array}{ll} j & \text{if } ij > 0 \,, \\ j + \frac{2\alpha}{1-\alpha}\mathbb{E}[\xi_n] & \text{if } j > 0, i < 0 \,, \\ j - \frac{2\alpha}{1-\alpha}\mathbb{E}[\xi_n] & \text{if } j < 0, i > 0. \end{array} \right\} \,.$$

Therefore, a direct calculation yields

$$\tilde{\sigma}^2_\infty = \sum_{j=1}^{m} j^2 p_j + \frac{2\alpha}{1-\alpha}(\mathbb{E}[\xi_n])^2 = \text{Var}(\xi_n) + (\mathbb{E}[\xi_n])^2 \frac{1+\alpha}{1-\alpha} \,.$$

$\square$

3.3 Mean Signature plot

In this section, we aim to provide through our Markov renewal model a quantitative justification of the signature plot effect, described in the introduction. We consider the symmetric and stationary case, i.e.:

(H)

i) The price return (J_n) is given by (3.1.2) with a probability transition matrix $\hat{Q}$ for $(\hat{J}_n) = (\text{sign}(J_n))$ in the form:

$$\hat{Q} = \left(\begin{array}{cc} \frac{1+\alpha}{2} & \frac{1-\alpha}{2} \\ \frac{1-\alpha}{2} & \frac{1+\alpha}{2} \end{array} \right) ,$$

for some $\alpha \in [-1, 1)$.

ii) (N_t) is a delayed renewal process: for $n \geq 1$, S_n has distribution function F (independent of i, j), with finite mean $\bar{\mu} = \int_0^\infty t dF(t) =: 1/\bar{\lambda} < \infty$, and finite second moment, and S_1 has a distribution with density $(1 - F(t))/\bar{\mu}$.

It is known that the process N is stationary under **(H)**(ii) (see [28]), and so the price process is also stationary under the stationary probability P_π, i.e. the distribution of $P_{t+\tau} - P_t$ does not depend on t but only on increment time τ. In this case, the empirical mean signature plot is written as:

$$\bar{\mathcal{V}}(\tau) := \frac{1}{T} \sum_{i\tau \leq T} \mathbb{E}_\pi \left[(P_{i\tau} - P_{(i-1)\tau})^2 \right] = \frac{1}{\tau}\mathbb{E}_\pi \left[(P_\tau - P_0)^2 \right] . \tag{3.3.1}$$

Notice that if $P_t = \sigma W_t$, where W_t is a Brownian motion, then $\bar{\mathcal{V}}$ is a flat function: $\bar{\mathcal{V}}(\tau) = \sigma^2$, while it is well known that on real data $\bar{\mathcal{V}}$ is a decreasing function on τ with finite limit when $\tau \to \infty$. This is mainly due to the anticorrelation of returns: on a short time-step the signature plot captures fluctuations due to returns that, on a longer time-steps, mutually cancel. We obtain the closed-form expression for the mean signature plot, and give some qualitative properties about the impact of price returns autocorrelation. The following results are proved in Appendix.

PROPOSITION 3.2. *Under* **(H)**, *we have*:

$$\bar{\mathcal{V}}(\tau) = \sigma^2_\infty + \left(\frac{-2\alpha(\mathbb{E}[\xi_n])^2}{1-\alpha} \right) \frac{1 - G_\alpha(\tau)}{(1-\alpha)\tau} ,$$

where σ^2_∞ *is the macroscopic variance given in (3.2.1), and* $G_\alpha(t) := \mathbb{E}[\alpha^{N_t}]$ *is given via its Laplace-Stieltjes transform*:

$$\widehat{G}_\alpha(s) = 1 - \bar{\lambda}(1-\alpha) \frac{1 - \widehat{F}(s)}{s(1 - \alpha\widehat{F}(s))} , \quad \alpha \neq 0 , \tag{3.3.2}$$

$\widehat{F}(s) := \int_{0-}^{\infty} e^{-st} dF(t)$. *Alternatively,* G_α *is given directly by the integral form*:

$$G_\alpha(t) = 1 - \bar{\lambda} \left(\frac{1-\alpha}{\alpha} \right) \left(t - (1-\alpha) \int_0^t Q_\alpha^0(u) du \right) , \tag{3.3.3}$$

where $Q_\alpha^0(t) = \sum_{n=0}^{\infty} \alpha^n F^{*(n)}(t)$, *and* $F^{*(n)}$ *is the n-fold convolution of the distribution function* F, *i.e.* $F^{*(n)}(t) = \int_0^t F^{*(n-1)}(t-u) dF(u)$, $F^{*(0)} = 1$.

COROLLARY 3.1. *Under* **(H)**, *we obtain the asymptotic behavior of the mean signature plot*:

$$\bar{\mathcal{V}}(\infty) := \lim_{\tau \to \infty} \bar{\mathcal{V}}(\tau) = \sigma^2_\infty ,$$

$$\bar{\mathcal{V}}(0^+) := \lim_{\tau \downarrow 0^+} \bar{\mathcal{V}}(\tau) = \bar{\lambda}\mathbb{E}[\xi_n^2] .$$

Moreover,

$$\alpha \left(\bar{\mathcal{V}}(0^+) - \bar{\mathcal{V}}(\infty) \right) \leq 0 .$$

REMARK 3.3. In the case of renewal process where F is the distribution function of the Gamma law with shape β and scale θ, it is known that $F^{*(n)}$ is the distribution function a the Gamma law with shape $n\beta$ and scale θ, and so:

$$F^{*(n)}(t) = \frac{\Gamma_{t/\theta}(n\beta)}{\Gamma(n\beta)} ,$$

where Γ is the Gamma function, and Γ_t is the lower incomplete Gamma functions defined in (3.1.12). Plugging into (3.3.3), we obtain an explicit integral expression of the mean signature plot, which is computed numerically by avoiding the inversion of the Laplace transform (3.3.2). Notice that in the special case of Poisson process for N, i.e. F is the exponential distribution of rate $\bar{\lambda}$, the function G_α is explicitly given by : $G_\alpha(t) = e^{-\bar{\lambda}(1-\alpha)t}$.

REMARK 3.4. The term σ^2_∞ equal to the limit of the mean signature plot when time step observation τ goes to infinity, corresponds to the macroscopic variance, and $\bar{\mathcal{V}}(0^+) = \bar{\lambda}\mathbb{E}[\xi_n^2]$ is the microstructural variance. Notice that while σ^2_∞ increases with the price returns autocorrelation α, the limiting term $\bar{\mathcal{V}}(0^+)$ does not depend on α, and the mean signature plot is flat if and only if price returns are independent, i.e. $\alpha = 0$. In the case of mean-reversion ($\alpha < 0$), $\bar{\mathcal{V}}(0^+) > \sigma^2_\infty$, while in the trend case ($\alpha > 0$), we have: $\bar{\mathcal{V}}(0^+) < \sigma^2_\infty$. We display in Figure 3.13 an example of the mean signature plot function for a Gamma distribution when varying α. We also compare in Figure 3.12 the signature plot obtained from empirical data on the Euribor, the signature plot simulated in our model with estimated parameters, and the mean signature for a Gamma distribution with the estimated parameters. This example shows how the signature plot decreasing form is a consequence (rather coarse) of the microstructure noise, and that the shape parameters of the gamma law, which is responsible for the volatility cluster, is able to reproduce the convexity of the signature plot shape.
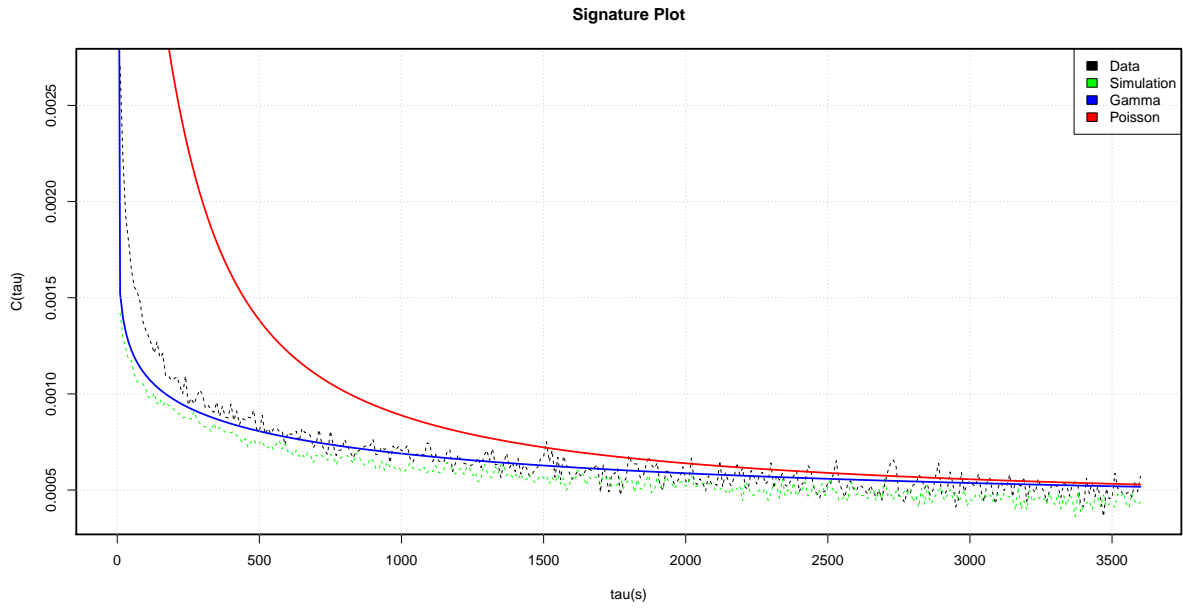
Signature Plot

Figure 3.12: Mean signature plot for the EURIBOR.
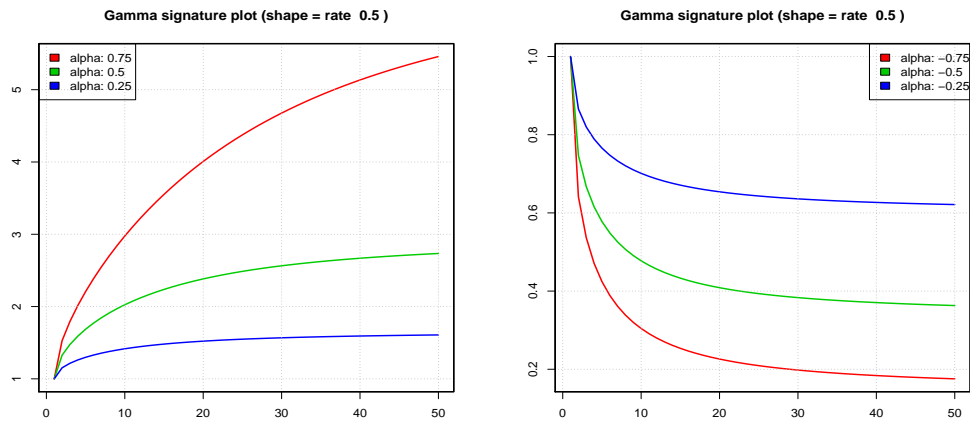
Figure 3.13: $\tau \to \bar{\mathcal{V}}(\tau)$ when varying price return autocorrelation α. Left: $\alpha > 0$. Right: $\alpha < 0$

Conclusion and extensions

In this paper we used a Markov renewal process (T_n, J_n) to describe the tick-by-tick evolution of the stock price and reproduce two important stylized facts, as the diffusive behavior and the decreasing shape of the mean signature plot towards the diffusive variance. Having in mind a direct application purpose, we decided to sacrifice the autocorrelation of inter-arrival times in order to have a fast and simple non-parametric estimation, perfect simulation and the suitable setup for a market making application, presented in a companion paper [37]. Aware of the model limits, and with an eye to statistical arbitrage, the next step is to extend the structure of the counting process (N_t), for example to Hawkes process, to have a better fit, and the structure of the Markov chain (J_n) to a longer memory binary processes, able to recognize patterns. Another direction of study will be the extension to the multivariate asset price case.

3.4 Appendix: the mean signature plot

The price process P_t is given by

$$P_t = P_0 + \sum_{k=1}^{N_t} J_k = \sum_{n=0}^{\infty} L_n \mathbb{1}\{N_t = n\}, \tag{3.4.1}$$

where

$$L_n = \sum_{k=1}^{n} J_k \, n \geq 1, \quad L_0 = 0.$$

LEMMA 3.3. *Under* **(H)**, *we have*

$$\mathbb{E}_\pi\left[L_n^2\right] = n\frac{\sigma_\infty^2}{\lambda} - \frac{2\alpha}{1-\alpha}\frac{1-\alpha^n}{1-\alpha}\left(\mathbb{E}[\xi_n]\right)^2,$$

where σ_∞ *is defined in* (3.2.1).

Proof. By writing that $L_n = L_{n-1} + \xi_n \hat{J}_n$, we have for $n \geq 1$:

$$\mathbb{E}_\pi\left[L_n^2\right] = \mathbb{E}_\pi\left[L_{n-1}^2 + \xi_n^2 \hat{J}_n^2 + 2\xi_n L_{n-1}\hat{J}_n\right],$$

$$= \mathbb{E}_\pi\left[L_{n-1}^2\right] + \mathbb{E}_\pi\left[\xi_n^2\right] + 2\left(\mathbb{E}\left[\xi_n\right]\right)^2 \sum_{k=1}^{n-1} \mathbb{E}_\pi\left[\hat{J}_k \hat{J}_n\right],$$

$$= \mathbb{E}_\pi\left[L_{n-1}^2\right] + \mathbb{E}_\pi\left[\xi_n^2\right] + 2\left(\mathbb{E}\left[\xi_n\right]\right)^2 \sum_{k=1}^{n-1} \mathbb{E}_\pi\left[\hat{J}_k \hat{J}_0\right], \tag{3.4.2}$$

where we used the fact that $\hat{J}_n^2 = 1$, (ξ_n) are i.i.d, and independent of $(\hat{J}_n)$ in the second equality, and the stationarity of $(\hat{J}_n)$ in the third equality. Now, from the Markov property of $(\hat{J}_k)_k$ with probability transition matrix $\hat{Q}$ in (3.1.3) and (3.1.5), we have for any $k \geq 1$:

$$\mathbb{E}_\pi\left[\hat{J}_k \hat{J}_0\right] = \mathbb{E}_\pi\left[\mathbb{E}_\pi\left[\hat{J}_k | \hat{J}_{k-1}\right] \hat{J}_0\right],$$

$$= \mathbb{E}\left[\left(\frac{1+\alpha}{2}\right)\hat{J}_{k-1}\hat{J}_0 - \left(\frac{1-\alpha}{2}\right)\hat{J}_{k-1}\hat{J}_0\right],$$

$$= \alpha\mathbb{E}_\pi\left[\hat{J}_{k-1}\hat{J}_0\right],$$

from which we obtain by induction:

$$\mathbb{E}_\pi\left[\hat{J}_k \hat{J}_0\right] = \alpha^k.$$

Plugging into (3.4.2), this gives

$$\mathbb{E}_\pi\left[L_n^2\right] = \mathbb{E}_\pi\left[L_{n-1}^2\right] + \mathbb{E}_\pi\left[\xi_n^2\right] + \frac{2\alpha}{1-\alpha}(1-\alpha^{n-1})\left(\mathbb{E}[\xi_n]\right)^2.$$

By induction, we get the required relation for $\mathbb{E}_\pi\left[L_n^2\right]$.

$\qquad\qquad\qquad\qquad\qquad\qquad\qquad\qquad\qquad\qquad\qquad\qquad\qquad\qquad\qquad\square$

Consequently, we obtain the following expression of the mean signature plot:

PROPOSITION 3.3. *Under* **(H)**, *we have*

$$\bar{\mathcal{V}}(\tau) = \sigma_\infty^2 - \frac{2\alpha}{1-\alpha}\frac{1-G_\alpha(\tau)}{(1-\alpha)\tau}\left(\mathbb{E}[\xi_n]\right)^2, \quad \tau > 0, \tag{3.4.3}$$

where $G_\alpha(t) := \mathbb{E}_\pi[\alpha^{N_t}] = \sum_{n=0}^{\infty} \alpha^n P_\pi[N_t = n]$.

Proof. From (3.3.1) and (3.4.1), we see that the mean signature plot is written as

$$\bar{\mathcal{V}}(\tau) = \frac{1}{\tau} \sum_{n=0}^{\infty} \mathbb{E}_{\pi}[L_n^2] P_{\pi}[N_{\tau} = n] \,,$$

since the renewal process N is independent of the marks (J_n). Together with the expression of $\mathbb{E}_{\pi}[L_n^2]$ in Lemma 3.3, this yields

$$\bar{\mathcal{V}}(\tau) = \frac{\sigma_{\infty}^2}{\bar{\lambda}} \frac{\mathbb{E}_{\pi}[N_{\tau}]}{\tau} - \frac{2\alpha}{1-\alpha} \frac{1 - G_{\alpha}(\tau)}{(1-\alpha)\tau} \left(\mathbb{E}[\xi_n]\right)^2 \,.$$

Finally, since $\mathbb{E}_{\pi}[N_{\tau}] = \bar{\lambda}\tau$ by stationarity of N, we get the required relation.

$$\square$$

We now focus on the finite variation function G_{α} that we shall compute through its Laplace-Stieltjes transform:

$$\widehat{G}_{\alpha}(s) := \int_{0^-}^{\infty} e^{-st} dG_{\alpha}(t) \,, \quad s \geq 0 \,,$$

We recall the convolution property for Laplace-Stieltjes transform

$$\widehat{G*H} = \widehat{G}\,\widehat{H} \,,$$

where

$$G*H(t) = \int_0^t G(t-s)dH(s) \,.$$

Let us consider the function Q_{α} defined by:

$$Q_{\alpha}(t) := \sum_{n=0}^{\infty} \alpha^n P_{\pi}[N_t \geq n] \,. \tag{3.4.4}$$

LEMMA 3.4. *Under* **(H)**, *we have for all* $\alpha \neq 0$,

$$G_{\alpha} = \left(1 - \frac{1}{\alpha}\right) Q_{\alpha} + \frac{1}{\alpha} \,, \tag{3.4.5}$$

$$\widehat{Q}_{\alpha}(s) = 1 + \alpha \frac{\bar{\lambda}}{s} \left(\frac{1 - \widehat{F}(s)}{1 - \alpha\widehat{F}(s)}\right) \,. \tag{3.4.6}$$

Proof.
For any $\alpha \neq 0$, $t \geq 0$, we have

$$G_{\alpha}(t) = \sum_{n=0}^{\infty} \alpha^n P_{\pi}[N_t = n] = \sum_{n=0}^{\infty} \alpha^n \left(P_{\pi}[N_t \geq n] - P_{\pi}[N_t \geq n+1]\right) \,,$$

$$= \sum_{n=0}^{\infty} \alpha^n P_{\pi}[N_t \geq n] - \frac{1}{\alpha} \left(\sum_{n=0}^{\infty} \alpha^n P_{\pi}[N_t \geq n] - P_{\pi}[N_t \geq 0]\right) \,,$$

$$= Q_{\alpha}(t) - \frac{1}{\alpha} \left(Q_{\alpha}(t) - 1\right) \,,$$

which proves (3.4.5).
Recall that for the delayed renewal process N, the first arrival time S_1 is distributed according to the distribution Δ with density $\bar{\lambda}(1 - F)$. Let us denote by N^0 the no-delayed renewal

process, i.e. with all interarrival times $S_n^0 = T_n^0 - T_{n-1}^0$ distributed according to F, and by Q_α^0 the function defined similarly as in (3.4.4) with N replaced by N^0. Then,

$$
\begin{aligned}
Q_\alpha(t) &= 1 + \alpha \sum_{n=0}^{\infty} \alpha^n P_\pi \left[N_t \geq n + 1 \right] \\
&= 1 + \alpha \sum_{n=0}^{\infty} \alpha^n P_\pi [S_1 + T_n^0 \leq t] \\
&= 1 + \alpha \mathbb{E}_\pi \left[\sum_{n=0}^{\infty} \alpha^n P_\pi [T_n^0 \leq t - S_1 | S_1 \leq t] \right] \\
&= 1 + \alpha \mathbb{E}_\pi \left[Q_\alpha^0 (t - S_1) \mathbb{1}\{S_1 \leq t\} \right] \\
&= 1 + \alpha Q_\alpha^0 * \Delta(t) \,.
\end{aligned}
\tag{3.4.7}
$$

By taking the Laplace-Stieltjes transform in the above relation, and from the convolution property, we get

$$
\widehat{Q}_\alpha = 1 + \alpha \widehat{Q_\alpha^0} \widehat{\Delta} \,.
\tag{3.4.8}
$$

By same arguments as in (3.4.7) and (3.4.8), we get $\widehat{Q_\alpha^0} = 1 + \alpha \widehat{Q_\alpha^0} \widehat{F}$, and so

$$
\widehat{Q_\alpha^0} = \frac{1}{1 - \alpha \widehat{F}} \,.
\tag{3.4.9}
$$

Now, from the relation $\Delta(t) = \int_0^t \bar\lambda (1 - F(u)) du$, and by taking Laplace-Stieltjes transform we get:

$$
\widehat{\Delta}(s) = \frac{\bar\lambda}{s} \left(1 - \widehat{F}(s) \right) \,.
\tag{3.4.10}
$$

By substituting (3.4.9) and (3.4.10) into (3.4.8), we get the required relation (3.4.6).

$$\square$$

From the relations (3.4.5)-(3.4.6) in the above lemma, we immediately obtain the expression (3.3.2) for the Laplace-Stieltjes transform $\widehat{G}_\alpha$. Let us now derive the alternative integral expression (3.3.3) for G_α.

LEMMA 3.5. *Under* **(H)**, *we have for all* $\alpha \neq 0$:

$$
Q_\alpha(t) = 1 + \bar\lambda t - \bar\lambda (1 - \alpha) \int_0^t Q_\alpha^0(u) du \,,
\tag{3.4.11}
$$

with

$$
Q_\alpha^0(t) = \sum_{n=0}^{\infty} \alpha^n F^{*(n)}(t) \,,
$$

and $F^{*(n)}$ *is the n-fold convolution of the distribution function* F.

Proof. We rewrite the expression (3.4.6) Laplace-Stieltjes transform as

$$
\begin{aligned}
\widehat{Q}_\alpha(s) &= 1 + \frac{\alpha \bar\lambda}{s} (1 - \widehat{F}) \sum_{n=0}^{\infty} (\alpha \widehat{F})^n \,, \\
&= 1 + \frac{\alpha \bar\lambda}{s} \sum_{n=0}^{\infty} \alpha^n \left((\widehat{F})^n - (\widehat{F})^{n+1} \right) \,.
\end{aligned}
\tag{3.4.12}
$$

Let us now consider the function G_α^0 (resp. Q_α^0) defined similarly as for G_α (resp. Q_α) with N replaced by N^0, the no-delayed renewal process with all interarrival times $S_n^0 = T_n^0 - T_{n-1}^0$ distributed according to F. Then,

$$G_\alpha^0(t) = \sum_{n=0}^\infty \alpha^n \left(P_\pi[N_t^0 \geq n] - P_\pi[N_t^0 \geq n+1] \right),$$

$$= \sum_{n=0}^\infty \alpha^n \left(P_\pi[T_n^0 \leq t] - P_\pi[T_{n+1}^0 \leq t] \right),$$

$$= \sum_{n=0}^\infty \alpha^n \left(F^{*(n)} - F^{*(n+1)} \right)(t).$$

Therefore, the Laplace-Stieltjes transform of G_α^0 is written also as

$$\widehat{G_\alpha^0} = \sum_{n=0}^\infty \alpha^n \left((\widehat{F})^n - (\widehat{F})^{n+1} \right).$$

By defining the function $I_\alpha^0(t) := \int_0^t G_\alpha^0(u)du$, we then see from (3.4.12) that

$$\widehat{Q}_\alpha(s) = 1 + \alpha\bar\lambda \widehat{I_\alpha^0},$$

and thus

$$Q_\alpha(t) = 1 + \alpha\bar\lambda \int_0^t G_\alpha^0(u)du. \tag{3.4.13}$$

Finally, by same arguments as in (3.4.5), we have

$$G_\alpha^0 = \left(1 - \frac{1}{\alpha} \right) Q_\alpha^0 + \frac{1}{\alpha},$$

and plugging into (3.4.13), we get the required result.

$$\square$$

By using (3.4.5) and (3.4.11), we then obtain the integral expression (3.3.3) of the function G_α as in proposition Proposition 3.2. Finally, we derive the asymptotic behavior of the mean signature plot.

PROPOSITION 3.4. *Under* **(H)***, we get:*

$$\bar{\mathcal{V}}(\infty) := \lim_{\tau \to \infty} \bar{\mathcal{V}}(\tau) = \sigma_\infty^2, \tag{3.4.14}$$

$$\bar{\mathcal{V}}(0^+) := \lim_{\tau \downarrow 0^+} \bar{\mathcal{V}}(\tau) = \bar\lambda \mathbb{E}[\xi_n^2], \tag{3.4.15}$$

and

$$\bar{\mathcal{V}}(0^+) > \bar{\mathcal{V}}(\infty) \Leftrightarrow \alpha < 0.$$

Proof. By observing that the function G_α is strictly bounded in τ by 1 for any $\alpha \in [-1,1)$, we easily obtain from the expression (3.4.3) the limit for $\bar{\mathcal{V}}(\tau)$ when τ goes to infinity. On the other hand, by substituting the integral formula (3.3.3) of the function G_α into the expression (3.4.3) of the mean signature plot, we have:

$$\bar{\mathcal{V}}(\tau) = \sigma_\infty^2 - \frac{2\alpha}{1-\alpha} (\mathbb{E}[\xi_n])^2 \left(\frac{\bar\lambda}{\alpha} \right) \left(1 - (1-\alpha)\frac{1}{\tau}\int_0^\tau Q_\alpha^0(s)ds \right).$$

Next, by noting that

$$\lim_{\tau \to 0^+} \frac{1}{\tau} \int_0^t Q_\alpha^0(s) ds = Q_\alpha^0(0) = 1 \,,$$

we deduce that

$$\lim_{\tau \to 0^+} \bar{\mathcal{V}}(\tau) = \sigma_\infty^2 - \frac{2\bar{\lambda}\alpha}{1-\alpha} \left(\mathbb{E}[\xi_n] \right)^2 \,, \tag{3.4.16}$$

which gives (3.4.15) from the expression (3.2.1) of σ_∞^2. Finally, we immediately see from (3.4.16) that $\bar{\mathcal{V}}(0^+) > \bar{\mathcal{V}}(\infty)$ if and only if $\alpha < 0$.

$\square$

3.5 Appendix: a comparison to the Eurostoxx50

For the sake of completeness, we have performed a (non-parametric) estimation on the Eurostoxx50 3M-future (large tick asset) contract exchanged on the EUREX platform.

For this kind of asset we have noticed a smaller microstructure noise, with $\alpha \approx -70\%$ (confidence interval $[-0.690, -0.674]$), mainly due to the different structure of the limit order book. While the EURIBOR contract is exchanged in a prorata matching engineering LOB, the EUROSTOXX market obeys to the FIFO (First In First Out) principle. This implies that while the EURIBOR's liquidity is concentrated only on the first level, the EUROSTOXX displays liquidity also on deeper ones, making reversion less important, but still significant.
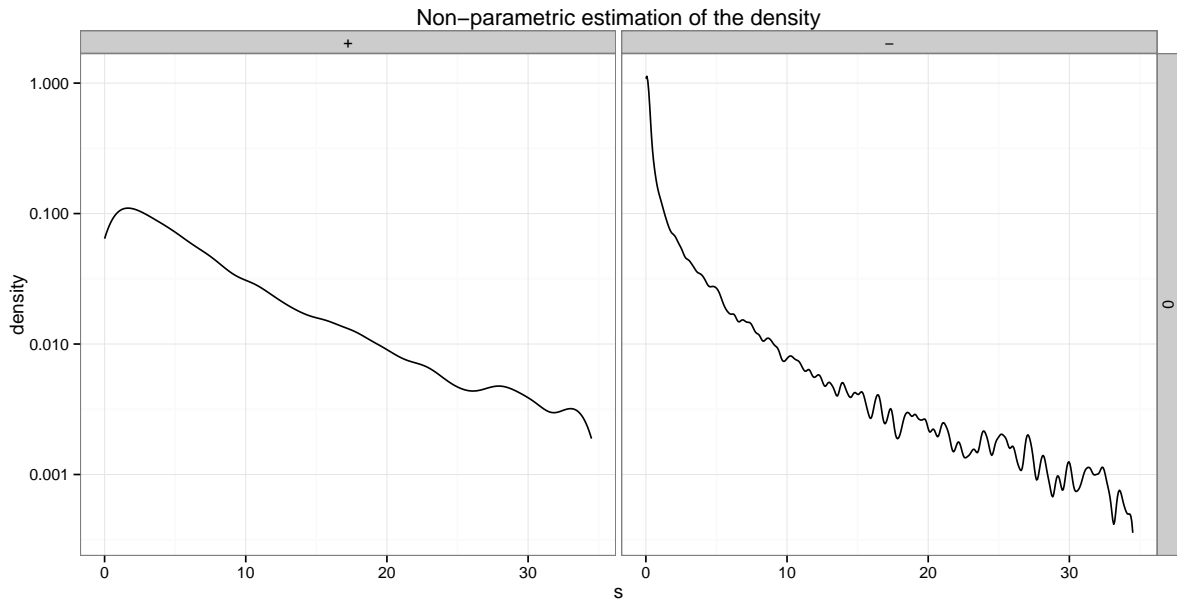
Figure 3.14: Log-density estimation of the density function $f_\pm$ on the EUROSTOXX.

Figure 3.14 shows how the shape of the density looks similar to the one displayed by Figure 3.7, even though the EUROSTOXX asset is much more volatile than the EURIBOR one: as a consequence, the inter-arrival times are usually much shorter, achieving a maximum of only 30 seconds. Figure 3.15 concerns the estimation of the hazard functions $h_\pm$. In this case as well, we notice a similar shape compared to Figure 3.10, even though both axis are rescaled.
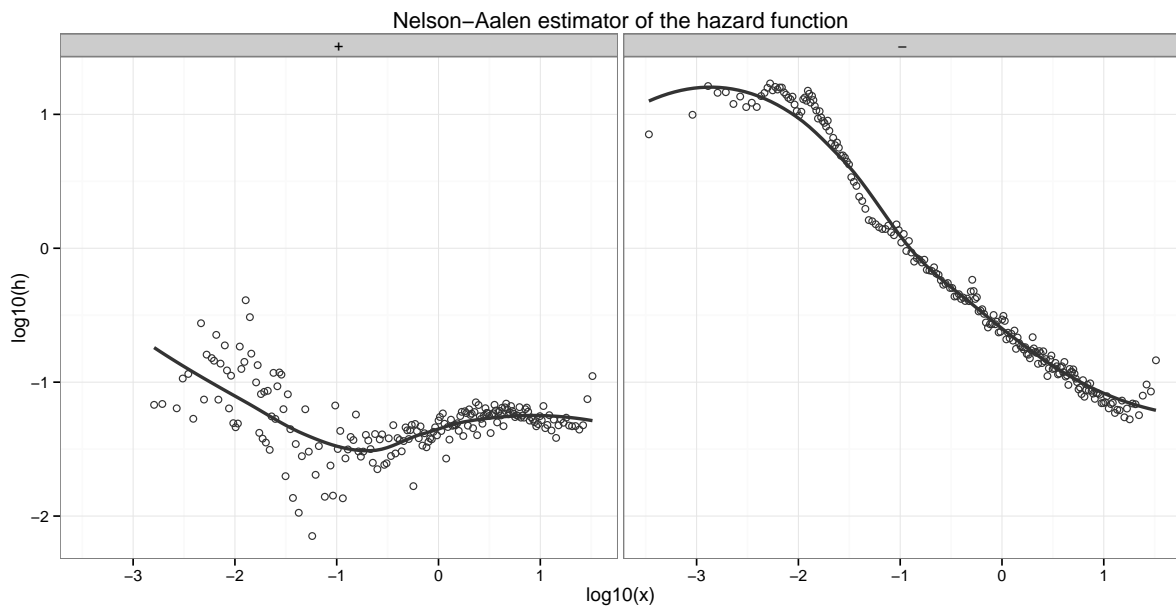
Figure 3.15: Log-density estimation of the hazard function $h_\pm$ on the EUROSTOXX.

Chapter 4

HFT and asymptotics for small risk aversion in a Markov renewal model

Abstract

We study an optimal high frequency trading problem within a market micro-structure model designed to be a good compromise between accuracy and tractability. The stock price is driven by a Markov Renewal Process (MRP), as described in [36], while market orders arrive in the limit order book via a point process correlated with the stock price itself. In this framework, we can reproduce the adverse selection risk, appearing in two different forms: the weak one, due to small market orders and reducing the probability of a profitable execution, and the strong one, due to big market orders impacting the stock price and penalizing the agent. We solve the market making problem by stochastic control techniques in this semi-Markov model. In the no risk aversion case, we provide explicit formula for the optimal controls and characterize the value function as a simple linear PDE. In the general case, we derive the optimal controls and the value function in terms of the previous result, and illustrate how risk aversion influences the trader strategy and her expected gain. Finally, using a perturbation method, optimal controls for small risk aversions are explicitly computed in terms of two simple PDE's, reducing drastically the computational cost and enlightening the financial interpretation of the results.

Introduction

Before illustrating the main results of the paper, let us recall some of the existing literature on high-frequency trading, that can be roughly divided into two main streams.

i) *Models of intra-day asset price*: this branch is devoted to the description of a tick-by-tick asset price in a limit order book, adopting two different philosophies. The **latent process** approach starts from a macroscopic unobserved process (typically a diffusion), which is contaminated by a noise reproducing the market micro-structure: discreteness of the price (valued on the tick grid), irregular spacing of price jump times (known as volatility clustering), and mean-reversion of price variations. Some papers in this direction are [39], [2], and [60]. The **micro-to-macro** approach instead models directly the observed stock price by means of point processes, see e.g. [9], [25], [1] or [7]. These papers consider sophisticated models, and are mainly intended to reproduce micro-structure stylized facts, as the explosion of the signature plot, the Epps effect, the volatility clustering and the short mean-reversion. Often the main purpose is volatility estimation, while trading applications are not studied: the complexity of these models leads to high dimensional equations in control problems, difficult to treat both analytically and numerically.

ii) *High frequency trading problems*: another important literature stream focuses on trading problems in the limit order book: stock liquidation and execution problems ([5], [4], [10], [45], etc ...), or market making problems ([6], [23], [44], [42], [49], [16], etc ...). These papers use stochastic control methods to determine optimal trading strategies, and they are mostly based on classical models for asset price, typically arithmetic or geometric Brownian motion, while the market order flow is usually driven by a Poisson process independent of the continuous price process.

The goal of this paper is to make a bridge between these two streams of literature, constructing a simple model for the limit order book, intended to be both

$\diamond$ *realistic*, capturing the main stylized facts of micro-structure, easy to estimate and simulate,

$\diamond$ *tractable*, (simple to analyze and implement) in order to lead to explicit formula in high-frequency trading applications with a nice financial interpretation.

Since our point of view is the market maker's one, that we allow to interact with the market only by limit orders, **we will speak of limit orders only for those posted by the agent, while trades, or equivalently called market orders, refer to non-agent market orders arriving in the market**, and potentially matching the agent limit orders.

The stock price

We shall rely on our previous work [36], where we show how Markov Renewal processes are an extremely flexible and pertinent tool to model the stock price at high frequency, as well as easy to estimate, simulate and understand. **We assume that the bid-ask spread is constantly one tick and the stock price jumps of one tick**, which is consistent with liquid assets with large tick.

By modeling the stock price through a pure jump process (and not a continuous one as e.g. a Brownian motion), we are able to introduce probabilistic and mechanical dependences between the price evolution and the trades arrival. We can easily introduce correlation between the next price jump and proportion of ask/bid trades before the next jump, and take into account the jump risk. In the context of option pricing, jumps represent a source of market incompleteness, leading to unhedgeable claims: similarly, jumps of the stock price in the electronic market are a real source of risk for the market maker. More precisely, the agent faces two kind of risk:

i) *Market risk:* when the price suddenly jumps, the whole agent inventory is re-evaluated, changing the portfolio value in no time (i.e. a finite amount of risk in no time, whereas the Brownian motion has quadratic variation proportional to the interval length).

ii) *Adverse selection risk:* in our model, we assume that an upwards (resp. downwards) jump at time t corresponds to a big market order clearing the liquidity on the best ask (resp. bid) price level. If the agent has posted a **small** limit order, say on the bid side, the latter has to be executed, since (we guess that) the goal of the big market order was to clear all the available liquidity (rather than consuming a fixed amount of it). In this sense, the agent does not affect the market dynamics. In this scenario, the agent is systematically penalized, since she sells liquidity at t_- for less than its value at t. This risk, known as **adverse selection**, will be incorporated, measured and hedged, thanks to our market model.

The market order flow

We introduce a suitable modeling of the market order flow, taking into account the real dependence with the stock price dynamics. The existing literature has provided several models for the arrival of trades in the limit order book. The seminal work [34] describes these events as a time series with an autoregressive behaviour, in order to model intensity spikes in the trading activity. Other authors (e.g. [19]) exploit renewal processes for modeling trades and describe the price formation in terms of this flow. One of the richest example is provided by [8], where a four-dimensional Hawkes process drives both trades and price, taking into account the mutual interaction of all its components: unfortunately, this elegant approach leads to a high-dimensional system, and consequently to computational issues. **Our model is price rather than trade centered**, since trades (no matter their side) are counted by a Cox process subordinated to the stock price. Trades arrive more frequently after a price jump, while their arrival rate decreases as the price stabilizes. In this sense, events have a much richer dynamic than a Poisson process, and they are not independent from the stock price, as often assumed. For this improvement, we pay no computational cost: we will see that the state variables describing the stock price are all we need. We do not include self-exciting components as in Hawkes process in order to keep the model dimension to the minimum.

The adverse selection risk

By adding marks (determining the trade exchange side) to the Cox process counting the trade events, we are able to reproduce the *adverse selection* risk appearing in its weak and strong form, the first limiting the agent profit, the second penalizing it, forcing the agent to play a less aggressive policy.

i) *Weak adverse selection:* it comes from the flow of small trades, made of those trades that are unable to move the market stock price. For this flow, a limit order is more likely to be matched on the less profitable side: if the price is likely to jump downwards (resp. upwards), few trades would arrive at the best ask (resp. bid) price, limiting the chances of building a short (resp. long) position (that would be profitable w.r.t. to the market direction). Thanks to this feature, the extra gain (w.r.t. to a market order) due to a limit order execution is compensated by an unfavorable execution probability.

ii) *Strong adverse selection:* differently from the weak adverse selection risk, the strong one comes from big trades affecting immediately the stock price. We assume that a limit order is automatically executed as soon as the stock price jumps over the corresponding level, i.e., for an order at the best ask (resp. bid), when the price jumps upwards (resp. downwards). In this scenario, the agent systematically loses, beyond the transaction cost, half-a-tick w.r.t. to the new mid-price. Making the stock price change its value, big trades put the market maker in a bad position, since the sudden execution forces her to sell liquidity at less than its current value.

The market making problem

In this context, we study the market making problem of an agent submitting optimally limit orders (market orders, as in [44], are not taken into account to improve the problem tractability) at best bid and best ask prices. The agent is not the unique market maker, but only one of the many participants of the exchange, and she has no constraint in terms of liquidity providing. Several authors in previous literature, as e.g. in the seminal paper [6] (see also [42]) consider limit orders, which are posted at a mid-price distance which may be nonpositive (some exception is the paper [23] which imposes a nonnegative constraint on the distance). This induces some problems with high frequency applications, in particular for large tick assets (see [31]) or pro-rata limit order book, where most of the liquidity is concentrated in few levels, making real-life rounding of the optimal quotes to the tick grid a non trivial issue. By replacing real controls with binary ones (limit order placed or not at the best price) we artificially add a policy constraint, but in such a specific context, the model fits better the reality: estimation is easier, policies are not subject to rounding as in the real case, no problem of negative posting distance exists, and the market spread is never improved; in other words **theoretical policies need no translation to real-trading ones**.

In this framework, we are able to derive explicit formula for both the value function and the (binary) optimal controls for an agent without risk aversion. Next, by a perturbation technique, we solve the market making problem for small risk aversions. This allows us to reduce drastically the problem dimension, and greatly improves the financial interpretability of the optimal strategy. In particular, we clearly understand the potential sources of gain and risk in the model, and how the introduction of risk aversion deforms them.

Plan of the paper

The structure of the paper is organized as follows. We briefly review in Section 4.1 the asset price model introduced in [36], and derive some useful results concerning the conditional mean of the stock price, i.e. a trend indicator. In Section 4.2, we describe the market order flow modeling small market trades, i.e. those trades leaving the stock price unchanged. On the contrary, big market orders, i.e. those affecting immediately the stock price value, are assumed to be incorporated into the price dynamics. For small trades, we introduce a marked Cox process subordinated to the stock price dynamics in order to reproduce the (weak) adverse selection risk and the intensity correlation between the two processes. Section 4.3 includes the formulation of the market making problem, and describes the agent process (wealth, inventory) dynamics, while Section 4.4 is devoted to the resolution of the market making problem, using a perturbation method for small risk aversion. Some numerical tests illustrate our results and show some useful results in the Appendixes.

4.1   Stock price in the limit order book

We consider a model for the mid-price of a stock (the arithmetic mean between the best-bid and best-ask price) in a limit order book (LOB) with a constant bid-ask spread $2\delta > 0$. For simplicity, we assume that the stock price jumps only of one tick. The mid-price (P_t) is then defined by the càd-làg piecewise constant process

$$P_t := P_0 + 2\delta \sum_{n=1}^{N_t} J_n, \tag{4.1.1}$$

where P_0 is the opening mid-price, N_t (representing the **tick times**) is the point process associated to the price jump times $(T_n)_n$, i.e.

$$N_t := \inf\left\{n : \sum_{k=1}^{n} T_k \leq t\right\}, \tag{4.1.2}$$

and J_n (called **price direction**) is the marks sequence valued in $\{-1, +1\}$ indicating whether the price has jumped upwards ($J_n = +1$) or downwards ($J_n = -1$) at time T_n.

4.1.1 Markov renewal model

We use a Markov renewal approach as in [36] for modeling the marked point process $(T_n, J_n)_n$, and briefly review the main features. The **price direction** is driven by the Markov chain

$$J_n = J_{n-1} B_n , \qquad (4.1.3)$$

where $B \equiv (B_n)$ is an i.i.d. sequence, independent of (J_n), and distributed according to a Bernoull iL aw on $\{-1, +1\}$ with parameter $(1+\alpha)/2$, $\alpha \in [-1, 1)$. In other words, the probability of two consecutive jumps in the same (resp. opposite) direction is given by

$$\mathbb{P}\left[J_n J_{n-1} = \pm 1\right] = \frac{1 \pm \alpha}{2} ,$$

where α represents the correlation between two consecutive price directions J_{n-1} and J_n under the stationary measure $\pi = (1/2, 1/2)$ associated to the Markov chain (J_n). For $\alpha = 0$, the jumps of the stock price are independent, for $\alpha > 0$, the price is short-term trended, while for $\alpha < 0$, the stock price exhibits a short-term mean-reversion, which is a well-known stylized fact about high-frequency data, usually called micro-structure noise.

In a second step, we model the counting process (N_t). Denoting by

$$S_n := T_n - T_{n-1} \geq 0 , \qquad (4.1.4)$$

the inter-arrival times of the price jump times, we assume that, conditioned on $J_n J_{n-1}$, (S_n) is an independent sequence of random variable with distribution

$$F_{\pm}(s) := \mathbb{P}\left[S_{n+1} \leq s \big| J_n J_{n-1} = \pm 1\right] ,$$

and density $f_{\pm}(s)$ with no masses. We can easily check that (S_n) is also unconditionally i.i.d., which implies that (N_t) is the renewal process with inter-arrival times distribution given by

$$F(s) := \frac{1+\alpha}{2} F_+(s) + \frac{1-\alpha}{2} F_-(s) . \qquad (4.1.5)$$

We define the pure jump process valued in $\{-1, +1\}$

$$I_t := J_{N_t} , \qquad (4.1.6)$$

which gives at time t the direction of the last jump of the stock price. (I_t) is a semi-Markov process in the sense that the pair (I_t, S_t) is a Markov process, where

$$S_t := t - \sup\{T_n : T_n \leq t\} \geq 0 , \qquad (4.1.7)$$

is the elapsed time since the last price jump. Finally, we set to

$$h_{\pm}(s) := \lim_{\Delta s \to 0^+} \frac{1}{\Delta s} \mathbb{P}\left[s \leq S_{n+1} \leq s + \Delta s, J_{n+1} = \pm J_n \big| S_n \geq s, J_n\right]$$
$$= \frac{1 \pm \alpha}{2} \frac{f_{\pm}(s)}{1 - F(s)} , \qquad (4.1.8)$$

the intensity function of price jump, assumed a bounded continuous function, in the same (resp. opposite) direction, and define $\mu(s)$ (resp. $\sigma^2(s)$) as the measure of the conditional trend (resp. agitation state) of the stock price:

$$\mu(s) := h_+(s) - h_-(s) , \qquad (4.1.9)$$
$$\sigma^2(s) := h_+(s) + h_-(s) . \qquad (4.1.10)$$

We recall that the elapsed time process (t, S_t) is an homogeneous Markov jump process with stochastic intensity $\sigma^2(S_t)$ (the same as the renewal process N_t, since they jump at the same time) and infinitesimal generator

$$\mathfrak{g}(t, s) \mapsto \frac{\partial \mathfrak{g}}{\partial t} + \frac{\partial \mathfrak{g}}{\partial s} + \sigma^2(s) \Delta \mathfrak{g}(t, 0) , \quad \Delta \mathfrak{g}(t, 0) := \mathfrak{g}(t, 0) - \mathfrak{g}(t, s) . \qquad (4.1.11)$$
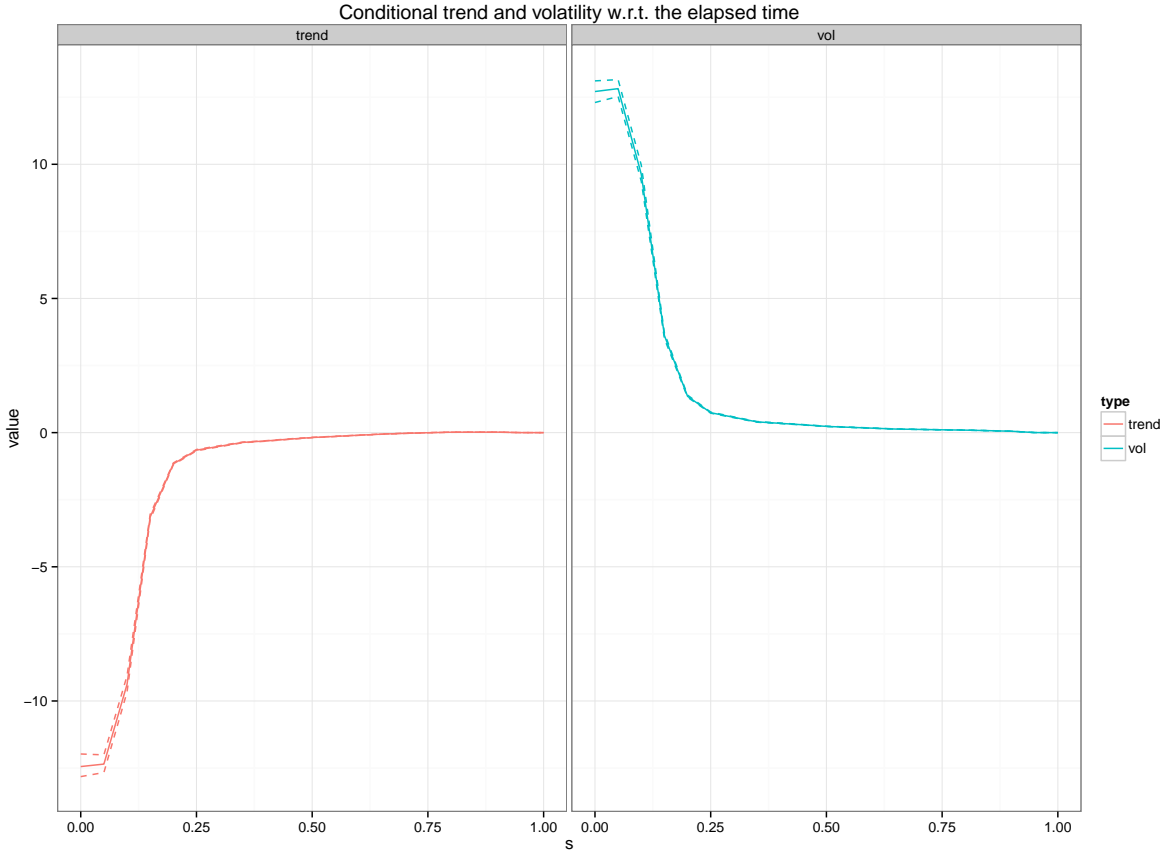
Figure 4.1: $\mu(s)$ (trend) and $\sigma^2(s)$ (volatility). For small s the renewal drift is negative, while for large s both functions tend to 0. For large s, $\mu(s)$ changes sign, reflecting a trending behavior of the stock price in the right queue of the renewal distribution. $\square$

Notations

From now on, in order to keep notations compact, we will use, for any function $f = f(x)$, $x \in \mathbb{R}^n$, the following notation:

$$\Delta_x f(x') := f(x') - f(x),$$

with the convention that the subscript in Δ_x will be omitted if it is clear from the context. Furthermore, since (N_t) is a renewal process associated to the renewal distribution F given in (4.1.5), we will often refer, in order to obtain a natural rescale for s, to

$$\hat{s} := F^{-1}(s) \in [0, 1],$$

as the renewal quantile associated to the elapsed time s. In order to increase the interpretability of the results, all the charts in this paper rescale the state variable s according to this transformation.

Data sample

We refer to [36] for the statistical estimation of the trendiness parameter α, the distribution $F_\pm$ of the renewal times, and the jump intensities $h_\pm(s)$. In the sequel, market data are taken from tick-by-tick observation of the 3-month future EUROSTOXX50, on February 2011, from 09:00:000 to 17:00:00.000 (CET). Figure 4.2 plots the form of $h_\pm(s)$ as a function of the renewal quantile: the reverting intensity $h_-(s)$ is dominant w.r.t. to the trending intensity $h_+(s)$ for small renewals, while this discrepancy tends to disappear for higher quantiles (> 0.50), ending with $h_+(s)$ dominating $h_-(s)$ on the right boundary. This tells that when the price is stable, i.e.

its quotation has been constant for a relatively long time, the micro-structural mean reversion disappears, and the price looks like a Bernoulli random walk.
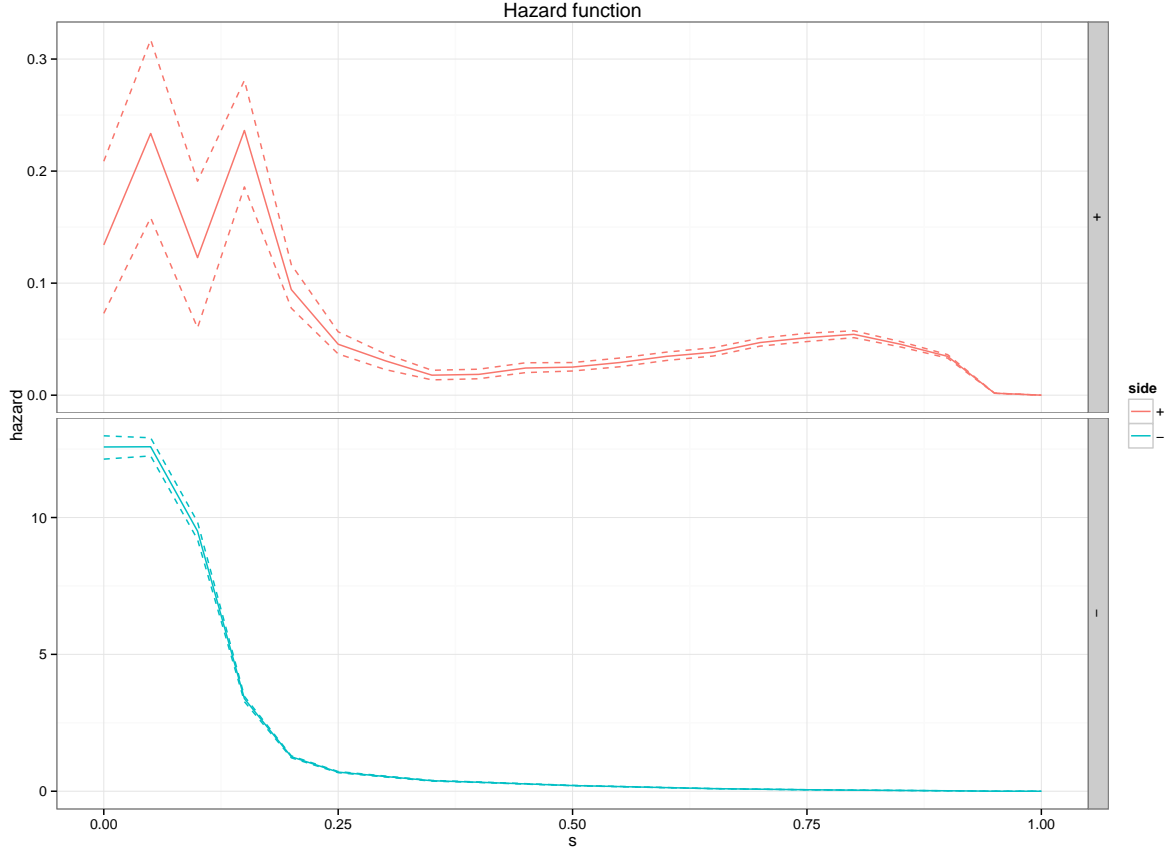
Figure 4.2: Non parametric estimation of $h_{\pm}(s)$ as a function of the renewal quantile ($\alpha = -0.75$), with bootstrap 95% confidence intervals. □

4.1.2   The stock price conditional mean and the trend indicator

We recall that the price process (t, P_t) is embedded into a Markov system with three observable state variables: (t, P_t, I_t, S_t) is a Markov process with infinitesimal generator:

$$\frac{\partial \mathfrak{g}}{\partial t} + \mathcal{L}\mathfrak{g}(t, p, i, s) = \frac{\partial \mathfrak{g}}{\partial t} + \frac{\partial \mathfrak{g}}{\partial s} + \sum_{\nu \in \pm} h_\nu(s) \Delta \mathfrak{g}(t, p + 2\nu\delta i, \nu i, 0).$$

In the sequel, for the applications of our model to market making problem, we shall extensively use properties of the mean value of the stock price at horizon, i.e.

$$\pi(t, p, i, s) := \mathbb{E}_{t,p,i,s}[P_T]. \tag{4.1.12}$$

Here, $\mathbb{E}_{t,p,i,s}$ denotes the expectation operator under the initial conditions

$$(t, P_t, I_t, S_t) = (t, p, i, s), \quad (t, p, i, s) \in [0, T] \times 2\delta\mathbb{Z} \times \{-1, +1\} \times \mathbb{R}_+.$$

We devote a separate part to the study of this function, which is fully developed in the Section 4.7. Here we concentrate the main results concerning $\pi(t, p, i, s)$ in the following proposition, which will be a useful reference in the remaining part of the paper.

PROPOSITION 4.1. *The function π in (4.1.12) is given by*

$$\pi(t, p, i, s) = p + i\theta(t, s), \tag{4.1.13}$$

where $\theta(t,s)$ is the unique bounded solution to

$$\langle \mathcal{Z}, \theta \rangle := -\frac{\partial \theta}{\partial t} - \frac{\partial \theta}{\partial s} - \mu(s)\theta(t,0) + \sigma^2(s)\theta(t,s) - 2\delta\mu(s) = 0\,, \tag{4.1.14}$$

$$\theta(T,) = 0\,,$$

for $(t,s) \in [0,T] \times \mathbb{R}_+$.

Furthermore, fixed $T \geq 0$, $\theta(t,s) := \theta^T(t,s)$ has the following properties:

  i) *it agrees with the sign of μ, i.e.*

$$\text{if } \mu(s) \geq 0\ (\leq 0), \forall s \geq 0 \Rightarrow \theta^T(t,s) \geq 0\ (\leq 0), \forall (t,s) \in [0,T] \times \mathbb{R}_+\,; \tag{4.1.15}$$

  ii) *it is bounded from below, uniformly in T, by the minus half-tick, i.e.*

$$\theta^T(t,s) \geq -\delta\,; \tag{4.1.16}$$

  iii) *it admits a limit for large horizons, i.e. fixed $t \geq 0$,*

$$\lim_{T \to \infty} \theta^T(t,s) = \frac{\bar{\alpha}(s)}{1-\alpha} := \bar{\theta}(s)\,, \tag{4.1.17}$$

  where

$$\bar{\alpha}(s) := \mathbb{P}\left[J_1 \middle| S_0 = s, J_0 = +1\right] = \sum_{\nu \in \pm} \nu \left(\frac{1+\nu\alpha}{2}\right)\left(\frac{1-F_\nu(s)}{1-F(s)}\right)\,, \tag{4.1.18}$$

  with i) $\bar{\alpha}(0) = \alpha$ and ii) $\bar{\alpha}(s) \equiv \alpha$ if marks and tick times are independent.

Proof. This proposition sums up all the main properties proved in Section 4.7: in particular the PDE representation (4.1.14) is given in Lemma 4.3, the inequalities (4.1.15) in Corollary 4.1, (4.1.16) in Corollary 4.2, and (4.1.17) is a direct consequence of Proposition 4.2, while (4.1.18) is shown in Corollary 4.3.

$\square$

From the definition of the function π, and relation (4.1.13), we see that θ admits the probabilistic representation:

$$\theta^T(t,s) = \mathbb{E}\left[P_T \middle| S_{t-} = s, P_{t-} = 0, I_t = +1\right]\,, \tag{4.1.19}$$

and can be interpreted as a martingale deviation of the stock price ($\theta \equiv 0$ means that price is martingale), as wellx as, in view of (4.1.15), a trend indicator of the stock price. The function θ can be computed either by the numerical resolution of the 1-dimensional PDE (4.1.14) via an implicit Euler scheme, or by a Monte Carlo method based on the linear Feynman-Kac representation (4.1.19). We plot in Figure 4.3 the form of θ for a fixed horizon T.

4.2   Market order flow modeling and adverse selection

In this section, we model the market order flow, that is the counterpart trade of the limit orders in a LOB. We distinguish two types of market orders:

  ◇ **big market orders** that affect the bid or ask price, inducing a jump of the mid-price;

  ◇ **small market orders** that do not affect the price.
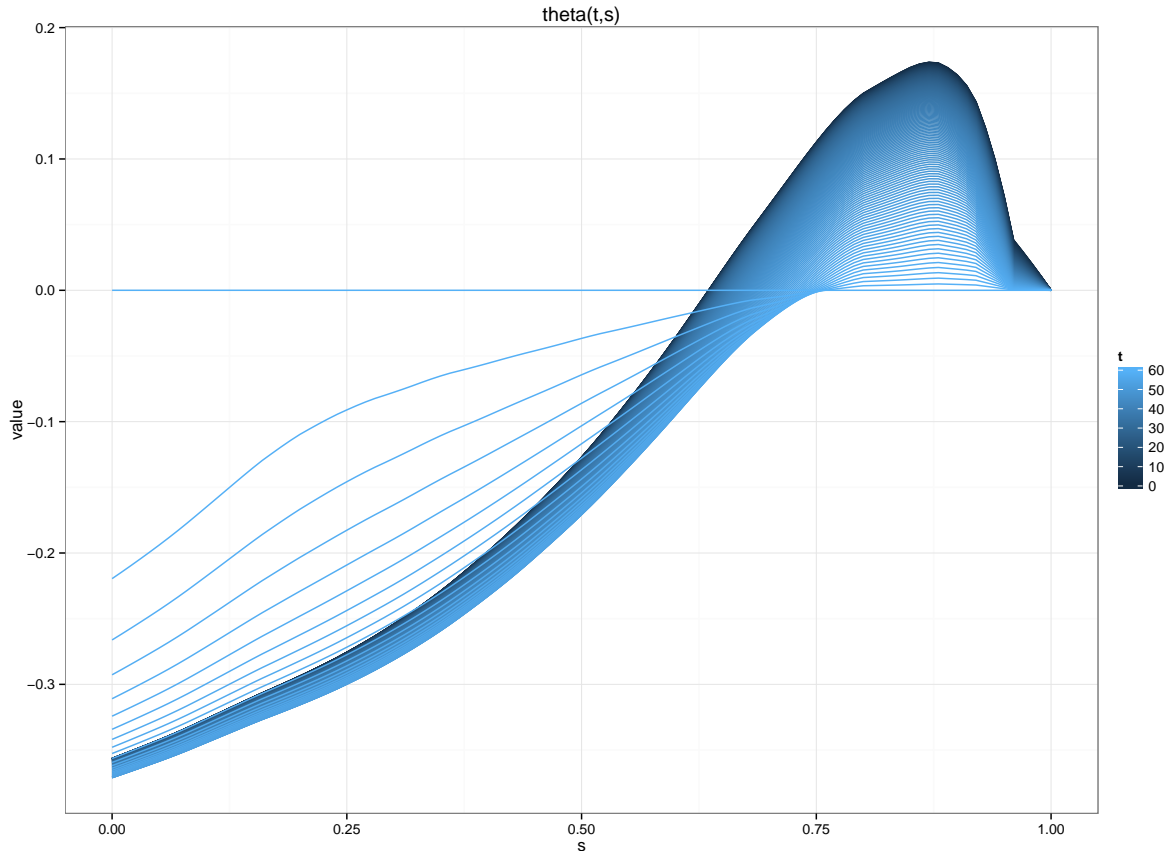
Figure 4.3: $\theta(t, s)$ for different t-sections. Its value is negative for small s, it inverts its sign for big s, and goes to 0 in the distribution queue. For $t = 0$, $\theta(, s)$ approximates its asymptotical behavior, given by (4.1.17).   □

Let us first describe the impact of big market orders. Suppose that a limit order is posted, say at the bid price. If a big market order arrives at the bid price, and consumes all the available liquidity, the price jumps downwards. The agent limit order is then executed at the new best ask price, i.e. it becomes a market buy order, hence is executed unfavorably. This phenomenon is know in the literature on market micro-structure as the **(strong) adverse selection**. We discuss more in detail this feature in the next section (see Remark 4.1). We now focus on small market orders that we model by a marked point process (θ_k, Z_k).

  i) *Timestamps:* the increasing sequence (θ_k) represents the arrival timestamps of (small) market orders.

 ii) *Marks:* the marks $(Z_k) \in \{-1, +1\}$, represent the side of the exchange, with the convention that when $Z_k = -1$(resp. $+1$), the trade is exchanged at the best bid (resp. ask) price, i.e. market sell (resp. buy) order has arrived.

In this paper, we do not take into account the size of trades. Here is an example of a database in a market with tick size $2\delta = 0.01$. To every trade, we attach the corresponding most recent quotes.

index k	θ_k	Traded price	ASK-BID	Z_k
1	09:00:01.123	98.47	98.47 - 98.46	+ 1
2	09:00:02.517	98.46	98.47 - 98.46	- 1
3	09:00:02.985	98.47	98.48 - 98.47	- 1
4	09:00:03.110	98.47	98.48 - 98.47	- 1
5	09:00:05.458	98.47	98.47 - 98.46	+ 1

The market order counting process

On one hand, we assume that the counting process (M_t) associated to (θ_k) is a Cox process with conditional intensity $\lambda(S_t)$, where S_t is the time spent since the last price jump given in (4.1.7). This approach extends the simple case where (M_t) is a Poisson process. A statistical procedure for the estimation of λ is described in the Section 4.5: Figure 4.4 shows the function λ as a function of renewal quantile. We recall that for small values the function $\sigma^2(s)$ defined at (4.1.10) is big (Figure 4.1): when the price is very unstable, many trades arrive in the limit order book. On the contrary, when the price stabilizes, the trading activity is weaker, but present.
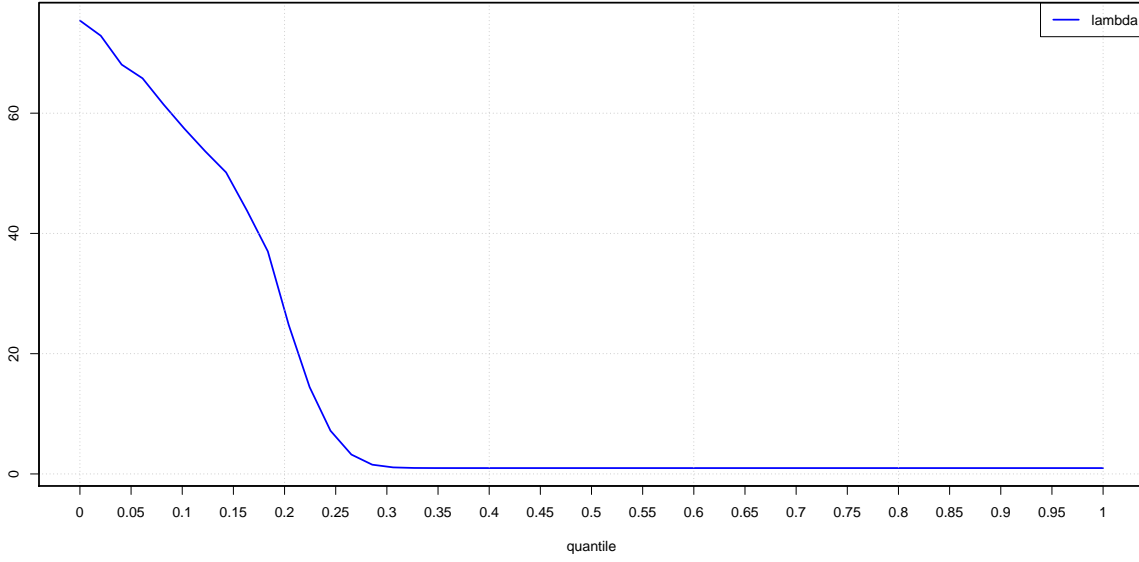
Figure 4.4: estimation of $\lambda(s) = \lambda_0 + a \exp(-ks)$. The conditional rate of order arrival decays exponentially with the time passing with no event occurring, but never completely disappears, as shown by $\lambda_0 > 0$, representing the base and minimal intensity of the process.   □

We shall assume that the intensity function λ is a continuous bounded function of s.

The market order exchange side

On the other hand, we assume that market order trade and stock price in the LOB are correlated via the relation:

$$Z_k := \Gamma_k I_{\theta_k-} \, , \tag{4.2.1}$$

where $\Gamma \equiv (\Gamma_k)$ is an i.i.d. sequence, independent of all other processes, and distributed according to a Bernoulli law on $\{-1, +1\}$ with parameter $(1 + \rho)/2$, with $\rho \in (-1, 1)$. It is straightforward to see that

$$\rho = \mathrm{Corr}(Z_k, I_{\theta_k^-}) \, ,$$

with the following interpretation:

i) for $\rho = 0$, the law of the trade side does not depend on the stock price, and market order flow arrives independently at best bid and best ask. This is the usual assumption made in the literature, see e.g. [6];

ii) for $\rho > 0$, most of the trade sides are **concordant** with the direction of the last jump of the stock price: market orders arrive more often on the **strong** side $(+)$ of the limit order book, i.e. on the same direction than the last jump - best ask (resp. bid) when price jumped upwards (resp. downwards);

iii) for $\rho < 0$, most of the trade sides are **discordant** with the direction of the last jump of the stock price: market orders arrive more often in the **weak** side $(-)$ of the limit order book, i.e. the side in the opposite direction than the last jump - best bid (resp. ask) when price jumped upwards (resp. downwards).

We define the concordant $(+)$ and discordant $(-)$ trade intensity as

$$\lambda_\pm(s) := \left(\frac{1 \pm \rho}{2} \right) \lambda(s) . \tag{4.2.2}$$

This definition is consistent with the one of $h_\pm(s)$, where $\pm$ indexes the concordance $(+)$ or discordance $(-)$ of two consecutive jumps.

The weak adverse selection risk

From (4.2.1), and by the strong law of large numbers, we have a consistent estimator of ρ given by

$$\hat{\rho}^{(n)} = \frac{1}{n} \sum_{k=1}^n \frac{Z_k}{I_{\theta_k -}} = \frac{1}{n} \sum_{k=1}^n Z_k I_{\theta_k^-} \longrightarrow \mathbb{E}\left[\Gamma_k \right] = \rho , \quad a.s. ,$$

as n goes to infinity. Estimation on real data leads to a value of ρ around -50%. This means that about 3 over 4 trades arrive on the weak side of the limit order book. Recall that stock price usually exhibits a short-term mean reversion, i.e. a negative correlation α of price increments, so that

$$\alpha\rho > 0 . \tag{4.2.3}$$

The fact that α and ρ are of the same sign is consistent with the execution dynamics. Suppose on the contrary that α and ρ are of opposite sign, say $\alpha < 0$ and $\rho > 0$, and assume e.g. that the last price jumped downwards. Then $\rho > 0$ means that most of the trades will occur at best bid, hence will execute buy limit orders in a bull market (since $\alpha < 0$), allowing market makers on best bid to open a low risk profitable position. The quantity $\alpha\rho$ is a measure of the inefficiency of limit orders w.r.t. to trend capturing: the bigger it is, the lower is the probability of building a profitable position via a limit order. This quantity compensates the intrinsic advantage of a limit order execution (one spread w.r.t. to a market order), and provides a first explanation of why market making is not a trivial game. We call this phenomenon the **weak adverse selection**, in comparison with the strong adverse selection considered above and related to big market orders.

4.3 The market making problem

The agent strategy

The agent strategy consists in placing continuously limit orders of constant small size $L \in \mathbb{N} \setminus (0)$, (where small is meant w.r.t. to the total liquidity provided by all the market makers) on both sides, and at the best price available. The market making strategy is then described by a pair of predictable processes (ℓ^+, ℓ^-) valued in $\{0, 1\}$. When $\ell_t^+ = 1$ (resp. $\ell_t^- = 1$), a limit order of size L is posted at time t on the strong (resp. weak) side, while in the opposite case no limit order is submitted or the limit order is cancelled. We denote by $\mathcal{A}$ the set of market making controls $\boldsymbol{\ell} = (\ell^+, \ell^-)$.

Every time a small market order arrives in the limit order book, if the agent has placed an order on the corresponding side, the latter is executed according to a random variable, whose distribution may differ according to the book matching rules. We recall the two main frameworks we can deal with.

⋄ *Price time priority (PTP)*: in a PTP order book, orders are matched according to their price (more priority to those closer to the mid price) and time (like in single file queue).

⋄ *Pro-rata*: in a (pure) pro-rata order book, there is price priority (as in PTP), but not the time one. Multiple market makers are executed when a single trade arrives, according to a proportion rewarding the limit orders of bigger size.

Notice that, if the price jumps upwards and the agent is in the condition to place her limit orders immediately after the jump, she will find a huge volume of concurrent limit order on the ask side (old orders), while very few on the bid side. The situation is symmetric when the price has jumped downwards. We then consider the distributions

$$\vartheta_\pm(dk, L) \text{ on } \{0, \ldots, L\},$$

where $\vartheta_-(dk, L)$ (resp. $\vartheta_+(dk, L)$) is the distribution of the executed quantity of limit order of size L in the concordant (resp. discordant), i.e. strong (resp. weak) side, of the limit order book (an estimation procedure for $\vartheta_\pm$ is provided in the Section 4.6). We denote by

$$\Phi_\pm^m(L) := \int k^m \vartheta_\pm(dk, L), \quad m = 1, 2,$$

the first and second moment of these distributions.

REMARK 4.1 (The strong adverse selection risk). *Recall once again that the sign $\pm$ indexing the distribution must not be interpreted as the ask/bid side of the limit order book but as the strong/weak side of the limit order book taking into account the last price direction. Moreover, in order to be consistent with the small agent assumption (the price is exogenous and not impacted by the agent strategy), we assume that, if the price jumps across the level of a limit order placed by the agent, the latter is automatically executed. This can be justified saying that, since the agent is small, the price jumps independently of the presence of her limit order, since a large market order whose goal was (at least) to clear the best level. Furthermore, since the spread is constantly one tick and orders are placed at the best price, when the price jumps, limit orders converts automatically to market ones, which are immediately executed. Notice that this scenario is particularly adverse to the agent: she is selling (resp. buying) a stock at ask price $P_{t-}+\delta$ (resp. bid price $P_{t-}-\delta$), while the current mid-price is $P_t = P_{t-}+2\delta$ (resp. $P_t = P_{t-}-2\delta$), so in both cases she is losing δ for each lot! The sudden execution is both against the market and does not let her the time to close the spread, leaving an open position: she faces both adverse selection and inventory risk. This phenomenon, refereed as* **strong adverse selection**, *is considered also in [19].* ☐

The wealth and the inventory process

We assume that each transaction is subject to a fixed cost $\varphi \geq 0$. Let us then denote by (X_t) and (Y_t) the wealth and inventory describing the agent portfolio, valued respectively in $\mathbb{R}$ and $\mathbb{Z}$.

LEMMA 4.1. *For a market making strategy $\boldsymbol{\ell} \in \mathcal{A}$, the dynamics of the portfolio value processes X and Y are given by*

$$dX_t = \sum_{\nu \in \pm} \int k\ell_{t-}^\nu \left(\nu P_{t-}I_{t-} + \delta - \varphi\right) \left(R_\nu^{trd}\left(dt, dk, S_{t-}\right) + R_\nu^{jmp}\left(dt, dk, S_{t-}\right)\right),$$

$$dY_t = -\sum_{\nu \in \pm} \int k\,\nu\,\ell_{t-}^\nu I_{t-} \left(R_\nu^{trd}\left(dt, dk, S_{t-}\right) + R_\nu^{jmp}\left(dt, dk, S_{t-}\right)\right),$$

where $R_\pm^{trd}$ (resp. $R_\pm^{jmp}$) is a random measure with intensity

$$\lambda_\pm(S_{t-})dt \otimes \vartheta_\pm(dk, L), \quad (resp.\ h_\pm(s)(S_{t-})dt \otimes \delta_L(dk)),$$

and δ_L is the Dirac measure at L.

Proof. To fix the ideas, assume that, at time t, $i = I_{t-} = +1$, i.e. the last jump of the price has been upwards (in the case $i = -1$ the proof is symmetric). Then if $\ell_{t-}^{\pm} = 1$, i.e. if the agent has placed a limit order on the strong (i.e. ask) or the weak (i.e. bid) side:

i) either she can be executed by an incoming trade of a random number of quantities k, where k has distribution $\vartheta_{\pm}(dk, L)$, with trade intensity $\lambda_{\pm}(S_{t-})$

ii) or she can be entirely executed, thus $k = L$, by a jump of the price, with rate $h_{\pm}(S_{t-})$.

In both cases, the agent inventory (Y_t) jumps of $\mp k$, while her wealth (X_t) jumps of k times $\pm P_{t-}$ (asset sold or bought), plus the market making prime of δ (the half spread), minus the fixed cost φ.

$\square$

We now consider the following criterion for the market making optimization problem, as usually adopted in [6], [19], [44]: the agent is looking for the optimal admissible market making strategy, which maximises her expected portfolio value at terminal date T, evaluated at the mid price:

$$V_T := X_T + Y_T P_T \,,$$

while controlling her final inventory through a quadratic penalization term ηY_T^2, with a risk aversion parameter $\eta \geq 0$.

We can now define in our MRP model the value function associated to the market making problem:

$$\mathbf{u}^{(\eta)}(t, p, i, s, x, y) := \max_{\ell \in \mathcal{A}} \mathbb{E}_{t,p,i,s,x,y} \left[X_T + Y_T P_T - \eta Y_T^2 \right] \,, \qquad (4.3.1)$$

for $(t, p, i, s, x, y) \in [0, T] \times 2\delta\mathbb{Z} \times \{-1, +1\} \times \mathbb{R}_+ \times \mathbb{R} \times \mathbb{Z}$, and where $\mathbb{E}_{t,p,i,s,x,y}$ denotes the expectation operator under the initial conditions $P_{t-} = p$, $I_{t-} = i$, $S_{t-} = s$, $X_{t-} = x$, $Y_{t-} = y$.

The choice of a linear/quadratic utility function rather than an exponential one is purely due to computational ease: the utility function being polynomial in the state variable y allows us to split PDE's according to their degree, reducing the problem dimension. The penalization term $-\eta Y_T^2$ limits the agent inventory risk: the agent does not want to close her trading day with a large position, that she would execute via a unique market order impacting the market. The quadratic form is consistent with a limit order book with constant liquidity shape, as explained in [20]: the risk aversion parameter η has to be considered as the subjective aversion of the agent to a final market order. This risk term was also recently demonstrated to stem from model ambiguity, see [18]. Since trading horizons are usually short (minutes), this penalisation affects the whole strategy, and provides an excellent inventory control throughout the whole trajectory, as we will illustrate later.

As an alternative, this penalisation can be replaced by $-\eta \int_t^T Y_u^2 du$, without changing substantially the arguments we are going to adopt to solve the control problem.

4.4 Value function and optimal controls: a perturbation approach

In order to solve the HJB equation associated to the optimal control problem (4.3.1), we will go through the following steps:

i) we consider an agent with no risk aversion ($\eta = 0$), and provide analytical formula for the optimal controls and a numerical method for the value function;

ii) thanks to a suitable variable change, we perform a dimension reduction of the HJB equation for $\eta > 0$, and obtain optimal controls as a non-explicit deformation of the previous case;

iii) finally, by a perturbation method for $\eta \to 0^+$, we provide optimal controls for small risk aversion in terms of the solution of **four linear PDE's**, and give a financial interpretation of this result.

From (4.1.11) and the dynamics of the controlled process (X_t, Y_t) in Lemma 4.1, the Hamilton-Jacobi-Bellman (HJB) equation arising from dynamic programming associated to the control problem (4.3.1) is given by

$$-\frac{\partial \mathbf{u}^{(\eta)}}{\partial t} - \frac{\partial \mathbf{u}^{(\eta)}}{\partial s} - \sum_{\nu \in \pm} \max_{\ell \in \{0,1\}} h_\nu(s)\langle \mathcal{J}_\nu[\ell], \mathbf{u}^{(\eta)}\rangle + \lambda_\nu(s)\langle \mathcal{T}_\nu[\ell], \mathbf{u}^{(\eta)}\rangle = 0\,, \tag{4.4.1}$$

$$\mathbf{u}^{(\eta)}(T,) = x + yp - \eta y^2\,,$$

for $(t,p,i,s,x,y) \in [0,T] \times 2\delta\mathbb{Z} \times \{-1,+1\} \times \mathbb{R}_+ \times \mathbb{R} \times \mathbb{Z}$, where

$$\langle \mathcal{J}_\pm[\ell], \mathfrak{g}\rangle := \Delta\mathfrak{g}(t, p \pm 2\delta i, \pm i, 0, x + L\ell(\pm ip + \delta - \varphi), y \mp iL\ell)\,, \tag{4.4.2}$$

$$\langle \mathcal{T}_\pm[\ell], \mathfrak{g}\rangle := \int \Delta\mathfrak{g}(t, p, i, s, x + k\ell(\pm ip + \delta - \varphi), y \mp ik\ell)\,\vartheta_\pm(dk, L)\,. \tag{4.4.3}$$

The interpretation of these operators is rather clear:

i) on one hand, $\langle \mathcal{J}_\pm[\ell], \mathbf{u}^{(\eta)}\rangle$ represents the variation of the value function when a limit order ℓ in the side $\pm$ of the LOB is executed due to a price jump (this occurs with intensity rate $h_\pm(s)$), hence the totality of size L is traded by the big market orders at the unfavorable price, right after jump (strong adverse selection);

ii) on the other hand, $\langle \mathcal{T}_\pm[\ell], \mathbf{u}^{(\eta)}\rangle$ represents the variation of the value function when a limit order ℓ on the side $\pm$ of the LOB is executed by a small market order (which arrives with intensity $\lambda_\pm(s)$), hence a quantity $k \in \{0, \ldots, L\}$ is traded with probability $\vartheta_\pm(dk, L)$ at the favorable current price.

The following lemma shows that the value function os this problem is actually bounded.

LEMMA 4.2. *There exists some positive constant C s.t.*

$$x + y\,\mathbb{E}_{t,i,s}[P_T] - \eta y^2 \leq \mathbf{u}^{(\eta)}(t,p,i,s,x,y) \leq x + yp + e^{C(T-t)}(1 + |y|)\,,$$

for all $(t,p,i,s,x,y) \in [0,T] \times 2\delta\mathbb{Z} \times \{-1,+1\} \times \mathbb{R}_+ \times \mathbb{R} \times \mathbb{Z}$.

Proof. Let us consider the function: $\varphi(t,p,x,y) := x + yp + e^{C(T-t)}(1 + |y|)$ for some positive constant C. Then, under the assumption that $h_\pm$ and $\lambda_\pm$ are bounded, say by B_∞, a straightforward calculation shows that:

$$-\frac{\partial \varphi}{\partial t} - \sum_{\nu \in \pm} \max_{\ell \in \{0,1\}} h_\nu(s)\langle \mathcal{J}_\nu[\ell], \varphi\rangle + \lambda\nu\langle \mathcal{T}_\nu[\ell], \varphi\rangle$$

$$\geq Ce^{C(T-t)}(1 + |y|) - 2B_\infty\big[L|\delta - \varepsilon| + 2\delta|y| + 2Le^{C(T-t)}\big] \geq 0\,,$$

for C large enough. By Dynkin's formula for pure jump processes, we deduce that the process $\varphi(t, P_t, X_t, Y_t)$ is a supermartingale for any ℓ admissible control, and so:

$$\mathbb{E}_{t,p,i,s,x,y}\big[X_T + Y_T P_T - \eta Y_T^2\big] \leq \mathbb{E}_{t,p,i,s,x,y}\big[\varphi(T, P_T, X_T, Y_T)\big] \leq \varphi(t,p,x,y)\,.$$

Since ℓ is arbitrary in the above inequality, this shows the required upper bound: $\mathbf{u}^{(\eta)} \leq \varphi$. The lower bound is instead given by holding the inventory ($\ell \equiv 0$) until the horizon T.

$\square$

4.4.1 The no risk aversion case

An agent with no risk aversion does not worry about her market position since neither any penalty for holding a large inventory affects her utility function, nor she has any inventory constraint. Our guess is that the value function can be decomposed as

i) the **hold** part, given by the average value at T of the current portfolio, and

ii) the **market making** part, obtained by an optimal strategy, completely independent from the current portfolio, i.e. from the variables (x, p, i, y).

This suggests the ansatz:

$$\mathbf{u}^{(0)} = \mathbf{u}^{(0)}_{hold} + \mathbf{u}^{(0)}_{mm}, \tag{4.4.4}$$

$$\mathbf{u}^{(0)}_{hold}(t, p, i, s, x, y) := x + y\, \mathbb{E}_{t,p,i,s}\left[P_T\right],$$

$$\mathbf{u}^{(0)}_{mm}(t, s) := \omega(t, s).$$

We will prove that $\mathbf{u}^{(0)}_{mm}$ is nonnegative: it corresponds indeed to the additional value with respect to the hold-strategy in $\mathbf{u}^{(0)}_{hold}$, and the key feature is to observe that it depends only on (t, s) in the no-risk aversion case. Thanks to Lemma 4.3, and setting the new state variable, called **strong inventory**

$$q := iy,$$

$\mathbf{u}^{(0)}_{hold}$ in (4.4.4) becomes

$$\mathbf{u}^{(0)}_{hold}(t, p, i, s, x, y) = (x + yp) + (q\theta(t, s)),$$
$$= \text{current portfolio value} + \text{martingale deviation}.$$

Notice that the latter decomposes as i) the sum of the current portfolio portfolio value, valued at the mid-price, and ii) a part proportional to q. The function $\theta(t, s)$ (studied in paragraph Section 4.7) represents the average distance from the martingale price, i.e. it measures the average behavior of the stock price in terms of drift and reversion. For $\theta > 0$ (resp. $\theta < 0$), the average value of stock price at maturity will reflect a drifting (resp. reverting) component, while for $\theta \equiv 0$, the stock price is a martingale.

By plugging the ansatz (4.4.4) into the HJB equation (4.4.1), we obtain the following characterization of the value function and optimal controls.

THEOREM 4.1. *For $\eta = 0$, the value function of the control problem (4.3.1) is given by*

$$\mathbf{u}^{(0)} = \mathbf{u}^{(0)}_{hold} + \mathbf{u}^{(0)}_{mm},$$

$$\mathbf{u}^{(0)}_{hold}(t, p, i, s, x, y) = x + yp + q\theta(t, s),$$

$$\mathbf{u}^{(0)}_{mm}(t, s) = \omega(t, s) \geq 0,$$

where $\omega(t, s)$ is the unique bounded viscosity solution to

$$-\frac{\partial\omega}{\partial t} - \frac{\partial\omega}{\partial s} - \sigma^2(s)\Delta\omega(t, 0) - \sum_{\nu \in \pm} \max\left(G_\nu(t, s), 0\right) = 0, \tag{4.4.5}$$

$$\omega(T,) = 0,$$

for $(t, s) \in [0, T] \times \mathbb{R}_+$, with

$$G_\pm(t, s) := \lambda_\pm(s)\left(\delta - \varphi \mp \theta(t, s)\right)\Phi^1_\pm(L) - h_\pm(s)\left(\delta + \varphi + \theta(t, 0)\right)L, \tag{4.4.6}$$

and admits the probabilistic representation

$$\omega(t,s) = \sum_{\nu \in \pm} \mathbb{E}_{t,s} \left[\int_t^T \max\left(G_\nu(u, S_u), 0\right) du \right].$$ (4.4.7)

Moreover, the optimal controls are given in feedback form by

$$\hat{\ell}_\pm(t,s) = \mathbb{1}\{G_\pm(t,s) > 0\}.$$ (4.4.8)

Proof. From the ansatz (4.4.4) and the definitions (4.4.2)-(4.4.3) of the operators $\mathcal{J}_\pm$ and $\mathcal{T}_\pm$, we have

$$\frac{\partial \mathbf{u}^{(0)}}{\partial t} + \frac{\partial \mathbf{u}^{(0)}}{\partial s} = q\left(\frac{\partial \theta}{\partial t} + \frac{\partial \theta}{\partial s}\right) + \left(\frac{\partial \omega}{\partial t} + \frac{\partial \omega}{\partial s}\right),$$

$$\langle \mathcal{J}_\pm[\ell], \mathbf{u}^{(0)} \rangle = q(\pm 2\delta \pm \theta(t,0) - \theta(t,s)) + \Delta\omega(t,0) + L\ell\left(-\delta - \epsilon - \theta(t,0)\right),$$

$$\langle \mathcal{T}_\pm[\ell], \mathbf{u}^{(0)} \rangle = \int k\ell\left(\delta - \varphi \mp \theta(t,s)\right) \vartheta_\pm(dk, L).$$

Now, plugging into (4.4.1),

$$-\frac{\partial \omega}{\partial t} - \frac{\partial \omega}{\partial s} - \sigma^2 \Delta\omega(t,0) - \sum_{\nu \in \pm} \max\left(G_\nu(t,s), 0\right)$$

$$-q\left(\frac{\partial \theta}{\partial t} + \frac{\partial \theta}{\partial s} + \mu(s)\theta(t,0) - \sigma^2(s)\theta(t,s) + 2\delta\mu(s)\right) = 0.$$

From (4.1.14), the expression in the bracket in front of q is zero, and we obtain the PDE satisfied by ω. The terminal condition is clear since $\mathbf{u}(T,p,i,s,x,y) = x + yp = \mathbf{u}_{hold}^{(0)}(T,p,i,s,x,y)$, and so $\omega(T,p,i,s,x,y) = 0$.

The probabilistic representation (4.4.7) is simply the Feynman-Kac representation of the linear PDE (4.4.5), recalling that (S_t) is a piecewise deterministic jump process with intensity $\sigma^2(S_t)$, see (4.1.11), and since h and λ are bounded and non-negative, so are G and ω.

Finally, the optimal feedback control on the side $\pm$ of the LOB is obtained for $\hat{\ell}_\pm$ attaining the argument maximum over $\ell \in \{0,1\}$ of

$$h_\pm(s)\langle \mathcal{J}_\pm[\ell], \mathbf{u}^{(0)} \rangle + \lambda_\pm \langle \mathcal{T}_\pm[\ell], \mathbf{u}^{(0)} \rangle.$$

In other words,

$$\hat{\ell}_\pm = 1 \iff h_\pm(s)\langle \mathcal{J}_\pm[1], \mathbf{u}^{(0)} \rangle + \lambda_\pm(s)\langle \mathcal{T}_\pm[1], \mathbf{u}^{(0)} \rangle > h_\pm(s)\langle \mathcal{J}_\pm[0], \mathbf{u}^{(0)} \rangle + \lambda_\pm(s)\langle \mathcal{T}_\pm[0], \mathbf{u}^{(0)} \rangle.$$

By substituting the decomposition $\mathbf{u}^{(0)} = \mathbf{u}_{hold}^{(0)} + \mathbf{u}_{mm}^{(0)}$, we see that $\hat{\ell}_\pm = \hat{\ell}_\pm(t,s)$ and

$$\hat{\ell}_\pm(t,s) = 1 \iff G_\pm(t,s) > 0,$$

i.e. the required assertion.

$\square$

Financial interpretation

The strong (resp. weak) optimal policies described in (4.4.8) are binary controls depending on $G_\pm(t,s)$. Cutting the surfaces $z = G_\pm(t,s)$ with the hyperplane $z = 0$ and projecting on (t,s)-plane the portions above the hyperplane, we obtain the trading regions. Since controls drive execution, and execution is due either on a trade or a price jump, optimal controls are naturally decomposed into two parts, as shown by the expression of $G_\pm$ in (4.4.6):

$$G_\pm(t,s) = G_\pm^{\text{trd}}(t,s) - G_\pm^{\text{jmp}}(t,s)$$

$$:= \lambda_\pm(s)\left(\delta - \varphi \mp \theta(t,s)\right) \Phi_\pm^1(L) - h_\pm(s)\left(\delta + \varphi + \theta(t,0)\right) L.$$

i) The **trade part** $G_\pm^{\mathrm{trd}}$: the agent orders are matched by small market orders (not impacting the stock price) of random size, distributed according to $\vartheta_\pm(dk, L)$, arriving at rate $\lambda_\pm(S_t)$. For each executed lot, she gains the half-spread thanks to passive execution (market making gain), she loses the transaction costs, and since her inventory changes, she loses the martingale distance $\theta(t, s)$ that she would gain (in average) keeping her position until the horizon (attention: this quantity might be negative). This scenario is favourable, since she has the time to close her spread before the stock price jumps again and she has gained half a tick w.r.t. to the mid-price evaluation of the stock: this profit comes from small uninformed traders, that are unable to make the stock price jump and need the liquidity provided by the market maker.

ii) The **jump part** $G_\pm^{\mathrm{jmp}}$: the agent orders are cleared (fulfilled) at rate $h_\pm(S_t)$ by big market orders impacting the stock price. As before, for each executed lot she gains the half-spread thanks to passive execution (market making gain), but loses a spread because of the stock price jumps, ending with a passive of half a spread, she loses the transaction costs, and since her inventory changes, she loses the martingale distance $\theta(t, 0)$ (the price has just jumped). Notice that, by Corollary 4.2,

$$h_\pm(s)\,(\delta + \varphi + \theta(t, 0)) \geq 0\,,$$

and looking at (4.4.6), it is clear that the limit order execution due to big orders is a source of risk, called **strong adverse selection**. This is due to the fact that large market orders make the price jump, and do not allow the agent to close her spread. On the contrary, the agent finds herself buying/selling L lots (the maximum admissible size) when the stock price is suddenly decreasing/increasing value (adverse selection).

As one can see, the "trade" case represents a positive event, since it leads to a proper market making strategy collecting spreads where buy and hold portfolio would not lead to substantial gains, while the "jump" one represents a negative event, since it leads to an unfavourable execution, where we sell (resp. buy) a stock whose value has decreased (resp. increased). Hence, the marked point process modeling of stock price leads to a much more realistic model, evaluating the risk of being executed under negative circumstances, which would not be possible if the stock price were continuous. The quantity $G_\pm$ is interpreted as the portfolio value arising from market making strategy, and naturally the value function $\mathbf{u}_{mm}^{(0)} = \omega$ in (4.4.7) is the expected gain of the portfolio value. Optimal controls are determined by a trade-off among

i) pure market making due to round-trip executions,

ii) trend or reversion anticipation thanks to the information associated to $\theta(t, s)$,

iii) limitation of strong adverse selection risk.

By stressing the dependence of optimal control on horizon T, we write $\hat{\ell}_\pm^T(t, s)$ for $\hat{\ell}_\pm(t, s)$, and we see from (4.4.8) and (4.1.17) that it converges for large horizon to the stationary value:

$$\lim_{T \to \infty} \tilde{\ell}_\pm^T(t, s) = \mathbb{1}\{\bar{G}_\pm(s) > 0\}\,, \tag{4.4.9}$$

with

$$\bar{G}_\pm(s) := \lambda_\pm(s)\,(\delta - \varphi \mp \bar{\theta}(s))\,\Phi_\pm^1(L) - h_\pm(s)\,(\delta + \varphi + \bar{\theta}(0))\,L\,,$$

We plot in Figure 4.5 the trade and jump parts functions $G_\pm^{\mathrm{trd}}$ and $G_\pm^{\mathrm{jmp}}$, in Figure 4.6 the market making performance ω, and in Figure 4.7 the optimal limit order controls.
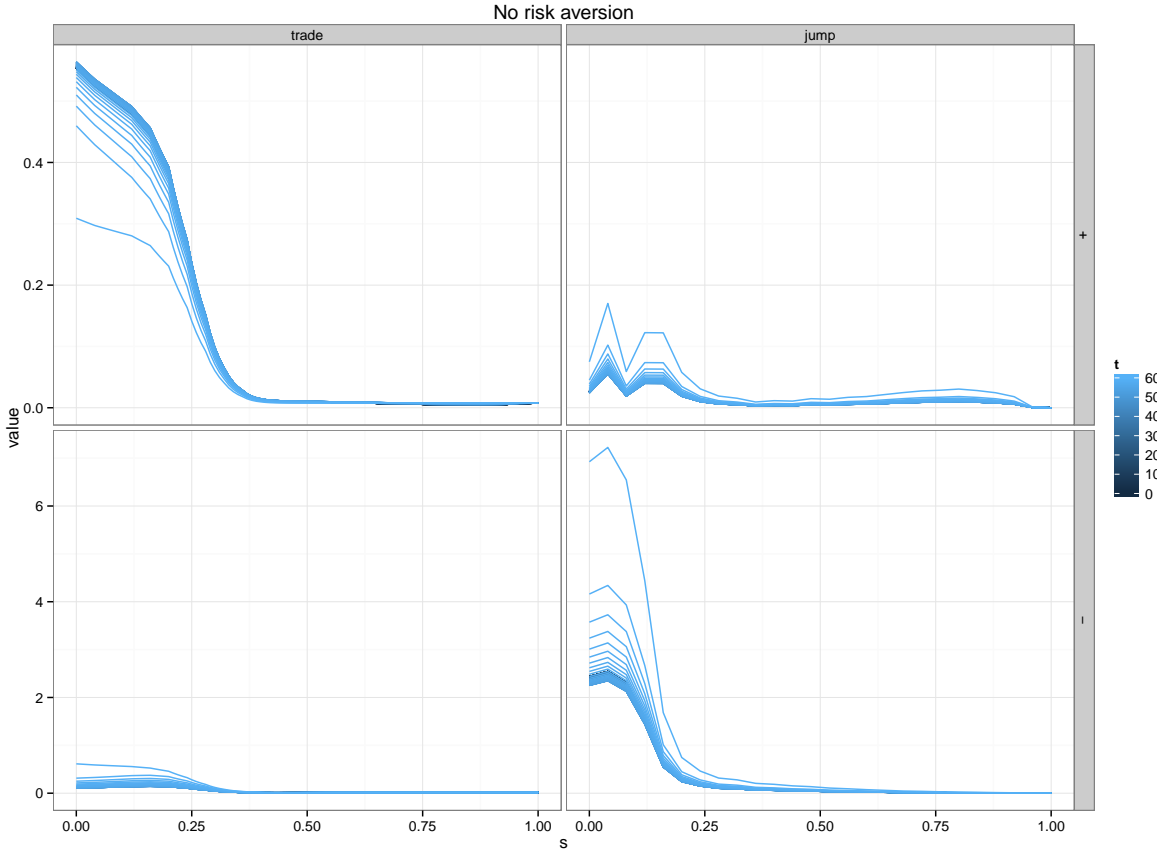
Figure 4.5: the trade part and the jump part in (4.4.6). The chart shows that the trade part dominates the jump part on the strong side, which leads the agent to place her orders on that side, while this scenario is inversed on the weak side. The risk due to jump execution on the weak side leads the agent to be more cautious, and to place her limit orders only under particular circumstances. □

4.4.2   The small risk aversion case

In this section, we prove that for small risk aversions, the solution of the HJB equation (4.4.1) associated to the optimal control problem (4.3.1) is a deformation of the solution in the case $\eta = 0$, and we explicitly characterize this deformation.

We first give the exact solution of the problem in terms of a non-explicit deformation of the $(\eta = 0)$-value function, that one can evaluate numerically if not wanting to involve approximation arguments. This result illustrates, in terms of probabilistic representation, how a particular strategy affects the value function.

THEOREM 4.2. *The value function associated to the control problem (4.3.1) is given by*

$$\mathbf{u}^{(\eta)} = \mathbf{u}^{(0)} - \mathbf{v}^{(\eta)},\tag{4.4.10}$$

where $\mathbf{u}^{(0)}(t, p, i, s, x, y)$ *is the solution of the control problem in the no risk aversion case (Theorem 4.1), while* $\mathbf{v}^{(\eta)}(t, s, q := iy)$ *is nonnegative and is the unique viscosity solution with quadratic growth in* q *to*

$$-\frac{\partial \mathbf{v}^{(\eta)}}{\partial t} - \frac{\partial \mathbf{v}^{(\eta)}}{\partial s} + \sum_{\nu \in \pm} \max_{\ell \in \{0,1\}} \left(\ell G_\nu(t, s) - \langle \mathcal{R}_\nu[\ell], \mathbf{v}^{(\eta)} \rangle \right) - \max \left(G_\nu(t, s), 0 \right) = 0, \tag{4.4.11}$$

$$\mathbf{v}^{(\eta)}(T,) = \eta q^2,$$

for $(t, s, q) \in [0, T] \times \mathbb{R}_+ \times \mathbb{Z}$, *where* $G_\nu(t, s)$ *is given by (4.4.6) and*

$$\langle \mathcal{R}_\pm[\ell], \mathbf{v}^{(\eta)} \rangle := h_\pm(s) \Delta \mathbf{v}^{(\eta)}(t, 0, \pm q - L\ell) + \lambda_\pm(s) \int \Delta \mathbf{v}^{(\eta)}(t, s, q \mp k\ell) \vartheta_\pm(dk, L). \tag{4.4.12}$$
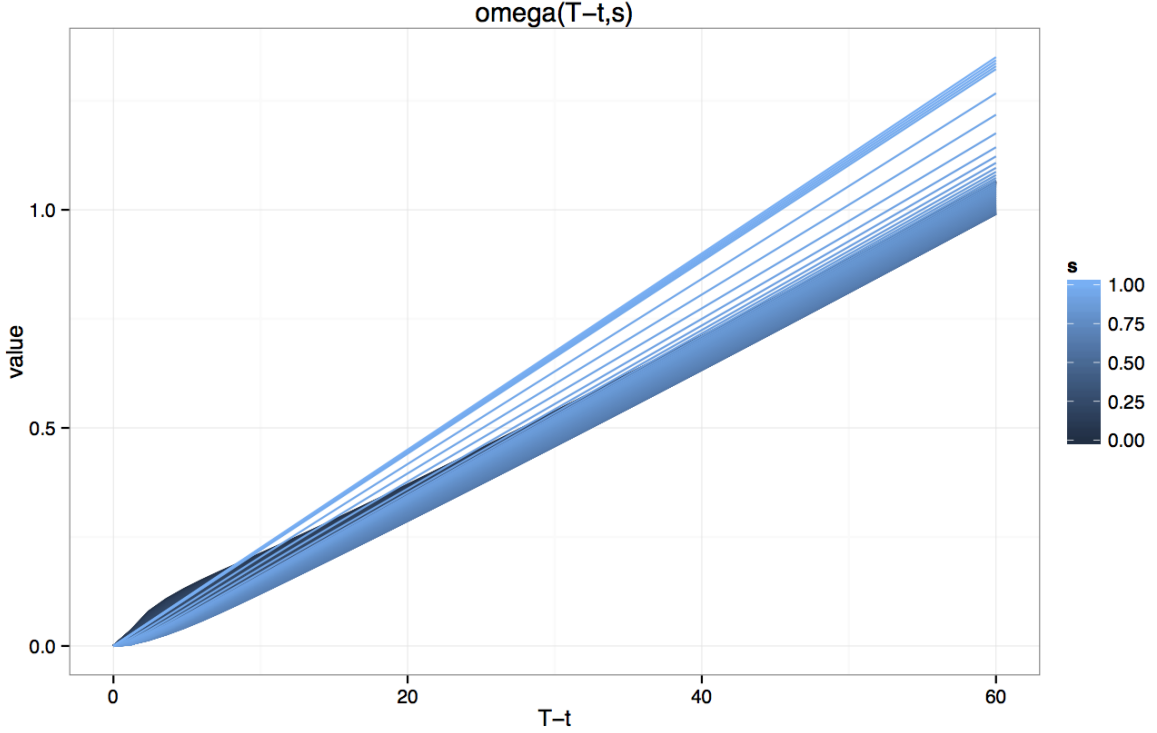
Figure 4.6: $\omega(T - t, s)$ for different s-sections. Far from the horizon, the agent has a linear average gain per time unit depending on the starting elapsed time. In the distribution queue, the agent gains more since she enters the market at a stable time, where the stock price is not likely to jump, representing a perfect scenario for the market maker. □

Moreover, the optimal controls for problem (4.3.1) are given in feedback form by

$$\hat{\ell}_\pm(t, s) := \hat{\ell}_\pm^{(\eta)}(t, s) = \mathbb{1}\{G_\pm(t, s) > \langle \mathcal{R}_\pm^1, \mathbf{v}^{(\eta)} \rangle\}, \tag{4.4.13}$$

where

$$\langle \mathcal{R}_\pm^1, \mathbf{v}^{(\eta)} \rangle := h_\pm(s) \left(\mathbf{v}^{(\eta)}(t, 0, \pm q - L) - \mathbf{v}^{(\eta)}(t, 0, \pm q) \right)$$
$$+ \lambda_\pm(s) \int \Delta \mathbf{v}^{(\eta)}(t, s, q \mp k) \vartheta_\pm(dk, L).$$

In particular $\langle \mathcal{R}_\pm^1, \mathbf{v}^{(0)} \rangle = \langle \mathcal{R}_\pm^1, 0 \rangle = 0$.

Proof. Injecting the ansatz (4.4.4) and (4.4.10) in (4.4.2) and (4.4.3), we have

$$\frac{\partial \mathbf{u}^{(\eta)}}{\partial t} + \frac{\partial \mathbf{u}^{(\eta)}}{\partial s} = \left(\frac{\partial \mathbf{u}^{(0)}}{\partial t} + \frac{\partial \mathbf{u}^{(0)}}{\partial s} \right) - \left(\frac{\partial \mathbf{v}^{(\eta)}}{\partial t} + \frac{\partial \mathbf{v}^{(\eta)}}{\partial s} \right), \tag{4.4.14}$$

$$\langle \mathcal{J}_\pm[\ell], \mathbf{u}^{(\eta)} \rangle = \langle \mathcal{J}_\pm[\ell], \mathbf{u}^{(0)} \rangle - \Delta \mathbf{v}^{(\eta)}(t, 0, \pm q - L\ell),$$

$$\langle \mathcal{T}_\pm[\ell], \mathbf{u}^{(\eta)} \rangle = \langle \mathcal{T}_\pm[\ell], \mathbf{u}^{(0)} \rangle - \int \Delta \mathbf{v}^{(\eta)}(t, s, q \mp k\ell) \vartheta_\pm(dk, L).$$

Plugging into (4.4.1), and using also (4.4.5), we see after some straightforward calculations that $\mathbf{v}^{(\eta)}$ should satisfy the PDE (4.4.11).

By definition of the control problem (4.3.1), it is clear that $\mathbf{u}^{(\eta)} \leq \mathbf{u}^{(0)}$, and so $\mathbf{v}^{(\eta)}$ is nonnegative. On the other hand, by taking the null strategy ($\ell^\pm \equiv 0$), we trivially obtain, since $\omega \equiv 0$,

$$\mathbf{u}^{(\eta)}(t, p, i, s, x, y) = x + y\pi(t, p, i, s) - \eta q^2 \Rightarrow \mathbf{v}^{(\eta)}(t, s, q) \leq \eta q^2,$$

which proves the quadratic growth of $\mathbf{v}^{(\eta)}$ in q.
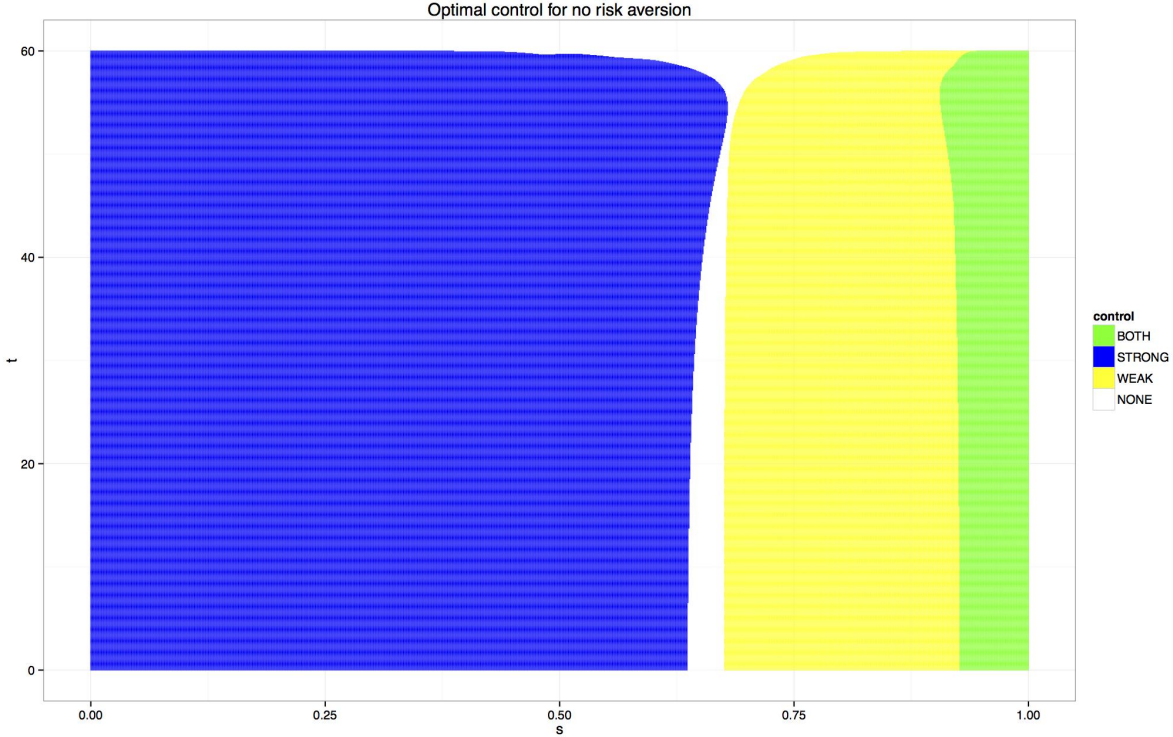
Figure 4.7: optimal policy for $\eta = 0$. The figures translated Figure 4.5 in terms of binary optimal policy, as described by (4.4.8). The agent places her limit order on the strong side for both small and big elapsed times, while posting on the weak side is restricted to large s: this is due to behavior of $\theta(t, s)$, changing signs in the right side of the cart, inducing the maker maker to place orders on the side to exploit the anticipation on the next jump. For $t \to 0$, the horizon is far and the policy stabilizes to her asymptotic value described in (4.4.9) $\square$.

Finally, optimal controls are determined choosing, for both strong and the weak side, the maximum between $\langle \mathcal{R}_\pm[0], \mathbf{v}^{(\eta)} \rangle$ and $\langle \mathcal{R}_\pm[1], \mathbf{v}^{(\eta)} \rangle$, which gives precisely the form (4.4.13).

$\square$

REMARK 4.2. The value function $\mathbf{u}^{(\eta)}$ of the market making control problem with risk aversion η is deformed with respect to the no risk aversion case $\mathbf{u}^{(0)}$ via the risk aversion function $\mathbf{v}^{(\eta)}$, which depends only on current time t, elapsed time s and strong inventory q. Is is also clear that $\mathbf{v}^{(0)} \equiv 0$, and $\mathbf{v}^{(\eta)}$ is non-decreasing in η, since $\mathbf{u}^{(\eta)}$ is non-increasing in η. Moreover, the optimal control $\hat{\ell}_\pm^{(\eta)}$ is a deformation of the optimal control $\hat{\ell}_\pm^{(0)}$ in the no risk aversion case through the barrier $\langle \mathcal{R}_\pm^1, \mathbf{v}^{(\eta)} \rangle$, which is null for $\eta = 0$. $\square$

The deformation function $\mathbf{v}^{(\eta)}$ due to risk aversion is solution to the semi-linear PDE (4.4.11), which can be solved numerically. We use instead a perturbation approach for deriving a first-order expansion of $\mathbf{v}^{(\eta)}$ for small risk aversion η.

THEOREM 4.3. *The function* $\mathbf{v}^{(\eta)}(t, s, q)$ *can be linearly approximated in* $\eta > 0$ *by*

$$\mathbf{v}^{(\eta)}(t, s, q) = \eta \left(q^2 + 2q\zeta_1(t, s) + \zeta_0(t, s) \right) - \mathbf{R}^{(\eta)}(t, s, q), \qquad (4.4.15)$$

where

i) $\zeta_1(t, s)$ *is the viscosity solution of*

$$-\frac{\partial \zeta_1}{\partial t} - \frac{\partial \zeta_1}{\partial s} - \mu(s)\zeta_1(t, 0) + \sigma^2(s)\zeta_1(t, s) + \sum_{\nu \in \pm} \nu \left(h_\nu(s)L + \lambda_\nu(s)\Phi_\nu^1(L) \right) \hat{\ell}_\nu^{(0)}(t, s) = 0,$$

$$\zeta_1(T,) = 0,$$

which is alternatively expressed as

$$\zeta_1(t,s) := \mathbb{E}\left[\hat{Y}_T \big| I_{t-} = i, S_{t-} = s, Y_{t-} = 0\right],$$

where $(\hat{Y}_t)$ is the inventory process controlled by the optimal strategy for $\eta = 0$ (see (4.4.13)) under particular initial conditions.

ii) $\zeta_0(t,s)$ is the viscosity solution of

$$-\frac{\partial \zeta_0}{\partial t} - \frac{\partial \zeta_0}{\partial s} - \sigma^2(s)\Delta\zeta_0(t,0)$$
$$-\sum_{\nu \in \pm}\left(h_\nu(s)\left(L^2 - 2L\zeta_1(t,0)\right) + \lambda_\nu(s)\left(\Phi_\nu^2(L) - 2\nu\Phi_\nu^1(L)\zeta_1(t,s)\right)\right)\hat{\ell}_\nu^{(0)}(t,s) = 0,$$
$$\zeta_0(T,) = 0;$$

iii) the remainder $\mathbf{R}^{(\eta)}(t,s,q)$ is a non-negative $o(\eta)$.

Proof. See Section 4.8.

$\square$

REMARK 4.3. The computation of $\mathbf{v}^{(\eta)}(t,s,q)$ through the equation (4.4.11) requires the numerical resolution of a non-linear system of 1-dimensional PDE indexed by $q \in \mathbb{Z}$. Alternatively, the first-order expansion for small risk aversion, with a quadratic in q leading term, involves the computation of (ζ_0, ζ_1) through a system of linear PDE's with an upper triangular structure: $\zeta_1(t,s)$ can be numerically solved without knowing $\zeta_0(t,s)$. It is worth noticing that:

i) thanks to the approximation methods, we are led to solve four linear simple PDE's (for $\theta, \omega, \zeta_1, \zeta_0$), reducing of one the dimension of the problem;

ii) since $\mathbb{Z}$ is an infinite set, a numerical solution needs a domain truncation and the specification of boundary conditions, while this problem does not affect the approximated solution;

iii) the numerical scheme can be trivially parallelized: the solution of $\omega(t,s)$ depends on $\theta(t,s)$, while the one of $\zeta_0(t,s)$ depends on $\zeta_1(t,s)$, but the two couples are independent, leading to a natural parallelization.

$\square$

We can also provide a probabilistic characterisation of ζ_1, as the average terminal inventory of the optimal strategy under no risk aversion.

REMARK 4.4. From the structure (4.4.13) of optimal control and the small expansion (4.4.15), we get an approximate optimal limit order control given by

$$\tilde{\ell}_\pm^{(\eta)}(t,s) := \mathbb{1}\{G_\pm(t,s) > \langle \mathcal{R}_\pm^1, \tilde{\mathbf{v}}^{(\eta)}\rangle\}$$
$$\tilde{\mathbf{v}}^{(\eta)}(t,s,q) := \eta\left(q^2 + 2q\zeta_1(t,s) + \zeta_0(t,s)\right).$$

The approximate optimal feedback control can be rewritten as:

$$\tilde{\ell}_\pm^{(\eta)}(t,s) := \mathbb{1}\{G_\pm(t,s) > \eta\left(\mathbf{C}_\pm^0(t,s) \mp 2\mathbf{C}_\pm^1(t,s)q\right)\},$$

where

$$\mathbf{C}_\pm^0(t,s) := h_\pm(s)\left(L^2 - 2L\zeta_1(t,0)\right) + \lambda_\pm(s)\left(\Phi_\pm^2(L) \mp 2\zeta_1(t,s)\Phi_\pm^1(L)\right), \qquad (4.4.16)$$
$$\mathbf{C}_\pm^1(t,s) := h_\pm(s)L + \lambda_\pm(s)\Phi_\pm^1(L) \geq 0. \qquad (4.4.17)$$

The control adjustment due to risk aversion can be understood as follows.

Optimal control for q = 0 : strong   **Optimal control for q = 0 : weak**
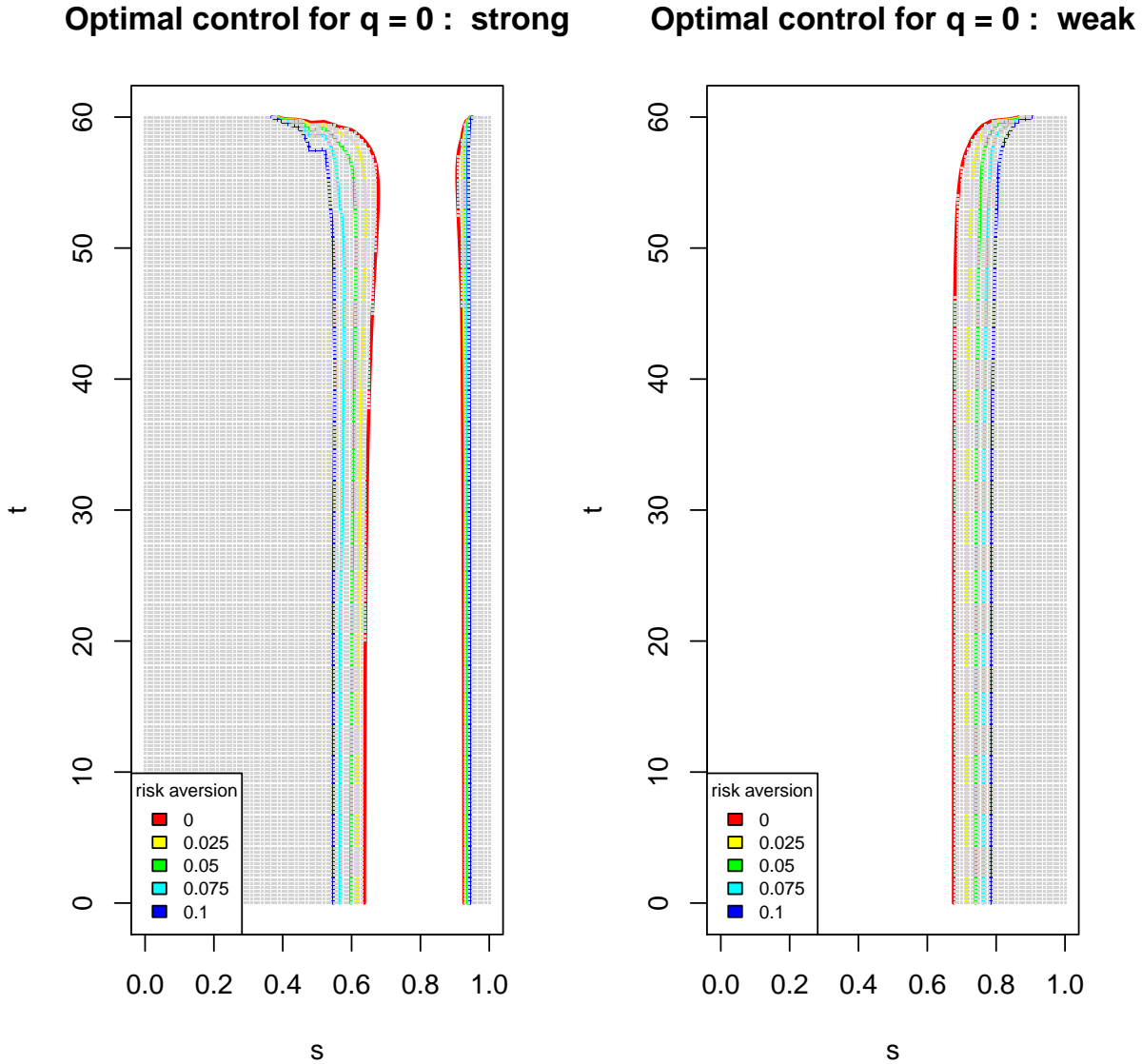
Figure 4.8: trading region for $q = 0$ and different risk aversion. The chart shows how increasing the risk aversion deforms the trading region, widening the zone where the agent does not send any order.   □

i) The **inventory independent part** in (4.4.16) affects the agent strategy even when her inventory is $q = y = 0$: in the no risk aversion case, the agent places a limit order if $G_{\pm}(t, s) > 0$, but when $\eta > 0$, this trading barrier - depending on the couple (t, s) - is raised by a multiple of the risk aversion itself. The agent becomes cautious and decides to enter the market only in the most profitable cases, but renounces to trade if expected gain is small, even if positive. This result is shown by Figure 4.8, where the non trading region for $q = 0$ grows w.r.t. the case $\eta = 0$, reflecting the increased trading aversion of the agent.

ii) The **linear part in the inventory** in (4.4.17) is in charge of controlling the absolute value of the inventory, in order to reduce the exposure of the agent to inventory and market risk. For $q > 0$ (i.e. $iy > 0$), the adjustment of the strong side (resp. weak side) turns the trading barrier down (resp. up) by a multiple of η: the agent decides to trade on the strong (resp. weak) side under less (resp. more) restrictive conditions in order to reduce (resp. not to increase) her absolute inventory. This result is summarized by Figure 4.9, where for large values of the inventory the agent plays, independently on s, on one side only, in order to revert the absolute position to a smaller value.

Optimal controls for t = 0 and risk aversion = 0.01
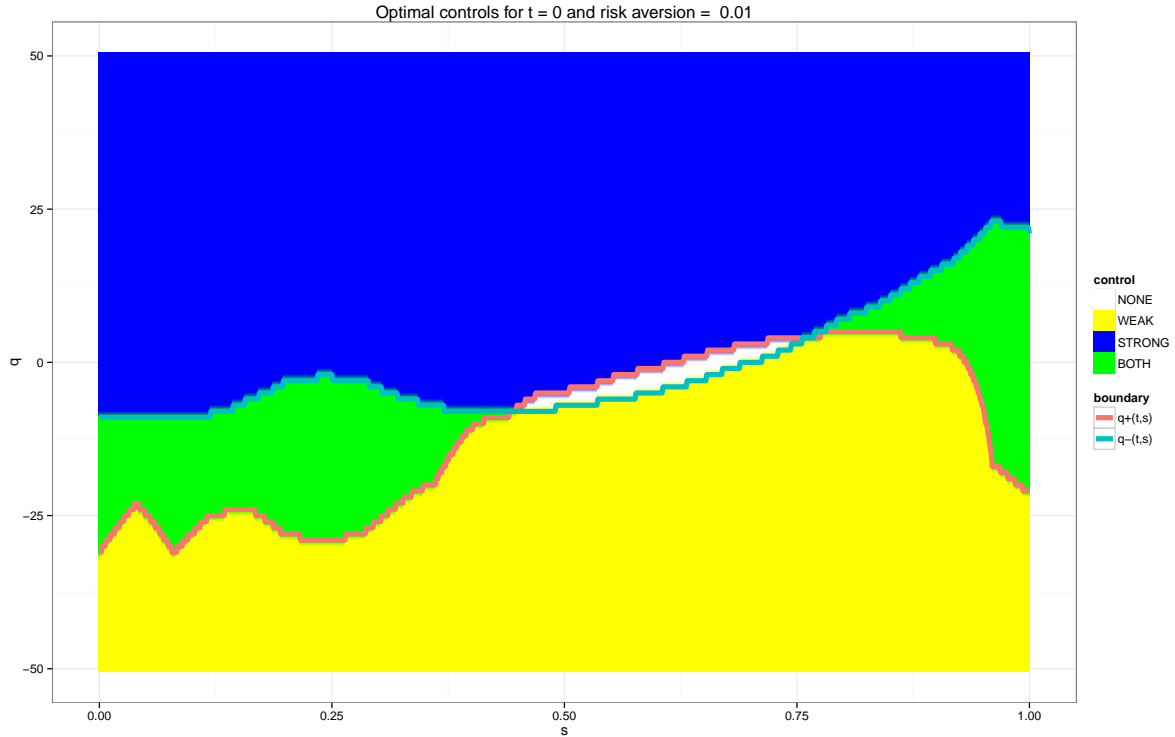
Figure 4.9: the optimal policy at time 0 for different values of q and s and positive risk aversion. The agent plays only only on the strong (resp. weak) side for large (small values) of the strong inventory in order not to be exposed to the inventory risk. For $q \approx 0$, the policy takes into account the inventory risk and the pure gain due to a market making strategy. The two lines denoted by $q_\pm(t,s)$ determines the trading boundary on the strong and the weak side. □

□

Conclusion and further developments

In this paper we have exploited the framework described in the companion paper [36] in order to provide an application to a market making problem. Thanks to a Cox model, we are able to include the matching engine and complete the order book model of the best levels: only small trades are described directly, while big market orders affecting the stock price are included in the stock price dynamics itself. The perturbation technique adopted to derive optimal controls as a deformation of the no risk aversion case has helped us to improve financial interpretability and reduce the dimension problem as well as the computational cost of its numerical solution. For further developments, more complicated stock price model can introduce statistical arbitrage opportunity, that we may capture by means of optimal control techniques. This part represents a work in progress, that will soon appear.

4.5 Appendix: the trade intensity function λ

We give a statistical procedure for the parametric estimation of the intensity function λ. The log-likelihood function associated to the counting process (M_t) with intensity $\lambda(S_t)$ is given over $[0, T]$ by

$$\ln L_T = \int_0^T \ln\left(\lambda(S_t)\right) dM_s - \int_0^T \lambda(S_t) dt \,.$$

Fix now $T = T_n$ the n-th jump time of the stock price. Since S_t jumps at $(T_k)_{k=1,\ldots,n}$, so does λ. This implies that:

$$\int_0^T \lambda(S_t)\,dt = \sum_{k=1}^n \int_{T_{k-1}}^{T_k} \lambda(S_t)\,dt = \sum_{k=1}^n \int_{T_{k-1}}^{T_k} \lambda(t - T_{k-1})\,dt = \sum_{k=1}^n \int_0^{S_k} \lambda(t)\,dt\,.$$

Moreover, trades arrive at $\theta_1, \ldots, \theta_m$, and so:

$$\int_0^T \ln\left(\lambda(S_t)\right)\,dM_s = \sum_{j=1}^m \ln \lambda(S_{\theta_j-})\,.$$

Putting all together, we have:

$$\ln L_T = \sum_{j=1}^m \ln \lambda(S_{\theta_j-}) - \sum_{k=1}^n \int_0^{S_k} \lambda(t)\,dt\,.$$

Assuming that λ is of parametric form, we can then obtain the MLE estimator for λ maximizing over the parameters the above log-likelihood function. For example, we can use the following parametric forms, reproducing the intensity decay when s is large:

$$\lambda^{exp}(s) = \lambda_0 + a\,s^r\,e^{-ks}\,,$$

for $\lambda_0, a, r, k \geq 0$. Notice that in both cases,

 i) λ is finite and smooth on $\mathbb{R}_+$;

 ii) when $a = 0$ we fall into the homogeneous Poisson case of intensity $\lambda = \lambda_0$;

 iii) when $r > 0$, $\lambda(0) = \lambda(\infty) = \lambda_0$ with a maximum reached at $s_* > 0$;

 iv) for special value of r and k (e.g. $r \in \mathbb{N}$ in the exponential case), $\int_0^s \lambda(t)\,dt$ has an explicit form, leading to a much faster optimization.

In our case we have chosen:

$$\lambda(s) = \lambda_0 + ae^{-ks} \quad \text{and so} \quad \int_0^s \lambda(t)\,dt = \lambda_0 s + a\,\frac{1 - e^{-ks}}{k}\,.$$

The estimated parameters on the data are: $\lambda_0 = 0.9772205$, $a = 77.0405310$, $k = 34.5428134$.

4.6 Appendix: the estimation of the agent execution distribution $\vartheta_\pm(dk, L)$

Unfortunately, the agent execution cannot be estimated before playing or backtesting a zero intelligence strategy, i.e. placing continuously limit orders on both sides of the limit order book. This problem cannot be overcome easily: a high-frequency backtest platform is necessary to estimate the execution rate.

Assuming that the agent is always placed with one lot on the strong/weak side - updating her position as soon as she is executed or she is not placed anymore at the best prices - $\vartheta_\pm(dk, L)$ is estimated by the ratio between the number of agent executions and the total amount of incoming market orders on the corresponding side. More in details, assume that

$$E_\pm^k := \text{number of trades on the } \pm \text{ side in } (T_{k-1}, T_k] - \mathbb{1}\{B_k = \pm\}\,,$$

where $B_k = J_k J_{k-1}$ is the same as (4.1.3). Following the strategy $\ell_\pm \equiv 1$, the agent places continuously on one side a limit order of size L. We can determine the statistics

$$e_\pm^k(i) := \text{number of agent trades of size } i \text{ on the } \pm \text{ side in } (T_{k-1}, T_k] - \mathbb{1}\{B_k = \pm, i = L\}\,,$$

Setting

$$E_\pm^N := \sum_{k=1}^N E_\pm^k\,, \quad e_\pm^N(i) := \sum_{k=1}^N e_\pm^k(i)\,,$$

by the Strong Law of the Large Number we have

$$\frac{e_N}{E_N} \to \mathbb{P}\left[\vartheta_\pm(dk, L) = i\right]\,, \quad i = 1, \ldots, L\,,$$

that provides an estimator for $\vartheta_\pm(dk, L)$. $\qquad \square$

4.7 Appendix: properties of the function $\theta^T(t, s)$

For the applications of our model to market making problem, we shall extensively use properties of the mean value of the stock price at horizon, i.e.

$$\pi(t, p, i, s) := \mathbb{E}_{t,p,i,s}\left[P_T\right]\,.$$

Here, $\mathbb{E}_{t,p,i,s}$ denotes the expectation operator under the initial conditions: $(P_t, I_t, S_t) = (p, i, s)$ for $(t, p, i, s) \in [0, T] \times 2\delta\mathbb{Z} \times \{-1, +1\} \times \mathbb{R}_+$. We devote this section to the study of this function, using both a PDE and a probabilistic approach.

4.7.1 The PDE representation

The next lemma gives first a decomposition of π guessed by the arithmetic nature of the stock price, as well as its particular symmetry.

LEMMA 4.3 (Feynman-Kac representation). *The function π is given by*

$$\pi(t, p, i, s) = p + i\theta(t, s)\,,$$

where $\theta(t, s)$ is the unique bounded solution to

$$\langle \mathcal{Z}, \theta \rangle := -\frac{\partial\theta}{\partial t} - \frac{\partial\theta}{\partial s} - \mu(s)\theta(t, 0) + \sigma^2(s)\theta(t, s) - 2\delta\mu(s) = 0\,, \qquad (4.7.1)$$

$$\theta(T,) = 0\,,$$

for $(t, s) \in [0, T] \times \mathbb{R}_+$.

Proof. By the Feynman-Kac representation theorem, $\pi(t, p, i, s)$ is solution to the linear PDE:

$$-\frac{\partial\pi}{\partial t} - \frac{\partial\pi}{\partial s} - \sum_{\nu\in\pm} h_\nu(s)\Delta\pi(t, p + 2\delta\nu i, \nu i, 0) = 0\,,$$

$$\pi(T,) = p\,,$$

for $(t, p, i, s) \in [0, T] \times 2\delta\mathbb{Z} \times \{-1, +1\} \times \mathbb{R}_+$. The result of the lemma follows injecting the ansatz (4.1.13) in the previous PDE, while the boundness of θ will be shown in the next section using an independent probabilistic argument.

$\qquad \square$

Notice that in particular, the following probabilistic representation holds:

$$\theta(t, s) = \theta^T(t, s) = \mathbb{E}\left[P_T \big| S_t = s, P_t = 0, I_t = +1\right]\,. \qquad (4.7.2)$$

Furthermore, the following two corollaries, based on the comparison theorem, provide bounds for $\theta^T(t, s)$ in different cases.

COROLLARY 4.1. *(Drift of constant sign) If $\mu(s) \geq 0$ (resp. $\mu(s) \leq 0$), then $\theta \geq 0$ (resp. $\theta \leq 0$). In particular if $\mu(s) \equiv 0$, then $\theta \equiv 0$.*

Proof. Looking at (4.7.1), it is straightforward to check that for $\mu(s)$ being identically bigger (resp. smaller) than 0, then $\langle \mathcal{Z}, 0 \rangle = -2\delta\mu(s) \leq 0$ (resp. ≥ 0). Since the terminal condition is 0, we have proved that the zero function is a sub (resp. super)-solution of (4.7.1), and we conclude by comparison principle.

$\square$

COROLLARY 4.2 (Lower bound). *The following lower bound holds:*

$$\theta(t,s) \geq -\delta, \quad (t,s) \in [0,T] \times \mathbb{R}_+ \,.$$

Proof. Observe that for constant function $c \in \mathbb{R}$, we have

$$\langle \mathcal{Z}, c \rangle = -\mu(s)(c + 2\delta) + \sigma^2(s)c \,.$$

Moreover, since $h_\pm(s) \geq 0$, we have

$$\frac{\mu(s)}{\sigma^2(s)} = \frac{h_+(s) - h_-(s)}{h_+(s) + h_-(s)} \geq -1, \quad s \in \mathbb{R}_+ \,,$$

and so for $c \geq -2\delta$, we get

$$\langle \mathcal{Z}, c \rangle \leq 2\sigma^2(s)(c + \delta) \,.$$

Therefore, taking any constant $c \in (-2\delta, -\delta)$, we have $\langle \mathcal{Z}, c \rangle \leq 0$, and we conclude by comparison principle that $\theta \geq c$, i.e. the required assertion.

$\square$

4.7.2   The probabilistic representation

We now investigate further bounds for $\theta(t,s)$, as well as its asymptotic behavior for large horizons, using a probabilistic approach based on the representation (4.1.19). The probabilistic angle allows to exploit the Markov property of the stock price to capture information that is hidden in the probabilistic representation of Lemma 4.3. In order to emphasize the dependence on the horizon T, we write $\theta^T(t,s)$ for $\theta(t,s)$ and define the conditional mean of the next jump w.r.t. to the elapsed time as

$$\bar{\alpha}(s) := \mathbb{E}\left[J_1 \middle| S_0 = s, J_0 = +1\right], \quad s \in \mathbb{R}_+ \,. \tag{4.7.3}$$

Notice that, by its very definition,

$$\bar{\alpha}(s) := \mathbb{E}\left[J_1 \middle| T_1 \geq s, J_0 = +1\right] = \mathbb{P}\left[B_1 \middle| T_1 \geq s, J_0 = +1\right], \quad s \in \mathbb{R}_+ \,,$$

where B_1 is given in (4.1.3).

LEMMA 4.4. *For a Markov Renewal Process (J_k, T_k) on a finite state space E with*

$$Q_{ij} := \mathbb{P}\left[J_k = j | J_{k-1} = i\right], \quad F_{ij} := \mathbb{P}\left[T_k - T_{k-1} \leq s | J_k = j, J_{k-1} = i\right], \quad i, j \in E \,,$$

we have

$$\mathbb{P}\left[J_k = j | J_{k-1} = i, T_k - T_{k-1} \geq s\right] = Q_{ij} \frac{1 - F_{ij}(s)}{1 - \sum_{j \in E} Q_{ij} F_{ij}(s)}, \quad i, j \in E \,. \tag{4.7.4}$$

Proof. A simple Bayes argument gives

$$
\begin{aligned}
\mathbb{P}\left[J_k = j | J_{k-1} = i, T_k - T_{k-1} \geq s\right] &= \frac{\mathbb{P}\left[J_k = j, T_k - T_{k-1} \geq s | J_{k-1} = i\right]}{\mathbb{P}\left[T_k - T_{k-1} \geq s | J_{k-1} = i\right]} \\
&= \frac{\mathbb{P}\left[T_k - T_{k-1} \geq s | J_{k-1} = i, J_k = j\right] \mathbb{P}\left[J_k = j | J_{k-1} = i\right]}{\sum_{j \in E} \mathbb{P}\left[T_k - T_{k-1} \geq s | J_{k-1} = i, J_k = j\right] \mathbb{P}\left[J_k = j | J_{k-1} = i\right]} \\
&= \frac{Q_{ij}\left(1 - F_{ij}(s)\right)}{\sum_{j \in E} Q_{ij}\left(1 - F_{ij}(s)\right)} = Q_{ij} \frac{1 - F_{ij}(s)}{1 - \sum_{j \in E} Q_{ij} F_{ij}(s)}\,.
\end{aligned}
$$

$\square$

As an immediate consequence of the previous lemma we obtain $\bar{\alpha}(s)$ specialising to our particular MRP.

COROLLARY 4.3. *For $s \in \mathbb{R}_+$,*

$$
\bar{\alpha}(s) = \sum_{\nu \in \pm} \nu \left(\frac{1 + \nu\alpha}{2}\right)\left(\frac{1 - F_\nu(s)}{1 - F(s)}\right)\,.
$$

In particular i) $\tilde{\alpha}(0) = \alpha$, while ii) if marks and tick times are independent, $\bar{\alpha}(s) \equiv \alpha$.

Proof. The claimed expression for $\bar{\alpha}(s)$ follows from Lemma 4.4 applied to the MRP driving the stock price: indeed, using the notation of the lemma with

$$
E = \{-1, +1\}\,, \quad Q_{ij} = \frac{1 + ij\alpha}{2}\,, \quad F_{ij} = \sum_{\nu \in \pm} F_\nu 1_{\{ij = \nu\}}\,,
$$

we have for any $i \in E$:

$$
\begin{aligned}
\sum_{j \in E} j\, \mathbb{P}\left[J_1 = j | J_0 = i, T_1 \geq s\right] &= \sum_{j \in E} j Q_{ij} \frac{1 - F_{ij}(s)}{1 - \sum_{j \in E} Q_{ij} F_{ij}(s)} \\
&= \sum_{\nu \in \pm} \nu \left(\frac{1 + \nu\alpha}{2}\right)\left(\frac{1 - F_\nu(s)}{1 - F(s)}\right)\,.
\end{aligned}
$$

In order to prove that $\bar{\alpha}(0) = \alpha$, we can either show it directly from (4.7.3), since

$$
\bar{\alpha}(0) = \mathbb{E}\left[J_1 | S_0 = 0, J_0 = +\right] = \mathbb{E}\left[B_1\right] = \alpha\,,
$$

or by the analytic formula (4.7.4), noticing that (no masses in 0 are assumed)

$$
F(0) = F_+(0) = F_-(0) = 0\,.
$$

For the final assertion, one can use (4.7.4), noticing that if the tick time (N_t) and mark process (J_k) are independent, then

$$
F_+ = F_- = F \Rightarrow \bar{\alpha}(s) = \sum_{\nu \in \pm} \nu \frac{1 + \nu\alpha}{2} = \alpha\,.
$$

$\square$

REMARK 4.5. Notice that $\alpha < 0$ does not imply that $\bar{\alpha}(s)$ shares the same property: α represents in fact the mean value of the trend variable B_n immediately after a price jump. The information brought by time passing without jumps may lead to a different behavior (trend/reversion) from the one described by α. $\square$

PROPOSITION 4.2. *The asymptotic behaviour of $\theta^T(t,s)$ is given by*

$$
\lim_{T \to \infty} \theta^T(t,s) = 2\delta \frac{\bar{\alpha}(s)}{1 - \alpha}\,, \quad \forall s \in \mathbb{R}_+. \tag{4.7.5}
$$

Proof. We assume that the first jump event, under $I_0 = +$ and $S_0 = s$, is described by the couple (J_1, T_1). At time T_1 ($T_1 < \infty$, since the process N_t is assumed non-explosive), $P_{T_1} = 2\delta J_1$, $I_{T_1} = J_1$, $S_{T_1} = 0$, while

$$\mathbb{E}\left[P_{T_1}\big|P_0 = 0, S_0 = s, I_0 = +1\right] = 2\delta\,\mathbb{E}\left[J_1\big|S_0 = s, I_0 = +1\right] = 2\delta\bar{\alpha}(s)\,.$$

We notice that $(P_u)_{u \geq T_1}$ conditionally on (T_1, J_1) is given by P_{T_1} plus the independent product of J_1 times an independent stochastic process (driven by the same dynamic of (P_t) conditionally on $S_0 = P_0 = 0$ and $I_0 = +1$), as shown by

$$P_t := P_{T_1} + 2\delta\sum_{k=2}^{N_t} J_k = P_{T_1} + J_1\left(2\delta\sum_{k=2}^{N_t}\prod_{i=1}^{k} B_i\right),$$

which proves that

$$P_t\big|J_1, T_1 \equiv P_{T_1} + J_1\hat{P}_{N_t-1}\,, \quad \hat{P}_n \equiv 2\delta\sum_{k=1}^{n}\prod_{i=1}^{k} B_i\,,$$

where $(\hat{P}_n)$ is independent from J_1. Now, by tower conditioning w.r.t. to (T_1, J_1),

$$\lim_{T\to\infty}\theta^T(t,s) = \lim_{t\to\infty}\theta^t(0,s) = \lim_{t\to\infty}\mathbb{E}\left[P_t\big|P_0 = 0, S_0 = s, I_0 = +1\right] = 2\delta\bar{\alpha}(s) + 2\delta\bar{\alpha}(s)\lim_{n\to\infty}\mathbb{E}\left[\hat{P}_n\right]$$

$$= 2\delta\bar{\alpha}(s) + 2\delta\bar{\alpha}(s)\sum_{k=1}^{\infty}\alpha^k = 2\delta\bar{\alpha}(s)\sum_{k=0}^{\infty}\alpha^k = 2\delta\left(\frac{\bar{\alpha}(s)}{1-\alpha}\right),$$

which concludes the proof. Notice that key element in the proof is finding a random time where (P_t) "regenerates" (we can apply somehow the Markov property), and from which its average long-run behavior can be deduced only by the embedded Markov chain (J_k) associated to the Markov renewal process (P_t).

$\square$

4.8   Appendix: proof of Theorem 4.3

The following proposition will be useful to improve the interpretation of the main result.

PROPOSITION 4.3. *Under a particular strategy* $\ell := (\ell_{\pm}(t,s))$,

$$\mathbb{E}_{t,s,i,y}\left[Y_T\right] = y + ig(t,s)\,,$$

where g is the viscosity solution of

$$-\frac{\partial g}{\partial t} - \frac{\partial g}{\partial s} - \mu(s)g(t,0) + \sigma^2(s)g(t,s) + \sum_{\nu\in\pm}\nu\left(h_\nu(s)L + \lambda_\nu(s)\Phi_{\pm}^1(L)\right)\ell_\nu(t,s) = 0\,,$$

$$g(T,) = 0\,.$$

Proof. Set

$$G(t,s,i,y) := \mathbb{E}_{t,s,i,y}\left[Y_T\right]\,,$$

which is associated to the Feymann-Kac equation

$$-\frac{\partial G}{\partial t} - \frac{\partial G}{\partial s} - \sum_{\nu\in\pm}h_\nu(s)\Delta G(t,0,\nu i, y - \nu i L\ell_\nu(t,s)) \qquad (4.8.1)$$

$$-\sum_{\nu\in\pm}\lambda_\nu(s)\int\Delta G(t,s,i,y-\nu ik\ell_\nu(t,s))\vartheta_\nu(dk,L) = 0\,,$$

$$G(T,) = y\,.$$

Using the ansatz

$$G(t, s, i, y) = y + i\mathfrak{g}(t, s),$$

we obtain

$$-\frac{\partial G}{\partial t} - \frac{\partial G}{\partial s} = i\left(-\frac{\partial \mathfrak{g}}{\partial t} - \frac{\partial \mathfrak{g}}{\partial s}\right),$$

$$\Delta G(t, 0, \nu i, y - \nu i L \ell_\nu(t, s)) = -\nu i L \ell_\nu(t, s) + i\left(\nu \mathfrak{g}(t, 0) - \mathfrak{g}(t, s)\right),$$

$$\int \Delta G(t, s, i, y - \nu i k \ell_\nu(t, s)) \vartheta_\nu(dk, L) = -\nu i \Phi_\pm^1(L) \ell_\nu(t, s),$$

$$\mathfrak{g}(T,) = 0.$$

The HJB equation (4.8.1) becomes

$$i\left(-\frac{\partial \mathfrak{g}}{\partial t} - \frac{\partial \mathfrak{g}}{\partial s}\right)$$
$$-\sum_{\nu \in \pm} h_\nu(s)\left(-\nu i L \ell_\nu(t, s) + i\left(\nu \mathfrak{g}(t, 0) - \mathfrak{g}(t, s)\right)\right) + \lambda_\nu(s)\left(-\nu i \Phi_\pm^1(L) \ell_\nu(t, s)\right) = 0,$$

$$\mathfrak{g}(T,) = 0,$$

and, by a further simplification,

$$\left(-\frac{\partial \mathfrak{g}}{\partial t} - \frac{\partial \mathfrak{g}}{\partial s}\right) - \mu(s)\mathfrak{g}(t, 0) + \sigma^2(s)\mathfrak{g}(t, s) + \sum_{\nu \in \pm} \nu\left(h_\nu(s)L + \lambda_\nu(s)\Phi_\pm^1(L)\right)\ell_\nu(t, s) = 0,$$

$$\mathfrak{g}(T,) = 0,$$

proving that $\mathfrak{g} = g$, which ends the proof.

$\square$

Proof of Theorem 4.3

We define $\eta\mathfrak{g} := \mathbf{v}^{(\eta)}$, that solves, thanks to (4.4.11):

$$\eta\left(-\frac{\partial \mathfrak{g}}{\partial t} - \frac{\partial \mathfrak{g}}{\partial s}\right) + \sum_{\nu \in \pm}\left(\max_{\ell \in \{0,1\}}\left(\ell G_\nu(t, s) - \eta\langle\mathcal{R}_\nu[\ell], \mathfrak{g}\rangle\right) - \max\left(G_\nu(t, s), 0\right)\right) = 0,$$

$$\eta\mathfrak{g}(T,) = \eta q^2,$$

with

$$\langle\mathcal{R}_\nu[\ell], \mathfrak{g}\rangle = h_\nu(s)\Delta\mathfrak{g}(t, \nu q - \ell, s) + \lambda_\nu(s)\int \Delta\mathfrak{g}(t, q \mp \ell k, s)\vartheta_\nu(dk, L) \tag{4.8.2}$$
$$:= \langle\mathcal{R}_\nu^0, \mathfrak{g}\rangle + \ell\langle\mathcal{R}_\nu^1, \mathfrak{g}\rangle,$$

and

$$\langle\mathcal{R}_\nu^0, \mathfrak{g}\rangle = h_\nu(s)\Delta\mathfrak{g}(t, \nu q, 0), \tag{4.8.3}$$
$$\langle\mathcal{R}_\nu^1, \mathfrak{g}\rangle = h_\nu(s)\left(\mathfrak{g}(t, \nu q - L, 0) - \mathfrak{g}(t, \nu q, 0)\right) + \lambda_\nu(s)\int \Delta\mathfrak{g}(t, q - \nu k, s)\vartheta_\nu(dk, L).$$

Using the (**sub**)-approximation for $\epsilon \to 0$:

$$\max\left(x - \varepsilon, 0\right) = \max\left(x, 0\right) - \varepsilon\mathbb{1}\{x > 0\} + o(\epsilon) \approx \max\left(x, 0\right) - \varepsilon\mathbb{1}\{x > 0\},$$

and since, by the operator continuity,

$$\lim_{\eta\to 0^+}\eta\langle \mathcal{R}^1_\nu, \mathfrak{g}\rangle = \lim_{\eta\to 0^+}\langle \mathcal{R}^1_\nu, \eta\mathfrak{g}\rangle = \langle \mathcal{R}^1_\nu, \lim_{\eta\to 0^+}\mathbf{v}^{(\eta)}\rangle = \langle \mathcal{R}^1_\nu, 0\rangle = 0\,,$$

the HJB equation is approximated by

$$\eta\left(-\frac{\partial\mathfrak{g}}{\partial t} - \frac{\partial\mathfrak{g}}{\partial s}\right) - \eta\langle\mathcal{R}^0_\nu, \mathfrak{g}\rangle + \sum_{\nu\in\pm}\left(\max\left(G_\nu(t,s) - \eta\langle\mathcal{R}^1_\nu, \mathfrak{g}\rangle, 0\right) - \max\left(G_\nu(t,s), 0\right)\right) \approx (\geq)$$

$$\eta\left(-\frac{\partial\mathfrak{g}}{\partial t} - \frac{\partial\mathfrak{g}}{\partial s}\right) - \eta\sum_{\nu\in\pm}\langle\mathcal{R}^0_\nu, \mathfrak{g}\rangle - \eta\sum_{\nu\in\pm}\langle\mathcal{R}^1_\nu, \mathfrak{g}\rangle\mathbb{1}\{G_\nu(t,s) > 0\} = 0$$

$$\eta\mathfrak{g}(T,) = \eta q^2\,.$$

Dividing by $\eta > 0$ and using (4.4.13) for $\eta = 0$, we obtain

$$-\frac{\partial\mathfrak{g}}{\partial t} - \frac{\partial\mathfrak{g}}{\partial s} - \sum_{\nu\in\pm}\langle\mathcal{R}^0_\nu, \mathfrak{g}\rangle - \sum_{\nu\in\pm}\langle\mathcal{R}^1_\nu, \mathfrak{g}\rangle\hat{\ell}^{(0)}_\nu(t,s) = 0 \tag{4.8.4}$$

$$\mathfrak{g}(T,) = q^2\,.$$

Since we have used a sub-approximation, by the comparison principle, any solution of (4.8.4) is an upper bound for $\mathfrak{g}$, which is positive since replacing $\mathfrak{g}$ by $\mathfrak{g}_* = 0$:

$$-\frac{\partial\mathfrak{g}_*}{\partial t} - \frac{\partial\mathfrak{g}_*}{\partial s} - \sum_{\nu\in\pm}\langle\mathcal{R}^0_\nu, \mathfrak{g}_*\rangle - \sum_{\nu\in\pm}\langle\mathcal{R}^1_\nu, \mathfrak{g}_*\rangle\hat{\ell}^{(0)}_\nu(t,s) \geq 0$$

$$0 \geq q^2\,.$$

Using the ansatz

$$\tilde{\mathfrak{g}}(t,s,q) := q^2 + q\tilde{\zeta}_1(t,s) + \zeta_0(t,s)\,,$$

and injecting in the equations at (4.8.3), we obtain

$$\langle\mathcal{R}^0_\nu, \tilde{\mathfrak{g}}\rangle = h_\nu(s)\left((\nu q)^2 - q^2 + (\nu q)\tilde{\zeta}_1(t,0) - q\tilde{\zeta}_1(t,s) + \Delta\zeta_0(t,0)\right)$$

$$= h_\nu(s)\left(q\left(\nu\tilde{\zeta}_1(t,0) - \tilde{\zeta}_1(t,s)\right) + \Delta\zeta_0(t,0)\right)$$

$$\langle\mathcal{R}^1_\nu, \tilde{\mathfrak{g}}\rangle = h_\nu(s)\left((\nu q - L)^2 - (\nu q)^2 + (\nu q - L)\tilde{\zeta}_1(t,0) - (\nu q)\tilde{\zeta}_1(t,0)\right)$$

$$+ \lambda_\nu(s)\int\left(((q - \nu k)^2 - q^2 + (q - \nu k)\tilde{\zeta}_1(t,s) - q\tilde{\zeta}_1(t,s)\right)\vartheta_\nu(dk, L)$$

$$= h_\nu(s)\left(L^2 - \nu 2Lq - \tilde{\zeta}_1(t,0)\right) + \lambda_\nu(s)\int\left(k^2 - \nu 2qk - \nu k\tilde{\zeta}_1(t,s)\right)\vartheta_\nu(dk, L)$$

$$= h_\nu(s)\left(L^2 - \nu 2Lq - \tilde{\zeta}_1(t,0)\right) + \lambda_\nu(s)\left(\Phi^2_\nu(L) - \nu 2q\Phi^1_\nu(L) - \nu\Phi^1_\nu(L)\tilde{\zeta}_1(t,s)\right)$$

$$= q\left(-2\nu\left(h_\nu(s) + \lambda_\nu(s)\Phi^1_\nu(L)\right)\right)$$

$$+ h_\nu(s)\left(L^2 - L\tilde{\zeta}_1(t,0)\right) + \lambda_\nu(s)\left(\Phi^2_\nu(L) - \nu\Phi^1_\nu(L)\tilde{\zeta}_1(t,s)\right)\,,$$

that, injected in (4.8.4), and splitting by the degree in q, lead to

$$-\frac{\partial\tilde{\zeta}_1}{\partial t} - \frac{\partial\tilde{\zeta}_1}{\partial s} - \sum_{\nu\in\pm}h_\nu(s)\left(\nu\tilde{\zeta}_1(t,0) - \tilde{\zeta}_1(t,s)\right) - \sum_{\nu\in\pm}\left(-2\nu\left(h_\nu(s) + \lambda_\nu(s)\Phi^1_\nu(L)\right)\hat{\ell}^{(0)}_\nu(t,s)\right) = 0\,,$$

$$\tilde{\zeta}_1(T,) = 0\,.$$

Setting $\tilde{\zeta}_1 := 2\zeta_1$, and noticing that

$$-\sum_{\nu\in\pm}h_\nu(s)\left(\nu\zeta_1(t,0) - \zeta_1(t,s)\right) = \mu(s)\zeta_1(t,0) - \sigma^2(s)\zeta_1(t,s)\,,$$

we obtain the characterisation for ζ_1, while the probabilistic representation of ζ_1 derives immediately from Proposition 4.3. Grouping the remaining terms non multiplying q, we obtain

$$-\frac{\partial \zeta_0}{\partial t} - \frac{\partial \zeta_0}{\partial s} - \sigma^2(s)\Delta \zeta_0(t,0)$$

$$-\sum_{\nu \in \pm} \left(h_\nu(s) \left(L^2 - 2L\zeta_1(t,0) \right) + \lambda_\nu(s) \left(\Phi_\nu^2(L) - 2\nu \Phi_\nu^1(L)\zeta_1(t,s) \right) \right) \hat{\ell}_\nu^{(0)}(t,s) = 0,$$

$$\zeta_0(T,) = 0.$$

We recall that, by the previous argument, $\tilde{\mathfrak{g}} \geq \mathfrak{g} \geq 0$, which are η-uniform bounds for $\mathfrak{g}$. For the error analysis, consider that

$$-\frac{\partial \mathfrak{g}}{\partial t} - \frac{\partial \mathfrak{g}}{\partial s} - \langle \mathcal{R}_\nu^0, \mathfrak{g} \rangle + \eta^{-1} \sum_{\nu \in \pm} \left(\max \left(G_\nu(t,s) - \eta \langle \mathcal{R}_\nu^1, \mathfrak{g} \rangle, 0 \right) - \max \left(G_\nu(t,s), 0 \right) \right) = 0$$

$$\langle \mathcal{A}, \tilde{\mathfrak{g}} \rangle := -\frac{\partial \tilde{\mathfrak{g}}}{\partial t} - \frac{\partial \tilde{\mathfrak{g}}}{\partial s} - \sum_{\nu \in \pm} \langle \mathcal{R}_\nu^0, \tilde{\mathfrak{g}} \rangle - \sum_{\nu \in \pm} \langle \mathcal{R}_\nu^1, \tilde{\mathfrak{g}} \rangle \mathbb{1}\{G_\pm(t,s) > 0\} = 0$$

$$\mathfrak{g}(T,) = \tilde{\mathfrak{g}}(T,) = 0.$$

We define $\delta^{(\eta)} := \tilde{\mathfrak{g}} - \mathfrak{g} \geq 0$, solving:

$$-\frac{\partial \delta^{(\eta)}}{\partial t} - \frac{\partial \delta^{(\eta)}}{\partial s} - \langle \mathcal{R}_\nu^0, \delta^{(\eta)} \rangle$$

$$-\sum_{\nu \in \pm} \langle \mathcal{R}_\nu^1, \tilde{\mathfrak{g}} \rangle \mathbb{1}\{G_\nu(t,s) > 0\} + \eta^{-1} \left(\max \left(G_\nu(t,s) - \eta \langle \mathcal{R}_\nu^1, \mathfrak{g} \rangle, 0 \right) - \max \left(G_\nu(t,s), 0 \right) \right) \geq$$

$$-\frac{\partial \delta^{(\eta)}}{\partial t} - \frac{\partial \delta^{(\eta)}}{\partial s} - \langle \mathcal{R}_\nu^0, \delta^{(\eta)} \rangle - \langle \mathcal{R}_\nu^1, \delta^{(\eta)} \rangle \hat{\ell}^{(0)} - \sum_{\nu \in \pm} \left| \langle \mathcal{R}_\nu^1, \mathfrak{g} \rangle \right| \mathbb{1}\{|G_\nu(t,s)| < \eta \left| \langle \mathcal{R}_\nu^1, \mathfrak{g} \rangle \right|\} =$$

$$-\frac{\partial \delta^{(\eta)}}{\partial t} - \frac{\partial \delta^{(\eta)}}{\partial s} - \langle \mathcal{R}_\nu[\hat{\ell}^{(0)}], \delta^{(\eta)} \rangle - \underbrace{\sum_{\nu \in \pm} \left| \langle \mathcal{R}_\nu^1, \mathfrak{g} \rangle \right| \mathbb{1}\{|G_\nu(t,s)| < \eta \left| \langle \mathcal{R}_\nu^1, \mathfrak{g} \rangle \right|\}}_{F_\eta(t,s,q)} =$$

$$\delta^{(\eta)}(T,) = 0,$$

where the inequality comes from the fact that

$$0 \leq \max\left(x - \varepsilon, 0\right) - \left(\max\left(x, 0\right) - \varepsilon \mathbb{1}\{x > 0\}\right) \leq |\epsilon| \, \mathbb{1}\{|x| < |\epsilon|\}.$$

Since $\langle \mathcal{A}^{(\eta)}, \delta^{(\eta)} \rangle = -\frac{\partial \delta^{(\eta)}}{\partial t} - \frac{\partial \delta^{(\eta)}}{\partial s} - \langle \mathcal{R}_\nu[\hat{\ell}^{(0)}], \delta^{(\eta)} \rangle$ is the infinitesimal generator of the Markov process (t, S_t, Q_t) under the trading strategy $\hat{\ell}^{(0)}$ (see (4.8.2)), we have the probabilistic representation

$$\delta^{(\eta)}(t, s, q) = \mathbb{E}_{t,s,q} \left[\int_t^T F_\eta(t, S_u, Q_u) \right].$$

Using the η uniform bound for $\mathfrak{g}$, we can provide a η uniform bound for $\left| \langle \mathcal{R}_\nu^1, \mathfrak{g} \rangle \right|$, so that $0 \leq F_\eta \leq \bar{F}_\eta \downarrow 0$, for $\eta \downarrow 0$: using the monotone convergence theorem, $\delta^{(\eta)} = \frac{1}{\eta} \mathbf{R}^{(\eta)} \to 0$, ending the proof. (Alternatively, an application of the stability principle of viscosity solution can be used).

Chapter 5

Long memory patterns in high-frequency trading

Abstract

In this paper we present a long memory model, based on marked point processes, which describes the stock price in the limit order book: its marks are driven by a VLMC (an efficient generalization of high-order Markov chains), while the inter-arrival times (between two consecutive jumps of the price) are represented by a self-exciting and independent univariate Hawkes process.

Instead of modeling directly the mid-price, we introduce a new price, called the fair one, with the intent to reduce the microstructure noise and represent the fundamental value of the asset: empirical evidences show that micro-structural trends, a potential source of statistical arbitrage, emerge after noise reduction.

The agent participates to the market both via impulsive (pseudo) market orders and limit orders, whose execution is modeled by Cox processes. Once the system is embedded into a Markovian one, we illustrate a trading algorithm based on optimal control techniques: we reduce the complex HJB equation associated to the problem to a simple system of variational ODE's, for which an explicit Euler scheme gives a computationally non-expensive solution.

Finally, Monte Carlo simulations show that the VLMC strategy over-performs the benchmark of a uninformed agent modeling the fair price as a simple Markov chain.

keywords: market micro-structure, self-exciting process, VLMC, optimal high-frequency trading

Introduction

One goal of this paper is to provide a model for the stock price in the limit order book and the execution mechanism for a single agent. The main difficulties arising in its conception are due to:

i) *The microstructure noise:* high-frequency mean reversion makes the best quotes move fuzzily, so that the very identification of a reference price represents a challenge.

ii) *The FIFO matching engine:* knowing how trades arrive is not sufficient to know how the agent limit orders are executed, since their position in the stack determines their execution priority.

iii) *Technical issues:* the way from a complex model (several state variables, non Markovianity, etc...) able to describe stylized facts (e.g. the volatility clusters) to an optimal trading algorithm is often a hard one, both computationally and mathematically.

Literature background

A vast literature exists on market microstructure: each author has tackled the subject from a different angle and with different techniques according to their main purpose being

⋄ modeling the stock price,

⋄ reproducing microstructure stylized facts,

⋄ describing the market impact,

⋄ providing an optimal trading application (mostly market making and optimal liquidation).

Roughly, this literature can be split into three big categories (since it is not the purpose of this paper, we omit optimal liquidation algorithms).

i) *Complex models on the observed price:* these papers exploit a complex system of mutually dependent point processes to reproduce several stylized effects characterizing the stock price at high-frequency, as the microstructure noise and the volatility clustering, the explosion of the mean signature plot, the Epps effect and the market impact. These models have become more and more sophisticated, going from the seminal paper [7], where the price is described by a couple of cross-exciting Hawkes processes, to [8], where the price and the market activity form a 4-dimensional Hawkes process with arbitrary kernel, for which a non-parametric estimation procedure is provided (see [7]). Limit theorems for large scale observations are available in the single and in the multi-asset case (see e.g. [7]), and recently [47] has shown a result concerning nearly unstable kernels. Using a different approach, [36] describes the mid-price using semi-Markov processes, choosing another perspective to represent the dependence among the tick times and the jump directions. Finally, in [25], the price is reconstructed endogenously from the interaction of market orders with the first levels of the book ([24]).

ii) *Hidden continuous price:* these papers describe the price as the representation of a hidden and continuous fundamental value: a microstructure noise due to the discrete nature of the book is supposed to hide the real value of the asset. A classic approach, with several further developments on the estimation of the quadratic volatility under noised observations, is due to [46]: the stock price observed at fixed frequency is seen as the sum of a Brownian motion and an independent noise. A new framework has been recently proposed by [60], who develops a very general model based on incertitude zones. Based on this work, [31] enlightens the role of the tick in the limit order book, and suggests the existence of an optimal tick size that guarantees the right liquidity distribution in the market.

iii) *Trading applications*: in most of these papers the price is a continuous martingale (usually a Brownian motion with constant volatility) while the agent execution is described by a complex system of stochastic intensity point processes, where market impact, news arrival and feedback execution are taken into account. In this list we can find the seminal papers [6] and [42] on optimal market making, where the agent limit orders are assumed to be filled by a Cox process with conditional intensity depending on the distance of the limit price from the mid one. In [23], the authors keep the hypothesis of a continuous price, and introduce a mean-reverting drift, while the agent execution is described by a complex system of Hawkes processes, and asymptotic formulas for small risk aversion describe explicitly the optimal posting distance. In [22], learning techniques are used to exploit information from the past in order to improve and stabilise the agent performance. The recent paper [33] focuses on option market making in a stochastic volatility framework with possibile parameter misspecification and provides explicit formula in the risk neutral case, that are deformed by the risk aversion of the agent. To conclude this non exhaustive list, [44] is one of the rare example where the stock price is not necessarily a continuous martingale, where the execution mechanism is pro-rata, rather than FIFO, and market orders are included in order to keep the inventory close to zero.

Our attempt is to bridge the first and the third group, looking for a good compromise between efficiency in price modeling and tractability. This paper aims a **high-frequency trader wanting to detect short-term patterns of the stock price, controlling the market risk associated to her portfolio**. We work with liquid large tick assets (see [31] for a rigorous quantitative definition), where the price jumps and the bid-ask spread are unitary.

The fair price

We first want to **reconstruct the symmetry broken by both the microstructure noise and the volatility clusters**, and then design a simple model able to describe all the market components. Replacing the mid-price by the fair one, defined as the best quote supplying the least liquidity immediately after a jump (see Figure 5.2), we obtain a new price

⋄ living on the tick grid,

⋄ being more stable,

⋄ such that the agent has a high probability to buy or sell the asset at that price before its value changes.

In this paper we choose an independent description of the tick times (the process counting the number of the fair price jumps) and the mark process (telling if the fair price jumps ↑ or ↓)[1]. With respect to [7] (where a bivariate Hawkes process drives upwards and downwards the price process) we model the tick times by a univariate marked point process: this dimensional reduction allows to add complexity somewhere else, in particular on the marks structure, the real source of statistical arbitrage.

i) *Tick times:* observing the inter-arrival times on a long period, we detect **clusters of several days, as shown by Figure 5.1**, during which the time between consecutive jumps is much shorter than its mean value: **a natural choice to reproduce this effect is a univariate self-exciting Hawkes process**. The tick times are the base ingredient for the description of other counting processes in the limit order book: we assume that **the jump intensity of the fair price provides a time change such that an observer in this system sees all the market events as Poisson processes**.

---

[1]The independence hypothesis allows parallel estimation, which is relevant under a computational point of view, since we are dealing with big data.
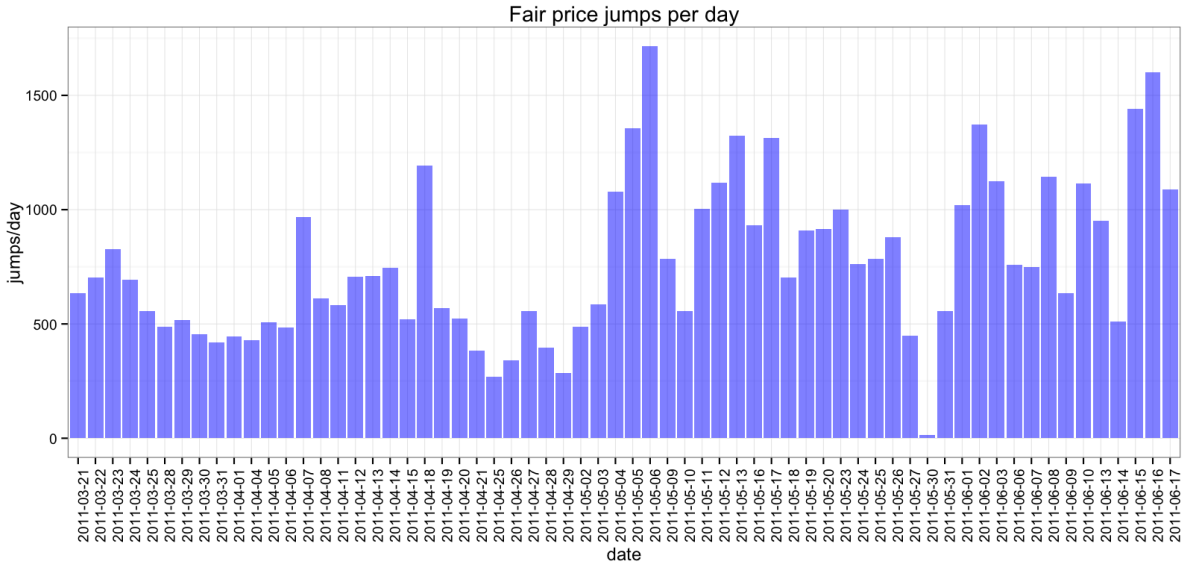
Figure 5.1: number of jumps of the fair price per day (taken from our dataset).

ii) *Marks:* at the microstructure level, **the fair price exhibits patterns of variable length** due to news anticipations, large order executions, trend following and several other reasons. Since the price jumps are either upwards (+) or downwards (-), we need a binary discrete process with long memory and efficient behaviour (parsimonious and quick to estimate). In [36], we exploit Markov chains, which have no memory but still a sufficiently rich dynamic to reproduce the microstructure noise. A natural candidate is represented by higher order Markov chains, which are unfortunately affected by dimensional curse: their state space grows exponentially with the memory depth, which makes their estimation extremely noisy and applications computationally involved. An efficient alternative, inspired by applications in DNA pattern recognition (see [15] for a complete theoretic framework) and text compressing (as in the original paper of [59]), are **VLMC**'s (Variable Length Markov Chain), **which generalizes higher order Markov chains, avoiding the dimensional curse**.

The matching engine (execution of limit and market orders)

We let the agent participate to the market in two ways:

i) *Pseudo market orders:* notice the fair price is close to a tradable reference price, i.e. a sell (resp. buy) limit order of small volume at that level is likely to be filled before the fair price changes. This is a natural consequence of the microstructure noise, that makes the mid-price oscillate several times around the fair one before the latter jumps (see Figure 5.3): before its next jump, the fair price is likely to coincide with the best-bid (resp. best-ask) price, leading to immediate execution (since the order is of small size and the limit order is sent at the market order level). Therefore, limit orders sent at that level are almost surely filled before the fair prices changes, so that they can be considered as market orders in a first approximation.

ii) *Passive limit orders:* in order to complement her strategy and compensate her lack of information, the agent can place passive limit orders at the fair price ±1 tick, in order to gain, in the market making fashion, an extra tick rewarding the provided liquidity.

This framework simplifies the execution model, since **the asymmetry due to microstructure noise and bid-ask imbalance is replaced by a system in equilibrium at the fair price**.

The trading algorithm

We use optimal control to exploit the pattern recognition technique previously described: we find a non-trivial policy capable of reaching an optimal trade-off between the rewards due to statistical arbitrages, and the risks associated to the trading activity. Taking care of transaction costs is essential, since many trades with low average expected gain take place during the day. Under the technical point of view, we reduce the complex system of variational PDE's characterizing the value function of the optimal trading problem to a system of variational ODE's by a suitable time change.
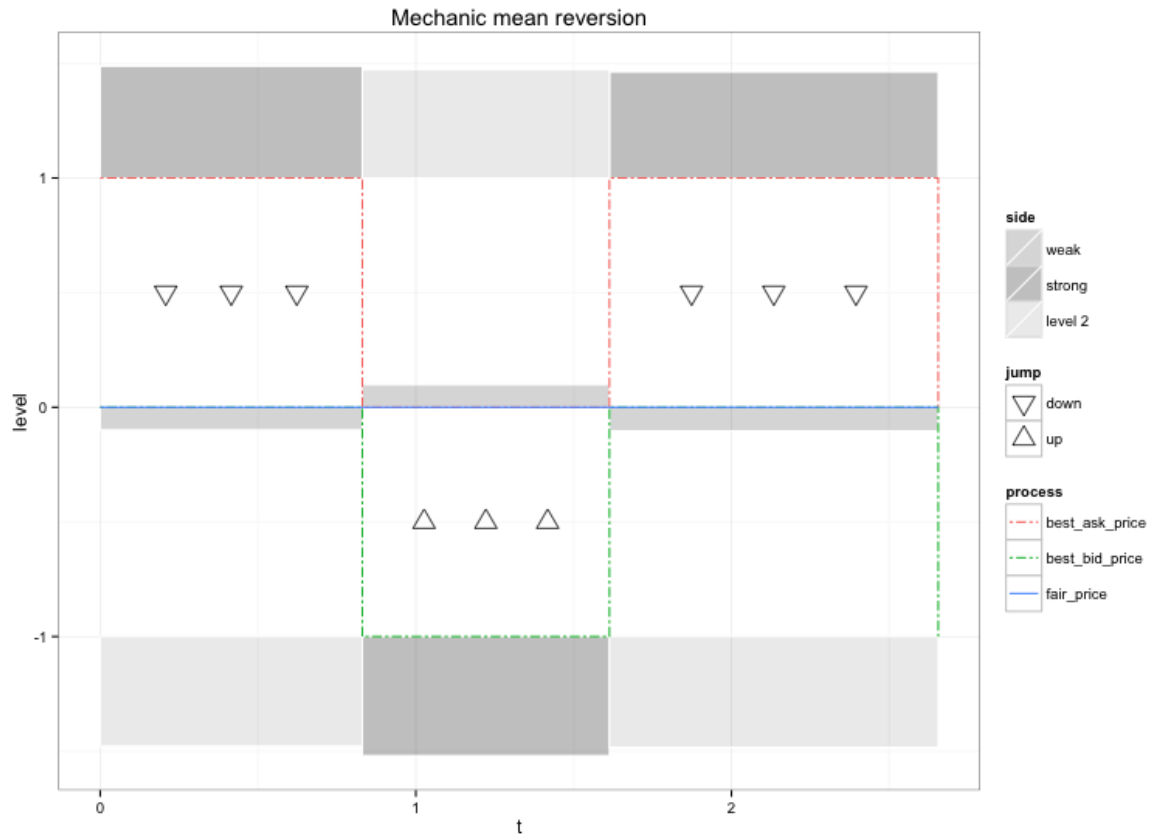
Figure 5.2: mechanical mean reversion. Starting from the left, the reader can see a low supply of liquidity at the best-bid level, which leads the price system to jump downwards. After the jump, a pre-existing liquidity block offers resistance on the bid side, while a brand new level provides only a modest support on the ask one, so that the price jumps upwards, and so on. Summing up, since the price is likely to jump over the weakest side on the limit order book, i.e. the one providing less liquidity, it is likely to revert. Notice that the weak side in the figure does not change since only reversions occur.

Plan of the paper

Section 5.1 is devoted to the reduction of the microstructure noise and the definition of the fair price. In Section 5.2 we provide a model for the fair price, independently describing the tick times (the process counting the number of jumps) and the mark process (telling if the price jumps upwards or downwards). Section 5.3 is devoted to the agent trading strategy and the matching engine, while Section 5.4 deals with application to statistical arbitrage. We conclude by commenting the numerical solution to the previously mentioned ODE: Monte Carlo simulations show that **this model theoretically outperforms the one presented in [36], where the fair price is seen a simple Markov chain**.

Framework and basic assumptions

In this paper we assume that the tick size is equal to 1 and that all the other quantities (e.g. the fees per transaction, bid-ask spread, etc...) are expressed in this unity measure. Furthermore, we assume that the bid-ask spread is constantly 1 tick, which is consistent with the data in our possession: in extremely liquid large tick assets, as the Eurostoxx future, the reaction of market participants is so fast that the bid-ask spread reverts instantaneously to its minimal value, i.e. one tick, which justifies our hypothesis.

Data

Data are taken from the 3-month future contract (front) on the Eurostoxx50 exchanged on EUREX, observed for 21 Mars to 17 June 2011 (contract maturity), from 09:30 to 16:00 Frankfurt TZ. All the empirical graphs are based on this database.

5.1   From the mid-price to the fair one

In our previous paper [36], and in several others in the market microstructure literature (e.g. [44] and [6]), the mid-price has been chosen as a reference price for market making application. For optimal execution instead, the mid-price is replaced either by one of the best quotes (e.g. [10]), depending if the agent is buyer or seller, while for some statistical papers on high-frequency stylized facts (e.g. [7]), the modeled price was the last traded one. Our main target is the pattern arbitrage and the mid-price does not seem a representative measure of the asset, since it is impossible to trade at that price (its value is not on the tick grid). Since our agent is both a buyer and a seller, the two best quotes are inappropriate as well, while the last traded price is subjected to an extremely high microstructure noise, which makes it difficult to describe. Our choice has been to **define a different reference price, based on the notion of weak side** (for which we send to [36] for further details): we obtain a process less affected by microstructure noise and which makes execution modeling less tricky.

The mid-price

We recall that the mid-price is defined as the arithmetic mean between the two best quotes in the limit order book. Let us fix some notations.

DEFINITION 5.1 (Mid-price). *We assume that the mid-price is described by* (M_n, T_n^M), *the latter being the only sequence such that*

$$J_n^M := M_{T_n^M} - M_{T_n^M -} \neq 0, \quad n \in \mathbb{N}^*, \tag{5.1.1}$$

$$M_t = M_{T_n^M}, \quad t \geq 0, \quad s.t., \quad T_n^M \leq t < T_{n+1}^M. \tag{5.1.2}$$

Notice that (5.1.1) means that (M_t) jumps exactly at (T_n^M-), while (5.1.2) that it is piecewise constant and cádlág. Notice that (M_t) is not on the tick grid $\mathbb{Z}$, which makes impossible to trade the asset at this price by sending any kind of order: our purpose is to replace this quantitative measure by a more representative and "tradable" one.

The fair price

It is well-known that the mid-price is subjected to micro-structural mean-reversion: as pointed out by the empirical literature (e.g. [36], [25] and [60]), at least on a big class of assets having large tick ([31]), two consecutive jumps of the mid-price are often in opposite directions. Consequently, **multiple jumps in the opposite direction clear themselves and do not affect the fundamental value of the asset**: they represent only an uninformative noise, whose

origin must be sought in the execution mechanism of the limit order book (see Figure 5.3 for further details). A natural candidate to replace the mid-price is given by:

DEFINITION 5.2 (Fair price). *We define the fair price at (T_n^M) as*

$$P_n := M_n - \frac{1}{2} sgn\left(J_n^M\right), \quad k \in \mathbb{N}^*, \tag{5.1.3}$$

and, as we did in Definition 5.1, we associate to (5.1.3) the sequence

$$\left(P_n, T_n^P\right) := (P_n, T_n),$$

describing its cádlág path, where (T_n) represents the timestamps of non-zero jumps of the fair price.

Notice that (P_t) jumps if and only if (M_t) does it twice consecutively in the same direction, while it is stable under noise reversion (see Figure 5.3). We choose (P_t) as the new reference price: **sending a limit order at that fair price level, the agent has a high probability of trading, independently if she is a buyer or seller** (we explain the execution dynamic in details in Section 5.3). In this sense, we say that the fair price is a representative measure of the asset value. Furthermore, its jump intensity (h_t) will define, in one of the following sections, a time change for which an observer in the new system sees all the events in limit order book as Poisson processes.
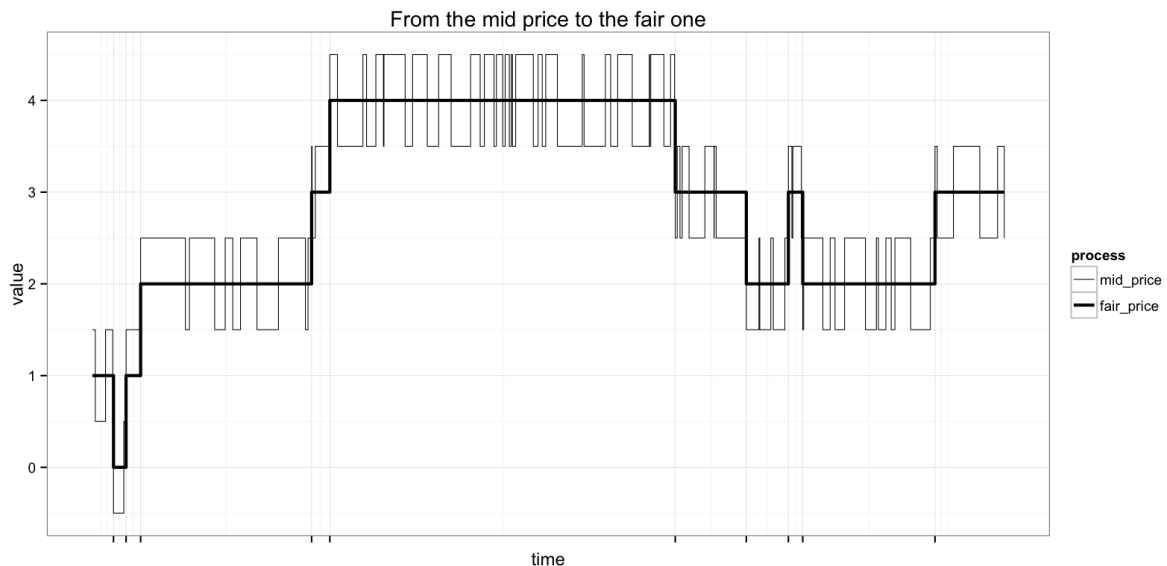
Figure 5.3: fair price corresponding to a path of the mid one (simulated data). Notice that the fair coincides either with the best-ask or the best-bid price and that it is stable under the reversion of the mid-price, i.e it jumps only if the mid-price jumps twice in the same direction.

5.2   The dynamic of the fair price

Before giving the price dynamic explicitly, we provide some (model independent) notations.

DEFINITION 5.3. *We call (N_t) the counting process associated to (T_n), i.e. the continuous cádlág process (here $T_0 = 0$) determining the number of jumps until t:*

$$N_t := \inf\{k \geq 0 : T_n \geq t\}, \quad t \geq 0.$$

DEFINITION 5.4. *We call (J_n) the $\{-1, +1\}$-valued discrete process describing the jump directions of the fair price:*

$$J_n := P_{T_n} - P_{T_n-}, \quad n \in \mathbb{N}^*.$$

DEFINITION 5.5. *Let I_t be the last direction taken by the fair price, i.e.*

$$I_t := J_{N_t}.$$

It is worth noticing that (N_t) and (J_n) characterize (P_t) thanks to:

$$P_t = P_0 + \sum_{k=0}^{N_t} J_n, \quad t \geq 0. \tag{5.2.1}$$

In our previous paper ([36]) we have given a description of the mid-price in terms of a semi-Markov process, where the tick times and the mark processes are mutually dependent and with short memory. In this paper instead, we assume that (N_t) and (J_n) are independent: this is not in contradiction with our previous work, since in this case the reference price is not the same. Getting free of the mutual dependence allows to use more complex models and describe **long memory patterns for both** (N_t) **and** (J_n) (a vast empirical literature, as e.g. [12, 52] has focused on the market persistence and long memory behavior).

Since the bid-ask spread is constantly 1 tick, the fair price - which coincides with the weak side of the limit order book, i.e. the best-bid (resp. best-ask) after an upward (resp. downward) jump, as shown in Figure 5.2 - is by definition one of the best prices: when the fair price is lower (resp. higher) than the mid one, it coincides with best-bid (resp. best-ask). This implies that a limit order at the fair price level is accepted by the trading platform as:

◇ a sell (resp. buy) limit order, sent when the fair price is the best-ask (resp. best-bid), is a passive limit order waiting for a match;

◇ a buy (resp. sell) limit order, sent when the fair price is the best-ask (resp. best-bid), is an aggressive limit order, which is automatically converted to a market one.

The difference between an aggressive limit order and a market one is that the first matches limit orders on the first level only, while the second seeks for liquidity in deeper levels of the LOB if necessary. Therefore, market orders have a bigger impact on the book, since they can clear multiple levels, making the price jumps of several ticks.

5.2.1   The tick times

As usual, the first point process to be tested for (N_t) is the Poisson one, which in this case leads to a poor fit, as shown by the qq-plot in Figure 5.5.

The Hawkes process approach

A renewal process is inappropriate as well, since, as shown by Figure 5.5, **inter-arrival times exhibit strong positive autocorrelation**: a natural candidate to model (N_t) is thus a univariate Hawkes self-exciting process. We quickly recall its definition (see [28] for a general introduction) in order to fix notations.

DEFINITION 5.6 (Hawkes process). *A self-exciting Hawkes process is a point process whose stochastic intensity is given by*

$$h_t = \mu_t + \sum_{T_n < t} \nu(t - T_n), \quad \mu_t > 0, \quad t \geq 0,$$

where ν is a positive integrable function called kernel, while $\mu_t > 0$ is called the base intensity. In order to guarantee the stability of the process, we impose the constraint $||\nu||_1 < 1$.

The intraday seasonality

Figure 5.4 shows the intraday seasonality of the fair price jump activity, i.e. the empirical density ρ for a fair price jump to be in a certain time region. As expected, it reproduces the typical U-shape form of the intraday volatility and the market volume distribution. We assume that μ_t depends on the day time, and to avoid the estimation of a collection of (μ_i), e.g. one for each hour, we rather assume that

$$\mu_t := \mu^{(0)} \rho(HH : MM(t)),$$

where $HH : MM(t)$ projects the current time to the corresponding day-time, expressed in hours and minutes after the midnight, and $\mu^{(0)} \in \mathbb{R}_+$ is a constant to estimate.
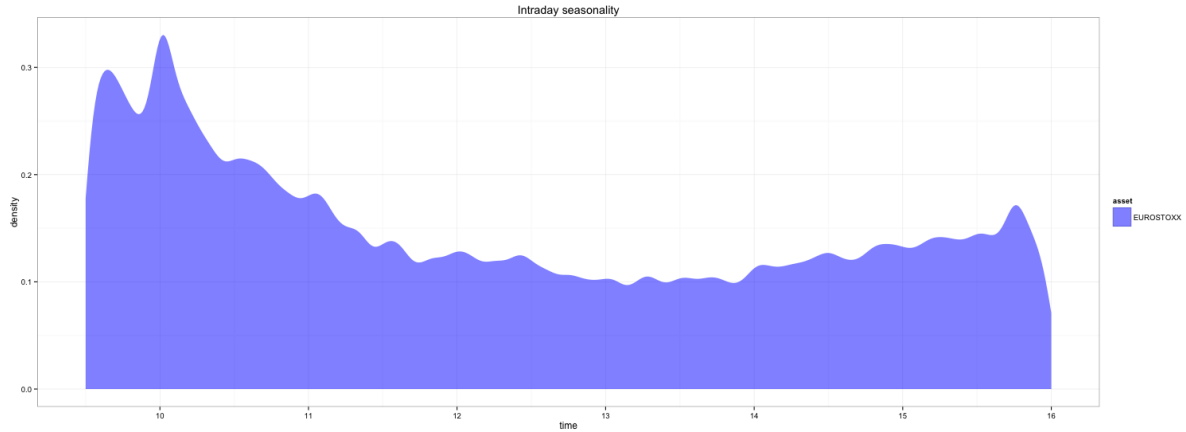
Figure 5.4: distribution of the fair price jumps according to the day time, reproducing the typical U shape (empirical data).

The exponential kernel

A common choice is taking the exponential kernel, even if the recent literature ([7]) has pointed out that the power one better represents the long memory of the limit order book. In order not to lose the Markov property, we keep the exponential assumption

$$\nu(t) := \alpha \exp(-\beta t), \quad 0 \le \alpha < \beta,$$

where the parameter constraint guarantees the stability of the process. For this particular kernel (which is not the case for the power one for example) (h_t) is a Markov process satisfying

$$dh_t = \alpha(\mu_t - h_{t-})dt + \beta dN_t. \tag{5.2.2}$$

Estimation and goodness-of-fit

We choose the MLE procedure for the estimation of the triplet (h, β, α): the process log-likelihood (see the original paper of [56]) is given by

$$\text{loglik} = \sum_{n=1}^{N_T} \left[\ln\left(h_{T_n-}\right) - \int_{T_{n-1}}^{T_n} h_s ds \right].$$

The exponential kernel guarantees an on-the-fly computation, which is a saving memory feature for big databases. The goodness-of-fit is given by testing that

$$\left(\zeta_n := \int_{T_{n-1}}^{T_n} h_t dt \right), \quad n = 1, \ldots, N_T, \tag{5.2.3}$$

is a i.i.d. sequence of exponential random variable of rate 1.
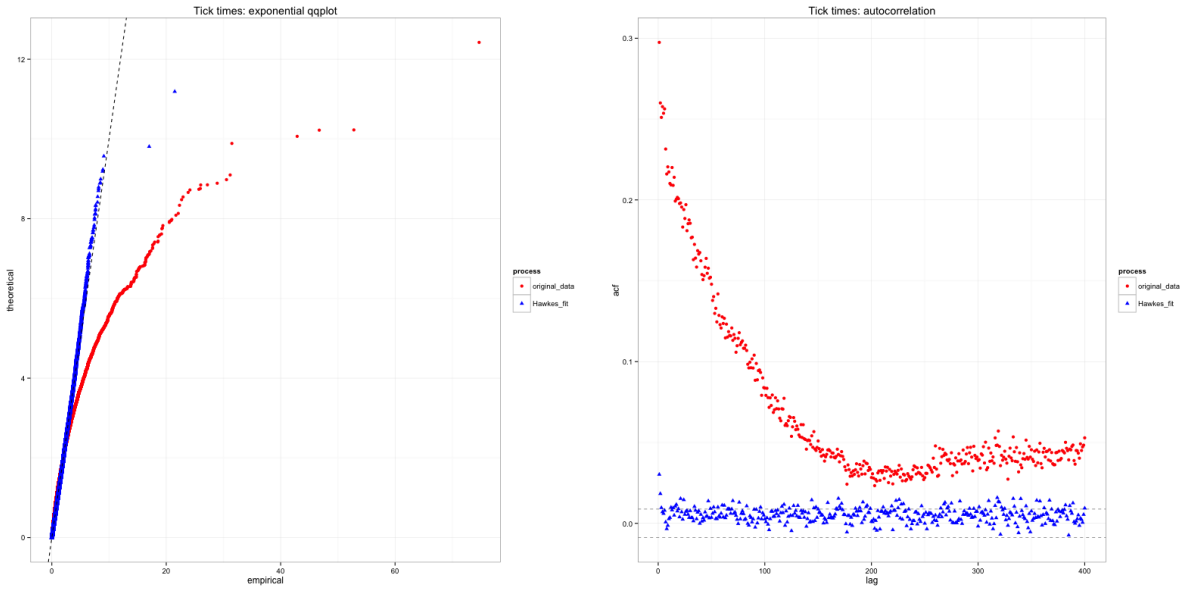
Figure 5.5: qq-plot (left) and autocorrelation function (right) of the original inter-arrival times $\left(\frac{T_n - T_{n-1}}{\mathbb{E}[T_n - T_{n-1}]}\right)$ and of Hawkes-transformed one $\left(\int_{T_{n-1}}^{T_n} h_s ds\right)$ against the exponential distribution (empirical data). This shows a Hawkes process with exponential kernel fits the data much better than a Poisson one.

The stochastic time change

Figure 5.5 shows an exponential qq-plot and an autocorrelation plot of the time series (ζ_n), proving that the model is consistent with data. Furthermore, the goodness-of-fit property (5.2.3) suggests a natural time change where (N_t) is a standard Poisson process.

DEFINITION 5.7 (Stochastic time change). *Let τ_t be the stochastic time change given by*

$$\tau_t := \langle P \rangle_t = \int_0^t h_s ds \, . \tag{5.2.4}$$

For every stochastic process Z we define its time changed by

$$\hat{Z} := Z \circ \tau^{-1} \, .$$

Notice that since $\langle P \rangle_t \geq \int_0^t \mu_u du$, $\tau^{-1}(s)$ is well defined for all s and bounded. In particular, $(\hat{N}_t)$ is a standard Poisson process, i.e. **an observer of the limit order book having a clock running (h_t) faster than the normal one, sees the inter-arrival times as an i.i.d. sequence of exponential random variables of parameter** 1. We will use this clock to get a Poisson normalization of all the other processes in the market.

The leverage effect

Figure 5.5 shows the fair price (P_t) and the jump intensity (h_t) processes. As for the Heston model, we suspected a negative correlation between volatility and price variation, usually called leverage effect. In order to test this assumption, we have replaced (5.2.2) by

$$dh_t = \alpha(\mu_t - h_{t-})dt + (\beta + lJ_{N_t})dN_t \, , \quad l \in \mathbb{R} \, ,$$

where the size of the jumps of the stochastic intensity depends on the side of the price jump: notice that (h_t) is not predictable anymore, but adapted to the filtration generated by the fair price. Surprisingly, a MLE estimation algorithm shows that this parameters is not statistically different from 0: at this scale **we have found no leverage effect**.

5.2.2   The marks of the stock price

Figure 5.6 shows that the autocorrelation function of the discrete time series (J_n) is not trivial, which leads to reject the i.i.d. model. **Marks exhibit positive auto-correlation**: most of the literature focuses on the short-term mean-reversion, but the latter seems to vanish once we pass from the mid-price price to the fair one. Furthermore, Figure 5.6 shows that while there are approximatively the same number of upwards and downwards jumps, this is not true for the number or trends and reversions, the first widely overcoming the second. These trends are caused by the strong positive autocorrelation of trade sides, mostly due to splitting of meta orders [52]: splitting algorithms avoid the instantaneous and tremendous impact that a single market order would have on the stock price, but they lead the agent to trade in the same sense for a rather long period. Trends in the fair price are a consequence, among other things, of this common practice. **The goal of this paper is to perform an arbitrage of these trends**, hedging against fees and market risk.

Since more than 99% of the price jumps are of the same size of the tick, we can assume that $|J_n| = 1$ a.s., even though the model can be easily extended to the general case introducing an independent law for the absolute size of the jumps.

DEFINITION 5.8. *We assume that*

$$J_n = J_{n-1}U_n, \quad n \in \mathbb{N}^*,$$

where (U_n) is valued in $\{-1,+1\}$ as well.

As we did in [36], rather than studying the law of sequences of marks, we focus on the probabilistic structure of sequences of trends $(U_n = 1)$ and reversions $(U_n = -1)$[2].
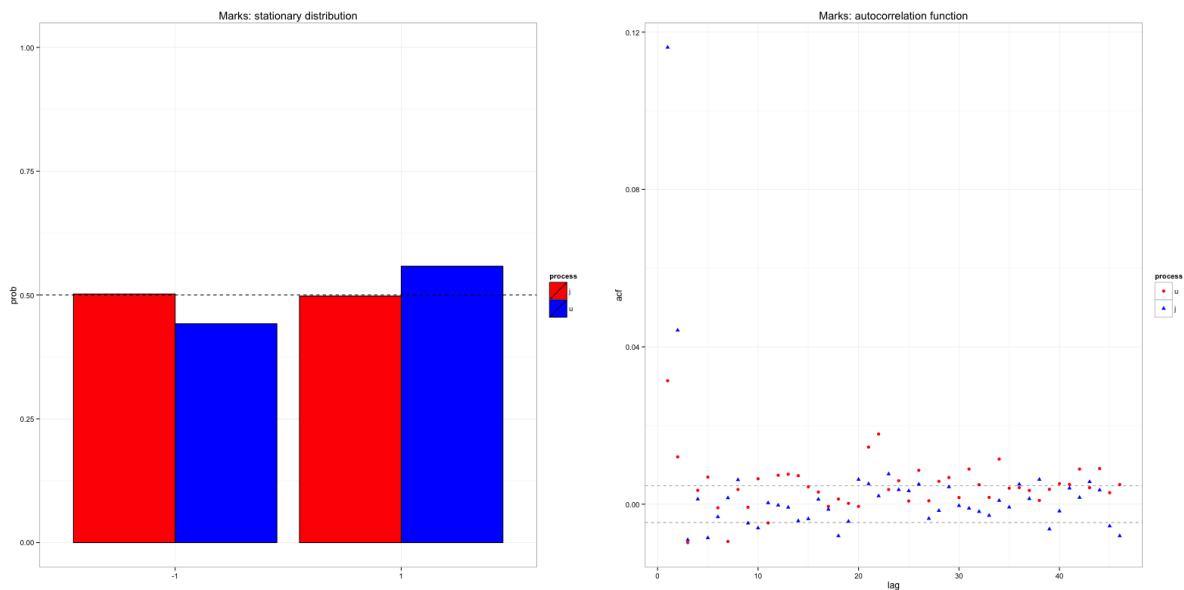
Figure 5.6: empirical distribution (left) and autocorrelation function of the time series (J_n) and (U_n). Differently from (J_n), the trend process (U_n) exhibits an asymmetric empirical distribution, while both of them shows a non-trivial autocorrelation function, proving the presence of memory in the two direction processes.

The Variable Length Markov Chain model

We assume that (U_n) is a stationary Variable Length Markov Chain (VLMC) of finite memory, and on the state space $E := \{-1,+1\}$. Formally (see [15] for a complete introduction to this model):

---

[2] The previous hypothesis is not necessary for the development of the model and its application, it just leads to a nice simplification for the solution of the control problem. If the reader feels uncomfortable with such an assumption, he/she can easily pass to the general case, where (J_n) is modelled directly.

DEFINITION 5.9 (VLMC). *The VLMC process describing the dynamic of (U_n) is given by*

i) a satured tree[3] with alphabet E, whose leaves (terminal nodes) are called "contexts" and form a set denoted by $\mathbb{C}$;

ii) a family of probability $\{\wp_{\pm}(c)\}_{c\in\mathbb{C}}$, such that for every u right infinite word on E

$$\mathbb{P}\left[U_0 = \pm \mid U_{-1}U_{-2}\cdots = u\right] = \wp_{\pm}\left(\pi(u)\right), \tag{5.2.5}$$

where

$$\pi : \prod_{k=1}^{\infty} E^{(k)} = E^{\mathbb{N}^*} \to \mathbb{C} \tag{5.2.6}$$

is the context function associated to the tree, mapping a right infinite sequence u to the only context $c := \pi(u)$ being prefix of u (continue reading for further details).

REMARK 5.1. *Notice that, since $E = \{-1, +1\}$,*

$$\wp_{\pm}(c) := \frac{1 \pm \alpha(c)}{2}, \quad c \in \mathbb{C},$$

where α is the conditional mean of the next state given c.

REMARK 5.2. *Notice that since the process is stationary, (5.2.5) holds shifting all the indexes by k.*

The formal Definition 5.9 is better understood by looking at
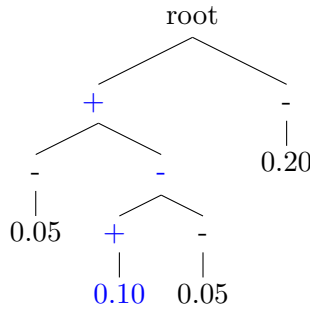
Assume that we want to predict U_0 and $u := U_{-1}U_{-2}U_{-3}U_{-4}\cdots = + - + + \ldots$: starting from the root, walk on the tree following the path given by u (drawn in blue). At the third step the walk ends at $c = + - +$, independently on $U_{-k}, k \geq 4$: the context $c := \pi(u)$ is called the context associated to u and $\alpha(c) = 0.10$ determines the conditional distribution of U_0 on the state space $E = \{-1, +1\}$. In this case the next state is $+1$ (resp. -1) with probability $0.55 = (1 + 0.10)/2$ (resp. $0.45 = (1 - 0.10)/2$).

DEFINITION 5.10 (Length function). *We define the length function as*

$$l(u) := d(root, \pi(u)),$$

where the distance d represents the length of the shortest path from the root to the context.

The function l of Definition 5.10 says how back in the past we need to go to have the conditional distribution of the next space. Notice that the contexts have variable length and thus the model has variable memory. If all the contexts had the same length, the tree would be complete of order $L_{\max}$ and describe the probabilistic structure of a high order Markov chain, of which the VLMC model is a generalization. By the assumption of finite memory, l is bounded by a certain $L_{\max} < \infty$.

REMARK 5.3. *Notice that the context function π can be trivially extended to all left finite the words, right finite and infinite, having one of the context as prefix (at most one context can enjoy this property), i.e. all the left finite words but the internal nodes of the tree.*

---

[3]In a satured tree, each node has either 0 or $|E|$ children

Estimation

The original **estimation procedure is performed by the CONTEXT algorithm of Rissanen** (see [59]), and several implementations are available in C/C++. The estimation depends on a confidence level and on a tuning parameter, called the threshold, giving a lower bound of the number of observation associated to a context. For example, the VLMC package of in R (see [54]) relies on one of these implementation and represents a user-friendly tool to estimate and manipulate this model. Here is the result of the estimation procedure both under tree representation (Section 5.2.2) and (c, α) scatterplot, as shown by Figure 5.7.
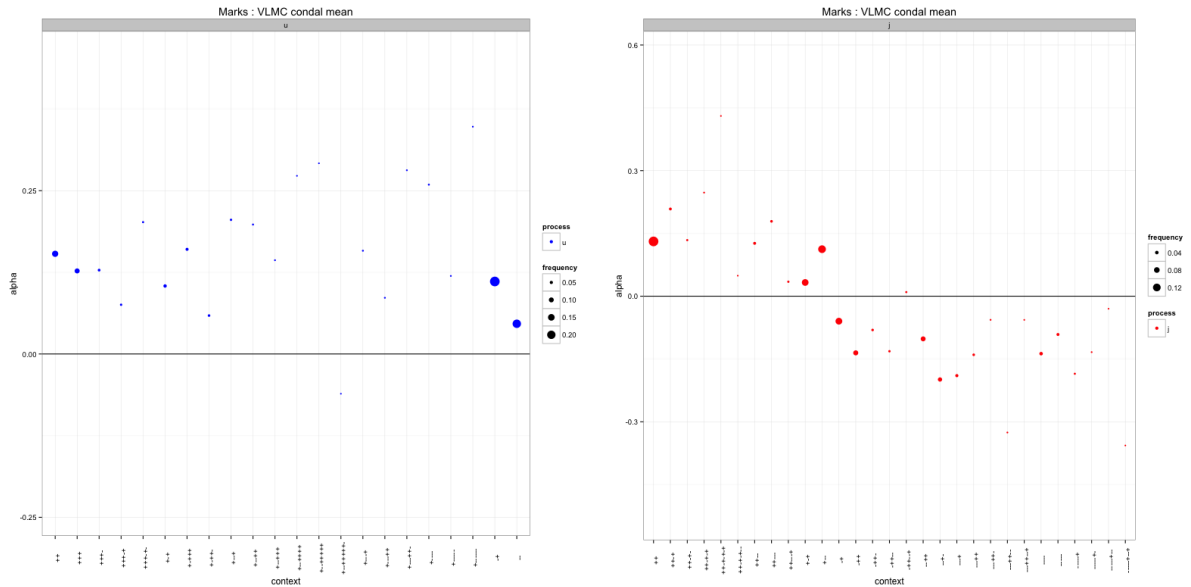
Figure 5.7: Estimation of $\alpha(c)$ on our dataset: the x axis contains the contexts, while the height (resp. the size) of the circles represents the function value (resp. the empirical estimator of the probability of that context to appear). Notice that α **is positive** almost everywhere, which is a further evidence of the fact that trends are dominant w.r.t. reversions. The importance of the VLMC model relies in its application: even if the next predicted state would almost always be $U_n = +$, knowing its conditional distribution allows to know if execution costs and market risk kill or not the expected return of the agent's arbitrage strategy.

The Markov embedding

The VLMC processes allows to describe the probabilistic structure of long patterns, but, on the contrary of higher order Markov chains, they are immune to the dimensional curse. Notice that

◇ a Markov chain of order n is a VLMC with on $\mathbb{C} = E^n$,

◇ a Markov chain of order n is a (embedded in a) Markov chain on E^n, but

◇ a VLMC **may not** be embedded in a Markov process on its context set $\mathbb{C}$.

The following example clarifies the previous statement: assume that the VLMC tree is given by

Table 5.1: estimation of the VLMC model on the process (U_n).

Figure 5.8: 10-fold cross validation for the estimation of the VLMC tree on (U_n). For a fixed level of confidence ($\alpha = 5\%$), the minus-log-likelihood is shown as a function of the "threshold" parameter: for small thresholds, the model over-optimises, while for big thresholds the model is an i.i.d. walk. The optimal threshold gives a non-trivial tree structure, shown in Section 5.2.2.

and that the current context is $c = -$ (red). If we could embed the VLMC in a Markov chain on $\mathbb{C}$, c is all we need to know to simulate the future trajectory of the process. We are able to simulate the next step, since $\alpha(c) = 0.20$ is its conditional mean: if the next state is $+$, all the information we own to simulate the next state is given by the sequence $+-$, which is an internal

node of the tree (green). Since π cannot be extended on internal node (see Remark 5.3), we cannot simulate the next step. This suggests that we need to embed the VLMC in a Markov chain on a state space larger than the context set.

We could embed the VLMC in a Markov chain of order L (the maximal length of a context), but this leads to a unnecessarily huge state space. A better solution is available. In order to provide a Markov embedding using the context function π, it is enough to define a Markov chain on $\mathbb{C}$ with probability $\mathbb{Q}$ defined as

$$\mathbb{Q}_c := \pi_*(\mathbb{P}_{\pi^{-1}(c)}), \tag{5.2.7}$$

where

$\diamond$ $\mathbb{Q}_c$ is the distribution of the next state of the Markov chain given c,

$\diamond$ $\mathbb{P}_u$ is the distribution of $(\ldots U_{-2}U_{-1}U_0)$ given $(u = U_{-1}U_{-2}\ldots)$.

The reason why VLMC's are not necessarily a Markov chain on their context set is that (5.2.7) is not necessarily well defined: (5.2.7) is equivalently stated in terms of transition probability as

$$\mathbb{Q}[c \to d] := \mathbb{P}[\pi^{-1}(c) \to \pi^{-1}(d)].$$

Going back to the previous example, choosing $c = -$ and $d = +-+$, we have

$$\mathbb{Q}[+ \to +-+] := \mathbb{P}[(+\omega\ldots) \to (+-+\ldots)] = 0, \qquad \omega = +,$$
$$= \frac{1+\alpha(c)}{2}, \qquad \omega = -,$$

which is not well defined, since it depends on ω. We would be done taking
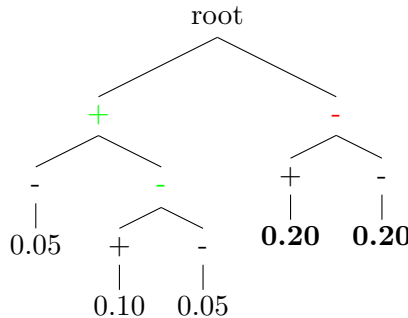
We simply add two children to the context $c = -$, and let them inherit their father's α function to preserve the probabilistic structure. Now $c = -$ is not a context anymore and it has been replaced by $-+$ and $--$. Notice that

$$\mathbb{Q}[-+ \to +-+] := \mathbb{P}[(-+\ldots) \to (+-+\ldots)] = \frac{1+\alpha(c)}{2},$$
$$\mathbb{Q}[-- \to +-+] := \mathbb{P}[(--\ldots) \to (+-+\ldots)] = 0,$$

i.e. they are well defined in both cases.

The procedure consists in adding leaves to the tree and extend α by parental inheritance (in order to preserve the probabilistic structure) until one finds a tree such that, for each context c (of the new tree), the words $+c$ and $-c$ are not internal nodes (so that π is well defined). A natural candidate is given by:

DEFINITION 5.11 (Embedding algorithm). *Call T the tree associated to the VLMC process and define the recursive sequence of trees given by*

$$T^0 = T,$$
$$T^{n+1} = T^n \cup T_+^n \cup T_-^n, \quad k > 0,$$

where $\cup$ denotes the union of trees (given by the set union of all the nodes) an $T_\pm^n$ are the subtrees of T^n attached to the nodes $\pm$ (i.e. the two nodes attached to the root of the tree).

By definition, if this algorithm converges, we are done.

LEMMA 5.1. *The algorithm given in Definition 5.11 converges, i.e.*

$$\exists T^\infty := \lim_{n \to \infty} T^n,$$

and T^∞ does not exceed the complete tree of order $L_{\max}$.

Proof. By assumption T^0 has maximal height $L_{\max} < \infty$: we can prove by induction that this holds for every T^n by the following argument. Assume T^n shares the same property for some index k: T^n_+ and T^n_- has maximal height less or equal than $L_{\max} - 1$, which implies that $T^{n+1} = T^n \cup T^n_+ \cup T^n_-$ has maximal height $L_{\max}$, and so this is true for all k's by induction. Since $T^n \subseteq T^{n+1}$, they are equal if and only if they have the same number of nodes, and since T^n has at most $2^{L_{\max}}$ nodes, we know that the algorithm eventually has a fixed point. In the worst case scenario, the fixed point is the complete tree of order $L_{\max}$.

$\square$

The resulting is usually much smaller than the complete one, and this helps us reducing the dimension of the state space we will work with. **From now on, we assume that $T = T^\infty$, i.e. that the VLMC process is a Markov chain on its context set $\mathbb{C}$.**

5.3   Execution via limit orders

In this section we illustrate how the agent trades in this electronic market. We **classify limit orders according to the distance of their limit price from the fair one**, dividing them into level-0 and level-1 type.

Level-0 limit orders

A level-0 limit order is sent at the fair price level. In this case its price

⋄ either improves the existing best quotes: since the spread is unitary, it is immediately converted to a market order and executed,

⋄ or coincides with the best quote: if the price reverts, the order is filled before the price reverts[4], otherwise a match is still possible before the fair price jumps.

Since reversions are frequent for large tick assets (see [36, 31]), **a first approximation is to consider level-0 limit orders as (pseudo) market orders, filled instantaneously with probability $\delta \in [0, 1]$.**

In order to prevent the agent to affect the exogenous dynamic of the price, i.e. to limit her market impact, and to make impulsive control easier, an admissible policy will allow only $k_{\max}$ pseudo market order per fair price jump.

DEFINITION 5.12. *We denote by*

⋄ (θ_j, m_j) *the sequence of timestamps θ_j at which the agent sends a level-0 limit order of size $|m_j| \in \mathbb{N}$, where if $I_{\theta_{j_-}} m_j > 0$ (resp. < 0), the order of buy (resp. sell) type.*

⋄ $(\tilde{K}_t)$ *the associated counting process, i.e.*

$$\tilde{K}_t := \inf\{j \geq 0 : \theta_j \geq t\}, \quad t \geq 0,$$

---

[4]In a backtest simulation, as soon as the price reverts, the agent limit order price coincides with the opposite best quotes and thus it is automatically executed as in the first scenario.

◇ (K_t) *the process counting the number of level-0 limit orders since the last fair price jump, i.e.*

$$K_t := \tilde{K}_t - \tilde{K}_{T_{N_t}}, \quad t \geq 0.$$

Notice that (K_t) *increments of* 1 *when the agent sends an order, while jumps to* 0 *at each fair price jump.*

Level-1 limit orders

A level-1 limit order is sent at the fair price level ± 1 tick, $+1$ (resp. -1) for sell (resp. buy) limit orders: they are used to gain an extra tick thanks to the execution, as in the market making case, when no statistical pattern is known, or simply to improve the performance. The blue (resp. red) band in Figure 5.9 shows a buy (resp. sell) limit order sent at the constant fair price minus (resp. plus) one tick.
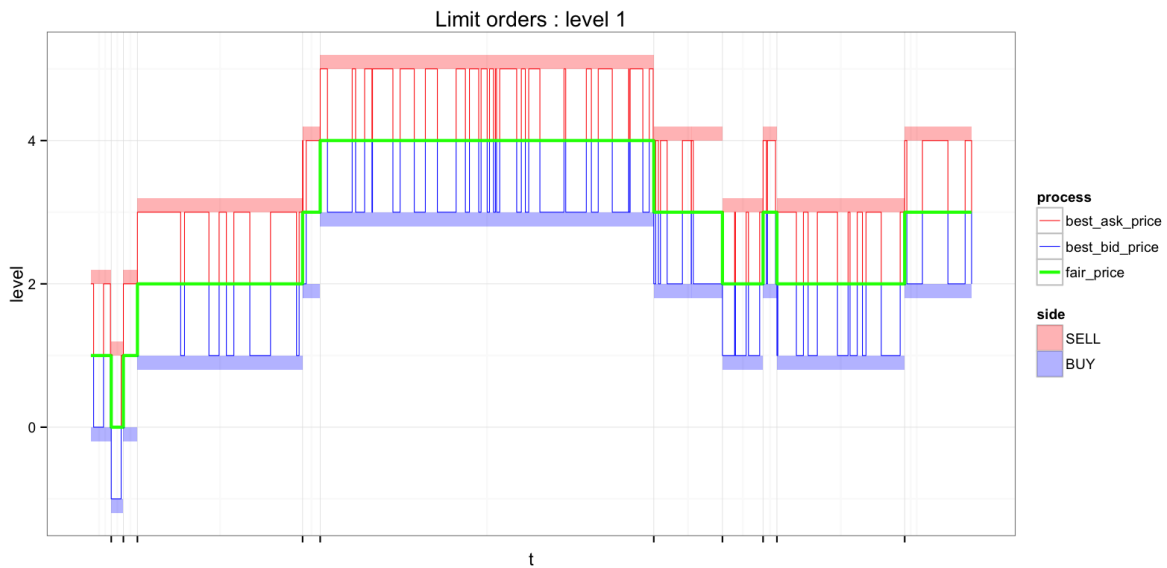
Figure 5.9: level 1 limit orders. According to the position of the fair price w.r.t. to the mid-price, a level 1 limit order coincides with either the first or the second level of the limit order book.

DEFINITION 5.13 (Level-1 limit orders). *They consist in sell (resp. buy) limit orders sent at the fair price level + 1 (resp. -1) tick. We assume that the agent sends orders of small size, that are entirely filled at a random time given by the first jump of a Cox process - independent from any other process in the market - having conditional intensity w.r.t. to the current context* c

$$h_t \lambda \frac{1 + I_t \alpha(c)}{2}, \quad \text{on the ASK side}, \tag{5.3.1}$$

$$h_t \lambda \frac{1 - I_t \alpha(c)}{2}, \quad \text{on the BID side} w$$

here $\lambda \geq 0$ *is non-negative constant. Notice that the total intensity of both sides is given by*

$$\sum_{\nu \in \pm} h_t \lambda \frac{1 + \nu I_t \alpha(c)}{2} = h_t \lambda, \tag{5.3.2}$$

which does not depend on the current context.

The coefficient $\frac{1 \pm I_t \alpha(c)}{2}$ tells that if the price is likely to jump in a certain direction, the same imbalance are reflected in the agent execution, adding **adverse selection** to the model, since an order is more likely to be executed if the price is going in the same direction: it is easier for

an agent to buy (resp. sell) an asset whose value is likely to decrease (resp. increase). In [37] we called this phenomenon weak adverse selection.

Notice that using level-1 limit orders, the agent tries to build a position gaining extra ticks thanks to the execution (as in market making strategies): the level-1 coincides either with the best or the second best price, depending on the relative position of the fair price w.r.t. to the mid one. In practice, sending limit orders to the second level, one is able to gain priority execution when the latter becomes the best one.

About the market impact, since the strong side (the opposite best quote of the weak side) usually offers liquidity, we assume that these orders have no impact on the fair price.

Estimation

For the estimation of the parameter λ:

  i) at T_0 send unitary limit orders at $P_{T_0} \pm 1$ on both sides on the book;

  ii) every time an order is executed, replace it with another one at the same level;

  iii) at every $(T_n), k \geq 1$, cancel all the existing limit orders and send new ones on both sides as in the step 1.

Since (N_t) (the fair price counting process) and (L_t) (the level-1 execution counting process) have intensity h_t and λh_t, in the time system given by $d\tau_t = hdt$ their are Poisson processes of intensity 1 $(\hat{N})$ and ϕ $(\hat{L})$. Using the Strong Law of the Large numbers,

$$\lim_{T \to \infty} \frac{L_T}{N_T} = \lim_{\tau \to \infty} \frac{\hat{L}_\tau}{\tau} \left(\frac{\hat{N}_\tau}{\tau} \right)^{-1} = \lambda,$$

which provides an estimator for λ (independent on the estimation of the Hawkes process driving (N_t)).

5.4 The optimal trading problem

In this section we formalize the optimal control problem, defining the admissible trading strategies and the corresponding value function. The final part of the section is devoted to the dimension reduction of the HJB equation associated to the control problem, leading to a numerical low dimensional problem.

5.4.1 The agent strategy and the portfolio dynamic

We describe the dynamic of the processes involved in the optimal control problem and define formally an agent strategy. We assume that every trade is subjected to an absolute transaction cost $\varphi \geq 0$. We denote by (X_t) and (Y_t) the agent wealth and inventory associated to her portfolio. We can reconstruct their dynamic using this straightforward lemma:

LEMMA 5.2. *Let $L_\pm(dt)$ the simple point process associated to the level 1 trading strategy (counting the number of trades matching her level-1 limit orders) at the side $\pm I_t$. The wealth and the inventory associated to the agent portfolio are given by (here $(B_j(p))$ is an i.i.d. sequence of Bernoulli random variable of parameter p):*

$$X_t = X_0 + \sum_{\nu \in \pm} \int_0^t \int (\ell_\nu)_{t-} \left[\nu I_{t-} P_{t-} + (1-\varphi) \right] L_\nu(dt) + \sum_{j:\theta_j \leq t} \left(I_{\theta_{j-}} P_{\theta_{j-}} m_j - \varphi|m_j| \right) B_j(\delta),$$

$$Y_t = Y_0 + \sum_{\nu \in \pm} \int_0^t \int (\ell_\nu)_{t-} \left(\nu I_{t-} \right) L_\nu(dt) + \sum_{j:\theta_j \leq t} \left(I_{\theta_{j-}} m_j \right) B_j(\delta).$$

DEFINITION 5.14 (The admissible strategies). *We assume that the agent admissible controls are given by* $((\ell_t),(I_j)) \in \mathcal{A}$*, where*

⋄ $\ell_t := (\ell_+, \ell_-)_t$ *is a continuously controlled process, with*

$$(\ell_\pm)_t \in \mathbb{L} := \{0, \dots, L\},$$

predictable w.r.t. $\mathbb{F}_t$ *(the market filtration), where* $(\ell_{\pm I_t})_t$ *represents the agent level-1 position at time* t *on the ask* $(+)$ *and bid* $(-)$ *side;*

⋄ $I_j := (\theta_j, m_j)$ *is an impulsive sequence of level-0 limit orders such that* $K_t \le k_{\max}$*,* $t \ge 0$*, and*

$$m_j \in \{-m_{\max}, \dots, -m_{\max}\} := \mathbb{M},$$

where $m_{\max} \in \mathbb{N}$*;*

⋄ *the inventory* (Y_t) *satisfies*

$$\mathbb{Y} := \{-y_{\max}, \dots, +y_{\max}\} = -\mathbb{Y},$$

where $y_{\max} \in \mathbb{N} \cup \infty$*.*

5.4.2 The HJB equation

The agent's goal is to arbitrate frequent short-term patterns in the stock price, controlling her exposure to market risk. So, as in the market making case, the agent faces an inventory risk, i.e. she is adverse to keep large position for a long time.

DEFINITION 5.15 (Portfolio value). *The value of the agent portfolio is given by the wealth plus the agent position valued at the fair price, i.e.*

$$V_t := X_t + Y_t P_t. \tag{5.4.1}$$

The agent's target is to maximize her profile over all the admissible execution strategies $\mathcal{A}$, i.e.

$$\text{value function at t} = \max_{((\ell_t),(I_j)) \in \mathcal{A}} \mathbb{E}\left[V_{t_{\max}} - \eta \int_t^{t_{\max}} Y_{u-}^2 d\langle P \rangle_u \Big| \mathbb{F}_{t-}\right],$$

where

⋄ $t \le t_{\max} < \infty$ is the agent horizon,

⋄ $\eta > 0$ is called the agent risk aversion,

⋄ $\mathbb{F}$ is the market filtration, generated all the processes mentioned so far.

Notice that if the system is Markovian, as in our case, the value function is a deterministic function of the state variables taken at $t-$. **In order to ease computation, it is simpler but still meaningful to consider the same problem, but with a very specific random horizon**, i.e.:

DEFINITION 5.16. *The agent optimal control problem is given by*

$$\mathbf{u}_k(t, \tau, h, x, y, p, c, i) := \max_{\ell \in \mathcal{A}} \mathbb{E}\left[V_T - \eta \int_t^T Y_{u-}^2 d\langle P \rangle_u \Big| \mathbb{F}_{t-}\right], \tag{5.4.2}$$

where T *is the random time (see* Figure 5.10*)*

$$T := \inf\{u \ge t : \tau_u = \tau_{\max}\}, \tag{5.4.3}$$

and $\tau_{t-} = \tau \in [0, \tau_{\max}]$*,* $h_{t-} = h \ge \mu_{t-} \ge 0$*,* $X_{t-} = x \in \mathbb{Z}$*,* $Y_{t-} = y \in \mathbb{Y}$*,* $P_{t-} = p \in \mathbb{Z}$*,* $K_{t-} = k \in \{0, \dots k_{\max}\}$*,* $C_{t-} = c \in \mathbb{C}$*,* $I_{t-} = i \in \{-1, +1\}$*.*
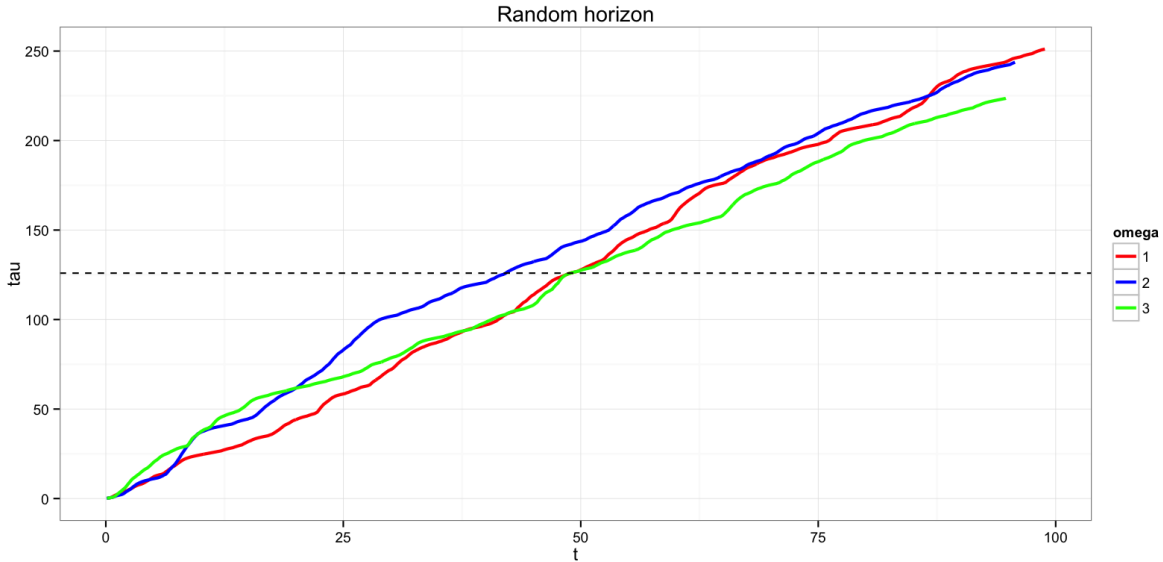
Figure 5.10: three simulated trajectories of the process τ_t, showing the random hitting time of the $\tau_{\max}$ barrier.

The following table summarize how different processes are seen in the two system, the real (dt) and the accelerated one $(d\tau)$.

clock	dt	$d\tau$
N_t	Hawkes	standard Poisson
level-1 arrival rate	$h_t\lambda$	λ
horizon	random T	deterministic $\tau_{\max}$

Here is the main result of the paper, concerning the characterization of the value function as viscosity solution of a system of ODE's. We use the notation convention that for a function usually denoted by $f = f(x_1, \ldots, x_n)$:

$$\Delta f(y_1, \ldots, y_n) := f(y_1, \ldots, y_n) - f(x_1, \ldots, x_n).$$

THEOREM 5.1. *The optimal control problem (5.4.2) is solved by*

$$\mathbf{u}_k(t, \tau, h, x, y, p, c, i) = x + yp + \mathbf{v}_k(\tau, iy, c),$$

where $\mathbf{v}_k(\tau, q, c)$ is the viscosity solution of

$$\min\left\{-\frac{\partial \mathbf{v}_k}{\partial \tau} - \mathcal{C}(\mathbf{v}_k), \mathcal{I}(\mathbf{v}_k)\right\} = 0, \qquad (\tau, q, c, k) \in [0, \tau_{\max}) \times \mathbb{Y} \times \mathbb{C} \times \{0, \ldots, k_{\max}\}, \quad (5.4.4)$$

$$\mathbf{v}_k(\tau_{\max},) = 0,$$

where

$$\mathcal{C}(\mathbf{v}_k) := \gamma^{(\eta)}(c,q) + \sum_{\nu\in\pm}\mathcal{J}_\nu(\mathbf{v}_k) + \mathcal{L}_\nu(\mathbf{v}_k),$$

$$\gamma^{(\eta)}(c,q) := \alpha(c)q - \eta q^2,$$

$$\mathcal{J}_\pm(\mathbf{v}_k) := \frac{1\pm\alpha(c)}{2}\Delta\mathbf{v}_0\left(\tau,\pm q,\pi\left(\pm c\right)\right),$$

$$\mathcal{L}_\pm(\mathbf{v}_k) := \frac{1\pm\alpha(c)}{2}\left(\max_{\ell\in\mathbb{L}:\,q\mp\ell\in\mathbb{Y}}\Delta\mathbf{v}_k\left(\tau,q\mp\ell,c\right) + \ell(1-\varphi)\right),$$

$$\mathcal{I}(\mathbf{v}_k) := \Delta\mathbf{v}_{k+1}(\tau,q,c) - \delta\left(\max_{m\in\mathbb{M}:\,q+m\in\mathbb{Y}}\Delta\mathbf{v}_{k+1}(\tau,q-m,c)-\varphi\,|m|\right),\quad k<k_{\max}$$

$$= \infty \qquad\qquad\qquad\qquad\qquad\qquad\qquad\qquad\qquad\qquad\qquad\qquad k = k_{\max}$$

Furthermore, optimal controls are given in feedback forms by

$$\hat{\ell}_\pm(\tau,q,c) := \underset{\ell\in\mathbb{L}:\,q\mp\ell\in\mathbb{Y}}{\arg\max}\ \Delta\mathbf{v}_k\left(\tau,q\mp\ell,c\right) + \ell(1-\varphi),$$

$$\hat{m}(\tau,q,c) := \underset{m\in\mathbb{M}:\,q+m\in\mathbb{Y}}{\arg\max}\ \Delta\mathbf{v}_{k+1}(\tau,q-m,c)-\varphi\,|m|,\quad k<k_{\max},$$

$$:= do\ nothing, \qquad\qquad\qquad\qquad\qquad\qquad k = k_{\max}$$

Proof. See Section 5.6.

$\square$

DEFINITION 5.17 (Strong inventory). *We define as strong inventory the state variable:*

$$q := iy.$$

Notice that the value function and the optimal control do not depend separately on the state variable i and y, on their product. This simplification (it induces a variable reduction) is due to the particular symmetry of the problem: the fair price and the limit order execution is described relatively to the process (I_t), as one can see in Definition 5.8 and Definition 5.13. In practice, when $q > 0$ (resp. $q < 0$), the agent inventory has the same (resp. opposite) sign of the last fair price jump.

The following simple lemma remarks a monotonicity property of the value function in the k state variable.

LEMMA 5.3. *The following inequalities hold:*

$$\mathbf{v}_k(\tau,q,c) \geq \mathbf{v}_{k+1}(\tau,q,c),\quad k<k_{\max}.$$

Proof. Assume that at time τ we have sent no pseudo market after the last fair price jumps again. Sending one of them of size $m = 0$, k increments and all the other state variables are unchanged. By the very definition of the value function:

$$x + yp + \mathbf{v}_k(\tau,q,c) \geq x + yp + \mathbf{v}_{k+1}(\tau,q,c).$$

Furthermore, since $\mathcal{I}(v) := \infty$ if $k = k_{\max}$, the optimal policy cannot send more than $k_{\max}$ pseudo market order per fair jump, concluding the proof.

$\square$

REMARK 5.4. *Notice that the value function $\mathbf{u}$ does not depend on the time variable t: this is a consequence of the random horizon defined at (5.4.3), which is reflected in the HJB equation by a t-independent terminal condition (which depends on τ instead). The proof of Theorem 5.1 is in fact based on the time change (5.2.4), thanks to which Hawkes processes become Poisson ones, and the random horizon becomes deterministic.*

The role of the stochastic intensity (h_t)

Looking at Theorem 5.1, one may wonder: where is the stochastic intensity (h_t) gone? We notice that neither the value function, nor the optimal controls depend on this state variable, while estimating the parameters of the Hawkes process can be even more expensive that computing the value function itself! Such an effort is unfortunately still necessary, since the role of the stochastic intensity is hidden behind the random horizon T in (5.4.3): $\langle P \rangle_t$ is indeed predictable w.r.t. to the agent filtration, but only once the parameters determining its dynamic are known. Long story short, the estimation of the Hawkes process N_t is necessary if and only if we want to to know when to know what the current τ is.

Luckily, we observe numerically that the optimal policy stabilizes after few backward steps. So, rather than a time dependent optimal policy, we can use its long-horizon version all over the trading day, losing more and more the optimal behaviour as we get closer to horizon. Using this recipe, the estimation of the Hawkes process parameters is less relevant under the performance point of view, though it is a good advice to perform it to validate the model assumptions.

The scaling property

The next proposition is particularly useful when the agent is able to in the position of trading a large amount of stocks. For assets like the DAX, because of the huge size of the contract (≈ 6 contracts for 1M EUR), a typical order consists in some unit, while for smaller assets like the EUROSTOXX ($\approx 30 - 40$ contracts for 1M EUR), a typical order has much bigger size. Since computing the optimal policy means numerically maximizing over all the possible order sizes, for contract having small face value we can construct a *quantum* policy, where all the orders are multiple of a certain minimal size $\aleph$, and the inventory lives in $\aleph\mathbb{Y}$. This will allow the agent to handle big inventory without maximizing over all the possible limit order sizes.

DEFINITION 5.18. *We call the $\aleph$-version of the stochastic optimal control of Definition 5.16 the problem where all the order sizes are a multiplied by $\aleph$, and the inventory process starts (and then lives) in $\aleph\mathbb{Y}$.*

PROPOSITION 5.1 (Scaling property for the quantum strategy). *Let $v^{(N,\eta)}$ be the viscosity solution of (5.4.4) associated to the $\aleph$-version of the optimal control problem of Definition 5.16, with risk aversion η. Then*

$$v_k^{(N,\eta)}(\tau, q, c) = \aleph v_k^{(1,\aleph\eta)}(\tau, q/\aleph, c), \quad q \in \aleph\mathbb{Y}.$$

Proof. See Section 5.7.

$\square$

5.5   Numerical results

In this section we illustrate numerical result concerning the optimal trading problem described in the previous section. We show both the numerical solution of the HJB equation (value function and optimal control) and perform a Monte Carlo simulation in order to obtain both the performance distribution (and its Sharpe ratio) and a stress scenario where the price does not behave as expected.

REMARK 5.5. *Notice that (5.4.4) is a system of variational ODE's, for which we can provide an explicit Euler scheme with no CFL condition, which is computationally parsimonious w.r.t. to an implicit scheme since system resolution is needed. For our parameter choice, our Java solver obtains both value function and optimal controls in less than a second.*

Thanks to numerical methods, we observe that the optimal policy stabilizes after few backward steps to a time-independent strategy. So, rather than the real optimal policy, we test only its long-run version all over the trading day. This has 2 advantages.

i) Using this recipe, the estimation of the Hawkes process parameters is less relevant under the performance point of view since knowing the current value of the process τ_t does not affect the trading strategy. Anyway, it is a good advice to perform the tick times model estimation to validate the model assumptions.

ii) No time interpolation is necessary: since the trading strategy is computed numerically, a real time application would require an interpolation over the points of the grid where the optimal solution has been computed: using the long-run version this problem does not occur.

Monte Carlo simulations must not be interpreted only as a tool to test and validate the numerical solution provided by the Euler scheme. Thanks to simulations, we can access the performance profile, i.e. its distribution at maturity rather the its mean only, but mostly important we can test any kind of strategy, despite its optimality. In this case, solving numerically the HJB equation leads us to an optimal strategy: its long-run version is not optimal anymore, but it is simpler to implement and understand, and it is likely to perform well. Monte Carlo simulations show that this intuition is correct.

The optimal controls

Figure 5.11 shows the both the continuous (level-1) and impulsive (level-0) policy, on the buy and on the sell side for the slice $k = \tau = 0$ (i.e. immediately after a fair price jump, and at the beginning of the trading day). We find the inventory on the x-axis and the current context on y-axis: a colored circle means that for the system occupying the state (q, c), the agent sends an order. The side convention is for $i = +$: in the opposite case the sell and the buy side are exchanged. Limit orders are of unitary size, i.e. $L = 1$, and $k_{\max} = 1$.

◇ Comparing the upper side with the lower one, we immediately notice that the agent is more active on the level-1 limit order, since it is almost always optimal to send a passive limit order one tick away from the fair price. Level-1 limit orders lead to a big potential gain with few risk. On the contrary, impulsive order are widely used for large values of $|q|$, in order to bring the agent inventory back to zero with few uncertainty on the execution. Furthermore, notice that the level-0 strategy is much more sensitive to the context variable c: this is due to the fact that impulsive order are able to change position quickly and allow the agent to follow the market, rather than being rewarded for providing liquidity, which is rather market independent instead.

◇ Comparing the left side with the right one, we notice an asymmetry: the agent tends to be more active on the buy side. In particular, for specify contexts, buying (for i= + , sell otherwise) is optimal both on level-0 and the level-1 even when q is already positive. This is due to the micro-structural trends emerging after the VLMC estimation (see Figure 5.7), that leads the agent to exploit her anticipation on the market to align her position to the market direction.

We do not show the result, for $k > 0$, since on the level-1 limit order no big changes emerge, while no level-0 limit orders are allowed.

The value function

Figure 5.12 and Figure 5.13 illustrate the behaviour of the value function for various values of the transaction costs (φ) and risk aversion (η). We plot

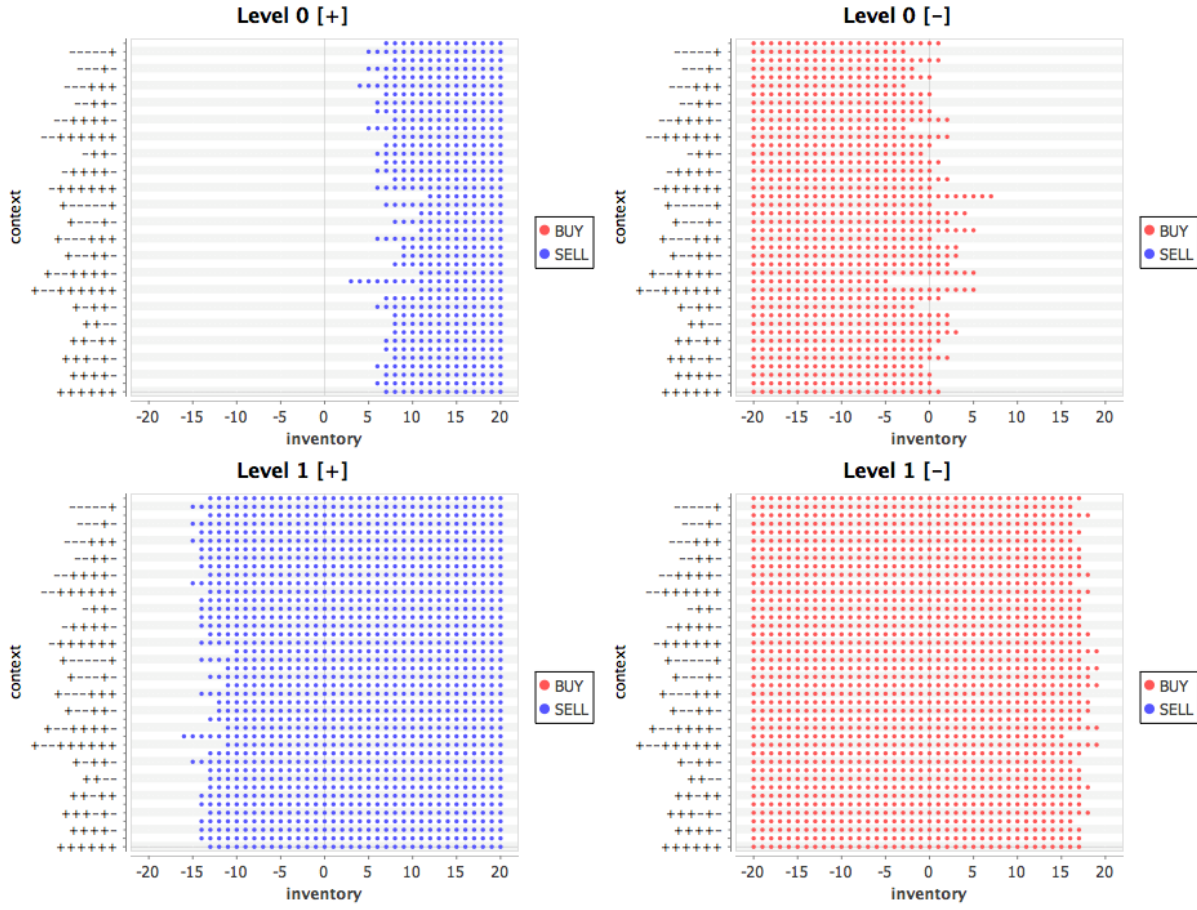$$q \mapsto \frac{1}{\tau_{\max}} \sum_{c \in \mathbb{C}} v(0, q, c) \, \mathbb{Q}^*(c), \, ,$$

Figure 5.11: optimal policy for $i = +$ and $k = \tau = 0$.

where $\mathbb{Q}^*$ is the stationary probability of the VLMC process seen as a Markov chain on its context set $\mathbb{C}$. Notice that:

⋄ the value function is concave in the q, since risk aversion penalizes large inventories;

⋄ incrementing the transaction costs penalizes the value function, reducing the agent performance;

⋄ incrementing the risk aversion increases the concavity of the value function in the variable q (strong inventory).

The no risk aversion case

We expect that reducing the η to 0, the value function has no concavity in q: this intuition is correct and can be formalized. Taking no inventory constraint, i.e. setting $\mathbb{Y} = \mathbb{Z}$, and assuming the polynomial growth of the value function, we can characterize the value function as an affine function on the state variable q. Using the ansatz

$$\mathbf{v}_k(\tau, q, c) = a(\tau, c)q + b_k(\tau, c),$$

(5.4.4) becomes

$$\min\left\{-\frac{\partial \mathbf{v}_k}{\partial \tau} - \mathcal{C}(\mathbf{v}_k), \mathcal{I}(\mathbf{v}_k)\right\} = 0, \quad (\tau, c, k) \in [0, \tau_{\max}) \times \mathbb{Y} \times \mathbb{C} \times \{0, \ldots, k_{\max}\}, \qquad (5.5.1)$$

$$\mathbf{v}_k(\tau_{\max},) = 0,$$

where

$$\mathcal{C}(\mathbf{v}_k) := \gamma^{(0)}(c, q) + \sum_{\nu \in \pm} \mathcal{J}_\nu(\mathbf{v}_k) + \mathcal{L}_\nu(\mathbf{v}_k) \,,$$

$$\gamma^{(0)}(c, q) := \alpha(c)q \,,$$

$$\mathcal{J}_\pm(\mathbf{v}_k) := \frac{1 \pm \alpha(c)}{2} \left(q \left(\nu a(\tau, \pi(\nu c)) - a(\tau, c) \right) \right) + \Delta b_0 \left(\tau, \pi(\pm c) \right) \,,$$

$$\mathcal{L}_\pm(\mathbf{v}_k) := \frac{1 \pm \alpha(c)}{2} \left(\max_{\ell : \ell \leq L} \ell \left(\nu a(\tau, c) + 1 - \varphi \right) \right) \,,$$

$$= \frac{1 \pm \alpha(c)}{2} L \left(\nu a(\tau, c) + 1 - \varphi \right)_+ \,,$$

$$\mathcal{I}(\mathbf{v}_k) := \Delta b_{k+1}(\tau, c) - \delta \max_{m \in \mathbb{M}} \left(-m a(\tau, c) - \varphi |m| \right) \,, \qquad k < k_{\max} \,,$$

$$:= \infty \,, \qquad k = k_{\max} \,.$$

Choosing $a(\tau, c)$ solution of

$$\frac{\partial a}{\partial \tau} - \alpha(c) - \alpha(c)a(\tau, \pi(\nu c)) + a(\tau, c) = 0 \,, \quad (\tau, c) \in [0, \tau_{\max}) \times \mathbb{C} \,, \qquad (5.5.2)$$

$$a(\tau_{\max},) = 0 \,, \qquad c \in \mathbb{C} \,,$$

the coefficient multiplying q in (5.5.1) disappear. Furthermore, we have

LEMMA 5.4. *The function $a(\tau, c)$ has the probabilistic representation*

$$a(\tau, c) = \mathbb{E}\left[P_T \big| \tau_{t-} = \tau, P_{t-} = 0, C_{t-} = c, I_{t-} = + \right] \,. \qquad (5.5.3)$$

Proof. Notice that, by the Feymann-Kac representation theorem,

$$G(t, \tau, h, p, c, i) := \mathbb{E}\left[P_T \big| \tau_{t-} = \tau, h_{t-} = h, P_{t-} = p, C_{t-} = c, I_{t-} = i \right]$$

solves

$$-\frac{\partial G}{\partial t} - h\frac{\partial G}{\partial \tau} - \beta(\mu_t - h)\frac{\partial G}{\partial h} - h \sum_{\nu \in \pm} \frac{1 + \nu\alpha(c)}{2} \Delta G(t, \tau, h + \alpha, p + \nu i, \pi(\nu c), \nu i) = 0 \,,$$

$$G(\tau_{\max},) = p \,,$$

Using the ansatz $G(t, \tau, h, p, c, i) = p + i\tilde{a}(\tau, c)$ and after tedious but straightforward calculations, one checks that $\tilde{a}(\tau, c)$ verifies (5.5.2), concluding the proof.

$\square$

Going back to value function characterization, the equation describing b_k has become (notice that it depends on $a(\tau, c)$):

$$\min \left\{ -\frac{\partial b_k}{\partial \tau} - \mathcal{C}^0(b_k), \mathcal{I}^0(b_k) \right\} = 0 \,, \qquad (\tau, c, k) \in [0, \tau_{\max}) \times \mathbb{C} \times \{0, \dots, k_{\max}\} \,, \qquad (5.5.4)$$

$$b_k(\tau_{\max},) = 0 \,,$$

where

$$\mathcal{C}^0(b_k) := \sum_{\nu \in \pm} \mathcal{J}^0_\nu(b_k) + \mathcal{L}^0_\nu(b_k) \,,$$

$$\mathcal{J}^0_\pm(b_k) := \frac{1 \pm \alpha(c)}{2} \Delta b_0 \left(\tau, \pi\left(\pm c\right)\right) \,,$$

$$\mathcal{L}^0_\pm(b_k) := \frac{1 \pm \alpha(c)}{2} L\left(\nu a(\tau, c) + 1 - \varphi\right)_+ \,,$$

$$\mathcal{I}^0(b_k) := \Delta b_{k+1}(\tau, c) - \delta \max_{m \in \mathbb{M}}\left(-ma(\tau, c) - \varphi\left|m\right|\right) \,, \quad k < k_{\max} \,,$$

$$:= \infty \,, \qquad\qquad\qquad\qquad\qquad k = k_{\max} \,.$$

We have proved that:

PROPOSITION 5.2. *In the special case when* $y_{\max} = \infty$ *(no inventory constraint) and* $\eta = 0$*, and if* $\mathbf{v}_k(\tau, q, c)$ *has polynomial growth, then*

$$\mathbf{v}_k(\tau, q, c) = a(\tau, c)q + b_k(\tau, c) \,,$$

where $a(\tau, c)$ *and* $b_k(\tau, c)$ *are given by (5.5.2) (or (5.5.3)) and (5.5.4). Optimal controls are given in feedback form by*

$$\hat{m}_k(\tau, c) = \arg\max_{m \in \mathbb{M}} -ma(\tau, c) - \varphi\left|m\right| \,,$$

$$\hat{\ell}_\pm(\tau, c) = L\mathbb{1}\{\pm a(\tau, c) + 1 - \varphi > 0\} \,.$$

In particular, $\mathbf{v}_k$ *is an affine function of* q *with no concavity.*

Monte Carlo simulations

Since we observe that, after few backward steps, the optimal policy stabilizes to a time asymptotic regime (a contribution to a formal proof is welcome), in these Monte Carlo simulations we inject the optimal policy for $\tau = 0$, calculated for $\tau_{\max} >> 0$. As for the initial condition, we took:

⋄ $k = 0$ (we assume that the price has just jumped),

⋄ i distributed according to $\delta_{1/2} + \delta_{-1/2}$,

⋄ c distributed according to the stationary distribution of the VLMC (seen as a Markov chain on its context set $\mathbb{C}$).

We investigate how risk aversion impacts the trading strategy[5]

⋄ Figure 5.14 shows the inventory of different agents: for high levels of risk aversion, the inventory reverts quickly to zero, and oscillates in small range, while for no risk aversion the inventory obeys only to its absolute constraint ($|Y_t| \leq y_{\max}$), which is a data of the problem.

⋄ Figure 5.15 shows the cumulative performance of the strategy: risk aversion penalizes the mean performance decreases, even though its variance is drastically reduced, as shown by Figure 5.16.

We claim an information advantage deriving from the VLMC model for (U_n) w.r.t. to a myopic agent that sees the process as a simple random walk (in which case (J_n) is a Markov chain, as in [36]).

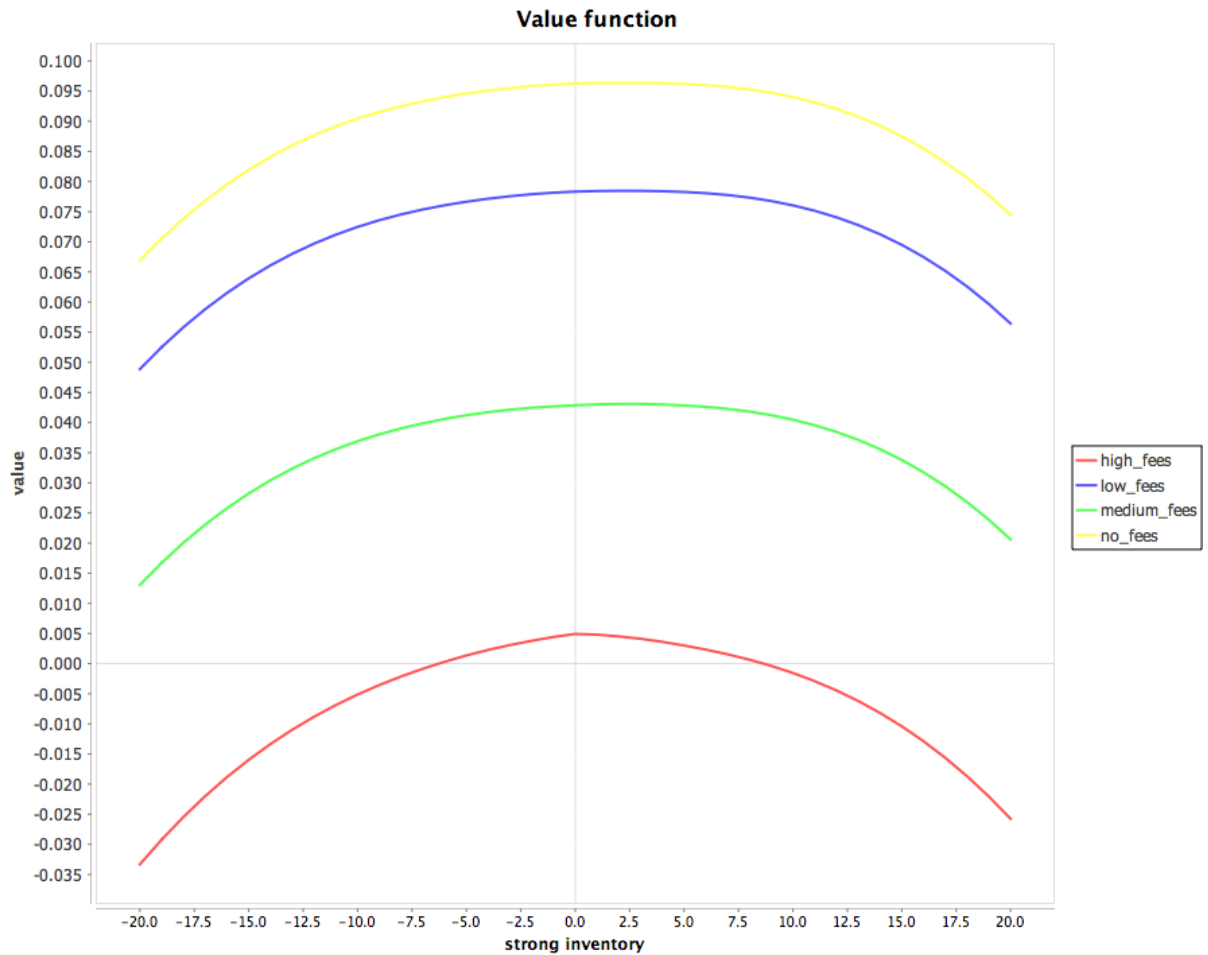[5]Low, medium and high risk aversions correspond to 0.0001, 0.001 and 0.01.

Figure 5.12: the computed value function for different levels of transaction cost.

⋄ Figure 5.17 shows the performance of a portfolio where the underlying asset is a VLMC: the first agent uses an optimal strategy based on this information, while the second one estimates the process as a simple random walk, and deduces her policy consequently. We notice that the informed agent, whose right tail is fatter, outperforms the previous one in terms of mean outcome.

⋄ Figure 5.18 shows a stress test where the fair price is driven by a random walk having the same stationary distribution of the VLMC process (seen as a Markov chain): the first agent is aware of the price dynamic, while the second thinks the process is VLMC. The impact of the model mis-specification is rather low compared to the information advantage previously described, which makes this approach rather robust.

Conclusion and further developments.

In this paper we essentially wanted to show how to combine long memory models to provide an efficient description of the stock price dynamic without precluding the development of an optimal trading applications. Because of the modeling of the agent execution, our choice has fallen on the fair price. Anyway, following the same idea, the model can be applied to the mid-price itself, possibly introducing dependence between tick times and marks.

For further developments, an application to stock liquidation is in program, but this needs to formalize the notion of impulsive market impact in these models keeping the global dimension within reasonable bounds.
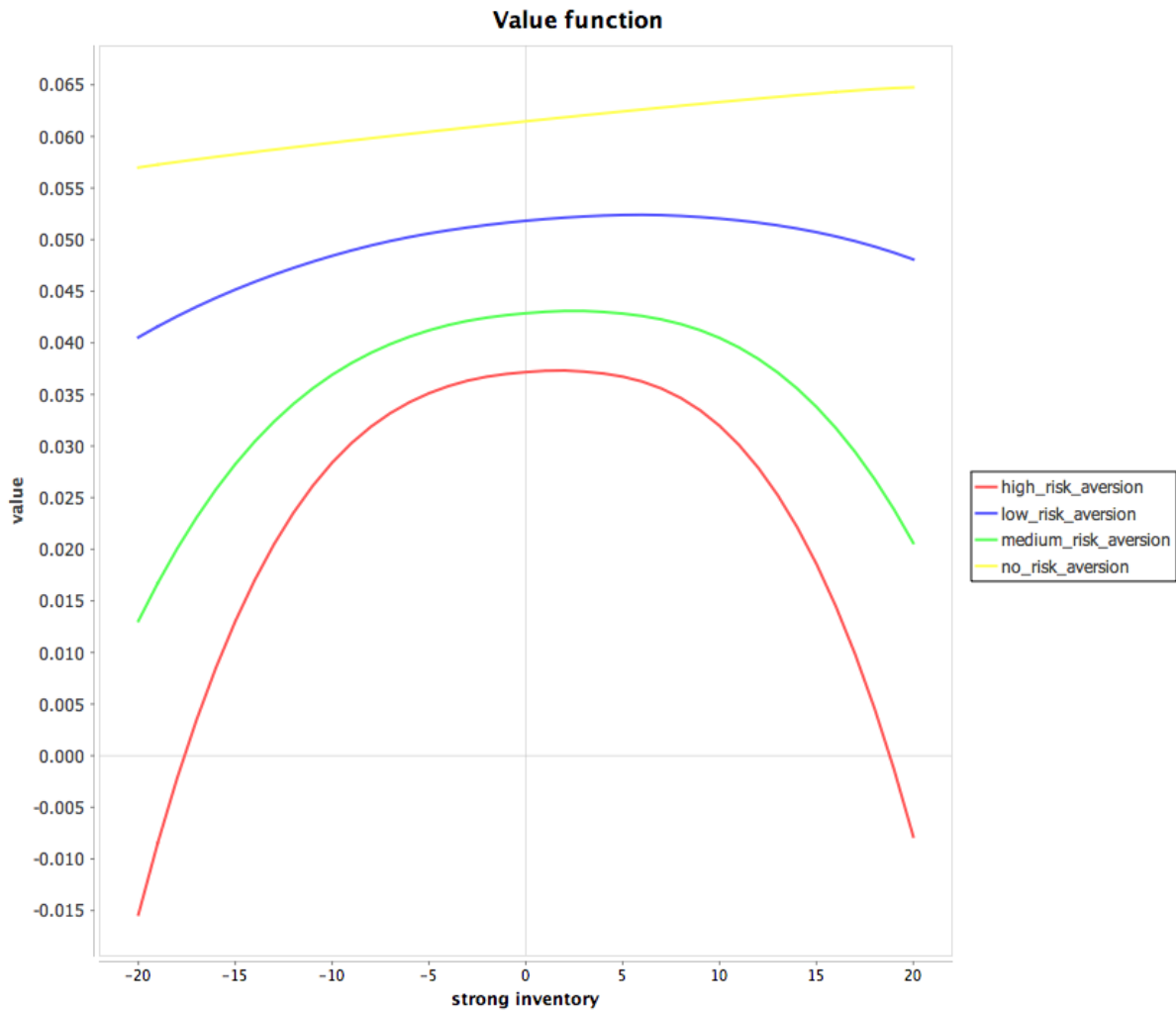
Figure 5.13: the computed value function for different levels of risk aversion.
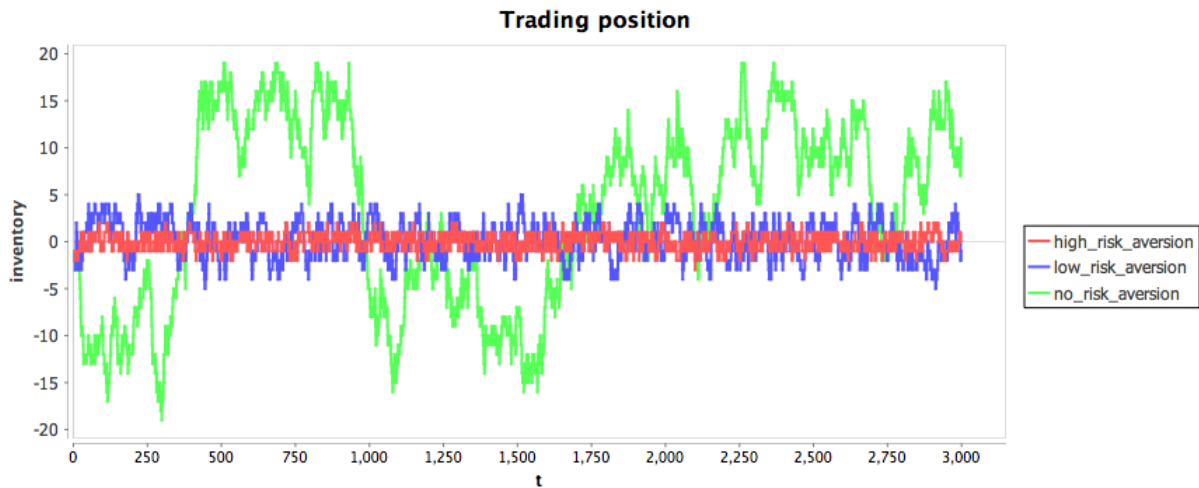

Figure 5.14: simulated evolution of the agent inventory for different risk aversions.

5.6   Appendix: proof of Theorem 5.1

Before giving the main result, we determine an upper and lower bound for the value function.
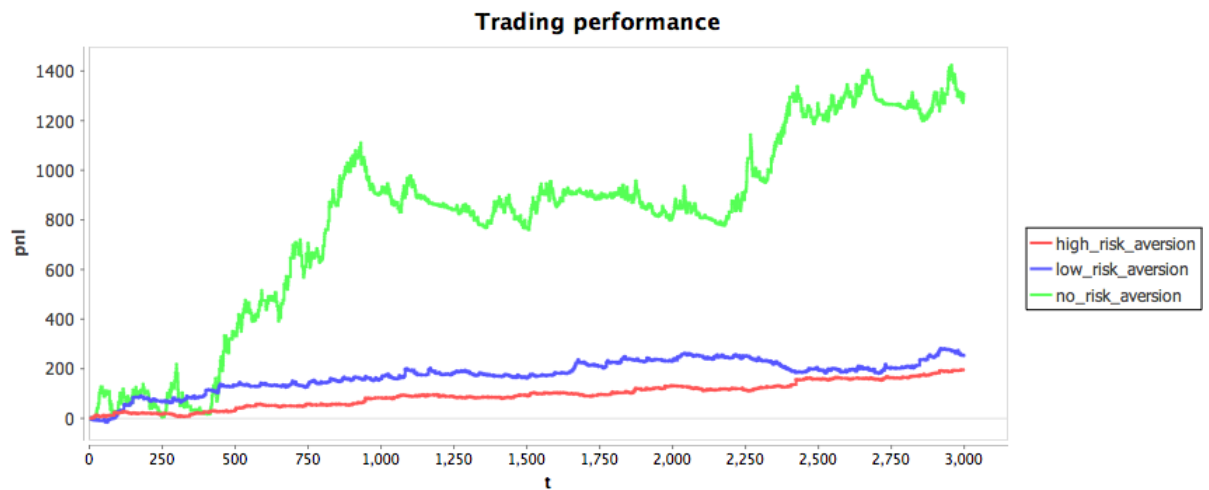
Figure 5.15: simulated evolution of the trading performance for different risk aversions.
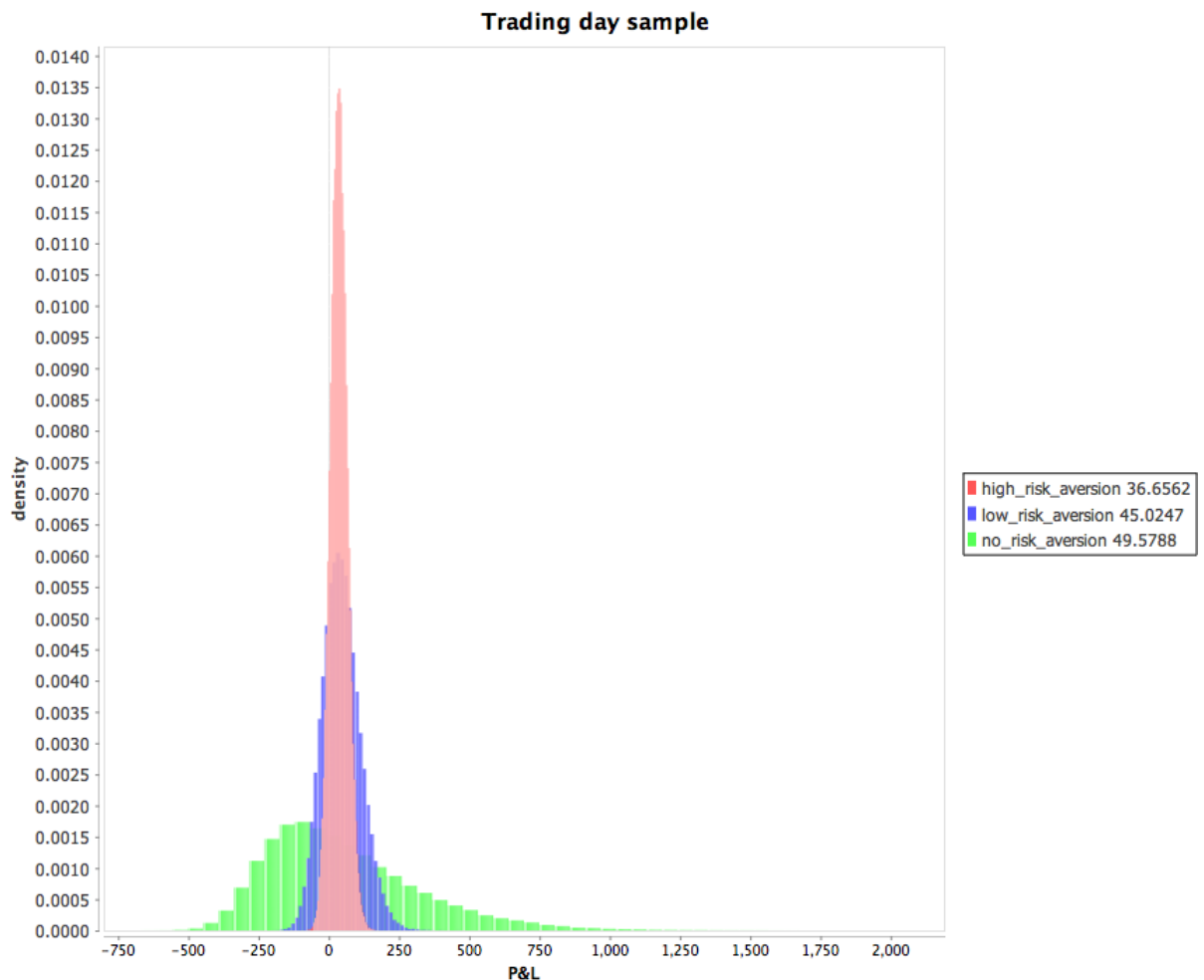

Figure 5.16: simulated histogram of the daily trading performance for different risk aversions.

Bounds of the value function

The first thing we to prove is that the value function is bounded by a function with polynomial growth in its arguments: this guarantees that the value is the unique viscosity solution of the HJB equation (with polynomial growth) associated to the optimal control problem (5.4.2).
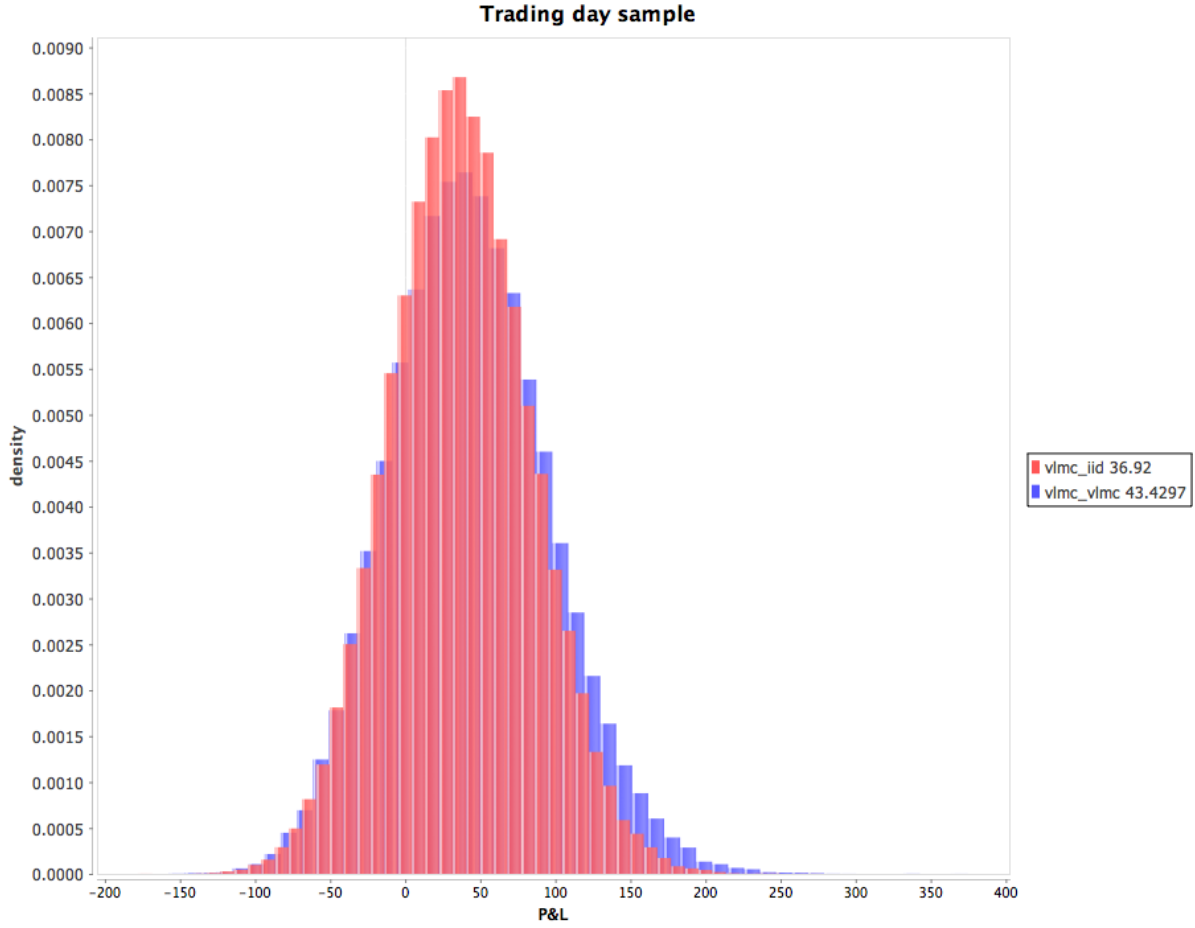
Figure 5.17: optimal policy and information advantage. The figure shows the simulation of different PnL distributions (given by the portfolio valued at the mid-price, with no inventory penalization) when (U_k) is driven by the VLMC model, and the first agent (red) estimates it as an i.i.d. sequence, while the second (blue) knows its real dynamic. The right blue tail exceeding the red one represents the information advantage due to the knowledge of the effective price dynamic.

PROPOSITION 5.3. *For the control problem of* Definition 5.16*:*

$$\mathbf{u}_k(t, \tau, h, x, y, p, c, i) \leq \left(\lambda L + \frac{1}{4\eta} \right) (\tau_{\max} - \tau).$$

Proof. The portfolio process V defined at (5.4.1) starts at $x + yp$ (which has polynomial growth), and its dynamic can be written as

$$dV_t = (dX_t + P_{t-}dY_t) + (Y_{t-}dP_t) + d\langle Y, P \rangle_t,$$
$$= (dX_t + P_{t-}dY_t) + (Y_{t-}dP_t),$$

where $d\langle Y, P \rangle_t = 0$ a.s. for all t since Y_t and P_t have no jumps in common. This leads to

$$V_t - \int_t^T Q_{u-}^2 d\langle P \rangle_u = x + yp + Z_t^1 + Z_t^2,$$

$$Z_t^1 := \int_0^t dX_u + P_{u-}dY_u,$$

$$Z_t^2 := \int_0^t Y_{u-}dP_u - \eta Y_{u-}^2 d\langle P \rangle_u.$$

It is thus enough to bound $\mathbb{E}[Z_T^1|\mathbb{F}_{t-}]$ and $\mathbb{E}[Z_T^2|\mathbb{F}_{t-}]$ uniformly in the strategy to achieve our goal. These bounds are given by Lemma 5.6 and Lemma 5.7.
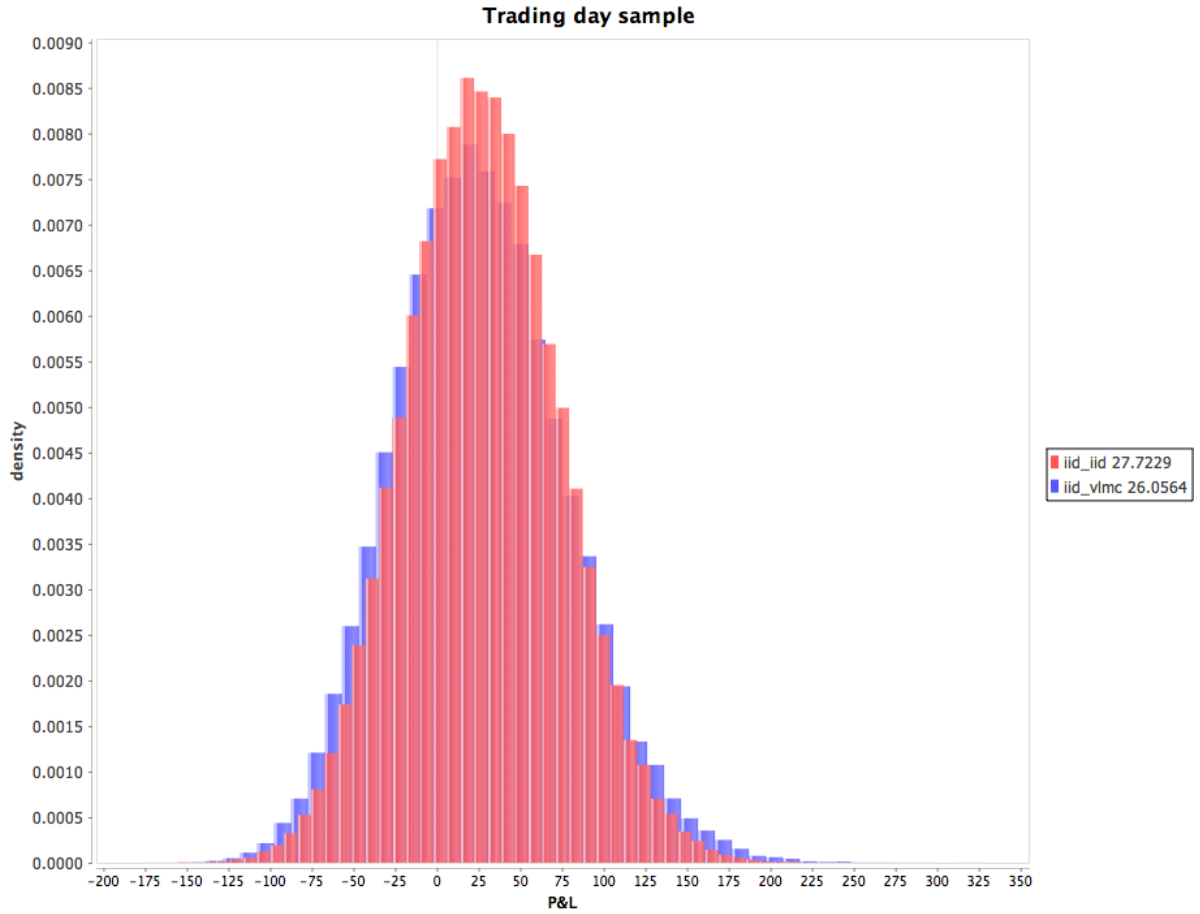
Figure 5.18: stress test against model mis-specification and robustness of the optimal policy. The figure shows the different simulated PnL distributions (given by the portfolio valued at the mid-price, with no inventory penalization) when (U_k) is driven by an i.i.d sequence, and the first agent (red) knows the exact dynamic, while the second one (blue) sees (U_k) as a VLMC process with the same stationary mean value of the real i.i.d. sequence underlying the stock price. The figure shows, that, despite the model error, the second agent is not particularly penalised by her mistake.

$\square$

LEMMA 5.5. *Let (N_t) (resp. $(L_t = L_t^+ + L_t^-)$) be the process counting the number of jumps of the fair price (resp. the number of times a level-1 limit order is executed). Then*

$$\mathbb{E}[N_T|\mathbb{F}_{t-}] = \tau_{\max} - \tau \,,$$
$$\mathbb{E}[L_T|\mathbb{F}_{t-}] = \lambda(\tau_{\max} - \tau) \,.$$

Proof. By (5.4.3):

$$\mathbb{E}[N_T|\mathbb{F}_{t-}] = \mathbb{E}\left[\int_t^T h_u du|\mathbb{F}_{t-}\right] = \tau_{\max} - \tau \,,$$
$$\mathbb{E}[L_T|\mathbb{F}_{t-}] = \lambda \mathbb{E}[N_T|\mathbb{F}_{t-}] = \lambda(\tau_{\max} - \tau) \,.$$

$\square$

LEMMA 5.6. *For the control problem of Definition 5.16:*

$$\mathbb{E}[Z_T^1|\mathbb{F}_{t-}] \le \lambda L(\tau_{\max} - \tau) \,.$$

Proof. Z_t^1 is a piecewise constant process jumping when the inventory does, and in particular of $-\varphi$ times the absolute size of the executed inventory plus an extra tick for each lot traded at

level-1. This process represents the gain and the loss due to the execution only. Z_t^1 can jump upwards of at most one tick for every level-1 limit order executed, while it has non-positive jumps for level-0 executions. Since the agent is allowed to place on both sides limit orders of size bounded by $L < \infty$ and level-1 execution arrives (independently on their side) at rate λ in the time changed dynamic,

$$\mathbb{E}\left[Z_T^1|\mathbb{F}_{t-}\right] \leq L\mathbb{E}\left[L_T|\mathbb{F}_{t-}\right] = \lambda L(\tau_{\max} - \tau),$$

which ends the proof.

□

LEMMA 5.7. *For the control problem of* Definition 5.16:

$$\mathbb{E}[Z_T^2|\mathbb{F}_{t-}] \leq \frac{1}{4\eta}(\tau_{\max} - \tau).$$

Proof. Z_t^2 is a piecewise constant process jumping when either the inventory or the stock price do. This process represents the gain due to the pattern anticipation. For $\eta > 0$

$$\begin{aligned}
\mathbb{E}\left[Z_T^2|\mathbb{F}_{t-}\right] &= \mathbb{E}\left[\int_t^T Y_{u-}dP_u - \eta Y_{u-}^2 d\langle P\rangle_u|\mathbb{F}_{t-}\right] \\
&\leq \mathbb{E}\left[\int_t^T |Y_{u-}|d\langle P\rangle_u - \eta Y_{u-}^2 d\langle P\rangle_u|\mathbb{F}_{t-}\right] \\
&\leq \mathbb{E}\left[\int_t^T \max_{Y_{u-}}(|Y_{u-}| - \eta Y_{u-}^2)\, d\langle P\rangle_u|\mathbb{F}_{t-}\right] \\
&\leq \frac{1}{4\eta}\mathbb{E}\left[\int_t^T d\langle P\rangle_u|\mathbb{F}_{t-}\right] = \frac{1}{4\eta}(\tau_{\max} - \tau),
\end{aligned}$$

which ends the proof. Notice that $\lim_{\eta \to 0+} \frac{1}{4\eta} = \infty$.

□

PROPOSITION 5.4. *For the control problem of* Definition 5.16:

$$\mathbf{u}_k(t, \tau, h, x, y, p, c, i) \geq x + yp - \left(|y| - \eta y^2\right)(\tau_{\max} - \tau).$$

Proof. For the lower bound of the value function, is in enough to bound the expected value of a single strategy. Canceling all the living limit orders and holding the inventory until the random horizon, we obtain

$$V_T = x + yP_T,$$
$$R_{t,T} = -\eta y^2 \int_t^T d\langle P\rangle_u.$$

We conclude by taking expectations:

$$\mathbb{E}[V_T|\mathbb{F}_{t-}] = x + yp + \mathbb{E}[P_T - p|\mathbb{F}_{t-}] \geq x + yp - |y|(\tau_{\max} - \tau),$$
$$\mathbb{E}[R_{t,T}|\mathbb{F}_{t-}] = -\eta y^2(\tau_{\max} - \tau).$$

□

Proof of Theorem 5.1

Thanks to Proposition 5.4 and Proposition 5.3, guaranteeing the problem is well-posed and that the value function grows sub-polynomially, we can characterize the value function as the unique viscosity solution (with polynomial growth) of the HJB equation

$$\min\left\{-\frac{\partial \mathbf{v}_k}{\partial t} - h\frac{\partial \mathbf{v}_k}{\partial \tau} - \mathcal{C}(\mathbf{v}_k), \mathcal{I}(\mathbf{v}_k)\right\} = 0\,, \qquad\qquad 0 \leq \tau < \tau_{\max}\,, \qquad\qquad (5.6.1)$$

$$\mathbf{v}_k(\tau_{\max},) = 0\,,$$

where

$$\mathcal{C}(\mathbf{v}_k) := \sum_{\nu \in \pm} \mathcal{J}_\nu^0(\mathbf{v}_k) + \mathcal{L}_\nu^0(\mathbf{v}_k)\,,$$

$$\mathcal{J}_\pm^0(\mathbf{v}_k) := \beta(\mu_t - h)\frac{\partial \mathbf{v}_k}{\partial h} + h\left(\frac{1\pm\alpha(c)}{2}\right)\Delta\mathbf{v}_0\left(t, \tau, h + \alpha, x, y, p \pm i, \pi\left(\pm c\right), \pm i\right)\,,$$

$$\mathcal{L}_\pm^0(\mathbf{v}_k) := \lambda h\left(\frac{1\pm\alpha(c)}{2}\right)\max_{\ell_\pm : y\pm i\ell_\pm \in \mathbb{Y}}\Delta\mathbf{v}_k\left(t, \tau, h, x \pm ip\ell - |i\ell|\varphi + |i\ell|, y \mp i\ell, p, c, i\right)\,,$$

$$\mathcal{I}(\mathbf{v}_k) := \max_{m : y + im \in \mathbb{Y}} \delta\mathbf{v}_{k+1}(t, \tau, h, x + ipm - \varphi\left|m\right|, y - im, p, c) + (1 - \delta)\mathbf{v}_{k+1}\,, \qquad k < k_{\max}\,,$$

$$:= \infty\,, \qquad\qquad\qquad\qquad\qquad\qquad\qquad\qquad k = k_{\max}\,.$$

Notice that:

⋄ $\mathcal{J}_\pm^0(\phi)$ is the operator associated to the jump of the fair price: the sign $\pm$ corresponds to a jump in the same (+) or the opposite (-) sign of the state variable i;

⋄ $\mathcal{L}_\pm^0(\phi)$ is the operator associated to activity at level-1: the sign $\pm$ corresponds to an execution of a limit order on the side i, where the side $= +$ (resp. side $= -$) is for the best ask (resp. bid);

⋄ $\mathcal{I}(\phi)$ is the operator associated to the impulsive activity (pseudo market orders): an impulse of size m correspond to a pseudo market order of volume $|m|$ of type $i\mathrm{sgn}(m)$, where type $= +$ (resp. type $= -$) is for sell (resp. buy) orders. Notice that $\mathcal{I}(\phi) = \infty$ if $k = k_{\max}$ guarantees the strategy admissibility: it is always suboptimal to send an impulse if the agent has already sent $k_{\max}$ after the last fair price jump.

Using the ansatz

$$\mathbf{u}_k(t, \tau, h, x, y, p, c, i) := x + yp + \mathbf{v}_k(\tau, q = iy, c)\,,\,,$$

we obtain

$$-\frac{\partial \mathbf{u}_k}{\partial t} = 0\,,$$

$$\mathcal{J}_\pm^0(\mathbf{u}_k) = h\left(\frac{1\pm\alpha(c)}{2}\right)\left(\mathbf{v}_0\left(\tau, \pm q, \pi\left(\pm c\right)\right) \pm q\right) := \lambda h\left(\mathcal{J}_\pm(\mathbf{v}_k) \pm q\right)\,,$$

$$\mathcal{L}_\pm^0(\mathbf{u}_k) = \lambda h\left(\frac{1\pm\alpha(c)}{2}\right)\max_{\ell_\pm : q\pm\ell^+ \in \mathbb{Y}}\mathbf{v}_k\left(\tau, q \mp \ell, c\right) + \ell(1 - \varphi) := h\mathcal{L}_\pm(\mathbf{v}_k)\,,$$

$$\mathcal{I}(\mathbf{u}_k) = \Delta\mathbf{v}_{k+1}(\tau, q, c) - \delta\max_{m : q+m \in \mathbb{Y}}\left(\Delta\mathbf{v}_{k+1}(\tau, q - m, c) - \varphi\left|m\right|\right) := \mathcal{I}(\mathbf{v}_k)\,, \quad k < k_{\max}\,,$$

$$:= \infty := \mathcal{I}(\mathbf{v}_k)\,, \qquad\qquad\qquad\qquad\qquad\qquad\qquad k = k_{\max}.$$

The HJB equation (5.6.1) becomes

$$\min\left\{h\left(-\frac{\partial \mathbf{v}_k}{\partial \tau} - \mathcal{C}(\mathbf{v}_k)\right), \mathcal{I}(\mathbf{v}_k)\right\} = 0, \qquad (5.6.2)$$

$$\mathbf{v}_k(\tau_{\max},) = 0,$$

where

$$\mathcal{C}(\mathbf{v}_k) := \alpha(c)q - \eta q^2 + \sum_{\nu \in \pm} \mathcal{J}_\nu(\mathbf{v}_k) + \mathcal{L}_\nu(\mathbf{v}_k) := \gamma^{(\eta)}(q,c) + \sum_{\nu \in \pm} \mathcal{J}_\nu(\mathbf{v}_k) + \mathcal{L}_\nu(\mathbf{v}_k)..$$

Since $h \geq \mu_t > 0$, we can divide by h, and conclude the proof.

REMARK 5.6. *Notice that we have simplified (5.6.1) introducing the extra state variable τ, and dividing by h at (5.6.2). For this proof to work, two crucial assumptions are necessary:*

  i) *the trade intensity on the level-1 is proportional to h (see (5.4.3)),*

  ii) *the terminal condition does not depend on t, which explains the choice of the random horizon rather than the standard deterministic one (see (5.3.1)).*

5.7   Appendix: proof of Proposition 5.1

The proof is somehow intuitive and straightforward, but handing notations needs some care. We start from the very equation and prove the result by a simple variable change. We know that $\mathbf{v}_k^{(N,\eta)}(\tau,q,c)$ satisfies (5.4.4), where $\mathcal{C}, \gamma^{(\eta)}$ and $\mathcal{J}$ are unchanged, while (following the notation of Theorem 5.1),

$$\mathcal{L}_\pm(\mathbf{v}_k) = \lambda\left(\frac{1 \pm \alpha(c)}{2}\right)\max_{\ell_\pm : q \pm N\ell^+ \in \mathbb{Y}} \mathbf{v}_k\left(\tau, q \mp \aleph\ell, c\right) + \aleph\ell(1 - \varphi),$$

$$\mathcal{I}(\mathbf{v}_k) := \max_{m \,:\, q + \aleph m \in \mathbb{Y}} \delta\left(V_{n+1}(\tau, q - \aleph m, c) - \varphi|m|\right) + (1-\delta)V_{n+1}(\tau,q,c) := \mathcal{I}(\mathbf{v}_k), \quad k < k_{\max},$$

$$:= \infty, \qquad\qquad\qquad\qquad\qquad\qquad\qquad\qquad\qquad\qquad\qquad\qquad\qquad k = k_{\max}.$$

Notice that $q \in \aleph\mathbb{Y}$, since that inventory can jump only of $\pm N$, and we assume it starts on the lattice $\aleph\mathbb{Y}$: by the variable change

$$\mathbf{v}_k(\tau,q,c) = \aleph\tilde{\mathbf{v}}_k(\tau, \tilde{q} = q/\aleph, c),,$$

we obtain

$$\mathcal{J}_\pm(\mathbf{v}_k)(\tau,q,c) = \aleph\mathcal{L}_\pm(\tilde{\mathbf{v}}_k)(\tau, q/\aleph, c),$$
$$\mathcal{L}_\pm(\mathbf{v}_k)(\tau,q,c) = \aleph\mathcal{L}_\pm(\tilde{\mathbf{v}}_k)(\tau, q/\aleph, c),$$
$$\mathcal{I}^\pm(\mathbf{v}_k)(\tau,q,c) = \aleph\mathcal{I}^\pm(\tilde{\mathbf{v}}_k)(\tau, q/\aleph, c),$$
$$\gamma^{(\eta)}(q,c) = \aleph\left[\alpha(c)(q/\aleph) - (\aleph\eta)(q/\aleph)^2\right] = \aleph\gamma^{(\aleph\eta)}(q/\aleph, c).$$

Since we can factor $\aleph$ everywhere, $\tilde{v}$ is the solution of the unitary problem ($N = 1$) where the risk aversion is multiplied by $\aleph$. This ends the proof.

Notations

Sets

We denote by

⋄ $\mathbb{N}, \mathbb{Z}, \mathbb{R}$ the natural, integers and real numbers;

⋄ $\mathbb{N}^*, \mathbb{Z}^*, \mathbb{R}^*$ the corresponding sets without 0;

⋄ $\mathbb{1}\{A\}$ the indicator function on the A set.

The agent portfolio

Throughout this work, we will assume that an agent participates to the market via a trading strategy. A single-asset agent portfolio contains a certain inventory of the asset: we denote by

⋄ $(P_t)_{t \geq 0}$ the reference price at which the portfolio is evalued: it can either be the mid-price, or any reference price chosen as representative of the intrinsic asset value;

⋄ $(X_t)_{t \geq 0}$ the agent bank account, also called wealth, which is subjected to no interest rate: it can be either positive, or negative, if the agent has a debt;

⋄ $(Y_t)_{t \geq 0}$ the agent inventory, either positive (long position) or negative (short position): short selling is allowed;

⋄ $(V_t)_{t \geq 0}$ the mark-to-market of the portfolio, i.e. $V_t := X_t + Y_t P_t$;

⋄ T is the agent horizon, which can be deterministic or random, but in both cases almost surely finite;

⋄ $\varphi \geq 0$ is the execution cost (fees) to which each transaction is subjected;

⋄ $\eta \geq 0$ is the agent risk aversion to hold a large inventory.

The piece-wise constant reference price

Most of the times the reference price will be described by a point process, i.e. a piece-wise constant process which jumps at random times of a random quantity. In this case we denote by

⋄ $(T_n)_{n \in \mathbb{N}}$ the timestamps at which the price jumps;

⋄ $(S_n)_{n \in \mathbb{N}^*}$ the inter-arrival times, i.e. $S_n := T_n - T_{n-1}$;

⋄ $(P_n)_{n \in \mathbb{N}}$ the value of the price during the interval $[T_n, T_{n+1})$, i.e. $P_n := P_{T_n}$;

⋄ $(J_n)_{n \in \mathbb{N}^*}$ the price jumps at T_n-, i.e. $J_n := P_n - P_{n-1} \neq 0$;

⋄ $(\widehat{J}_n)_{n \in \mathbb{N}^*}$ the direction of the stock price jumps at T_n-, i.e. $\widehat{J}_n := \text{sgn}(J_n)$;

⋄ $(U_n)_{n \in \mathbb{N}^*}$ the type of direction taken by the stock price at T_n-, i.e. $U_n := \hat{J}_n \hat{J}_{n-1}$;

⋄ $(N_t)_{t\geq 0}$ the counting process $N_t := \inf\{n : \sum_{k=1}^n T_k \leq t\}$, with the convention that $N_0 = 0$.

⋄ $(P_t)_{t\geq 0}$ the real time value of the reference price, i.e. $P_t := P_0 + \sum_{k=1}^{N_t} J_k$;

⋄ $(I_t)_{t\geq 0}$ the last direction taken by the stock price, i.e. $I_t := \widehat{J}_{N_t}$;

⋄ $(S_t)_{t\geq 0}$ the elapsed time since the last price jump, i.e. $S_t := t - T_{N_t}$;

Markov processes

We will often use conditional expectation in this work. For a general (multi-dimensional) Markov process $(X_t)_{t\geq 0}$ we denote by

⋄ $\mathbb{E}_{t,x}[X_T] := \mathbb{E}[X_T | X_t = x]$;

⋄ if the reference price $(P_t)_{t\geq 0}$ is Markovian, we denote by

$$\pi(t,p) := \mathbb{E}_{t,p}[P_T] =: p + \varepsilon(t,p) =: p + i\theta(t,p);$$

For any Markov process (X_t) such that $X_t = x$ we will denote by

$$\Delta_{t,x}\mathfrak{g}(t,y) = \mathfrak{g}(t,y) - \mathfrak{g}(t,x),$$

where $\mathfrak{g}$ denotes a generic test function. In practice, we will omit the subscript "t, x" when it is clear from the context. This notation will be particularly useful for the description of the infinitesimal generators of jump processes appearing in the HJB equations.

Bibliography

[1] Frédéric Abergel and Aymen Jedidi. A mathematical approach to order book modeling. *International Journal of Theoretical and Applied Finance*, 16(05), 2013.

[2] Yacine Aït-Sahalia, Per A Mykland, and Lan Zhang. How often to sample a continuous-time process in the presence of market microstructure noise. *Review of Financial studies*, 18(2):351–416, 2005.

[3] Yacine Ait-Sahalia, Per A Mykland, and Lan Zhang. Ultra high frequency volatility estimation with dependent microstructure noise. *Journal of Econometrics*, 160(1):160–175, 2011.

[4] Aurélien Alfonsi, Antje Fruth, and Alexander Schied. Optimal execution strategies in limit order books with general shape functions. *Quantitative Finance*, 10(2):143–157, 2010.

[5] Robert Almgren and Neil Chriss. Optimal execution of portfolio transactions. *Journal of Risk*, 3:5–40, 2001.

[6] Marco Avellaneda and Sasha Stoikov. High-frequency trading in a limit order book. *Quantitative Finance*, 8(3):217–224, 2008.

[7] Emmanuel Bacry, Sylvain Delattre, Marc Hoffmann, and Jean-François Muzy. Modelling microstructure noise with mutually exciting point processes. *Quantitative Finance*, 13(1):65–77, 2013.

[8] Emmanuel Bacry and Jean-François Muzy. Hawkes model for price and trades high-frequency dynamics. *to appear on Quantitative Finance*, 1:1–20, 2014.

[9] Luc Bauwens and Nikolaus Hautsch. *Modelling financial high frequency data using point processes*. Springer, 2009.

[10] Erhan Bayraktar and Michael Ludkovski. Liquidation in limit order books with controlled intensity. *Mathematical Finance*, 2012.

[11] Alain Bensoussan and C Tomson. *Perturbation methods in optimal control*. Gauthier-Villars Paris, 1988.

[12] Jean-Philippe Bouchaud, J Doyne Farmer, and Fabrizio Lillo. How markets slowly digest changes in supply and demand. *Handbook of financial markets: dynamics and evolution*, 1:57, 2009.

[13] Jean-Philippe Bouchaud, Marc Mézard, Marc Potters, et al. Statistical properties of stock order books: empirical results and models. *Quantitative Finance*, 2(4):251–256, 2002.

[14] Jean-Philippe Bouchaud and Marc Potters. *Theory of financial risk and derivative pricing: from statistical physics to risk management*. Cambridge university press, 2003.

[15] Peter Bühlmann, Abraham J Wyner, et al. Variable length markov chains. *The Annals of Statistics*, 27(2):480–513, 1999.

[16] R. Carmona and K. Webster. High frequency market making. *Available at arXiv:1210.5781*, 2012.

[17] Álvaro Cartea. Derivatives pricing with marked point processes using tick-by-tick data. *Quantitative Finance*, 13(1):111–123, 2013.

[18] Álvaro Cartea, Ryan Donnelly, and Sebastian Jaimungal. Algorithmic trading with model uncertainty. *Available at SSRN 2310645*, 2014.

[19] Álvaro Cartea and Sebastian Jaimungal. Modelling asset prices for algorithmic and high-frequency trading. *Applied Mathematical Finance*, 20(6):512–547, 2013.

[20] Álvaro Cartea and Sebastian Jaimungal. Risk metrics and fine tuning of high-frequency trading strategies. *Mathematical Finance*, 2013.

[21] Álvaro Cartea and Sebastian Jaimungal. A closed-form execution strategy to target vwap. *Available at SSRN 2542314*, 2014.

[22] Álvaro Cartea, Sebastian Jaimungal, and Damir Kinzebulatov. Algorithmic trading with learning. *Available at SSRN*, 2013.

[23] Álvaro Cartea, Sebastian Jaimungal, and Jason Ricci. Buy low sell high: a high frequency trading perspective. *Preprint SSRN*, 2011.

[24] Alvaro Cartea and Thilo Meyer-Brandis. How duration between trades of underlying securities affects option prices. *Review of Finance*, page rfp013, 2009.

[25] Rama Cont and Adrien De Larrard. Price dynamics in a markovian limit order market. *SIAM Journal on Financial Mathematics*, 4(1):1–25, 2013.

[26] Rama Cont, Sasha Stoikov, and Rishi Talreja. A stochastic model for order book dynamics. *Operations research*, 58(3):549–563, 2010.

[27] John C Cox, Jonathan E Ingersoll Jr, and Stephen A Ross. A theory of the term structure of interest rates. *Econometrica: Journal of the Econometric Society*, pages 385–407, 1985.

[28] Daryl J Daley and David Vere-Jones. *An introduction to the theory of point processes*, volume 2. Springer, 1988.

[29] Guglielmo D'Amico and Filippo Petroni. A semi-markov model with memory for price changes. *Journal of Statistical Mechanics: Theory and Experiment*, 2011(12):P12009, 2011.

[30] Guglielmo D'Amico and Filippo Petroni. Weighted-indexed semi-markov models for modeling financial returns. *Journal of Statistical Mechanics: Theory and Experiment*, 2012(07):P07015, 2012.

[31] Khalil Dayri and Mathieu Rosenbaum. Large tick assets: implicit spread and optimal tick size. *arXiv preprint arXiv:1207.6325*, 2012.

[32] J Doyne Farmer 5, Laszlo Gillemot, Fabrizio Lillo, Szabolcs Mike, and Anindya Sen. What really causes large price changes? *Quantitative finance*, 4(4):383–397, 2004.

[33] Sofiene El Aoud and Frédéric Abergel. A stochastic control approach for option market making. *Available at SSRN 2491446*, 2014.

[34] Robert F Engle and Jeffrey R Russell. Autoregressive conditional duration: a new model for irregularly spaced transaction data. *Econometrica*, pages 1127–1162, 1998.

[35] Alexis Fauth and Ciprian A Tudor. Modeling first line of an order book with multivariate marked point processes. *arXiv preprint arXiv:1211.4157*, 2012.

[36] Pietro Fodra and Huyên Pham. Semi markov model for market microstructure. *arXiv preprint arXiv:1305.0105*, 2013.

[37] Pietro Fodra and Huyen Pham. High frequency trading and asymtpotics in a markov renewal model. *arXiv:1310.1756 (accepted by SIAM Journal of Financial Mathematics)*, 2014.

[38] Ramazan Gençay, Michel Dacorogna, Ulrich A Muller, Olivier Pictet, and Richard Olsen. *An introduction to high-frequency finance*. Academic Press, 2001.

[39] Arnaud Gloter and Jean Jacod. Diffusions with measurement errors. i. local asymptotic normality. *ESAIM: Probability and Statistics*, 5:225–242, 2001.

[40] Peter W Glynn and Peter J Haas. On functional central limit theorems for semi-markov and related processes. *Commun. Statist. Theory Methods*, 33(487-506), 2004.

[41] Olivier Guéant, Charles-Albert Lehalle, and Joaquin Fernandez-Tapia. Optimal portfolio liquidation with limit orders. *SIAM Journal on Financial Mathematics*, 3(1):740–764, 2012.

[42] Olivier Guéant, Charles-Albert Lehalle, and Joaquin Fernandez-Tapia. Dealing with the inventory risk: a solution to the market making problem. *Mathematics and financial economics*, 7(4):477–507, 2013.

[43] Fabien Guilbaud and Huyên Pham. Optimal high frequency trading in a pro-rata microstructure with predictive information. *http://arxiv.org/abs/1205.3051*, 2012.

[44] Fabien Guilbaud and Huyen Pham. Optimal high-frequency trading with limit and market orders. *Quantitative Finance*, 13(1):79–94, 2013.

[45] Xin Guo and Mihail Zervos. Optimal execution with multiplicative price impact. *SIAM Journal of Financial Mathematics (to appear)*, 2013.

[46] Jean Jacod. La variation quadratique du brownien en presence d'erreurs d'arrondi. *Astérisque*, 236(1):155–162, 1996.

[47] Thibault Jaisson and Mathieu Rosenbaum. Limit theorems for nearly unstable hawkes processes. *arXiv preprint arXiv:1310.2033*, 2013.

[48] Andrei Kirilenko, Albert S Kyle, Mehrdad Samadi, and Tugkan Tuzun. The flash crash: The impact of high frequency trading on an electronic market. *Manuscript, U of Maryland*, 2011.

[49] Mauricio Labadie and Pietro Fodra. High-frequency market-making with inventory constraints and directional bets. *Available at arXiv:1206.4810*, 2012.

[50] Jeremy Large. Measuring the resiliency of an electronic limit order book. *Journal of Financial Markets*, 10(1):1–25, 2007.

[51] Sophie Laruelle, Charles-Albert Lehalle, et al. Optimal posting price of limit orders: learning by trading. *arXiv preprint arXiv:1112.2397*, 2011.

[52] Fabrizio Lillo and J Doyne Farmer. The long memory of the efficient market. *Studies in Nonlinear Dynamics & Econometrics*, 8(3), 2004.

[53] Nikolaos Limnios and Gheorghe Oprisan. *Semi-Markov processes and reliability*. Springer, 2001.

[54] M. Maechler. *VLMC Package*, 2014.

[55] Albert J Menkveld and Bart Z Yueshen. Anatomy of the flash crash. *Available at SSRN 2243520*, 2013.

[56] Yoshiko Ogata. The asymptotic behaviour of maximum likelihood estimators for stationary point processes. *Annals of the Institute of Statistical Mathematics*, 30(1):243–261, 1978.

[57] Gu Olivier, Guillaume Royer, et al. Vwap execution and guaranteed vwap. Technical report, arXiv. org, 2013.

[58] Marc Potters and Jean-Philippe Bouchaud. More statistical properties of order books and price impact. *Physica A: Statistical Mechanics and its Applications*, 324(1):133–140, 2003.

[59] Jorma Rissanen et al. A universal data compression system. *IEEE Transactions on information theory*, 29(5):656–664, 1983.

[60] Christian Y Robert and Mathieu Rosenbaum. A new approach for the dynamics of ultra-high-frequency data: The model with uncertainty zones. *Journal of Financial Econometrics*, 9(2):344–366, 2011.

[61] Christian Yann Robert and Mathieu Rosenbaum. Volatility and covariation estimation when microstructure noise and trading times are endogenous. *Mathematical Finance*, 22(1):133–164, 2012.

[62] Ioanid Roşu. A dynamic model of the limit order book. *Review of Financial Studies*, page hhp011, 2009.